UNIVERSIDAD AUTÓNOMA DE MADRID

FACULTAD DE CIENCIAS

Departamento de Biología Molecular

REQUERIMIENTO DE FACTORES DE INICIACIÓN PARA LA TRADUCCIÓN DE mRNAs DE PICORNAVIRUS

TESIS DOCTORAL

Natalia Redondo Sevillano

Madrid, 2012

UNIVERSIDAD AUTÓNOMA DE MADRID

FACULTAD DE CIENCIAS

Departamento de Biología Molecular

REQUERIMIENTO DE FACTORES DE INICIACIÓN PARA LA TRADUCCIÓN DE mRNAs DE PICORNAVIRUS

TESIS DOCTORAL

Memoria presentada por **Natalia Redondo Sevillano** para optar al grado de Doctora en Ciencias por la Universidad Autónoma de Madrid

Madrid, 2012

El trabajo presentado en esta tesis doctoral ha sido realizado en el **Centro de Biología Molecular "Severo Ochoa"**, bajo la dirección del Dr. Luis Carrasco Llamas, la Dra. MªVanesa Madan Renes y el Dr. Miguel Ángel Sanz Fernández, mediante la concesión de una beca FPI del Ministerio de Ciencia e Innovación. Ha sido financiado por el proyecto BFU2009-07352 otorgado por la Direccion General de Investigacion Cientifica y Tecnica, Ministerio de Educacion y Ciencia.

AGRADECIMIENTOS

Me gustaría, en primer lugar, dar las gracias a Luis por haberme dado la oportunidad de incorporarme a su grupo de trabajo e introducirme en el mundo de la virología.
Tengo que agradecer mucho también a mis co-directores, Vanesa, que me enseñó a manejarme en el laboratorio, y Miguel Ángel, que siempre sabe resolver todas mis dudas

Doy las gracias a las amigas que he hecho en el laboratorio, grandes amigas que permanecerán mucho más allá de mi estancia en el CBM, como Valva, Diana y Ruth. También tengo que agradecer al resto de personas que han estado o están en el 120 y que han sido una parte importante para el desarrollo de mi trabajo: Kike, gracias por tus consejos; Juan, gracias por ayudarme con todos los clonajes, que habría hecho sin ti! y Alfredo, que incluso en la distancia ha sido de gran ayuda. También tengo que mencionar a Tinka y Esther. Como no a Alfonsito, siempre tan atento y que con sus locuras me alegra los días. A Lorena, que me hace compañía cuando me quedo la última en el laboratorio. A Héctor, que siempre está ahí para tomarnos un descanso entre experimento y experimento. Y en definitiva quiero agradecer a toda la gente con la que empecé con un simple "Hola" por los pasillos y al final acaban siendo buenos amigos dentro y fuera del CBM.

Una parte muy importante ha sido mi familia, que aunque nunca han entendido muy bien lo que hago, nunca han dejado de apoyarme. Sobre todo le tengo que agradecer a Paula, mi sobrina de tres años, que con ella desaparece todo el estrés, los agobios y en general todas las malas vibraciones.

Importantísimas son mis amigas Bea y May, mi amiga Ana "la del molino", que es una parte insustituible de mi vida. Mi primi Olga, que tan buenos consejos me da y que tanto me entiende. Gema, que aunque no nos vemos todo lo que quisiéramos siempre está ahí. Iker, que es la persona que más me hace reír en el mundo. Y no me puedo olvidar de mis amigas "las Biólogas"… algún día cambiaremos el mundo! Y a todas las personas que no nombro porque si no no acabaríamos nunca…Tampoco puedo olvidarme de Ana, que tan buenos valores ha sabido transmitirme.

Y por último tengo que hacer una mención especial a mis gatas, Ébola y África…

ÍNDICE

RESUMEN EN INGLÉS (SUMMARY)

Viruses are intracellular parasites that rely on the components of the host cell for gene expression and replication. Soon after infection, the host cell often tends to limit viral production and replication by shutting-off global translation. Many viral genomes have evolved mechanisms to bypass this general inhibition of translation by developing strategies of initiation independent of the classical recognition of an m^7G cap structure at the 5′ end of the mRNA. These mechanisms imply the utilization of internal ribosome entry sites (IRES) which can promote 5′ end independent initiation. The IRES were first recognized within the RNA genomes of picornaviruses 20 years ago. Since the initial characterization of picornavirus IRES, other RNA virus have shown to initiate translation internally. Each class of IRES varies in size, structure and requirements for cellular protein to allow them to function.

Poliovirus IRES translation is not blocked when eIF4G is cleaved either when eIF2 is inactivated by phosphorylation at late times of infection. However, RNA is blocked when eIF2 is inactivated at earlier times. Thus, poliovirus RNA translation exhibits a dual mechanism for the initiation of protein synthesis as regards to the requirement for eIF2. Analysis of individual poliovirus non-structural proteins indicates that the presence of $2A^{pro}$ alone is sufficient to provide eIF2 independence for IRES-driven translation. This effect is not observed with a $2A^{pro}$ variant unable to cleave eIF4G. The level of $2A^{pro}$ synthesized in culture cells is crucial for obtaining eIF2 independence. Expression of the N-or C-terminus fragments of eIF4G did not stimulate IRES-driven translation, nor provide eIF2 independence, consistent with the idea that the presence of $2A^{pro}$ at high concentrations is necessary. The finding that $2A^{pro}$ provides eIF2-independent translation opens a new and unsuspected area of research in the field of picornavirus protein synthesis.

The hepatitis A virus (HAV) IRES is thought that requires intact eIF4F complex for translation. In line with previous results we report that poliovirus (PV) $2A^{pro}$ strongly blocks protein synthesis directed by HAV IRES. However, in contrast to previous findings we now demonstrate that eIF4G cleavage by foot-and-mouth disease virus (FMDV) L^{pro} strongly stimulates HAV IRES-driven translation. Thus, this is the first observation that $2A^{pro}$ and L^{pro} exhibit opposite effects to what was previously thought to be the case in HAV IRES. Notably, in presence of this FMDV protease, translation directed by HAV IRES takes place when eIF2α has been inactivated by phosphorylation. Our present findings clearly demonstrate that protein synthesis directed by HAV IRES can occur when eIF4G has been cleaved and after inactivation of eIF2. Therefore, factorless translation directed by HAV IRES is similar to that observed with other picornavirus IRESs.

INTRODUCCIÓN

El estudio de la traducción y de su regulación está produciendo en los últimos años resultados muy novedosos y de alto interés científico. Los estudios de traducción de mRNAs virales han sido especialmente relevantes y han permitido el descubrimiento de nuevos mecanismos de traducción "no canónicos", diferentes del mecanismo predominante en la traducción de los mRNAs celulares. Entre los mecanismos no canónicos descritos se encuentran el denominado *leaky scanning*, utilizado por algunos mRNAs de retrovirus, papilomavirus y coronavirus, cuyo fin es economizar espacio en el material genético. Por otro lado la traducción mediada por IRES (Internal Ribosome Entry Site), se descubrió estudiando los picornavirus y el mecanismo conocido como *shunting* se ha observado en adenovirus[1]. Además no sólo se están descubriendo nuevos factores de iniciación implicados en la síntesis de proteínas celulares [2, 3], sino que también se han identificado algunas proteínas virales capaces de reemplazar funciones de la maquinaria de traducción celular [4].Asimismo, se está analizando el papel regulador de la traducción de diversos gránulos de RNA, como son los cuerpos de procesamiento (*processing bodies*) ó los gránulos de estrés (*stress granules*) [5]. También se ha descrito la compartimentalización subcelular de la traducción de diversos mRNAs [6, 7]. De gran interés ha sido el estudio de la regulación de la expresión genética mediante RNAs de interferencia (siRNAs), tanto en células infectadas por virus como en células sanas [8, 9]. También se está estudiando el uso de codones de iniciación distintos al AUG y la posibilidad de traducir en las tres fases posibles de lectura dando lugar a proteínas aberrantes (RAN translation) y la implicación de estos procesos en la patogénesis de distintas enfermedades humanas[10, 11]. Se ha descubierto que un gran porcentaje (casi el 50%) de mRNAs celulares contienen ORFs (open reading frames o fases de lectura abierta) cortas antes del AUG iniciador y que la traducción de estas "upstream open reading frame" (UORF) regula la expresión genética de diversas formas [12]. Nuestro grupo también ha realizado recientes aportaciones en el campo de la traducción viral, describiendo cómo diferentes mRNAs virales pueden traducirse en ausencia de factores de iniciación concretos [13-16]. Además, hemos encontrado evidencias que apoyan la participación de dos mecanismos en la traducción de mRNAs virales durante la infección. En el inicio de las infecciones diferentes mRNAs virales se traducen siguiendo un mecanismo canónico, mientras que en las fases tardías, cuando la infección prospera y el entorno celular es alterado tras la expresión de las proteínas virales, predomina un mecanismo no canónico [14, 16]. Por último, hemos descrito que una proteína viral, la proteasa 2A de poliovirus, confiere traducibilidad a los mRNAs virales cuando el factor eIF2α está fosforilado y es inactivo [17]. Todos estos descubrimientos hacen del estudio de la traducción y de los

mecanismos de iniciación de la síntesis de proteínas un campo dinámico y de gran interés en la actualidad.

1. MECANISMO DE LA TRADUCCIÓN DE mRNAS.

En células de mamíferos existen, principalmente, dos mecanismos de iniciación de la traducción de mRNAs: el mecanismo "canónico", que es usado por la mayoría de los mRNAs celulares, y el mecanismo de iniciación interna de la traducción [18-20].

1.1. Mecanismo de traducción cap-dependiente

El mecanismo canónico tiene lugar en mRNAs que poseen una estructura *cap* (m^7GpppN) en su extremo 5' (Fig. 1A), requiere más de diez factores de inicio de la traducción (eIFs) y ocurre en dos etapas: i) formación del complejo de iniciación 48S, y ii) unión a la subunidad ribosomal 60S [21].

Por un lado, i) el extremo 5´del mRNA es reconocido por el complejo eIF4F que está formado por tres factores: el eIF4E, que reconoce la estructura cap, el eIF4G, que es una proteína de ensamblaje que interacciona y regula la actividad de distintos componentes que participan en la traducción, y el eIF4A, que tiene actividad helicasa. Además, la cola de poli(A), que se localiza en el extremo 3' del mRNA, se une a la proteína de unión a la cola de poli(A) (PABP, *poly(A)-binding protein*). PABP interacciona con eIF4G e induce que el mRNA adopte una conformación circular, facilitando el reciclado de los ribosomas (Fig. 1B y 1C). Por otro lado, el eIF2 se une al tRNA iniciador (Met-$tRNA_i$) y a GTP para formar el complejo ternario Met-$tRNA_i$-eIF2-GTP, que junto a los factores eIF3, eIF1 y eIF1A se une a la subunidad ribosómica 40S para formar el complejo de pre-iniciación 43S [22-24] (Fig. 1B). Este complejo interacciona a través del eIF3 con el eIF4F y el mRNA [18, 25, 26]. A continuación comienza desde el extremo 5' el "scanning" de la secuencia lider del mRNA hasta alcanzar el AUG iniciador (Fig. 1C). Una vez posicionada la subunidad 40S en este AUG iniciador, se establece el apareamiento de bases (codon:anticodon) con el Met-$tRNA_i$, dando lugar al complejo de iniciación 48S [18, 25, 27]. Posteriormente, ii) la incorporación del eIF5 a este complejo promueve la hidrólisis de GTP del complejo ternario [18, 22, 25, 26], mientras que la entrada de eIF5B-GTP promueve la interacción con la subunidad 60S y la salida del eIF2-GDP y del resto de los factores de iniciación, excepto el eIF1A y el eIF5B (Fig. 1D). El complejo eIF2-GDP que se produce después de cada ronda de traducción tiene que ser reciclado para dar lugar de nuevo a eIF2-GTP antes del comienzo de una nueva ronda de traducción. Este proceso está facilitado por el factor de reciclaje eIF2B (*guanine nucleotide exchange factor* o GEF) [22, 24, 26]. Una

vez que el Met-tRNA$_i$ queda unido al ribosoma 80S en el sitio P, el proceso de iniciación de la traducción termina y da comienzo entonces la etapa de elongación ó polimerización (Fig. 1D).

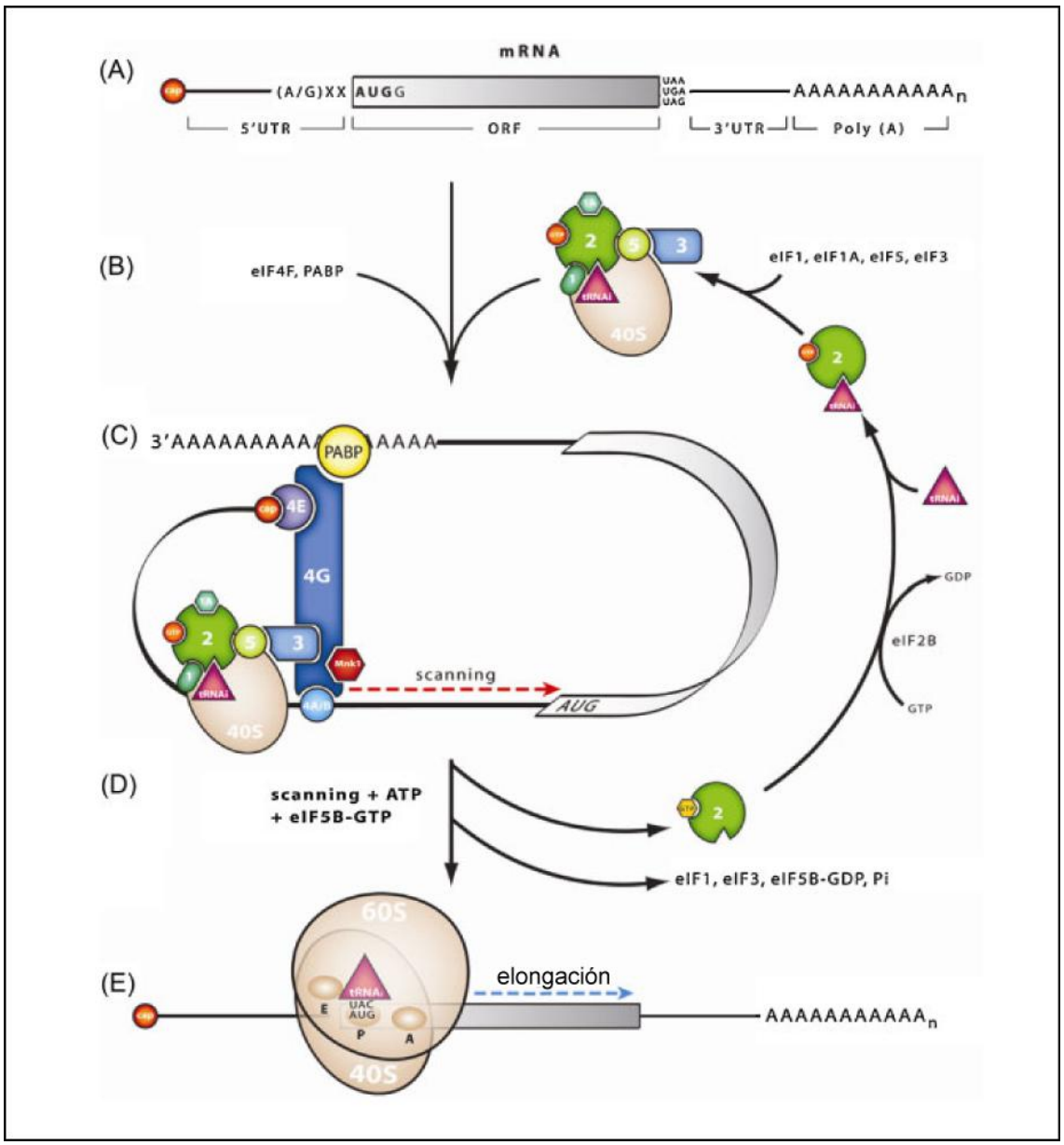

Figura 1. Esquema del mecanismo de traducción cap-dependiente. A) Estructura de un mRNA canónico. B) Formación del complejo de pre-iniciación 43S. C) Posicionamiento de la subunidad 40S sobre el AUG iniciador. Formación del complejo de iniciación 48S. D) El factor eIF5B promueve la hidrólisis de GTP. Salida de factores. E) Ensamblaje de la subunidad 80S. Comienza la etapa de elongación. Adaptado de López-Lastra y col., 2010.

1.2. Mecanismo de traducción cap-independiente

Algunos mRNAs se traducen mediante un mecanismo cap-independiente gracias a la presencia de unas estructuras conocidas como sitio de entrada interna del ribosoma o IRES. La presencia de estas estructuras se descubrió a finales de la década de los años 80 estudiando la traducción de mRNAs de picornavirus [28].

La clasificación de los diversos IRES descritos hasta la actualidad se realiza en función de su origen, su estructura y su funcionalidad [29-31]. Se pueden distinguir dos grupos principales: IRES celulares ó IRES virales. El último, a su vez, engloba cuatro grupos en función de su origen: 1) IRES de picornavirus; 2) IRES de flavivirus; 3) IRES de lentivirus y 4) IRES de dicistrovirus [29] (Tabla 1).

Los IRES permiten la unión del mRNA a la subunidad 40S del ribosoma sin necesidad de la presencia de una estructura cap en el extremo 5´. Además, permiten la traducción en condiciones extremas tales como la falta de aminoácidos, hipoxia, choque térmico, o durante la muerte celular. Los IRES confieren a los virus, además, la posibilidad de traducir sus mRNAs en ausencia de determinados eIFs, de forma que el requerimiento de dichos factores es diferente en función del origen del IRES (Fig. 2). Por ejemplo, en el caso de los picornavirus, la mayoría de los IRES no requieren el complejo eIF4F intacto y pueden traducirse cuando el factor eIF4G ha sido hidrolizado por las proteasas de picornavirus (Fig. 2). Además, recientemente se ha demostrado que los RNAs de picornavirus son capaces de traducirse cuando el eIF2α está fosforilado [16, 17, 32]. Actualmente se están llevando a cabo muchos estudios para determinar cuales son los requerimientos de eIFs de los diferentes IRES, tanto en sistemas *in vitro* como en células, lo que conllevará un cambio en los requerimientos descritos hasta la fecha.

Familia de virus	Género	Virus
Picornaviridae (ssRNA+)	*Enterovirus*	Polio
		Rhinovirus
	Hepatovirus	Hepatitis A
	Avihepatovirus	Hepatitis A aviar
	Aphtovirus	Fiebre aftosa
	Teschovirus	Teschovirus porcino
	Kobuvirus	Aichivirus
Retroviridae (ssRNA+)	*Lentivirus*	HIV-1
		HIV-2
		FIV
Flaviviridae (ssRNA+)	*Hepacivirus*	Hepatitis C
Dicistroviridae	*Cripavirus*	Parálisis del grillo

Tabla 1. Virus que poseen estructuras IRES.

Aparte de los eIFs, la actividad de los IRES también está regulada por los factores específicos de IRES, ITAFs (**I**RES-specific **T**rans **A**cting **F**actors). La lista de ITAFs está en continuo crecimiento, pero dos de los más estudiados son el La *autoantigen* (La) y la *polypyrimidine tract binding protein* (PTB), los cuales son importantes para la actividad de algunos picornavirus. Los ITAFs pueden condicionar el reclutamiento del ribosoma al IRES, aunque

hoy en día se desconoce el mecanismo por el que actúan. Una teoría propone que los ITAFs podrían poseer actividad chaperona, y que su interacción con el RNA ayudaría a los IRES a adquirir la conformación adecuada para obtener traducibilidad [1].

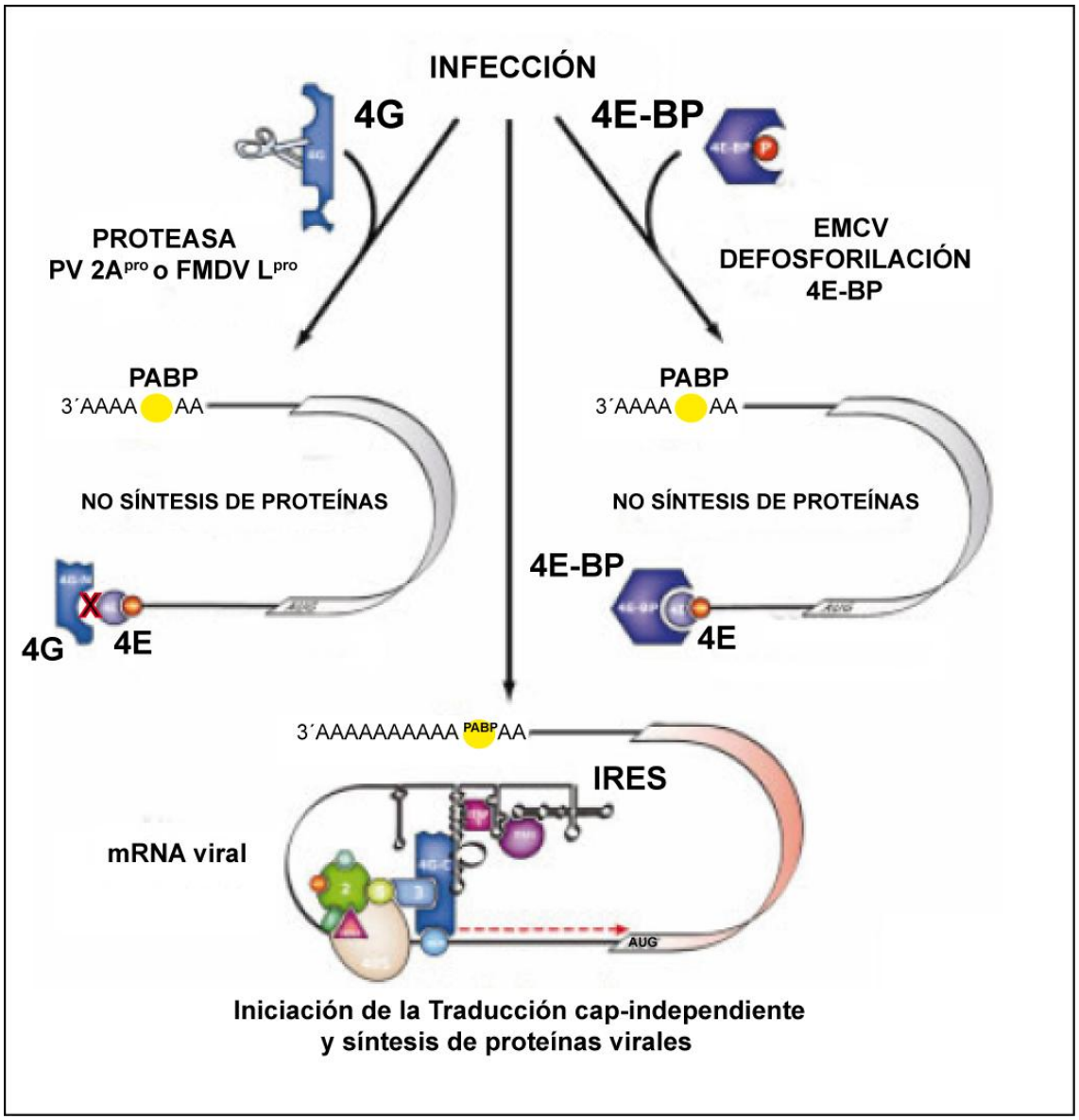

Figura 2. Inhibición de la traducción cap-dependiente. La infección causada por el virus de la polio (PV) o el virus de la fiebre aftosa (FMDV) produce una rápida hidrólisis del factor eIF4G por acción de las proteasas 2A y L, respectivamente. El corte de eIF4G inhibe la traducción cap-dependiente y favorece la traducción dirigida por los IRES virales. Otros picornavirus, como el virus de la encefalomiocarditis (EMCV) inhibe la traducción cap-dependiente induciendo la defosforilación de las proteínas de unión a 4E (4E-BPs). Las 4E-BPs se unen al factor eIF4E desplazando al factor eIF4G. Adaptado de López-Lastra y col., 2010.

2. REPLICACIÓN DE LOS PICORNAVIRUS

Los Picornavirus forman una gran familia de virus animales ampliamente extendidos en la naturaleza. Algunos miembros han sido estudiados en profundidad dada su implicación en problemas de salud pública. En la actualidad los virus de la familia *Picornaviridae* se clasifican en 12 géneros: Enterovirus, Cardiovirus, Aphthovirus, Rhinovirus, Hepatovirus, Parechovirus, Erbovirus, Kobuvirus, Teschovirus, Sapelovirus, Senecavirus y Tremovirus.

Los Picornavirus forman partículas pequeñas icosahédricas que contienen una molécula de RNA de cadena sencilla y polaridad positiva de aproximadamente 7500 nucleótidos. El RNA no posee la estructura cap en el extremo 5´, pero sí contiene una cola de poli(A) en su extremo 3´ con una longitud variable entre 65 y 100 nucleótidos. El RNA viral se traduce en una larga poliproteína la cual es procesada proteolíticamente por las proteasas virales, dando lugar a 11 proteínas maduras en el caso de poliovirus y un número variable, dependiendo del virus, de productos parcialmente procesados. Cuatro de estas proteínas, VP1-VP4, son las proteínas estructurales que forman la cápsida viral, mientras que las demás proteínas serán las encargadas de llevar a cabo la replicación viral [33] (Fig. 3A)

El ciclo infectivo de los picornavirus comienza con la unión de la partícula viral a los receptores presentes en la superficie celular, los cuales para la mayoría de los picornavirus son miembros de la superfamilia de las inmunoglobulinas [33]. Esta unión conlleva la internación del virus y la desestabilización de la cápsida, volviéndose ésta menos compacta. A continuación se produce la liberación del RNA viral en el citoplasma, que interaccionará con la maquinaria de traducción celular para dar lugar a la síntesis de proteínas virales durante la fase temprana de la infección (Fig. 3B).

Como se mencionó anteriormente, la poliproteína viral sintetizada es proteolíticamente procesada para dar lugar a las proteínas virales maduras. Se han descrito tres eventos proteolíticos: i) el llevado a cabo por proteasas virales. Por un lado, la proteasa 2A ($2A^{pro}$) corta en su extremo amino terminal dentro de la poliproteína dando lugar al precursor P1, que codifica las proteínas estructurales del virus y, por otro lado, la proteasa 3C ($3C^{pro}$) libera el precursor P2 (2ABC) de P3 (3ABCD). En los aftovirus, además, existe una tercera proteasa, la proteasa *leader* (Lpro), que es la encargada del procesamiento de la poliproteína viral en estos virus; ii) cortes de numerosos factores celulares que tienen lugar en el citoplasma llevados a cabo fundamentalmente por la proteasa 3C [33], y iii) la hidrólisis de VP0 (VP4-VP2), responsable de la morfogénesis de las partículas virales [34, 35].

Todos los eventos proteolíticos conducen a la formación de once proteínas maduras y varios precursores que son P1, P2, P3, VP0, VP3, VP1, 2BC, 3AB y 3CD. Este último precursor, 3CD, en el caso de PV, puede actuar como sustrato de la $2A^{pro}$ o de la $3C^{pro}$. El corte

alternativo llevado a cabo por la proteasa 2A da lugar a los productos maduros denominados 3C´y 3D´, mientras que $3C^{pro}$ genera las proteínas canónicas $3C^{pro}$ y $3D^{pol}$. Sin embargo, el significado biológico de este corte alternativo no está claro, ya que en virus mutados, en los que se ha eliminado la capacidad proteolítica de $2A^{pro}$ en el precursor 3CD, no se observan defectos en replicación [36].

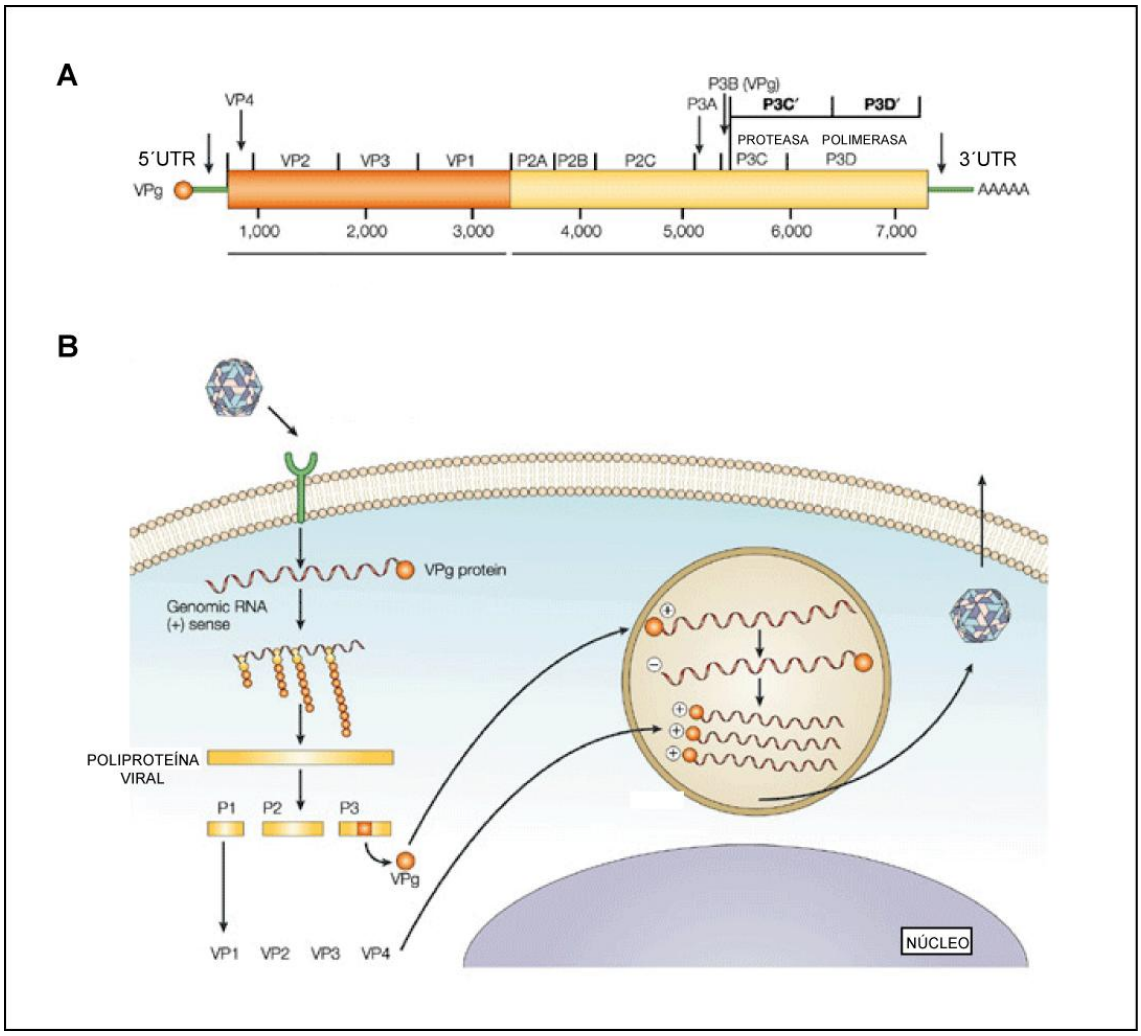

Figura 4. Esquema de la infección de PV. A) Procesamiento proteolítico de la poliproteína viral. B) Representación del proceso en la célula hospedadora. Adaptado de Minor, 2004.

Las proteínas no estructurales generadas participan en la replicación del genoma viral [33, 37, 38], para ello, la molécula de RNA es reconocida en su extremo 3´por las proteínas que conforman el complejo replicativo, dando lugar a una molécula de RNA complementaria de polaridad negativa. En este proceso la proteína 3B, conocida también como VPg, actúa como cebador (primer) para iniciar la transcripción del RNA viral [39]. Esto conduce a la formación de una mólecula de RNA de doble cadena, también llamada forma replicativa. La cadena de polaridad negativa sirve de molde para la síntesis de varias copias de polaridad positiva, las cuales actuarán en tres procesos: i) como moldes para sintetizar más moléculas de polaridad

negativa, que a su vez producirán más copias de RNA de polaridad positiva, ii) como mRNAs que intervendrán en el proceso de traducción, y iii) como genomas que serán encapsidados en las partículas virales en formación [40].

Una vez que se han producido varios miles de moléculas de RNA de polaridad positiva, tiene lugar la fase tardía de la infección, en la cual se inhibe la traducción canónica de mRNAs celulares como consecuencia de la hidrólisis del factor eIF4G, llevada a cabo por la proteasa 2A, y sólo son sintetizadas las proteínas virales [41]. En el caso de los picornavirus, el proceso de transcripción es dependiente de una continua síntesis de proteínas virales [42], ya que la inhibición de la traducción provoca el bloqueo de la síntesis de mRNAs virales. Por tanto, estos dos procesos de biosíntesis de macromoléculas virales están estrechamente relacionados, así como la producción continua de lípidos y componentes de las membranas celulares [43].

La morfogénesis de las partículas virales en formación tiene lugar junto con la traducción y replicación del virus. La liberación de los nuevos virus se produce tras la lisis de la célula, como consecuencia de una alteración previa en la permeabilización de la membrana durante la fase tardía de la infección [44] (Fig. 3B). En los picornavirus, la viroporina 2B y su precursor 2BC son las responsables del aumento de la permeabilización debido a la formación de poros en las membranas celulares [45-47].

Los picornavirus, y en concreto poliovirus (PV), han sido una herramienta muy útil en el campo de la biología molecular y expresión génica. De hecho, un gran número de descubrimientos fueron realizados con PV, como por ejemplo, la detección de mRNAs sin estructura cap, la secuenciación y desarrollo de clones virales infectivos, el estudio de estructuras tridimensionales de partículas virales, la descripción de secuencias IRES, la síntesis de un virus infeccioso en un sistema in vitro o la síntesis química de un genoma viral completo, entre otros [48-53]. Asimismo el corte proteolítico del factor de inicio de la traducción eIF4G se observó por primera vez durante la infección de PV [48-53].

3. PROTEASAS DE PICORNAVIRUS

Los picornavirus codifican diferentes proteasas dependiendo de la especie viral, aunque es común en todas las especies la presencia de $3C^{pro}$ y su precursor $3CD^{pro}$. En PV, estas dos proteínas poseen actividad proteasa y son las responsables de la mayoría de eventos proteolíticos que tienen lugar durante el procesamiento de la poliproteína viral [34, 35, 54]. Aparte de estas dos proteasas, los picornavirus contienen el gen 2A, cuyo producto posee actividad proteolítica en algunas especies, tales como PV y rhinovirus (HRV). Su papel en el procesamiento de la poliproteína viral es limitado, estando más implicada en la alteración de diversas funciones celulares mediante el corte de diferentes proteínas. En este sentido, el evento

proteolítico mejor estudiado es el que se produce sobre los factores de iniciación de la traducción, y en concreto, el producido sobre el eIF4G [40, 41].

Algunas especies de picornavirus, además, codifican para una proteína *Leader* (L) situada delante de P1 [55]. En el caso de los aphtovirus, como FMDV (foot and mouth disease virus), la proteína L tiene actividad proteasa y es conocida como L^{pro}[56, 57]. L^{pro} es la primera proteína en ser sintetizada, de forma que su actividad autocatalítica la libera del resto de la poliproteína viral. Debido a que L^{pro} no desempeña un papel directo en la replicación viral [58] y su actividad proteasa tiene una función limitada en el procesamiento de la poliproteína viral, su función principal consiste en su interacción con la célula hospedadora [59-61].

Las proteasas $2A^{pro}$ y L^{pro} ejercen su actividad proteolítica sobre eIF4GI en una posición muy cercana [62-64], sin embargo, estas dos proteínas no poseen actividad proteolítica en todas las especies de picornavirus, como es el caso de EMCV [65]. En general, las proteasas se clasifican en relación a tres parámetros: i) su centro catalítico, ii) su especificidad por el sustrato y iii) su estructura tridimensional [40].

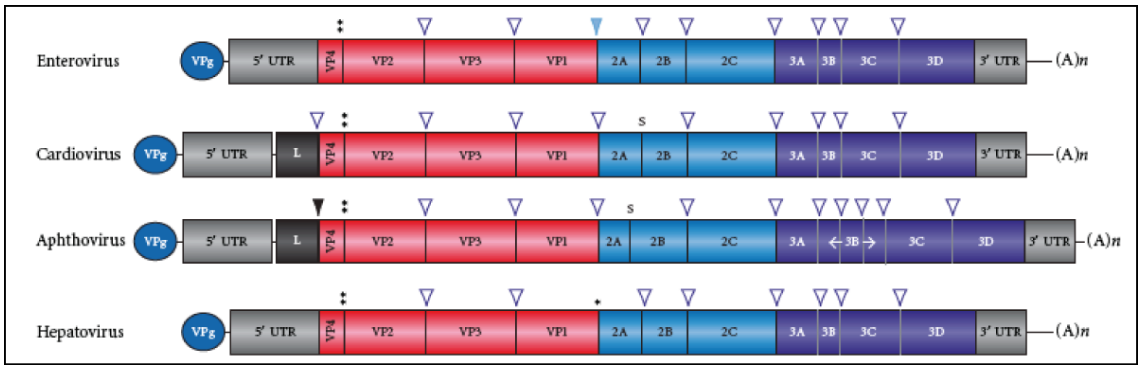

Figura 4. Estructura del genoma de diferentes miembros de la familia picornaviridae. Las flechas negras indican los sitios de corte de L^{pro}; la flecha azul indica el corte de la $2A^{pro}$; los dos asteriscos indican el sitio de corte entre los productos VP4-VP2; las flechas vacías indican los sitios de corte de la $3C^{pro}$. Adaptado de Castelló y col., 2011.

3.1. La proteasa 2A de PV

La proteasa 2A de PV, $2A^{pro}$, es una proteína formada por 149 aminoácidos que pertenece al grupo de las cisteín-proteasas [66]. $2A^{pro}$ es procesada autocatalíticamente en su extremo amino terminal entre la proteína de la cápsida VP1 y 2A [67]. Para identificar las secuencias de los sustratos que interaccionan con $2A^{pro}$ se utilizó el sistema del doble híbrido o "*yeast two-hybrid system"* [68]. Todas las secuencias identificadas contienen un motivo Leu-X-Thr-Z (donde X es cualquier aminoácido y Z es un residuo hidrofóbico) en las posiciones de P4 a P1, lo que sugiere la presencia de un sitio común de interacción de la $2A^{pro}$ en todos sus sustratos.

El evento proteolítico mejor caracterizado de la $2A^{pro}$ es el que efectúa sobre el factor eIF4G. El corte de eIF4G impide la interacción de los mRNAs con estructura cap con la subunidad ribosomica 40S [69]. $2A^{pro}$, sin la presencia de ningún factor adicional, cataliza la proteólisis de eIF4G entre los aminoácidos 681 y 682, lo que conlleva la separación de los factores eIF4E y eIF3 del extremo N-terminal (Nt) y C-terminal (Ct) del factor eIF4GI, respectivamente [70, 71]. Sin embargo, el hecho de que al purificar el factor eIF4G de extractos de células infectadas con PV no se co-purifique la $2A^{pro}$, sugiere que esta proteasa podría estar a su vez activando una proteasa celular que hidrolizaría el factor eIF4G [72]. También se ha sugerido que el factor eIF3 y alguna proteína celular no identificada hasta ahora, podrían estar actuando como cofactores de la 2A para llevar a cabo el corte de eIF4G [73]. En este sentido se ha sugerido que la infección de PV activaría dos proteasas celulares que, junto con la 2A, hidrolizarían el factor eIF4G [74]. Sin embargo, estas proteínas celulares no han sido identificadas y no existe ninguna otra evidencia a favor de esta hipotésis. Por otro lado, varios estudios han demostrado que la cinética de inhibición de la síntesis de proteínas celular y el corte de eIF4G no se correlacionan en células infectadas con PV [75-77].

La levadura *Saccharomyces cerevisiae* se ha utilizado para la obtención de variantes de $2A^{pro}$ [78]. El hecho de que esta proteasa sea muy tóxica para las levaduras ha sido aprovechado para la obtención de variantes carentes de esta citotoxicidad. Así, se han obtenido variantes de $2A^{pro}$ que han perdido su capacidad de cortar el factor eIF4G. La caracterización de estos mutantes reveló la presencia de una región implicada en la interacción con los sustratos, pero en ninguno de los mutantes estaba afectado el centro catalítico. Además, también se ha observado un paralelismo entre la habilidad de estas variantes de $2A^{pro}$ para bloquear la síntesis de proteínas y el corte de eIF4G [79]. Por otro lado, virus con mutaciones en $2A^{pro}$ que inhiben su capacidad catalítica en *trans* pero no en *cis*, poseen un procesamiento proteolítico normal de la poliproteína, mientras que no ejercen ninguna acción sobre eIF4G [80]. Sin embargo, la replicación del RNA de estos mutantes se ve alterada, lo que sugiere una correlación entre la replicación del RNA de PV y la actividad de $2A^{pro}$. Existe mucha controversia sobre cómo la $2A^{pro}$ puede contribuir o no a la replicación viral. A pesar de la presencia de una fracción de $2A^{pro}$ en las proximidades de los complejos replicativos, no se ha demostrado una implicación directa de la proteasa en el proceso de replicación viral [81].. Estudios más recientes demuestran que $2A^{pro}$ no es imprescindible para formar la progenie viral [82]. No obstante, $2A^{pro}$ juega un papel importante en la inducción del efecto citopático y evita la inhibición de la replicación del virus en células tratadas con interferón α (IFNα) [83].

Otro efecto observado en las infecciones con PV sobre la maquinaria de traducción celular es el corte de la proteína de unión a poli(A), PABP (Poly(A)Binding-Protein). Sin embargo, el corte que efectúa $2A^{pro}$ sobre PABP resulta ser ineficaz *in vivo* e *in vitro* [84].

Además del corte del eIF4G y su implicación con la replicación viral, se ha descubierto que la $2A^{pro}$ está involucrada directa o indirectamente en la alteración del complejo del poro nuclear (NPC, *Nuclear Pore Complex*) durante la infección con PV y HRV. Esta alteración del NCP, también puede ser prevenida *in vitro* con inhibidores de $2A^{pro}$ [85]. De hecho, esta perturbación del transporte núcleo-citoplasma, que podría ser debida a la hidrólisis de ciertas nucleoporinas, afecta al transporte de mRNAs, rRNAs y U snRNAs [86]. Además, la hidrólisis de las nucleoporinas podría actuar como un mecanismo de evasión de la respuesta inmune mediada por el IFN-γ [86].

Asimismo, en la presente tesis obtuvimos claras evidencias que demuestran la capacidad de la $2A^{pro}$ para conferir independencia del factor eIF2α a los IRES de PV y del EMCV [17]. Así, a tiempos tardíos de la infección con diversos picornavirus se producen proteínas virales cuando eIF2α se encuentra fosforilado [32, 87].

3.2. La proteasa L de FMDV

Varios picornavirus poseen el gen de la proteasa L^{pro}, la cual puede diferir considerablemente, tanto en relación a su tamaño como a su función, incluso entre virus del mismo género. Sólo la mitad de los picornavirus descritos poseen proteína L^{pro}, y de éstos, sólo la de los aftovirus y cardiovirus ha sido estudiada con más detalle.

Las proteínas L de aftovirus (FMDV) y erbovirus (ERBV) son cistein-proteasas de la superfamilia de las papaínas (*papain-like cisteine protease*) [57, 88]. Su actividad proteolítica les sirve para liberarse de la poliproteína viral en el extremo amino terminal. Una vez liberada, la L^{pro} de los aftovirus corta las dos isoformas del factor eIF4G, diferenciándose únicamente en siete aminoácidos del sitio de corte de la $2A^{pro}$ [89, 90], lo que se traduce en una inhibición de la traducción celular cap-dependiente, mientras la traducción viral se mantiene cap-independiente a través del IRES [62, 90, 91]. A partir del IRES de FMDV se producen dos formas de L^{pro}, la forma larga, denominada Lab^{pro} (de unos 200 aminoácidos) y la forma corta, denominada Lb^{pro} (de unos 170 aminonácidos). Ambas formas se diferencian en el extremo amino terminal, ya que la traducción comienza en diferentes sitios, separados por 84 nucleótidos [92, 93].

Al igual que la $2A^{pro}$, la L^{pro} también hidroliza el factor eIF4G, pero lo hace entre los aminoácidos 674-675. También se ha observado que PABP se hidroliza en las células infectadas con FMDV, y aunque se desconocen los sitios de procesamiento, se ha propuesto que L^{pro} podría llevar a cabo esta proteólisis.

Las dos proteínas sintetizadas, la Lab^{pro} y la Lb^{pro} , son activas durante la infección de FMDV [94], aunque la forma Lb es más abundante y ha sido mejor caracterizada. Estudios comparativos de secuencia sugieren que la forma corta no posee ningún motivo en el extremo

amino terminal lo suficientemente básico para actuar como señal nuclear. Si esto fuera cierto, la producción de ambas proteasas actuaría como mecanismo frente a las defensas del hospedador. De hecho, Lab^{pro} se localiza en el núcleo, donde produce la degradación de p65/RelA, una subunidad de NF-κB, y presumiblemente conlleva a una reducción de la respuesta inflamatoria durante la replicación del virus en el hospedador [95]. Además, mutantes de L^{pro} incapaces de degradar p65/RelA son aún capaces de hidrolizar el factor eIF4G, lo cual indica la existencia de diferentes mecanismos de actuación de la L^{pro} [60].

Se ha observado que virus defectivos en L^{pro} no replican eficientemente en los sitios primarios de infección y no son capaces de diseminar la infección a otros focos del hospedador. Además, aunque tanto los virus defectivos como los virus wt (Wild-type) inducen la producción de interferón alfa y beta (IFN-α/β) en cultivos tisulares, la actividad de dichos IFNs sólo se detecta en presencia del virus defectivo. Esto se explica porque sólo los virus con L^{pro} intacta son capaces de inhibir la traducción *cap* dependiente de los mRNAs de IFN, permitiendo por tanto, una rápida diseminación de la infección por el hospedador [96, 97]. Posteriormente se observó que esta inhibición de IFN mediada por L^{pro} se producía a nivel de la transcripción de IFN-β y de la traducción del mRNA de IFN-α/β [59]. Recientemente se ha propuesto que esta inhibición podría ser debida a la posible actividad deubiquitinasa de L^{pro} sobre diferentes moléculas involucradas en la vía de señalización del IFN-β[98].

4. IRES DE PICORNAVIRUS

Los IRES de picornavirus se han subdividido en cuatro clases, aunque recientemente se ha publicado la existencia de un nuevo tipo de IRES de picornavirus que no encajaría en los grupos ya descritos [99]. La clase I está representada por los IRES de PV y HRV (Fig. 5A), mientras que a la clase II pertenecen los IRES de FMDV y EMCV (Fig. 5B). La clase III contiene como especie representativa el virus de la hepatitis A (HAV) (Fig. 5C) y la clase IV incluye los IRES de picornavirus que poseen similitudes con el IRES del virus de la hepatitis C (HCV), siendo el más representativo el IRES del teschovirus porcino (PTV) (Fig. 5D).

4.1. IRES de Entero/Rhinovirus

Los IRES de tipo I tienen una longitud aproximada de 450 nucleótidos (nt) y su estructura secundaria ha sido ampliamente estudiada [100, 101]. Se caracterizan por un funcionamiento ineficiente en sistemas de traducción *in vitro* de lisados de reticulocitos de conejo (RRLs, *Rabbit Reticulocyte Lysate*). Sin embargo, se observó que la adición de extractos de células HeLa aumentaba la eficacia de la traducción del mRNA de PV en este sistema [102].

Esta observación permitió el descubrimiento de los factores activadores de IRES o ITAFs. Entre los ITAFs que inducen una estimulación funcional del IRES de PV se encuentran, entre otros, PTB (polypirimidine tract binding protein), PCBP2 (poly r(C) binding protein) y unr (upstream de N-ras) [100].

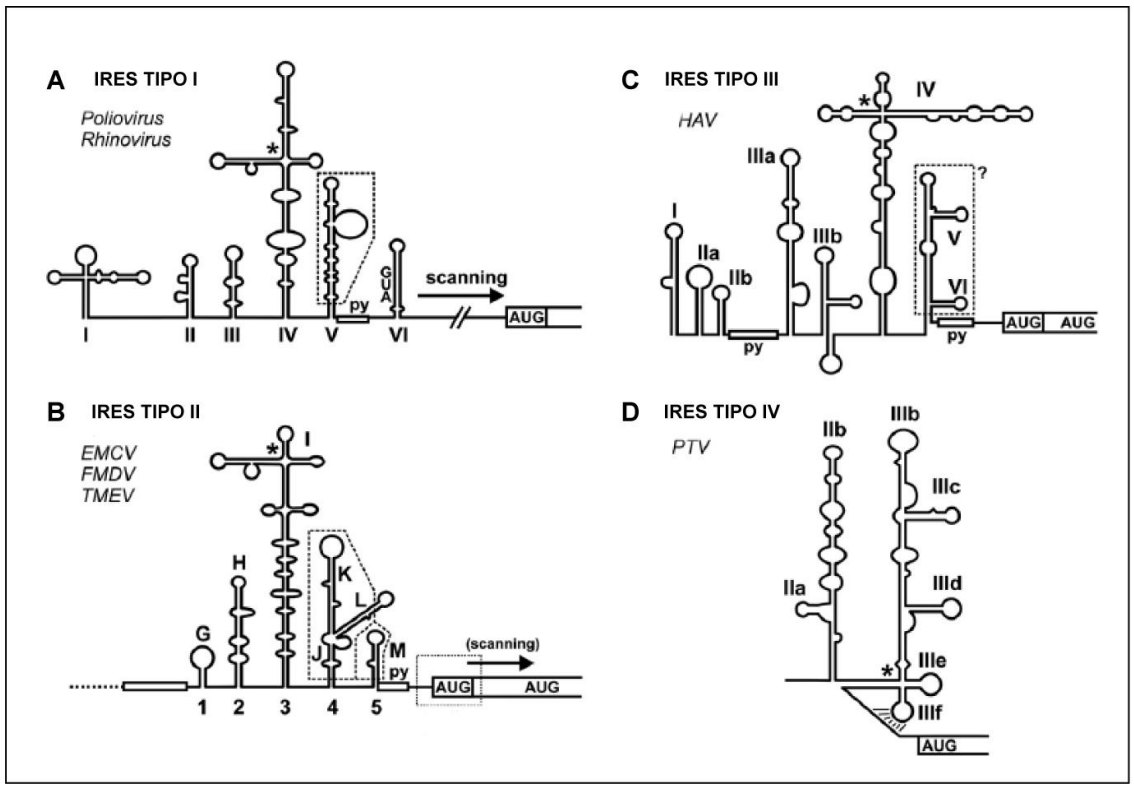

Figura 5. Estructuras IRES de picornavirus. Adaptado de Niepmann, 2009.

En cuanto al requerimiento de factores de inicio de la traducción de los IRES de tipo I, se ha descrito que son sensibles a mutantes dominantes negativos del factor eIF4A [103] y al hipuristanol, que es un inhibidor de este factor [104]. Esto indica que el factor eIF4A es necesario en la traducción del mRNA viral de PV y HRV. En cambio, la funcionalidad de estos IRES no se ve alterada por el corte del factor eIF4G [30, 40]. Además, es interesante destacar que la presencia de la proteasa $2A^{pro}$ de enterovirus estimula potentemente la traducibilidad de estos IRES [87, 105-109]. La $2A^{pro}$ induce el corte del factor eIF4G con la consecuente inhibición de la síntesis de proteínas celulares, sin embargo, estos dos procesos no parecen estar directamente relacionados con el efecto estimulante que ejerce la $2A^{pro}$ sobre el IRES. De hecho, la supresión de la traducción cap-dependiente mediante la inhibición del factor eIF4E no estimula la traducción viral [108]. Por otro lado, en el presente estudio demostramos que la traducción mediada por el IRES de PV se mantiene activa en presencia de $2A^{pro}$ cuando el factor eIF2 está fosforilado [17].

4.2. IRES de cardio/aphtovirus

Los IRES de tipo II también constan de aproximadamente 450 nt y entre ellos tienen una similitud de aproximadamente el 50%, siendo a su vez muy diferentes de los de enterovirus y rhinovirus. En contraste con el primer grupo, se observó que estos IRES funcionaban muy bien en RRLs sin necesidad de proteínas o extractos adicionales. El proceso de iniciación de la traducción dirigido por los IRES de tipo II y la implicación de los diferentes factores que intervienen, ha sido estudiado en detalle [110, 111]. Estos trabajos demostraron que el IRES de EMCV por sí solo no es capaz de formar un complejo de iniciación estable que se una a la subunidad 40S, aunque sin embargo, puede formar el complejo 48S en presencia de la región carboxilo terminal del eIF4G, los factores eIF4A, eIF3 y el complejo ternario eIF2/GTP/Met-tRNA. Otros estudios con el IRES de FMDV mostraron evidencias de que las proteínas PTB y Ebp1, se requieren para el correcto ensamblaje del complejo 48S [111]. Además, Ebp1 estimula la traducción mediada por estos IRES [112].

El requerimiento del factor eIF4A se confirmó posteriormente en varios estudios mediante el empleo de mutantes dominantes negativos [103] e inhibidores de dicho factor [113]. Asimismo, se ha observado que al igual que en el caso del IRES de PV, la traducción mediada por los IRES de EMCV y FMDV puede prescindir del factor eIF2 en las fases tardías de la infección [16].

4.3. IRES del virus de la hepatitis A

El IRES de HAV fue inicialmente caracterizado por Glass et al (1993) y Brown et al (1994) [114, 115]. Su estructura parece ser diferente a la de los otros tipos de IRES, teniendo una longitud de aproximadamente 750 nt y además comparativamente, la traducibilidad mediada por este IRES es mucho menor que la observada con el IRES de EMCV. A diferencia de los IRES de tipo II, el IRES de HAV puede ser estimulado tras la adición de extractos de células de hígado, pero no por extractos de células HeLa. Respecto a los factores implicados en la traducción mediada por este tipo de IRES, hasta el momento sólo se ha descrito que la presencia del complejo eIF4F intacto es esencial para la funcionalidad del IRES. [116-118]. Además, el ITAF La, que ejerce un efecto estimulante de la traducción del IRES de PV, en cambio inhibe la traducción mediada por el IRES de HAV. Asimismo, la interacción de la gliceraldehido-3-fosfato deshidrogenasa con el IRES de HAV también inhibe la actividad del mismo [119]. Al igual que para los IRES de tipo I, PTB y PCBP2 estimulan la función de este IRES [30].

4.4. IRES de picornavirus HCV-like

Finalmente, dentro del grupo de los IRES de picornavirus hay que nombrar aquellos IRES que poseen una estructura muy similar a la encontrada en el IRES del virus de la Hepatitis C (HCV). Este tipo de IRES se describió en el teschovirus porcino tipo 1 (PTV-1), siendo ésta la especie tipo, pero posteriormente se observaron características comunes en el IRES de otros picornavirus (simian virus 2, porcine enterovirus-8, simian picornavirus tipo 9 o el virus de la encefalomielitis aviar). Los estudios iniciales mostraron que el IRES de PTV-1 tiene una longitud de unos 405 nt y no requiere la expresión de secuencias codificantes para traducirse eficientemente en RRLs o en células tranfectadas [30], al contrario de lo que ocurre en el IRES de HCV [29]. Este IRES no se estimula por la co-expresión de la proteasa $2A^{pro}$ y por tanto tampoco por el corte del factor eIF4G y la subsecuente inhibición de la traducción cap-dependiente. Por otro lado, las secuencias de los IRES de los diferentes teschovirus están muy conservadas entre sí [120], no existiendo gran similitud con los demás tipos de IRES descritos anteriormente [121].

En cuanto al requerimiento de factores en el proceso de iniciación de la traducción, se ha observado, que al igual que el IRES de HCV, el IRES de PTV-1 no requiere ningún factor eIF4, ya que es capaz de formar el complejo 48S directamente con la subunidad 40S y con el complejo ternario eIF2-GTP-Met-tRNA [122].

4.5. OTROS TIPOS DE IRES

4.5.1. IRES de Flavivirus

Los miembros de la familia Flaviviridae son virus con envuelta lipídica que possen como genoma una molécula de RNA de cadena sencilla y polaridad positiva. A esta familia pertenecen el HCV, el virus de la diarrea viral bovina (BVDV) y el virus de la fiebre porcina clásica (CSFV). Todos ellos contienen un IRES en su 5´UTR (Fig. 6A). El virus prototipo de esta familia es HCV y el mecanismo por el cual lleva a cabo el reclutamiento de ribosomas es muy diferente al descrito en los picornavirus. El requerimiento de factores en la traducción mediada por el IRES de HCV ha sido investigado en detalle, observándose que el ensamblaje del complejo 48S ocurre en ausencia de los factores eIF4A, eIF4B y eIF4F [123, 124]. También se ha observado que el IRES de HCV puede traducirse en condiciones de estrés en las que disminuye la disponibilidad del complejo ternario eIF2-GTP-$tRNA_i^{Met}$ [125]. Recientemente se ha descrito que en esta situación de estrés el factor eIF2A juega un papel fundamental en la traducción del IRES de HCV [126]. Asimismo, se ha demostrado mediante ensayos *in vitro* que

el IRES de HCV puede unirse directamente a la subunidad 80S del ribosoma y comenzar la etapa de elongación en presencia de altas concentraciones de Mg^{++} [127].

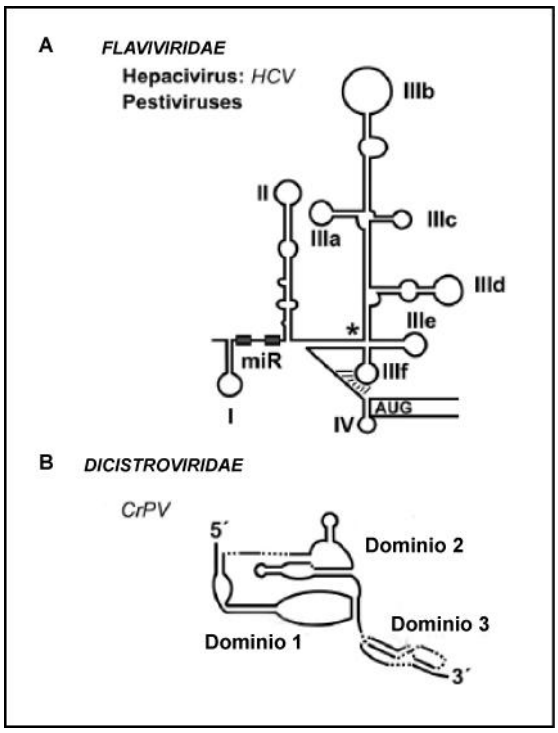

Figura 6. Representación esquemática de la estructura de los IRES de la familia *Flaviviridae* A) y *Dicistroviridae* B). Adaptado de Niepmann, 2009.

4.5.2. IRES de Dicistrovirus

La familia *Dicistroviridae* pertenece al orden Picornavirales y está constituida por virus que infectan insectos. Estos virus poseen un genoma lineal, no segmentado, de RNA de polaridad positiva que está organizado en dos grandes marcos de lectura abierta u ORFs (*Open Reading Frame*) , separados por una región intergénica (IGR). Cada uno de los ORFs posee un IRES en su extremo 5´. El primero se encuentra en la región 5´UTR y su funcionalidad se ha comprobado en multitud de sistemas de traducción, mientras que el segundo IRES está localizado en la región IGR y es el único IRES descrito que posee la habilidad de reclutar el ribosoma en ausencia de factores de iniciación y sin $tRNA_i^{Met}$ [128] (Fig. 6B). La total ausencia de factores de inicio de la traducción confieren a este IRES la capacidad de producir proteínas virales en condiciones extremas en la célula, como pueden ser elevados niveles de fosforilación del factor eIF2 o en situaciones de baja disponibilidad de aminoácidos [129]. Esta baja dependencia de factores de inicio de la traducción da muestra del gran nivel de adaptación del virus a la célula hospedadora.

4.5.3. IRES de Lentivirus

El género Lentivirus está compuesto por nueve especies de virus, entre los que se incluyen los virus de la inmunodeficiencia humana tipo-1 y 2 (HIV-1 y HIV-2) y el virus de la inmunodeficiencia felina (FIV). Su genoma está compuesto por una molécula de RNA de cadena sencilla y polaridad positiva, con una longitud de unos 9000 nt. Todos los mRNAs producidos por los lentivirus poseen una estructura cap en su extremo 5´ y una cola de poli(A) en su extremo 3´, de forma que están estructuralmente en disposición de traducirse de forma canónica, aunque existen muchas evidencias de que los lentivirus poseen la capacidad de traducirse de forma cap-independiente. Así, se sabe que las infecciones por lentivirus inducen, en un momento determinado de la infección, el arresto de la célula en la fase G2 del ciclo celular [130]. En este contexto aunque la traducción cap-dependiente no es viable, no se impide que exista una importante producción de poliproteína viral [131]. Además, en fases tardías de la infección la proteasa de HIV-1 induce el corte de determinados factores de inicio de la traducción como eIF4GI, eIF4GII y PABP [132-134]. En conclusión, la habilidad para traducirse bien mediante un mecanismo cap dependiente o bien a través del IRES, constituye para los lentivirus una sofisticada estrategia para asegurar de forma eficiente la síntesis de proteínas virales.

OBJETIVOS

Los objetivos propuestos en esta tesis doctoral han sido:

1. Estudiar el efecto de la proteasa $2A^{pro}$ de PV en la traducibilidad de mRNAs dirigida por diferentes IRES de Picornavirus cuando el factor eIF2α se encuentra fosforilado.

2. Analizar la importancia de la actividad proteolítica de $2A^{pro}$ así como la función de los productos generados tras la hidrólisis del factor eIF4GI en la traducibilidad de diferentes IRES de Picornavirus cuando el factor eIF2α se encuentra fosforilado.

3. Estudiar la traducción mediada por el IRES de HAV cuando el factor eIF4GI está hidrolizado por la acción de la proteasa L^{pro}.

4. Estudiar la traducibilidad del IRES de HAV en presencia de L^{pro} cuando los factores eIF2α y eIF4A están inhibidos.

MATERIALES Y MÉTODOS

1. MATERIAL BIOLÓGICO

1.1. Líneas celulares de mamífero.

En este trabajo se utilizaron las siguientes líneas celulares:

BHK-21 (clon BSR T7/5): células de riñón de hámster que expresan constitutivamente la RNA polimerasa del bacteriófago T7 (RNA pol T7). Seleccionables con el antibiótico G418. [135]. En esta tesis se han denominado BHKT7.

BHK-21(ATCC CCL 10): células de riñón de hámster

Huh7-T7: Células de hepatocarcinoma humano que expresan constitutivamente la RNA pol T7. Seleccionables con el antibiótico Zeomicina. En esta tesis se han denominado HuhT7

1.2. Bacterias.

Se utilizaron las siguientes cepas de *E.coli*:

DH5α [F^-, recA1, hsdR17, (rK^-, mK^-), LacZY, argF, U169, supE44, thi1, gyrA96, relA1] [136]. Esta cepa se transformó con los plásmidos descritos en esta tesis.

BL21 (DE3): estas bacterias contienen insertado como profago en la cepa BL21 [F^-, $ompT^-$, rB^-, mB^-, $recA^+$, $1on^-$, dcm^-] el gen de la RNA polimerasa del fago T7 bajo el control del promotor *lac UV*5 [137].

BL21 (DE3)pLys: estas células son lisógenos que expresan la lisozima del fago T7 (un inhibidor natural de la RNA polimerasa de este fago) a bajos niveles [138].

1.3. Plásmidos.

1.3.1. Plásmidos derivados de pTM1

pTM1: contiene el promotor para la RNA polimerasa del bacteriófago T7, seguido por la secuencia del IRES (Internal Ribosome Entry Site) del EMCV (Encefalomiocarditis virus),

que dirige la traducción independiente de *cap* del gen que se sitúa a continuación. Se requiere la expresión de la RNA pol T7 en las células transfectadas con estos plásmidos. Para ello, se utilizó la línea celular BHK-T7 y Huh-T7. Por otro lado este plásmido puede ser utilizado en una reacción de transcripción *in vitro* usando la RNA pol T7 purificada (*Promega*).

pTM1-Luc: Este plásmido posee el gen de la luciferasa de luciérnaga (*Photinus pyralis*) [87].

pTM1-2A^{pro}: Este plásmido posee el gen de la proteasa 2A de PV tras el IRES de EMCV [139, 140].

pTM1-2A(G60R): Este plásmido posee el gen de un mutante de la proteasa 2A de PV tras el IRES de EMCV [139, 140].

pTM1-2B: Este plásmido posee el gen de la proteína 2B de PV tras el IRES de EMCV [139, 141, 142].

pTM1-2C: Este plásmido posee el gen de la proteína 2C de PV tras el IRES de EMCV [139, 141, 142].

pTM1-2BC: Este plásmido posee el gen de la proteína 2BC de PV tras el IRES de EMCV [139, 141, 142].

pTM1-3A: Este plásmido posee el gen de la proteína 3A de PV tras el IRES de EMCV.

pTM1-3AB: Este plásmido posee el gen de la proteína 3AB de PV tras el IRES de EMCV.

pTM1-3C: Este plásmido posee el gen de la proteasa 3C de PV tras el IRES de EMCV. [139].

pTM1-3D: Este plásmido posee el gen de la polimerasa 3D de PV tras el IRES de EMCV.

pTM1-3CD: Este plásmido posee el gen de la proteína precursora 3CD de PV tras el IRES de EMCV.

pTM1-eIF4GInt: Este plásmido posee la secuencia del extremo amino terminal del factor eIF4GI [17].

pTM1-eIF4GIct: Este plásmido posee la secuencia del extremo carboxilo terminal del factor eIF4GI [17].

pTM1-Lb^{pro}: Este plásmido posee la secuencia de la proteasa Lb^{pro}.

1.3.2. Otros plásmidos.

pCDNA.3.1.IRES HAV-Luc: este plásmido posee el promotor para la RNA polimerasa del bacteriófago T7, seguido por la secuencia del IRES de HAV y, a continuación, el gen de la luciferasa de luiciérnaga. En esta tesis se ha denominado pHAV-luc. Este plásmido fue amablemente cedido por el Dr. Y.Kusov.

pCDNA.3.1.IRES PV-Luc: este plásmido posee el promotor para la RNA polimerasa del bacteriófago T7, seguido por la secuencia del IRES de PV y, a continuación, el gen de la luciferasa de luciérnaga. En esta tesis se ha denominado pPV-luc Este plásmido fue amablemente cedido por el Dr. Y.Kusov.

pT7 Rluc ΔEMCV IGR-Fluc: este plásmido posee el promotor para la RNA polimerasa del bacteriófago T7, seguido por la secuencia de la región intergénica (IGR) del CrPV y, a continuación, el gen de la luciferasa de luicérnaga. En esta tesis se ha denominado pIGR CrPV-luc. Este plásmido fue amablemente cedido por el Dr. P. Sarnow.

pKS-IRES FMDV-L^{pro}: este plásmido posee la secuencia completa del IRES de FMDV seguido de la secuencia de la proteasa L^{pro}.

1.4. Replicones

pRLuc31: contiene la secuencia completa del genoma de PV [143]. Fue amablemente prestado por el Dr. Y. Kusov.

1.5. Oligonucleótidos.

Oligonucleótido	Secuencia (5' →3')
3A 5´ NcoI	**GGCCGGCCATGGGACCACTCCAGTATAAAG**
3A 3´ BamHI	**GGGCCCGGATCCTTACTGGTGTCCAGCAAACAG**
3AB 5´ NcoI	**GGCCGGCCATGGGACCACTCCAGTATAAAG**
3AB 3´ BamHI	**GGGCCCGGA TCCTT A TTGT ACCTTTGCTGTCCG**
5´SpeI-FMDV L	**GGGACTAGTGGATCCTTGAAAGGGGGCGCTAGGGT**
3´XhoI-FMDV L	**GGGCTCGAGTGGAAGGCCAGCGTTCAGCG**
5′NcoI4GInt	**GCGCGCCCCATGGCCACGCCTTCTCAG**
3′BclI4GInt	**GCGCTGATCATTAGCCAAGGTTGGCCAAG**
5′EcoRI4GIct	**GCGCGCAAATTCGGACAACCCTTAGC**
3′BclI4GIct	**CCGCTGATCAGTTGTGGTCAGACTCCTCC**

Tabla 2. Oligonucleótidos empleados en las construcciones plasmídicas realizadas.

2. MATERIAL NO BIOLÓGICO

2.1. Sueros y anticuerpos.

Anti-eIF4GI: anticuerpo policlonal frente al factor de iniciación de la traducción eIF4GI. Se obtuvieron tras la inmunización de conejos con péptidos sintéticos derivados de la región C-terminal del factor 4GI humano, como se describe en la tesis de la Dra. Isabel Novoa [144]. Se utilizó a una dilución 1:1000 para western blot.

Anti-eIF2 Total: anticuerpo policlonal que reconoce específicamente la región correspondientes a los aminoácidos 1-315 del factor eIF2 humano. Se utilizó a una dilición 1:1000 para western blot. Fue adquirido de Santa Cruz *Biotechnology*.

Anti-eIF2 fosforilado: anticuerpo policlonal que reconoce específicamente el grupo fosfato de la Serina 51 de la subunidad α del factor de iniciación eIF2. Se utilizó a una dilución 1:500 para western blot. Fue adquirido de *Cell Signaling Technology*.

Anti-Luciferasa: suero de conejo inactivado que reacciona específicamente con la proteína luciferasa. Se obtuvo en nuestro laboratorio por el Dr. M.A. Sanz. Se utilizó en para western blot a 1:1000.

Anti-PKR: anticuerpo que reconoce la *protein kinase-R.* Fue amablemente cedido por el Dr. JJ. Berlanga. Fue utilizado para western blot a una dilución 1:500.

Anticuerpos secundarios: los anticuerpos secundarios conjugados a peroxidasa, utilizados en la técnica de western blot, fueron adquiridos a *Promega* y se utilizaron a una dilución 1:5000.

2.2. Compuestos e inhibidores.

Arsenito (Riedel-de Haën): compuesto químico que induce la fosforilación de la subunidad α del factor eIF2 a través de la quinasa HRI (Inhibidor Regulado por Hemina).

Tapsigargina (Sigma): compuesto químico que induce estrés en el retículo endoplásmico mediante la inhibición de la bomba Ca^{+2} –ATPasa. Como consecuencia se activa la quinasa PERK (PKR-like ER *kinase*).

Hipuristanol: es una molécula pequeña producida por el coral *Issis hippuris*. Posee la capacidad de inhibir el factor eIF4A, que es una helicasa que forma parte del complejo eIF4F. Este compuesto fue adquirido del Dr. J. Pelletier (Universidad McGill).

Geneticina (G418) (Sigma): antibiótico aminoglicósido de la misma familia que la gentamicina. Usado a una concentración de 2 mg/ml selecciona las células BHK-T7.

Zeocin™ (Invitrogen): es un antibiótico miembro de la familia de la bleomicina. Es un potente inhibidor de líneas celulares de mamíferos e insectos, así como de levaduras y bacterias. Actúa intercalándose y cortando el DNA. Se utilizó a una concentración 5 μM para seleccionar las células Huh-T7.

Ácido poliinosínico:polycitidílico (Poli I:C) (Amersham) : mimetiza un mRNA de doble cadena. Induce la fosforilación de la quinasa PKR, con la consiguiente fosforilación de la subunidad α del factor eIF2. Se emplearon 50 ng por reacción.

3. MANIPULACIÓN DE CÉLULAS BACTERIANAS

3.1. Medios de cultivo para *E. coli.*

Para el cultivo de *E. coli* se utilizó medio LB (Luria-Bertani) suplementado con 100 µg/ml del antibiótico ampicilina. Los cultivos de colonias en medio sólido se realizaron en el mismo medio con bacto-agar (*Difco)* al 1,5% y ampicilina (100 µg/ml). Los clones bacterianos se conservaron a -70ºC en medio LB suplementado con glicerol al 20% (v/v). La composición de estos medios viene detallada en el manual de protocolos de Sambrock y col. [145].

3.2. Transformación de *E. coli* por choque térmico.

Para transformar bacterias competentes, previamente se descongelaron durante 15 minutos en hielo. Posteriormente se mezclaron 100 µl de bacterias con 5 µl de β-mercaptoetanol y se añadió el DNA transformante y se incubaron en hielo 30 minutos. El choque térmico consistió en una incubación de 45 segundos a 42ºC. Seguidamente, las bacterias se enfriaron en hielo durante 2 minutos y se añadieron 900 µl de medio LB para volver a incubarlas 1 hora a 37ºC con agitación suave. Posteriormente se recogieron por centrifugación (3 minutos a 3000 rpm), se extendieron sobre una placa de LB-agar suplementada con el antibiótico correspondiente y se incubaron en una estufa a 37ºC durante toda la noche.

3.3. Purificación de DNA plasmídico.

En función de la cantidad de DNA que se desease obtener se utilizaron diferentes procedimientos. Para la obtención de pequeñas cantidades, con fines analíticos, se recurrió al *kit* comercial Wizard *Plus* SV Minipreps de *Promega*. Cuando se requirieron mayores cantidades se emplearon los *kits* comerciales de *Qiagen* y se siguieron las instrucciones de estos proveedores.

4. MANIPULACIÓN DE ÁCIDOS NUCLEICOS

4.1. Manipulación de DNA en procesos de clonación.

Para realizar las construcciones plasmídicas descritas en esta tesis se siguieron los métodos recomendados por las casa comerciales suministradoras de los enzimas de restricción

(*New England Biolabs*), de la DNA ligasa del bacteriófago T4 (*New England Biolabs*) y de la DNA polimerasa Taq (*Perkin Elmer*). Asimismo se utilizaron los protocolos del manual de laboratorio "*Molecular Cloning*" [145].

4.2. Electroforesis en geles de agarosa y extracción de DNA.

Los fragmentos de DNA se separaron mediante electroforesis en geles de agarosa del 0,8-2% (p/v), en función su tamaño, usando tampón de electroforesis TAE (Tris-acetato; EDTA). Tras la separación, se tiñó el gel con bromuro de etidio (5 mg/ml) y se visualizaron las bandas de DNA en un transiluminador con luz ultravioleta. La extracción de los fragmentos de DNA del gel de agarosa se llevó a cabo utilizando el *kit* comercial de purificación de banda de *Qiagen*.

4.3. Reacción en cadena de la polimerasa (PCR).

Las reacciones de PCR se realizaron en un volumen final de 50-100 µl con el tampón suiministrado por la casa comercial (Tris-HCl 10 mM; pH 8.0, KCl 50 mM, $MgCl_2$ 1,5 mM, gelatina al 0.01%), 0,5 µM de cada oligonucleótido iniciador, 200 µM de cada dNTP, 0,5-1 ng de DNA molde y 5 unidades (U) de DNA polimerasa Taq (*Perkin Elmer*). El programa estándar de amplificación fue el siguiente: 1 ciclo de 2 minutos a 92ºC, 30 ciclos de 35 segundos a 92ºC, 1 minuto a 50ºC, 2,5 minutos a 72ºC y un ciclo final de 2 minutos a 92ºC, 1 minuto a 50ºC y 15 minutos a 72ºC. Los productos amplificados se purificaron en columnas *Wizard PCR preps* (*Promega*).

4.4. Transcripción *in vitro.*

Para la reacción de transcripción se linealizó el DNA molde, previamente purificado (por el protocolo de *Qiagen*), con *Xho*I en el caso de los plásmidos pTM1, excepto para el plásmido pTM1-2A que se empleó el enzima *SalI*. En el caso del plásmido pHAV-Luc se linealizó con *NotlI*. El replicón pRLuc31 se linealizó con el enzima *MluI*. Para llevar a cabo la reacción se usó la RNA polimerasa del fago T7 (*Biolabs*) .La reacción se llevó a cabo en un volumen final de 50 µl con tampón de transcripción 5x (*Biolabs*), 0,5 mM de cada ribonucleótido trifosfato (A, C, U, de *Amersham*), 20 U de inhibidor de RNAasas (RNAsin, *Promega*), 3 µg de DNA molde y 80 U de RNA polimerasa. Para los plásmidos que no expresaban secuencias IRES, se añadió a la reacción el análogo del cap, $m^7G(5')ppp(5')G$ (*Bio Labs*), para obtener RNAs con la estructura cap en el extremo 5´, de forma que en estos casos se

redujo la cantidad de GTP a 0,25 mM y se añadió análogo de cap a 0,25 mM. Las reacciones se incubaron a 37ºC durante 2 horas.

4.5. Traducción *in vitro* en reticulocitos de conejo tratados con nucleasa (RRL, *rabbit reticulocyte lysates*)

El mRNA sintetizado *in vitro* y purificado (kit *Qiagen*) fue empleado en reacciones de traducción *in vitro* en extractos celulares. Las reacciones se realizaron a una temperatura de 30º C. Una vez pasado el tiempo requerido para el experiemnto las muestras se recogieron bien para medir actividad luciferasa o bien se realizó un marcaje metabólico. En el primer caso, se añadieron 50µl de buffer de lisis de luciferasa para parar las reacciones y, posteriormente, se midieron 5µl de muestra. En el segundo caso, para realizar un marcaje metabólico de las proteínas sintetizadas, se prepararon las mezclas de reacción en ausencia de metionina y cisteína y suplementándolas, en su lugar, con 2 µCi de la mezcla *translabel* (*Amersham*), constituida por dichos aas marcados con el isótopo [S^{35}] ([S^{35}]-metionina y [S^{35}]-cisteína). Al finalizar el tiempo de incubación se añadió a cada muestra tampón de carga para proteínas (2% SDS, 11,6% glicerol, DTT 0,1M y azul de bromofenol al 0,033%) y se analizaron las muestras por SDS-PAGE, fluorografía y autorradiografía.

5. MANIPULACIÓN DE PROTEÍNAS

5.1. Electroforesis en geles de poliacrilamida.

Las muestras de proteínas se analizaron mediante electroforesis en geles de poliacrilamida en condiciones desnaturalizantes (SDS-PAGE) [145]. De forma rutinaria, se utilizaron geles con un porcentaje de acrilamida del 15%, si bien se usaron geles del 10% para separar proteínas de alto peso molecular y del 17,5% para proteínas de bajo peso molecular.

5.2. Fluorografía.

Las muestras de proteínas marcadas radiactivamente con [^{35}S]Met/Cys y separadas mediante SDS-PAGE se sometieron a la fluorografía. Los geles se fijaron en una mezcla de ácido acético al 7.5% y etanol al 20% en agua durante 15 minutos. Se lavaron abundantemente con agua y por último se sumergieron en una solución de salicilato sódico 1 M durante 1 hora. Tras el tratamiento fluorográfico, los geles se secaron sobre papel *Whatman* 3MM a 80ºC y al vacío en un secador de geles y se expusieron en películas autorradiográficas.

5.3. Inmunodetección de proteínas mediante *western blot.*

Las proteínas se separaron mediante SDS-PAGE y se electrotransfirieron a una membrana de nitrocelulosa (*Bio-Rad*) en tampón de transferencia (Tris-HCl 25 mM; pH 8.3, glicina 190 mM, metanol al 20% y SDS al 0,1%) a un amperaje de 200 mA durante 15 horas aproximadamente (Harlow y Lane. 1988). La membrana de nitrocelulosa se saturó con una solución de leche desnatada en polvo o con albúmina de suero bovino (BSA) purificada, al 5% en tampón PBS o TBS durante una hora con agitación suave. A continuación se añadió el anticuerpo primario a la dilución adecuada y se incubó durante al menos 2 horas con agitación suave. En algunos casos se incubó el anticuerpo primario durante toda la noche. Después de esta incubación se realizaron tres lavados sucesivos de 15 minutos cada uno con tampón TPBS o TTBS (Tween-20 al 0,05% en tampón salino PBS o TBS, respectivamente) y después se incubó la membrana con el anticuerpo secundario correspondiente conjugado a peroxidasa, a una dilución 1:5000 en TPBS o TTBS durante una hora. Una vez realizados tres nuevos lavados, se procedió al revelado utilizando el sistema comercial ECL (*Amersham Biosciences*) o *Supersignal westFemto Maximum Sensitivity Substrate* (*ThermoScientific*). Finalmente, las membranas se expusieron en una película autorradiográfica.

Para la reutilización de la membrana de nitrocelulosa con otro anticuerpo ("stripping"), se incubó la membrana con un tampón de lavado (Tris-HCl 62,5 mM; pH 6.7, SDS al 2% y β-mercaptoetanol 100mM) durante 30 minutos a 55ºC (con agitación). Posteriormente se realizaron varios lavados de 30 minutos con Tween-20 al 0,05% en tampón salino PBS o TBS y se procedió nuevamente a la saturación de la nitrocelulosa, continuando con el protocolo descrito anteriormente.

5.4. Medida de la actividad luciferasa

La actividad luciferasa (de *Photinus pyralis*) se midió usando el kit comercial *Luciferase Assay System* (*Promega*) y 5µl de muestra en un luminómetro *Monolight 2010* (*Molecular Dynamic*). La representación de las mediciones de actividad luciferasa en gráficas se realizó tomando tres mediciones independientes de, al menos, tres experimentos. Las barras de error representan la desviación estándar obtenida.

6. MANIPULACIÓN DE CÉLULAS EUCARIOTAS

6.1. Medios de cultivo para células de mamífero.

Para cultivar las distintas líneas celulares de mamífero se utilizó medio mínimo de Eagle modificado por Dulbecco (DMEM de *Difco*) [146] suplementado con suero fetal de ternera (*Flow)* al 5% o al 10% (v/v), 50 U/ml de penicilina, 50 U/ml estreptomicina y 0,2 mg/ml del éster butírico del ácido p-hidroxibenzoico (*Sigma)*. Además, se añadieron aminoácidos no esenciales y glutamina 4 mM (*Merck*). Las células BHK-21 que expresan la RNA pol T7 constitutivamente deben seleccionarse con el antibiótico G418 a una concentración final de 2 mg/ml cada tres pases. En el caso de las células Huh-T7, las células se sleccionas añadiendo al medio de cultivo Zeomicina al 5%. Las células se conservaron en nitrógeno líquido en DMEM con suero fetal de ternera al 20% y dimetilsulfóxido (DMSO) al 7% como agente crioprotector. Los marcajes metabólicos de proteínas con [S^{35}] Met/Cys se realizaron en medio DMEM sin metionina ni cisteína.

6.2. Transfección de células con lipofectaminas.

Este método se empleó para la expresión transitoria de proteínas virales a partir de plásmidos que contienen el promotor de la RNA pol T7. Para ello se empleó como transfectante la lipofectamina 2000 (*Invitrogen*). Se sembraron las células el día anterior con medio DMEM sin antibióticos ni antimicóticos de tal forma que las células estuvieran a una confluencia de 85-90% en el momento de la transfección. Para preparar la mezcla de transfección se mezclaron 1 µg de DNA diluido en 50 µl de Opti-Mem (*Invitrogen)* y 2µl de lipofectamina 2000 en 50 µl de Opti-Mem. En el caso de las co-transfecciones, se mezcló 1 µg de cada plásmido. Se incubaron durante 20 minutos a temperatura ambiente y, posteriormente, se añadió a las células, gota a gota, sobre 200 µl de Opti-Mem. Se dejó actuar durante 2 horas en el caso de las BHK-T7 y 3 horas en el caso de las Huh-T7, transcurridas las cuales se retiró la mezcla de transfección y se dejaron incubando las células en medio normal el tiempo necesario según el estudio. Para transfectar mRNA se empleó el mismo procedimiento con las concentraciones adecuadas de mRNA.

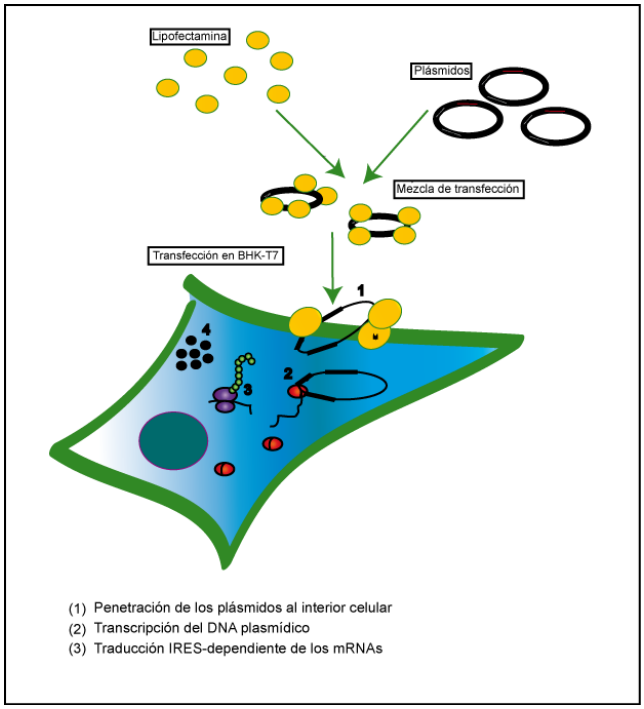

Figura 6. Representación esquemática del método de transfección con Lipofectamina.

6.3. Electroporación de células con RNAs sintetizados *in vitro.*

La electroporación de células de mamífero es una técnica utilizada para introducir RNAs recombinantes, con el fin de estudiar el efecto de la expresión de diferentes proteínas virales. El protocolo seguido fue el descrito por Liljeström y col. [147] con algunas modificaciones. Los RNAs se obtuvieron por transcripción *in vitro* como se describe en el apartado 4.4. Se utilizaron células BHK-21, las cuales crecieron activamente hasta alcanzar un grado de subconfluencia, para lo cual se sembraron 24 horas antes. Se levantaron con tripsina y se centrifugaron (2 minutos a 2000 rpm). Se lavaron con 3 ml de PBS (phosphate-buffered saline) frío y tras una nueva centrifugación se resuspendieron en un volumen de PBS adecuado para conseguir una concentración celular de 2.5×10^6 células/ml. La electroporación se llevó a cabo a temperatura ambiente añadiendo una alícuota de la mezcla de transcripción (50 µl) a 0,4 ml de células. La mezcla resultante se transfirió a una cubeta de electroporación de 0,2 cm (*Bio-Rad*) y se realizaron 2 pulsos consecutivos (1500 V, 25 µF y R= ∞) en el electroporador (*Gene Pulser* de *Bio-Rad*). Las células electroporadas se diluyeron en medio de cultivo (0,7 ml) y se centrifugaron. Posteriormente se resuspendieron en el volumen deseado de medio de cultivo y se sembraron en placas multipocillos.

6.4. Marcaje metabólico de proteínas.

El marcaje radiactivo de proteínas se realizó incubando las células en placas de L-24 con 200 µl de medio DMEM sin metionina ni cisteína suplementado con 1 µl de la mezcla [^{35}S] durante el tiempo necesario del experimento. Posteriormente las células se recogieron en tampón de carga de proteínas (SDS al 2%; pH 7.2, glicerol al 11,6%, DTT 100 mM, Tris-HCl 160 mM; pH 6.8 y azul de bromofenol al 0,03%) y se hirvieron a 95ºC durante 4 minutos. El análisis de proteínas se realizó mediante SDS-PAGE, fluorografía y autorradiografía.

RESULTADOS

1. TRADUCCIÓN EN AUSENCIA DEL FACTOR eIF2α PROMOVIDA POR LA PROTEASA 2A DE PV

Las células eucariotas presentan mecanismos de defensa que pueden ser activados en respuesta a diferentes tipos de estrés. La infección por virus es una de las causas de activación de estos mecanismos defensivos. Uno de los más importantes es la fosforilación del factor eIF2α, y la consecuente inhibición de la traducción cap-dependiente. En el caso de virus con secuencias IRES, como CrPV, HCV o CSFV, se ha descrito que la traducción de sus mRNAs tiene lugar de una manera eIF2α-independiente [125, 126, 129, 148]. Algunos picornavirus también son capaces de producir sus proteínas virales cuando eIF2α no está disponible a tiempos tardíos de la infección [16]. Este es el caso de PV, que induce la fosforilación del factor eIF2α durante la infección [149, 150]. En la presente tesis estudiaremos el mecanismo por el cual el genoma de PV es capaz de traducirse cuando eIF2α está fosforilado [17, 32].

1.1. Fosforilación del factor eIF2α en la replicación de PV

La traducción de algunos mRNAs virales en el contexto de la infección requiere determinados eIFs, que pueden ser diferentes a los que se necesitarían para la traducción de los mismos mRNAs *in vitro* o en células transfectadas [13, 14, 129]. Este es el caso del mRNA 26S del virus Sindbis, que no requiere de los factores eIF4GI o eIF2α para traducirse en células infectadas, pero sí para iniciar la síntesis de proteínas en lisados celulares [15].

Aunque la idea de que los picornavirus necesitan el factor eIF2α para iniciar la traducción de sus mRNAs está aceptada, existen evidencias que demuestran que este factor se encuentra fosforilado e inactivo a tiempos tardíos de la infección. Para estudiar si la traducción de PV puede tener lugar en presencia del factor eIF2α inactivo, analizamos la síntesis de proteínas virales a diferentes tiempos y en paralelo comprobamos el estado de fosforilación del factor eIF2α. Para ello utilizamos el replicón de PV pRLuc31 (Rep PV) que se caracteriza porque contiene el gen de la luciferasa (luc) en lugar de la secuencia de las proteínas estructurales. Además, el plásmido del que deriva este replicón posee el promotor de la polimerasa del fago T7 delante de la secuencia del IRES de PV (Figura 8A). Así, una vez transfectado este plásmido en células BHKT7, que son células que expresan constitutivamente la RNA polimerasa del fago T7, se producen grandes cantidades de mRNAs pertenecientes al Rep PV.

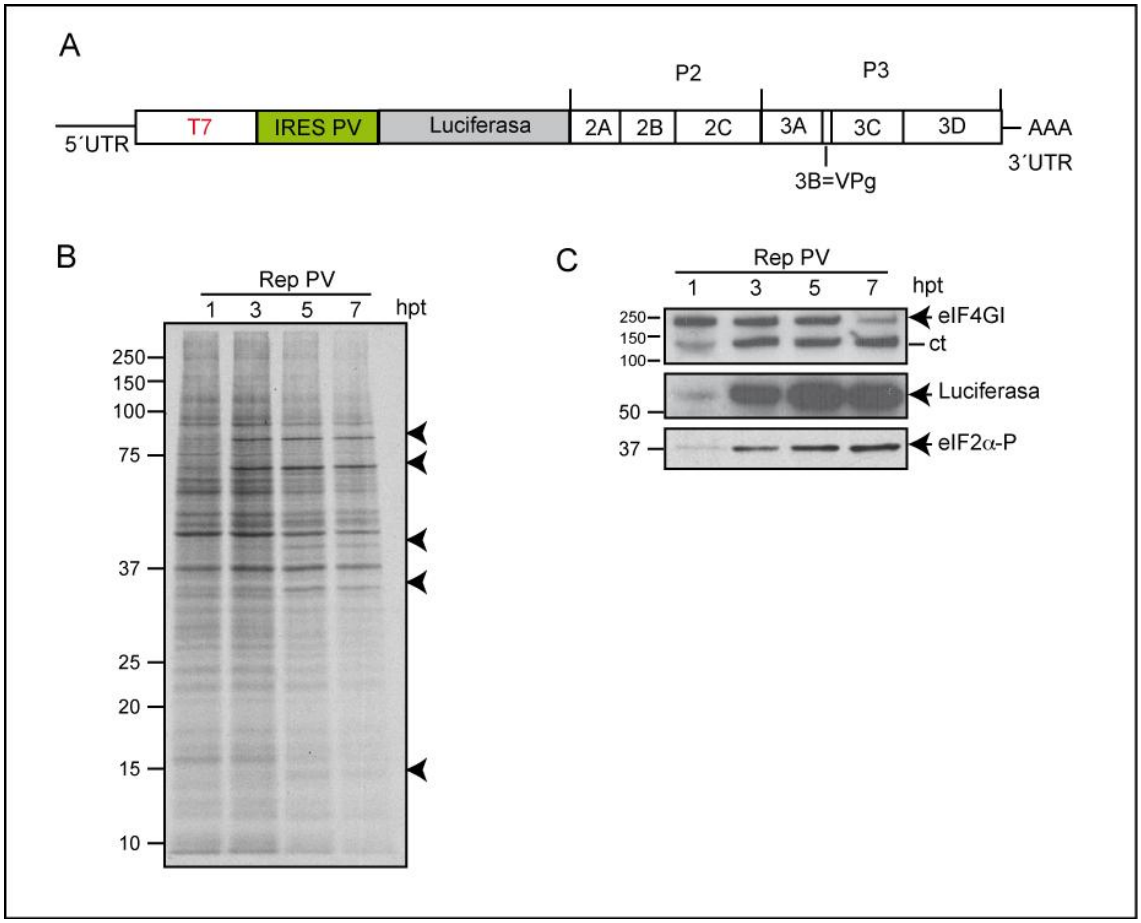

Figura 8. Replicación de PV a partir del Rep PV en células BHK-T7. Se transfectaron células BHK-T7 con el plásmido pRLuc31. A diferentes hpt se realizó un marcaje metabólico de proteínas con [^{35}S]Met/Cys durante 45 min. Finalmente, las muestras se procesaron mediante SDS-PAGE, fluorografía y autorradiografía. A) Representación esquemática del replicón de PV. B) Autorradiografía de las proteínas sintetizadas a las diferentes h.p.t. A las 3 h.p.t pueden detectarse proteínas virales (◀). C) En paralelo las muestras se analizaron mediante western blot utilizando diferentes anticuerpos frente a eIF4GI, eIF2α-P y luciferasa.

Tras transfectar las células con Rep PV se analizó la síntesis de proteínas a las 1, 3, 5 y 7 horas post-transfección (hpt) mediante un marcaje radioactivo con [^{35}S]-Met/Cys. Las células se recogieron y posteriormente se procesaron mediante SDS-PAGE, fluorografía y autorradiografía (Figura 8B). Las proteínas virales se pueden detectar a partir de las 3 hpt, y su síntesis aumenta a lo largo del tiempo. Además las muestras se analizaron mediante Western blot con diferentes anticuerpos. Por una parte, como control indirecto de la replicación de Rep PV, se analizó la cantidad de luc acumulada a las diferentes hpt usando anticuerpos específicos. En la figura 1C se puede observar que la cantidad de luc aumenta a lo largo del experimento, dando una medida indirecta del nivel de replicación viral. Por otra parte, también se analizó el corte del factor eIF4GI (Fig. 8C). El procesamiento proteolítico de eIF4GI incrementa con el tiempo. Así, el eIF4GI completo disminuye a la vez que se detecta el aumento del producto catalítico correspondiente a su extremo carboxilo terminal (Ct). A las 7 horas hpt prácticamente la totalidad del eIF4GI está cortado, aunque todavía una pequeña proporción del mismo es detectable, presumiblemente debido a que el porcentaje de transfección no fue del 100%.

El estado de fosforilación del factor eIF2α, se analizó mediante Western blot con anticuerpos que reconocen específicamente la forma fosforilada de este factor (Figura 8C). La cantidad de eIF2α fosforilado aumenta con el tiempo así como la inhibición de la síntesis de proteínas celulares (Figura 8B). Por tanto, estos datos nos indican que la traducción de PV tiene lugar en condiciones en las que eIF2α está fosforilado (de 3 a 7 hpt.).

1.2. Traducción temprana y tardía del replicón de PV.

A partir de este resultado, establecimos la hipótesis de que PV podría tener diferentes requerimientos del factor eIF2α según la etapa del ciclo viral. Así, eIF2α sería necesario para el comienzo de la síntesis de proteínas virales en la fase temprana de la infección, mientras que podría ser dispensable para el virus a tiempos tardíos, cuando la síntesis de proteínas celulares ha sido inhibida y sin embargo la síntesis de proteínas virales es máxima. Para testar esta posibilidad, estudiamos la traducción de PV en su fase temprana y en su fase tardía. Para estudiar la traducción de PV durante la fase temprana empleamos el mRNA Rep PV que fue obtenido mediante transcripción *in vitro* del correspondiente plásmido previamente linealizado. Para inactivar el factor eIF2α utilizamos Arsenito (Ars), un compuesto comúnmente utilizado que induce estrés oxidativo y fosforilación de eIF2α [125, 151, 152]. Como control negativo utilizamos un mRNA con estructura cap seguido de la secuencia de la luc (mRNA cap-luc). La traducción de este mRNA será inhibida al no disponer de eIF2α activo. Por otro lado, como control positivo utilizamos un mRNA CrPV IGR-luc, que expresa el gen de luc dirigido por la región intergénica (IGR) de CrPV, que le confiere la capacidad de traducirse en presencia de eIF2α inactivo (Fig. 9A). Para recrear las fases iniciales de la infección, llevamos a cabo una electroporación con los diferentes mRNAs. A tiempo cero post electroporación (hpe), tratamos las células con diferentes concentraciones de Ars (0, 50, 100 ó 200 μM) durante una hora y posteriormente recogimos las células para medir la actividad luc. La electroporación de estos mRNAs en las células BHK-21 conduce a la síntesis de luc desde el comienzo de la transfección, de forma que consideramos que se están traduciendo en condiciones similares a las que tienen lugar en el inicio de la infección. Podemos observar que en el caso del mRNA Rep PV, la traducción de luc es drásticamente bloqueada por el tratamiento con Ars al igual que ocurre en el caso del mRNA cap-luc, mientras que en el caso del mRNA CrPV IGR-luc, sólo se observa una ligera inhibición del 20% aproximadamente respecto a la traducción de luc en ausencia de Ars (Fig. 9B).

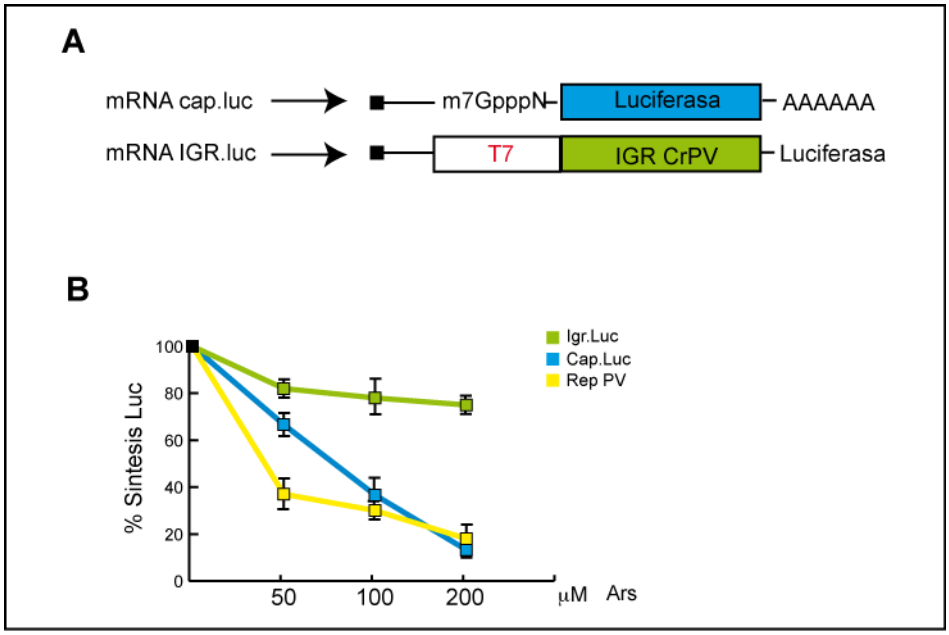

Figura 9. Efecto de la fosforilación del factor eIF2α inducida por Ars en la traducción del Rep de PV a tiempos tempranos. Se obtuvieron los mRNAs del Rep de PV, cap-luc y CrPV IGR-luc mediante transcripción *in vitro* con la polimerasa del fago T7. Posteriormente se electroporaron células BHK-21 con los mRNAs y se sembraron en DMEM con 10% de SFT y diferentes concentraciones de Ars (0, 50, 100, 200) durante una hora. Después se recogieron las células y se midió la actividad luciferasa. A) Representación esquemática de los mRNAs controles cap-luc y CrPV IGR-luc. B) Gráfica que representa los valores de síntesis de luciferasa de los diferentes mRNAs. Las barras de error representan la desviación estándar (D.E.) obtenida de tres medidas de cada muestra de dos experimentos independientes.

A continuación, utilizamos el mismo tratamiento con Ars para estudiar la traducción de PV a tiempos tardíos de infección. Para ello electroporamos el mRNA Rep PV en células BHK-21 y a las 7 hpe pre-tratamos las células durante 15 minutos con 400µM de Ars para inducir la fosforilación del factor eIF2α previamente al marcaje metabólico de proteínas. Seguidamente se retiró el medio y se añadió el medio de marcaje radiactivo con las concentraciones correspondientes de Ars, e incubamos durante una hora. En este caso no medimos actividad luc porque la alta cantidad de luc acumulada durante las 7 horas anteriores no nos permitiría observar claramente el efecto del Ars. Por esto, las células se recogieron y se procesaron mediante SDS-PAGE, fluorografía y autorradiografía (Figura 10A).

En la figura 3A se observa que el tratamiento con Ars inhibe la síntesis de proteínas celulares aproximadamente en un 90%, mientras que la síntesis de proteínas virales no está afectada, y se mantiene estable incluso con las concentraciones más altas de Ars. Asimismo, el aumento en la concentración de Ars, produce un defecto en el procesamiento de la poliproteína viral, que se manifiesta en un acúmulo de productos de reducida movilidad electroforética. Este efecto ha sido descrito previamente y podría indicar que altas dosis de Ars afectan la actividad proteasa de PV $2A^{pro}$ y $3C^{pro}$ [32].

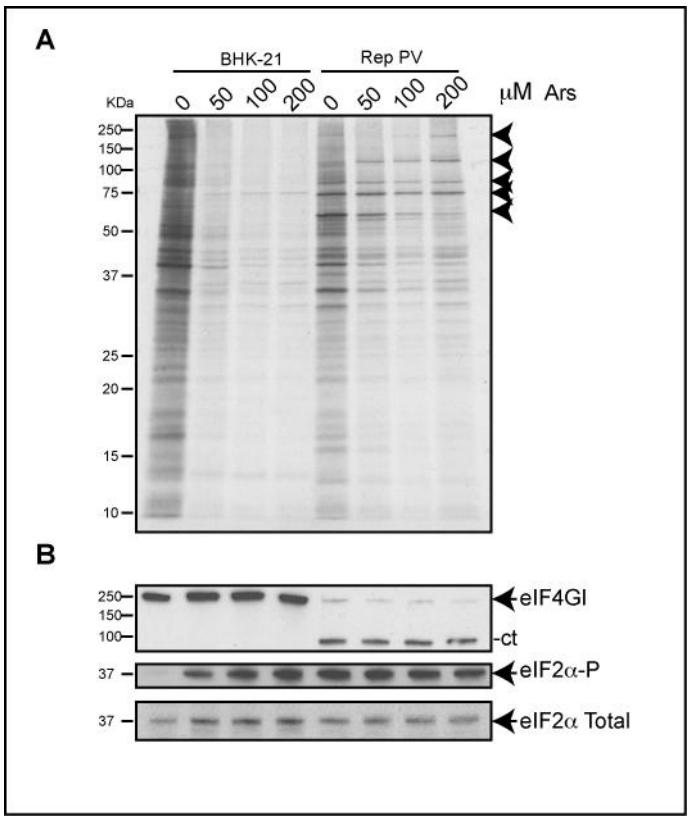

Figura 10. Efecto de la fosforilación de eIF2α inducida por Ars en la síntesis de proteínas de PV a tiempos tardíos. A) Se electroporó el mRNA obtenido a partir de la transcripción *in vitro* del plásmido pRLuc31. A las 7 hpe las células se trataron con diferentes concentraciones de Ars y se realizó un marcaje de proteínas con [^{35}S]Met/Cys durante 45 min. Las muestras se procesaron mediante SDS-PAGE (17,5%), fluorografía y autorradiografía. Las puntas de flecha (◀) indican las proteínas virales. B) En paralelo eIF4GI, eIF2α-P y eIF2α total fueron detectados mediante western blot.

Las mismas muestras se analizaron mediante western blot para comprobar el corte de eIF4GI y el estado de fosforilación de eIF2α tras el tratamiento con Ars. Como se observa en la Fig. 3B el tratamiento con Ars induce la fosforilación de eIF2α en las células control. En las células que expresan el Rep PV el estado de fosforilación de eIF2α es máximo incluso en ausencia de Ars (Fig. 10B, panel intermedio). Esto indica que el Rep PV induce potentemente la fosforilación del eIF2α total en la célula así como el corte de eIF4GI a tiempos tardíos (7 hpe). Estos resultados demuestran que el mRNA de PV puede traducirse de una forma dual en cuanto a los requerimientos del factor eIF2α, de forma que a tiempos tempranos y antes de que ocurra la replicación viral, eIF2α es requerido para traducir el RNA de PV, mientras que este factor es dispensable a tiempos tardíos cuando la síntesis de proteínas virales está ocurriendo a niveles máximos.

1.3. Estudio del papel de las proteínas no estructurales de PV en la traducción

Puesto que el Rep PV no posee la secuencia de las proteínas estructurales, decidimos estudiar si alguna de las proteínas no estructurales por sí misma es capaz de conferir traducibilidad a los mRNAs virales cuando eIF2α está fosforilado. Para analizar esta posibilidad, utilizamos de nuevo el sistema basado en células BHK que expresan de forma

estable la RNA polimerasa del fago T7 (BHK-T7). Esta polimerasa no tiene capacidad para incorporar cap en los mRNAs, por ello se usa en combinación con plásmidos que contienen, detrás de la secuencia promotora para la polimerasa, la secuencia de un IRES de picornavirus. De este modo, a partir de los plásmidos transfectados se sintetizan grandes cantidades de mRNAs en el citoplasma celular que son eficazmente traducidos mediante un mecanismo mediado por el IRES. Como método de transfección se utilizó lipofectamina, con la cual obtenemos una eficiencia de transfección que oscila entre el 80-100% (ver Figura 7 en la sección materiales y métodos).

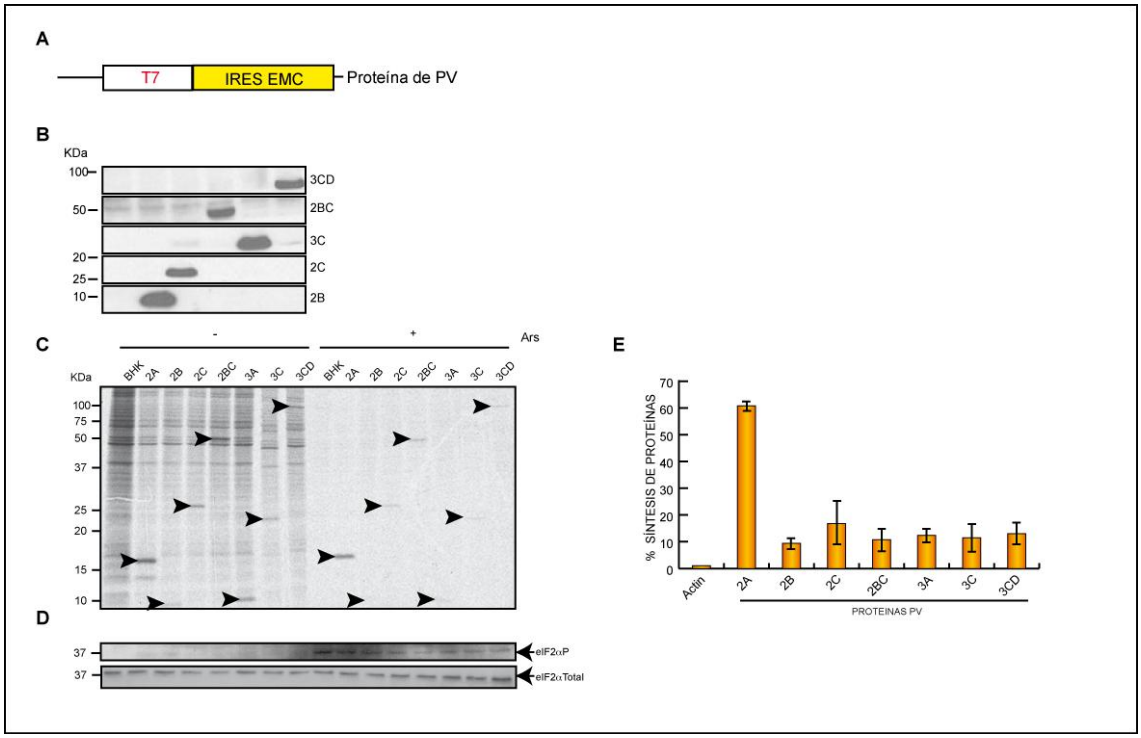

Figura 11. Expresión individual de las proteínas no estructurales de PV. A) Representación esquemática de los diferentes plásmidos pTM1 que contienen la secuencia de las proteínas no estructurales de PV. B) Detección de las proteínas de PV a las 3 hpt mediante western blot. C) Efecto del Ars sobre la traducción de las proteínas no estructurales de PV. Las células BHK-T7 fueron transfectadas con los correspondientes plásmidos. A las 3 hpt se pretrataron con Ars durante 15 min y posteriormente se realizó un marcaje radiactivo de proteínas con [^{35}S]Met/Cys durante 45 min en presencia (+) o ausencia (-) de Ars. Las muestras fueron procesadas por SDS-PAGE (17,5%), fluorografía y autorradiografía. D) Una alícuota de las mismas muestras se usó para analizar el eIF2α-P y eIF2α total mediante western blot. E) El porcentaje de síntesis de actina y de las proteínas de PV de las muestras tratadas con Ars respecto al de las no tratadas se cuantificó mediante densitometría de las bandas correspondientes (puntas de flecha ➤). La gráfica muestra la media de tres experimentos independientes. Las barras de error indican la D.E.

Para expresar las diferentes proteínas no estructurales de PV utilizamos el sistema de expresión pTM1-"proteína de PV" que posee el gen promotor de la polimerasa T7 seguido del IRES de EMC y a continuación contiene la secuencia de la proteína de PV a estudiar (Fig. 11A).

La expresión de las proteínas virales se confirmó primero mediante western blot, aunque no pudimos detectar por esta técnica las proteínas 2A^{pro} ni 3A, ya que no disponemos de anticuerpo específico para ellas (Fig.11B). A continuación, transfectamos cada plásmido por separado y a

las 3 hpt pre-tratamos las células BHK-T7 durante 15 minutos con Ars para inducir la fosforilación del factor eIF2α antes de realizar el marcaje radiactivo. En la figura 4C se observa que todas las proteínas de PV expresadas pueden ser claramente detectadas cuando las células no están expuestas al tratamiento con Ars. Sin embargo, sólo la proteína $2A^{pro}$ mantiene un elevado nivel de síntesis cuando el factor eIF2α está fosforilado (Fig. 11C y 11E).

En paralelo verificamos la foforilación del factor eIF2α analizando las mismas muestras mediante western blot (Fig. 11D). Para cuantificar los niveles de síntesis de proteínas y su inhibición tras el tratamiento con Ars, realizamos un análisis densitométrico de las bandas correspondientes a las proteínas de PV y a una proteína celular (actina) (Fig. 11E). La traducción de actina se inhibió un 90%, mientras que la síntesis de $2A^{pro}$ sólo se inhibió un 35%. La inhibición del resto de las proteínas estructurales también fue elevada (alrededor del 80%) siendo prácticamente indetectables las proteínas 2B, 3A y 3C (Fig. 11C y 11E).

Por tanto, la expresión de una única proteína, la proteasa $2A^{pro}$, puede conferir independencia del factor eIF2α en la traducción mediada por un IRES de picornavirus.

La infección con PV induce una degradación parcial así como la fosforilación de la proteína kinasa R (PKR). La activación de PKR a su vez correlaciona con el aumento en la fosforilación del eIF2α conforme avanza la infección [153, 154]. Para estudiar la posibilidad de que la $2A^{pro}$ pudiera estar afectando los niveles de PKR, analizamos mediante western blot la acumulación de PKR en células BHK-T7 transfectadas con pTM1-2A que fueron tratadas o no con Ars .

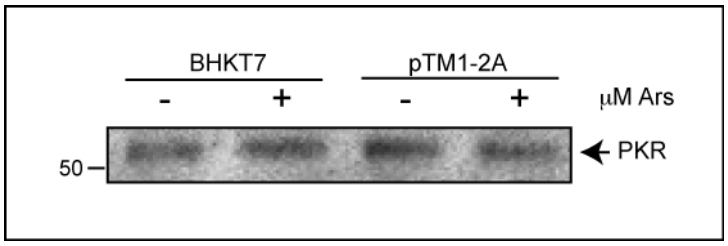

Figura 12. Efecto de $2A^{pro}$ sobre PKR. Las células BHK-T7 fueron transfectadas con el plásmido pTM1-2A durante 2 horas o se dejaron sin transfectar. Pasado este tiempo se añadió DMEM fresco y a las 2 hpt se trataron las células con (+) o sin (-) Ars. Finalmente se procesaron las muestras para analizar PKR por western blot.

En la figura 12 se puede apreciar que no hay cambios significativos en los niveles de PKR tras la expresión de la $2A^{pro}$. Por tanto, la $2A^{pro}$ no es la proteína responsable de la degradación ni de la fosforilación de PKR durante la infección de PV.

1.4. Traducción de mRNAs que contienen diferentes IRES de picornavirus en presencia de la proteasa 2A

Nuestro siguiente objetivo fue estudiar si la proteasa 2A expresada en *trans* era capaz de conferir independencia del factor eIF2α en la traducción de mRNAs que contienen otros IRES de picornavirus. Para ello utilizamos plásmidos que contienen el promotor de la polimerasa del fago T7 y los IRES de EMC, PV o HAV delante del gen de la luc (Fig. 13A, 13B y 13C, respectivamente).

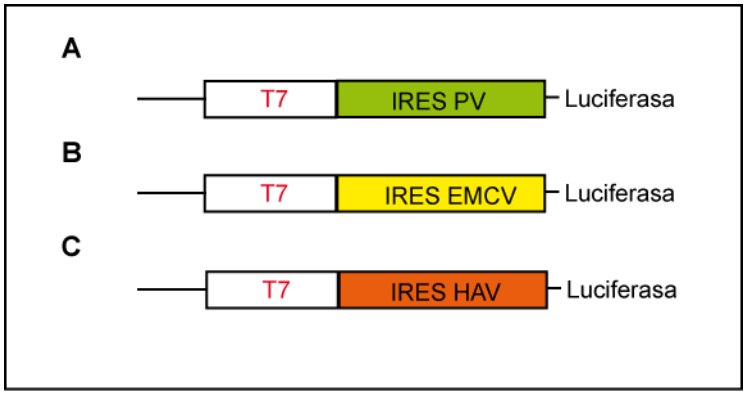

Figura 13. Representación esquemática de los plásmidos pPV-luc, pTM1-luc, y pHAV-luc.

Siguiendo el procedimiento indicado anteriormente, transfectamos estos plásmidos en las células BHK-T7, solos o en combinación con pTM1-2A, y posteriormente se realizó el tratamiento con Ars. La traducibilidad de los diferentes IRES se analizó mediante el ensayo de la medida de la actividad de luc (ver materiales y métodos). En el caso de los IRES de EMC y PV la expresión de la proteasa $2A^{pro}$ en ausencia de Ars estimula la traducción hasta 8 y 5 veces, respectivamente, con respecto a la de las células que no expresan $2A^{pro}$(Fig. 14A y 14C). En presencia de Ars, la traducción se inhibe pero la expresión de $2A^{pro}$ es capaz no sólo de recuperar los niveles de traducción iniciales, sino que de nuevo potencia la traducción mediada por el IRES de EMC y PV hasta 9 y 8 veces, respectivamente (Fig. 14A y 14C).

En cambio, en el caso del IRES de HAV, se observa una inhibición de la expresión de luc en presencia de $2A^{pro}$, que es independiente del tratamiento con Ars (Fig. 14E). Este resultado coincide con estudios previos que indican que el IRES de HAV requiere el complejo eIF4F intacto para ser funcional [117, 155]. Además de analizar la actividad luc, las muestras se procesaron mediante western blot para detectar el factor eIF4GI, eIF2α forforilado y eIF2α total (Fig. 14B, 14D y 14E). En los tres casos se observa que $2A^{pro}$ es activa y ha hidrolizado el factor eIF4GI por completo. Asimismo el eIF2α aparece fosforilado indicando que el tratamiento con Ars también fue eficaz.

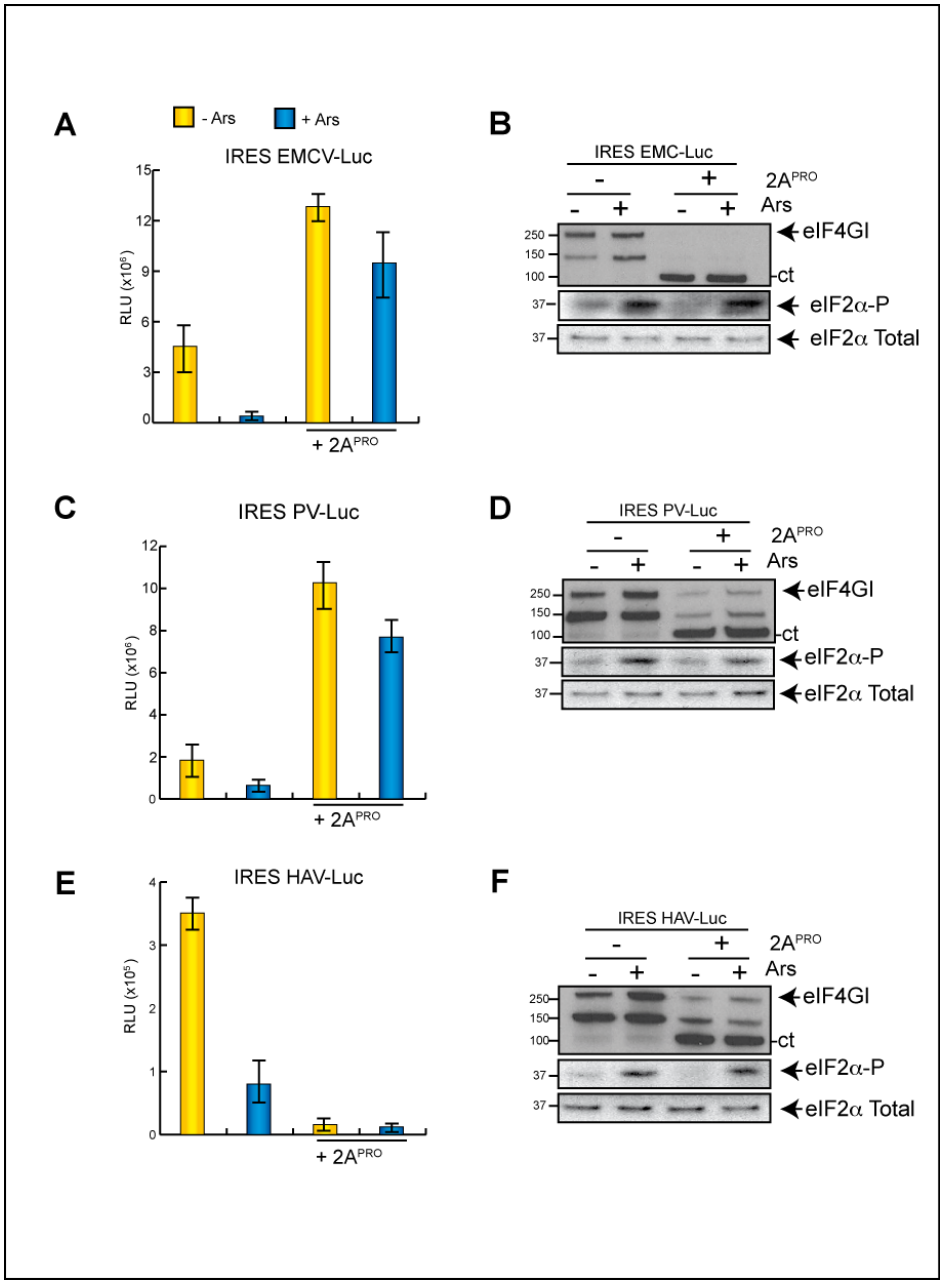

Figura 14. Inhibición de la traducción de los IRES de EMCV y PV en presencia de Ars. Rescate por la 2A^{pro}. A, C y D) Las células BHK-T7 fueron transfectadas con los plásmidos pTM1-luc, pPV-luc y pHAV-luc solos o co-transfectadas con el plásmido pTM1-2A. A las 2 hpt las células fueron tratadas o no con Ars durante 1h. Después, las células fueron recogidas y lisadas en buffer para medir la actividad luciferasa. Las barras de error representan la D.E.. B, D y E) Una alícuota de las mismas muestras se usó para analizar eIF4GI, eIF2α-P y eIF2α por western blot.

PV es un virus que infecta a humanos o primates, por ello quisimos comprobar si este efecto estimulador de la traducción y el rescate de la misma cuando eIF2α está fosforilado era inherente a la proteasa 2A^{pro} y no un artefacto de inespecificidad celular. Para ello empleamos la línea celular Huh-T7, constituida por células de hepatoma humano que expresan constitutivamente la polimerasa del fago T7.

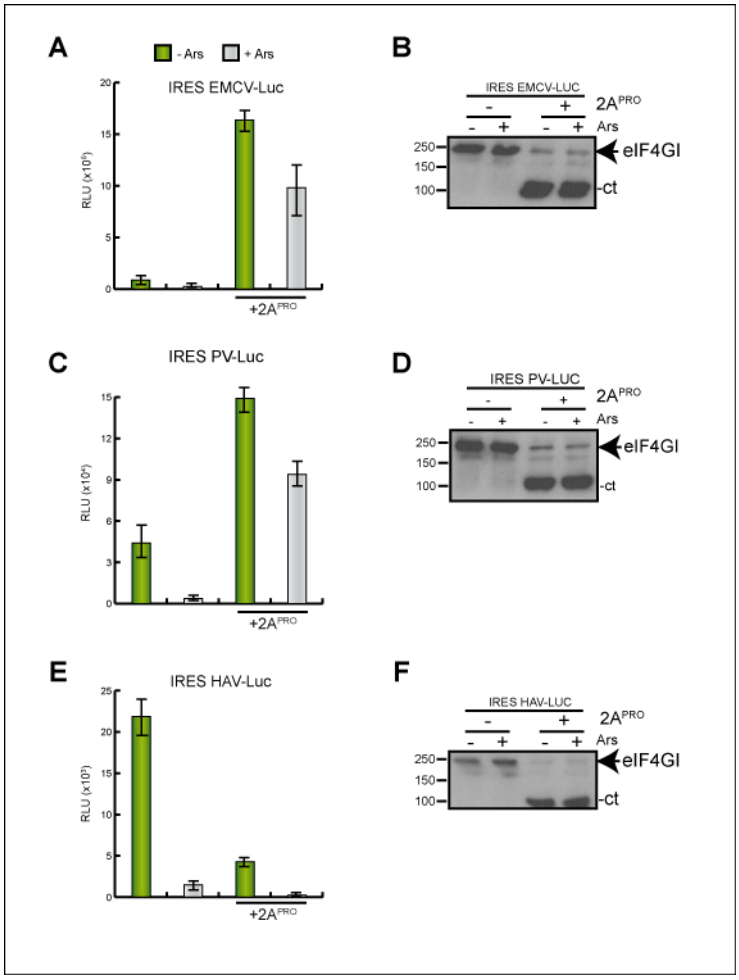

Figura 15. Inhibición de la traducción de los IRES de EMCV y PV en presencia de Ars en células Huh-T7. Rescate por la $2A^{pro}$. A, C y E) Las células Huh-T7 fueron transfectadas con los plásmidos pTM1-luc, pPV-luc y pHAV-luc solos o co-transfectadas con el plásmido pTM1-2A. A las 2 hpt las células fueron tratadas o no con Ars durante 1h. Después, las células fueron recogidas y lisadas en buffer para medir la actividad luciferasa. Las barras de error representan la D.E.. B, D y F) Una alícuota de las mismas muestras se usó para analizar eIF4GI, eIF2α-P y eIF2α por western blot.

Al igual que en las células BHK-T7, se observa un fuerte efecto estimulador de la traducción en ausencia de Ars (15 veces más en el caso del EMC IRES y 3 veces más en el de PV) y el rescate de la misma mediados por la proteasa $2A^{pro}$ (en presencia de Ars) que alcanzó entorno al 75% en el caso de los IRES de EMC y PV (Fig. 15A y 15C). En el caso de HAV de nuevo observamos la inhibición de la traducción cuando está presente $2A^{pro}$ (Fig. 15E). Al detectar el factor eIF4GI mediante western blot, comprobamos que se encuentra completamente hidrolizado por acción de la proteasa (Fig. 15B, 15D y 15F).

De estos resultados concluímos que la traducción mediada por los IRES de EMC y PV, fuera del contexto de la infección, es sensible a la fosforilación del factor eIF2α. Además, la proteasa $2A^{pro}$ permite y, aún más, potencia de manera específica la traducción mediada por dichos IRES cuando el factor eIF2α está fosforilado.

1.5. Rescate de la traducción por la proteasa $2A^{pro}$ de PV en diferentes condiciones de estrés

Existen diferentes situaciones de estrés que conducen a la fosforilación del factor eIF2α y, por tanto, a la inhibición de la traducción. Estos mecanismos se activan por diferentes vías celulares. En el caso del Ars la fosforilación se induce activando la quinasa HRI (Heme-Regulated Inhibitor). Pero existen otros inhibidores que inducen la fosforilación del factor eIF2α, como la tapsigargina (Tg), que activa la PKR-like ER kinase (PERK) [156] o el dithiothreitol (DTT) [157]. Además de compuestos químicos, determinadas situaciones en la célula también desencadenan la fosforilación del factor eIF2α, como alteraciones en la migración celular, procesos de *splicing* o la presencia de un medio hipertónico.
Por tanto, estudiamos la traducción del IRES de EMC en algunas de estas situaciones y en presencia de la proteasa $2A^{pro}$.

1.5.1. Traducción mediada por el IRES de EMC en condiciones hipertónicas y en presencia de $2A^{pro}$

En levaduras se describió que el medio hipertónico induce una fuerte, aunque reversible, forforilación del eIF2α [158], por lo que este tratamiento ha sido utilizado en diversos trabajos para inhibir este factor [15, 159]. Por ello estudiamos si en estas condiciones la PV $2A^{pro}$ era capaz de promover la traducción del IRES de picornavirus en células de mamífero.
Transfectamos las células BHK-T7 con el plásmido pTM1-luc, con el plásmido pTM1-2A o con ambos, y dos horas después expusimos las células a estrés bien incubándolas en medio hipertónico (+/-), con Ars (-/+) o con una combinación de ambas situaciones (+/+) y realizamos un marcaje radiactivo de proteínas para estudiar el efecto producido sobre la traducción. En la figura 16A se puede observar que la traducción de proteínas celulares, así como la síntesis de luc resultan fuertemente inhibidas con cualquiera de los dos tratamientos o con la combinación de los mismos, en ausencia de $2A^{pro}$ (Fig. 16A, carriles 1-8). Sin embargo, en presencia de $2A^{pro}$ la síntesis de luc se estimula significativamente (Fig. 16A, carriles 5 y 13) en ausencia de estrés. Mientras, en condiciones de estrés, aunque la síntesis de $2A^{pro}$ disminuye, ésta es aún suficiente para potenciar la expresión de luc por encima de los niveles obtenidos en ausencia de Ars (Fig 16A, carriles 6-8 y 14-16).

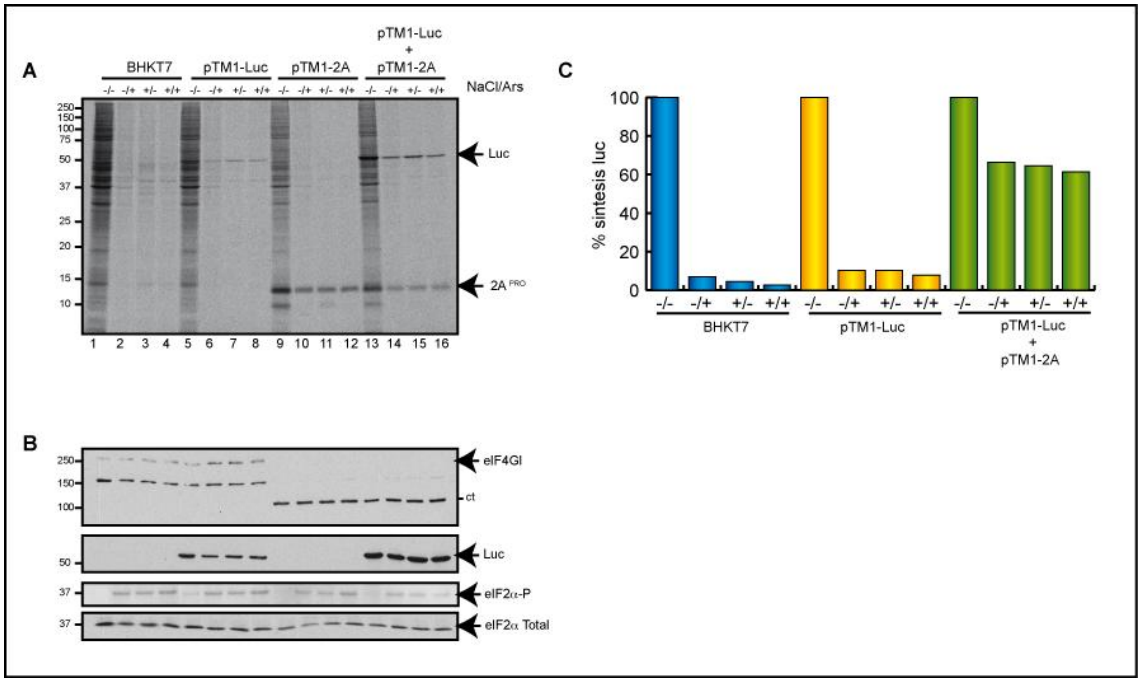

Figura 16. Efecto de un medio hipertónico sobre la traducción dirigida por el IRES de EMC. Efecto de la $2A^{pro}$. A) Células BHK-T7 fueron transfectadas con pTM1-luc, pTM1-2A o con ambos plásmidos. A las 2 hpt las células fueron pretratadas con Ars (-/+), NaCl (+/-) o con los dos tratamientos (+/+) durante 15 min. Después se marcaron con [^{35}S]Met/Cys durante 45 min en presencia de los inhibidores. Posteriormente las células se procesaron mediante SDS-PAGE (17,5%), fluorografía y autorradiografía. B) Las muestras del panel A también se emplearon para detectar eIF4GI, luciferasa, eIF2α-P y eIF2α total.

También analizamos el factor eIF4GI mediante western blot (Fig. 16B, panel superior) y comprobamos que en cualquiera de las condiciones del experimento $2A^{pro}$ es completamente activa y el corte de eIF4GI es total. En paralelo también confirmamos que sólo cuando sometemos las células a estrés se detecta la fosforilación del factor eIF2α (Fig. 16B). También analizamos la cantidad total de este factor, no existiendo diferencias significativas (Fig. 16B, panel inferior). Para observar mejor el rescate de la traducción del mRNA EMC-luc, en la gráfica 16C están representados los valores del porcentaje de síntesis de una proteína celular y de luc, siendo el 100% los valores sin tratamiento (-/-).

Por tanto, $2A^{pro}$ no solo rescata la traducción del IRES de EMC cuando el factor eIF2α está fosforilado mediante tratamiento con Ars, sino que también tiene lugar cuando dicha inhibición es inducida en presencia de un medio hipertónico. De hecho, en condiciones extremas de estrés en las que las células están sometidas a ambos tratamientos, $2A^{pro}$ rescata la traducción del mRNA EMC-luc.

1.5.2. Traducción del mRNA EMC-2A en presencia de tapsigargina

Otro inhibidor utilizado para inducir fosforilación del factor eIF2α es la tapsigargina [129, 160]. En este caso comprobamos el efecto de un medio hipertónico, de un medio con

tapsigargina o de un medio con ambos tratamientos sobre la traducción del mRNA EMC-2A. Para ello transfectamos las células con el plásmido pTM1-2A o las dejamos sin transfectar. Posteriormente, previo pre-tratamiento, expusimos las células a las diferentes condiciones de estrés y realizamos un marcaje radiactivo de proteínas antes de analizar las muestras mediante SDS-PAGE, fluorografía y autorradiografía (Fig. 17A).

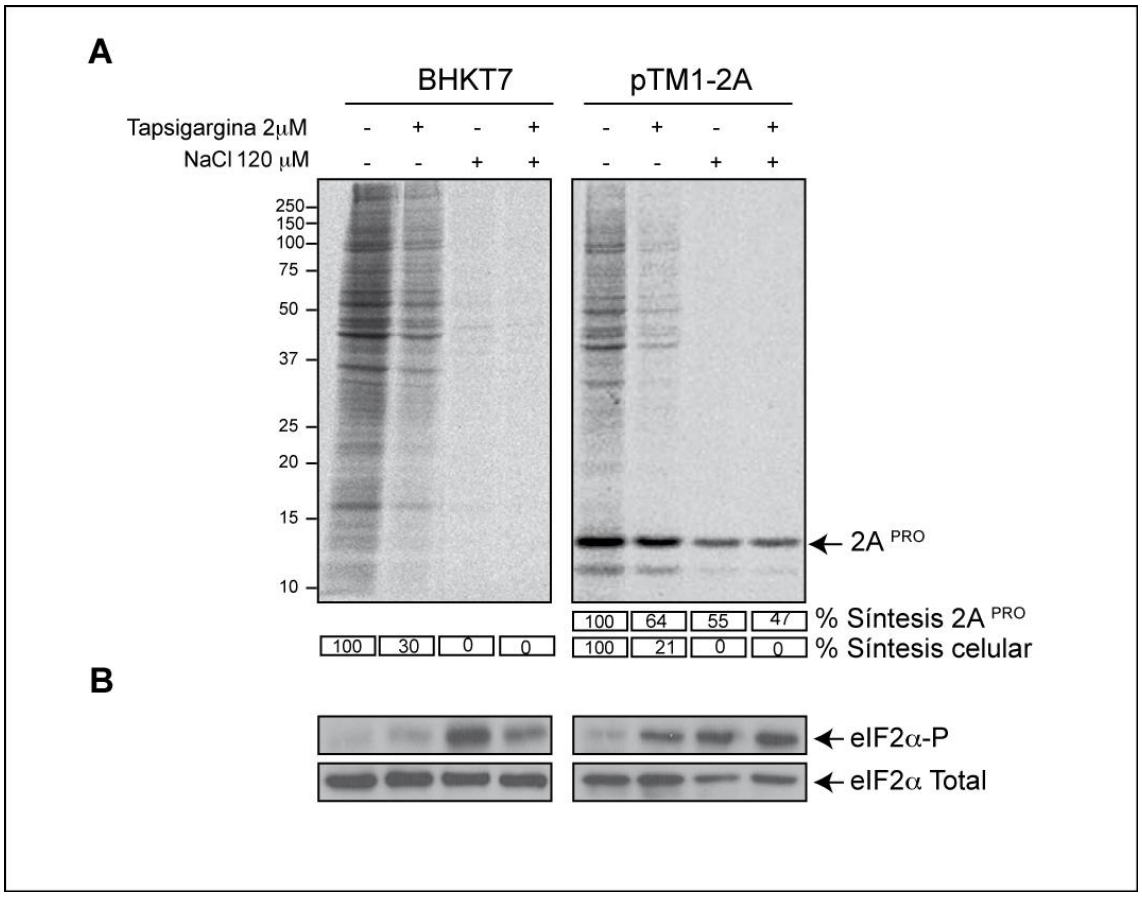

Figura 17. Efecto de la tapsigargina sobre la traducción del mRNA EMC-2A. A) Las células BHK-T7 se transfectaron con pTM1-2A o se dejaron sin transfectar. A las 2 hpt las células se pretrataron con 1μM de Tapsigargina, con 120 mM de NaCl o con ambos tratamientos durante 15 min. Posteriormente se marcaron con [^{35}S]Met/Cys durante 45 min en presencia de los mismos compuestos. Después del marcaje las células se analizaron por SDS-PAGE (17,5%), fluorografía y autorradiografía. El porcentaje de síntesis respecto de las células no tratadas está representado debajo de cada línea, calculado mediante densitometría de las bandas correspondientes a una proteína celular (*) o a la 2A^{pro}. B) En paralelo se detectaron eIF2α-P y eIF2α total por western blot.

Al igual que en los experimentos anteriores, mientras que la traducción celular ha sido prácticamente inhibida en su totalidad, la traducción de la proteasa 2A^{pro} se mantiene en un 50% (Fig. 17A, panel derecho). Las mismas muestras las analizamos por western blot, confirmando que este factor resulta fosforilado cuando sometemos las células a los diferentes tratamientos (Fig.17B). Estos resultados respaldan la idea de que el mRNA EMC-2A mantiene su traducibilidad en un 50% o más en diferentes situaciones de estrés en las que el factor eIF2α se encuentra fosforilado y la traducción celular totalmente anulada.

1.6. Análisis de la actividad proteolítica de $2A^{pro}$ y su papel para conferir independencia del factor eIF2α

Hasta el momento, el principal efecto directo que se conoce de $2A^{pro}$ sobre la traducción celular es su actividad proteolítica sobre el factor eIF4GI, lo que ha permitido especular que esto conduce a una estimulación de la traducción de los mRNAs de picornavirus [30]. Por tanto estudiamos si la capacidad de $2A^{pro}$ para estimular la traducción cuando el factor eIF2α está fosforilado, podía estar relacionado con su actividad proteasa sobre el factor eIF4G.

Con este fin, empleamos un plásmido que expresa un mutante de la proteasa $2A^{pro}$, pTM1-2A(G60R), que no posee actividad proteasa sobre el factor eIF4GI [79]. En este caso, además, utilizamos el plásmido pTM1-2C para estudiar el efecto en traducción.

Procedimos de la siguiente manera, co-transfectamos el plásmido pTM1-2C con el plásmido pTM1-2A o con pTM1-2A(G60R); como controles transfectamos cada plásmido por separado. A continuación, tratamos las células con dos concentraciones de Ars diferentes y marcamos radiactivamente para estudiar el efecto sobre la síntesis de proteínas (Fig.18A). En paralelo analizamos por western blot el estado de fosforilación del eIF2α, así como la cantidad total de este factor. También estudiamos el corte del factor eIF4GI, observándose una ausencia de actividad proteolítica por parte del mutante 2A(G60R) (Fig.18B).

En la figura 18 puede observarse como la expresión de la proteína $2A^{pro}$ resulta débilmente afectada por el tratamiento con Ars (carriles 4-6), mientras que la síntesis de 2C está fuertemente inhibida (carriles 7-9). Sin embargo, cuando se coexpresan $2A^{pro}$ y 2C, la traducción de esta última experimenta un fuerte rescate, de forma que no se aprecia inhibición en presencia de $2A^{pro}$ (carriles 10-12). Por último, cuando se expresa el mutante 2A(G60R) (carriles 13-15) o cuando se coexpresan 2A(G60R) y 2C (carriles 16-18), el tratamiento con Ars afecta drásticamente a la traducción y, por tanto, a la síntesis de ambas proteínas. Realizamos un análisis cuantitativo densitometrando la banda correspondiente a una proteína celular, así como las correspondientes a las proteínas 2C, $2A^{pro}$ y 2A(G60R), y expresamos los valores en porcentaje de síntesis. Como se muestra en la figura 18C, cuando estas proteínas se expresan por separado, sólo $2A^{pro}$ es capaz de mantener los niveles de síntesis alrededor del 75% tras el tratamiento con Ars, mientras que las demás son inhibidas en aproximadamente un 80%. En cambio, si observamos la figura 18D, el panel de la izquierda muestra una clara recuperación de la proteína 2C en presencia de $2A^{pro}$ con unos valores de síntesis del 70% aproximadamente en contraste con lo observado cuando se expresa con la 2A mutante, donde los niveles de síntesis se inhiben más del 80%, como ocurre cuando se expresa por separado.

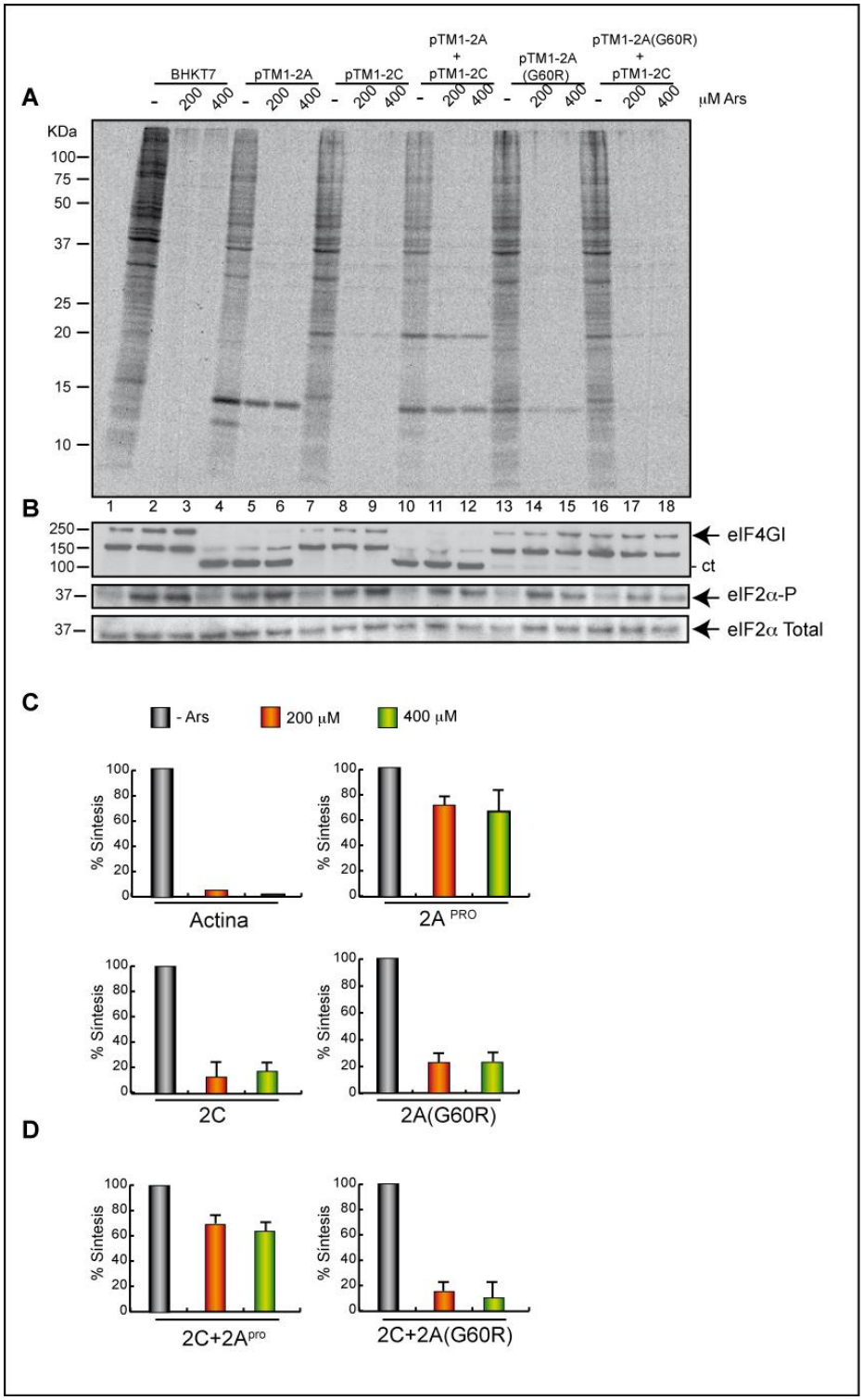

Figura 18. La actividad proteolítica de 2A^{pro} es necesaria para propiciar una traducción independiente de eIF2α. Se transfectaron células BHK-T7 con pTM1-2A, pTM1-2C o pTM1-2A(G60R), o se co-transfectaron con pTM1-2A o pTM1-2A(G60R) con el plásmido pTM1-2C. A) A las 2hpt las células se trataron con diferentes concentraciones de Ars(200 µM y 400 µM) y se incubaron durante 45 min con [^{35}S]Met/Cys. Después, las muestras fueron procesadas por SDS-PAGE (17,5%), fluorografía y autorradiografía. B) Las mismas muestras fueron utilizadas para detectar eIF4GI, eIF2α-P y eIF2α total por western blot. **C)** Se densitometraron las bandas correspondientes a una proteína celular, 2A^{pro}, 2A(G60R) y 2C. Los valores obtenidos se expresaron en % de síntesis, siendo el 100% la síntesis en ausencia de Ars. Las barras de error representan la D.E. de tres experimentos independientes. D) Están representados los valores de la síntesis de la proteína 2C tras el tratamiento con Ars y en presencia de 2A^{pro} o de 2A(G60R) obtenidos por densitometría de las bandas correspondientes. Las barras de error representan la D.E. de tres experimentos independientes

Por tanto, este resultado indica que es necesaria la actividad catalítica de $2A^{pro}$ para conferir traducibilidad al IRES de EMC cuando el factor eIF2α está fosforilado.

1.7. Análisis del corte del factor eIF4GI y su implicación en la traducción eIF2α-independiente

Teniendo en cuenta los resultados anteriores, es posible que la independencia del factor eIF2α que proporciona $2A^{pro}$ fuera resultado de la producción de los fragmentos de eIF4GI generados tras ejercer su actividad proteolítica. Por otro lado, también podría estar ocurriendo, que la presencia de $2A^{pro}$ sea necesaria, lo que significaría que actuaría como un ITAF.

Para diferenciar estas posibilidades estudiamos, en primer lugar, el efecto de la concentración de $2A^{pro}$. Ha sido ensayado previamente en nuestro laboratorio que la transfección de pequeñas cantidades del mRNA EMC-2A sintetizadas *in vitro* conducen al corte completo del factor eIF4GI [13]. Este mismo efecto se puede observar con el sistema utilizado en esta tesis, con la diferencia de que las cantidades producidas son mucho mayores.

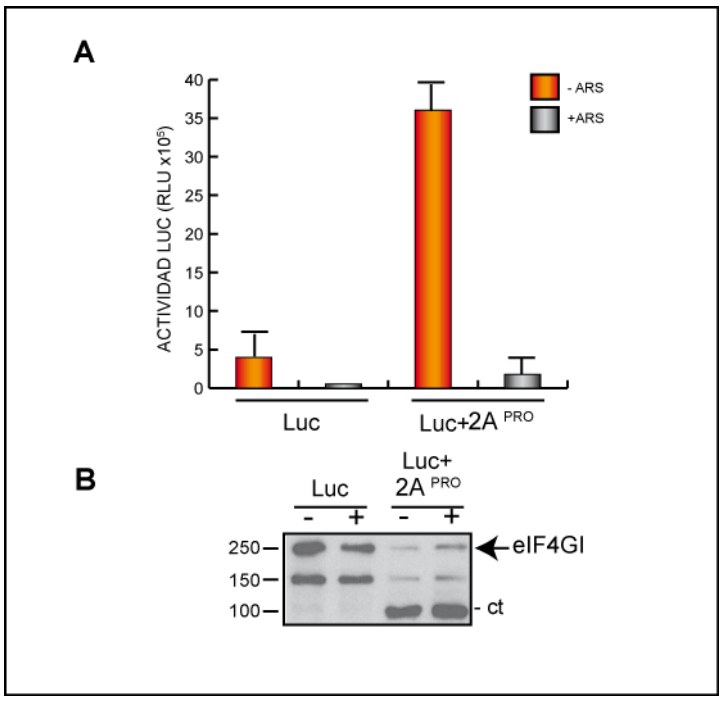

Figura 19. El corte del factor eIF4GI no es suficiente para conferir independencia del factor eIF2. A) Las células BHK-T7 fueron transfectadas con el mRNA EMC-2A. A las 2 hpt se cambió el medio de transfección por medio fresco. Se dejaron durante 1 h para asegurar el corte del factor eIF4GI. Después, se transfectó pTM1-luc durante 2h. Pasado este tiempo se lavaron las células y se volvió a añadir medio fresco; tras 15 min se añadió 200 μM de Ars y se dejó actuando 1h. Por último, las células se recogieron para medir actividad luciferasa. Las barras de error representan la D.E. de tres experimentos independientes. B) El corte del factor eIF4GI fue detectado por western blot.

Por tanto, transfectamos las células con el mRNA EMC-2A, previamente sintetizado *in vitro*, para inducir el corte de eIF4GI. A continuación transfectamos el plásmido pTM1-luc. Por último analizamos la producción de luc en ausencia o presencia de Ars (Fig. 19A).

En estas condiciones de baja producción de proteína $2A^{pro}$ y corte total de eIF4GI (Fig.19B), el tratamiento con Ars inhibe profundamente la síntesis de luc. Estos resultados indican que la

presencia de los fragmentos de eIF4GI, o el corte de algún otro sustrato celular, pueden ser necesarios pero no suficientes para conferir independencia del factor eIF2α si la cantidad de $2A^{pro}$ presente es muy pequeña.

Existen trabajos previos en los que se observó estimulación de la traducción IRES-dependiente sólo con la presencia del fragmento carboxilo terminal del factor eIF4GI [161]. Por ello, estudiamos más en detalle el papel que podría ejercer cada fragmento expresado por separado sobre la traducción del IRES de EMC cuando eIF2α está fosforilado. Por tanto clonamos cada fragmento de eIF4GI en plásmidos pTM1. Transfectamos pTM1-luc con diferentes plásmidos en las células BHK-T7 como se muestra en la figura 20A. A continuación fueron pre-tratadas o no con Ars.

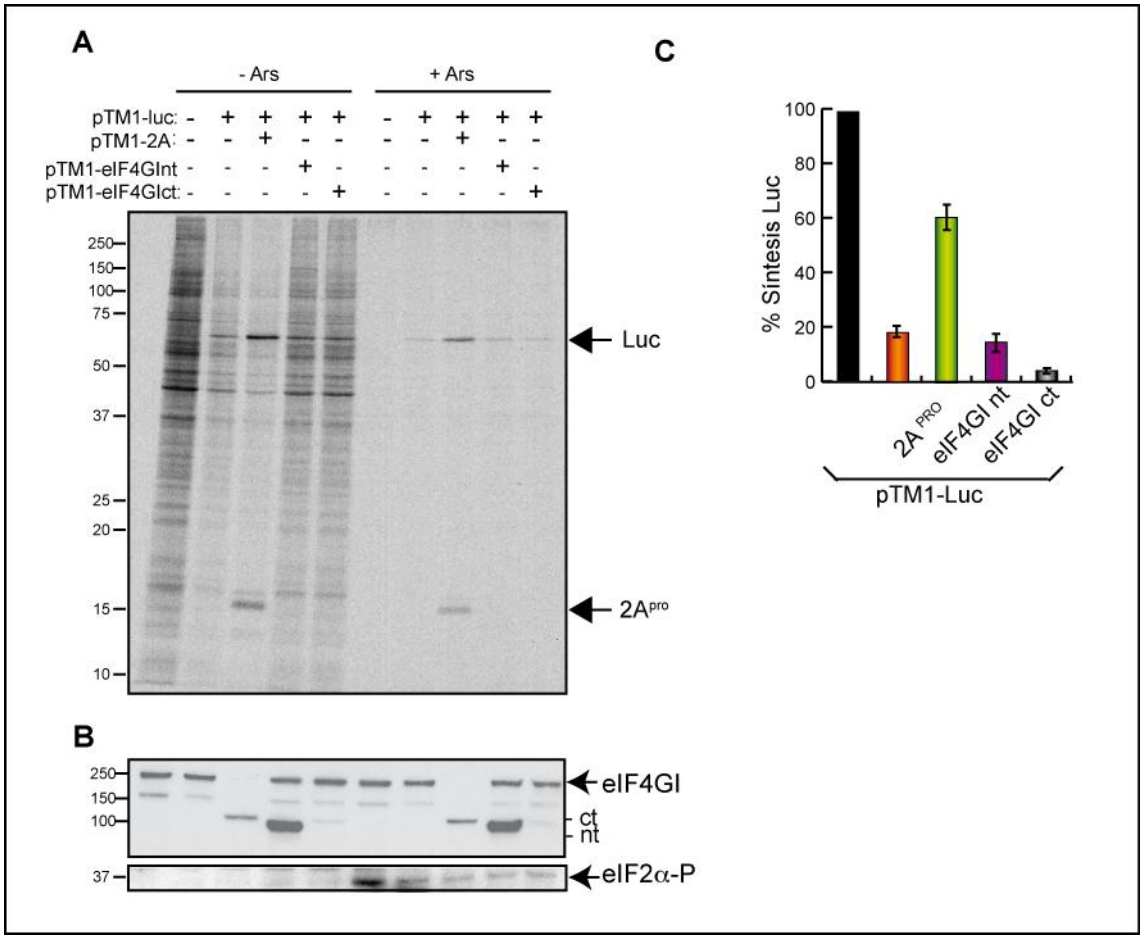

Figura 20. Estudio de la expresión de los fragmentos Nt ó Ct de eIF4GI. pTM1-luc fue transfectado solo o cotransfectado con los siguientes plásmidos: pTM1-2A, pTM1-eIF4GINt y pTM1-eIF4GCt. A) A las 2 hpt las células fueron pre-tratadas con 200 μM de Ars durante 15 min y luego se marcaron durante 45 min con [^{35}S]Met/Cys en presencia del inhibidor. Después las muestras se procesaron por SDS-PAGE (17,5%), fluorografía y autorradiografía. B) eIF4GI y eIF2αP fueron detectados en una alícuota de las mismas muestras utilizadas en A por western blot. C) Representación del porcentaje de la síntesis de luciferasa en presencia de pTM1-2A, pTM1-eIF4GINt o pTM1-eIF4GICt obtenido por densitometría de la banda de luciferasa en cada caso. El 100% corresponde a los valores sin Ars.

Posteriomente realizamos un marcaje radiactivo de proteínas en presencia o ausencia de Ars y analizamos las muestras mediante SDS-PAGE, fluorografía y autorradiografía. En la figura 20A se puede observar que la síntesis de luc está inhibida en presencia de Ars a pesar de la presencia de los fragmentos Nt o Ct de eIF4GI, a diferencia de lo que ocurre cuando $2A^{pro}$ está presente. Para verificar la correcta transfección y expresión de los fragmentos, éstos fueron detectados mediante western blot (Fig. 20B, panel superior). Por último, densitometramos la banda correspondiente y comparamos los valores de síntesis de luc, tomando como 100% los valores obtenidos en ausencia de Ars en cada caso. Como se muestra en la figura 20C, la síntesis de luc se mantuvo en torno al 60% en las células tratadas con Ars en presencia de $2A^{pro}$, mientras que en los demás casos no llegó al 20%.

A partir de los resultados anteriores, estudiamos la posibilidad de que la presencia de altos niveles tanto del fragmento Ct de eIF4GI como de una $2A^{pro}$ proteolíticamente inactiva, 2A(G60R), pudieran rescatar la traducción del IRES de EMC en presencia de Ars. Con este fin, transfectamos o co-transfectamos las células como se indica en la figura 21A. Posteriormente realizamos el ensayo de marcaje radiactivo de proteínas en presencia o ausencia de Ars.

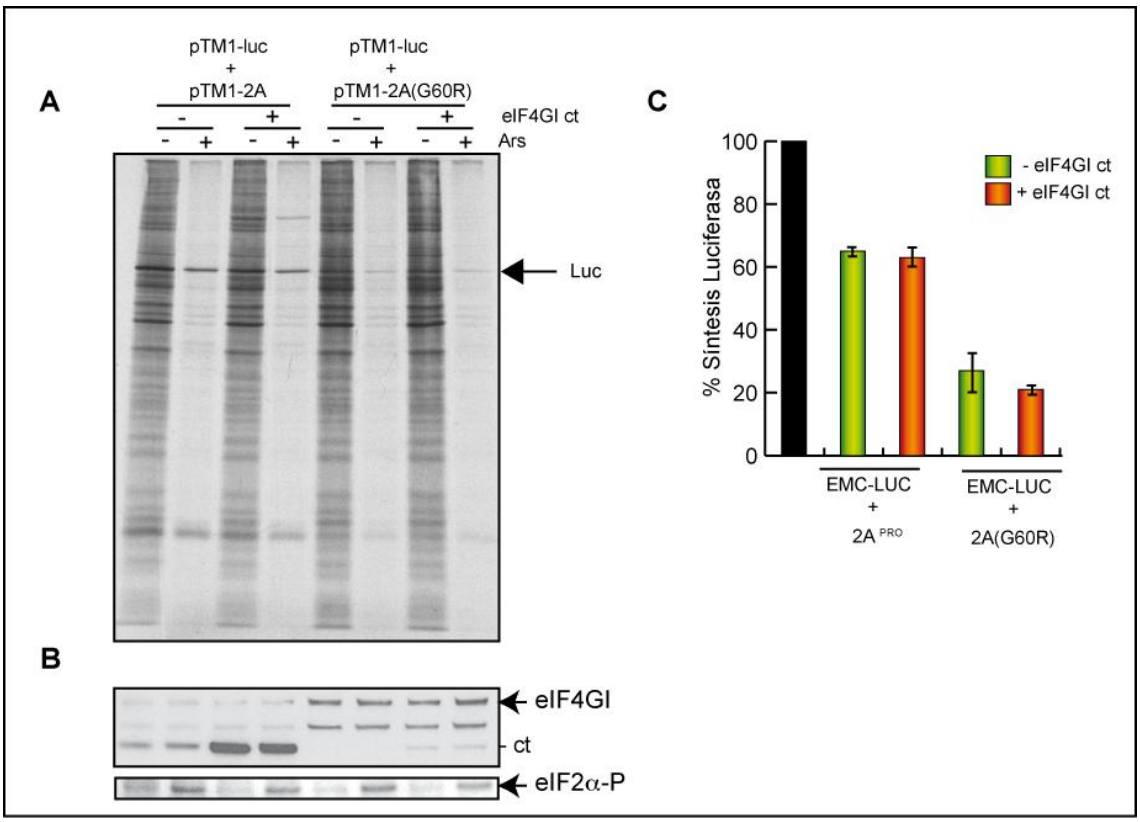

Figura 21. Efecto de coexpresar el fragmento Ct de eIF4GI y 2A(G60R) sobre la traducción del mRNA EMC-luc. Se co-transfectaron células BHK-T7 con pTM1-luc y con pTM1-$2A^{pro}$ o pTM1-2A(G60R). Las mezclas de transfección se incubaron con o sin pTM1-eIF4GICt. A las 2 hpt las muestras se pretrataron durante 15 min con Ars y posteriormente se marcaron durante 45 min con [^{35}S]Met/Cys en presencia o ausencia del inhibidor. A) Las muestras se procesaron por SDS-PAGE (17,5%), fluorografía y autorradiografía. B) En paralelo eIF4GI y eIF2αP fueron detectados por western blot. C) Representación del porcentaje de síntesis de luc obtenido mediante densitometría de la banda correspondiente. Las barras de error representan la D.E. de al menos tres experimentos independientes.

Como se muestra en la figura 21A, la traducción de luc mediada por el IRES de EMC se inhibe un 80% tras el tratamiento de Ars, tanto en presencia del fragmento Ct de eIF4GI solo, o cuando se encuentra además 2A(G60R) (Fig. 21A y 21C). Sin embargo, cuando $2A^{pro}$ wt está presente, no sólo detectamos síntesis de luc en un 65% (Fig. 21C), sino que también está estimulada la síntesis del extremo Ct. Estas observaciones indican que para aportar independencia de la fosforilación del factor eIF2α, es necesaria la presencia de una $2A^{pro}$ proteolíticamente activa

De los resultados obtenidos hasta el momento, dos posibilidades podrían estar ocurriendo. Por un lado, podría ser que $2A^{pro}$ estuviera ejerciendo su actividad proteolítica sobre otra proteína celular que no fuera el factor eIF4GI, y de esta forma se vea favorecida la traducción de los IRES cuando el factor eIF2α está fosforilado. Otra posibilidad podría ser que, además, $2A^{pro}$ tuviera que estar presente. Para distinguir entre estas dos posibilidades utilizamos el compuesto methoxysuccinyl-Ala-Ala-Pro-Val-chloromethylketone (MPCMK), que se une covalentemente a $2A^{pro}$ inhibiendo su actividad proteolítica [162].

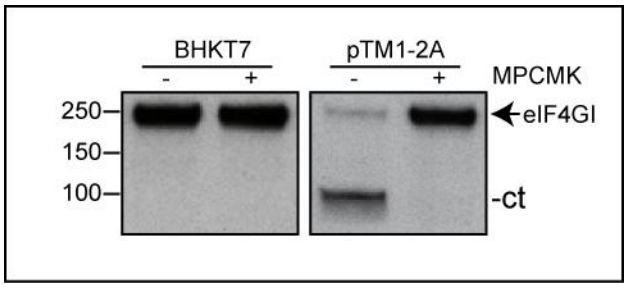

Figura 22. Efecto del inhibidor MPCMK sobre la actividad proteasa de $2A^{pro}$. Se transfectaron células BHK-T7 con el plásmido pTM1-2A o se dejaron sin transfectar. Durante la transfección las células se incubaron sin (-) o con (+) 750 μM de MPCMK durante 1h. Después se cambió la mezcla de transfección y las células se siguieron incubando en presencia o ausencia del compuesto. Para comprobar el efecto inhibitorio del compuesto se analizó el factor eIF4GI por western blot.

Por tanto, para estudiar el efecto de este inhibidor transfectamos células BHK-T7 con el plásmido pTM1-2A o las dejamos sin transfectar. En la mezcla de transfección las células se incubaron (+) o no (-) con 750μM de MPCMK. Tras dos horas de transfección se cambió el medio y las células se incubaron con el inhibidor durante una hora más. Posteriormente analizamos el corte del factor eIF4GI por western blot. Como se puede ver en la figura 22, en las células transfectadas con pTM1-2A e incubadas con el inhibidor, hay ausencia de corte de eIF4GI.

Una vez comprobados los efectos del inhibidor, transfectamos el plásmido pTM1-2A en las células BHK-T7, y después de una hora de incubación, cuando el factor eIF4GI y, posiblemente, otros sustratos celulares pudieran haber sido hidrolizados, añadimos el plásmido pTM1-luc en presencia o ausencia del inhibidor, además del tratamiento con Ars. Lo que se obtuvo tras medir la producción de luc fue que en presencia del inhibidor MPCMK, $2A^{pro}$ no es capaz de conferir independencia traduccional al IRES de EMC (Fig. 23A), a pesar de estar cortado prácticamente

por completo el factor eIF4GI (Fig. 23B). Por tanto, para que el IRES de EMC pueda traducirse independientemente del factor eIF2α, debe estar presente una $2A^{pro}$ activa.

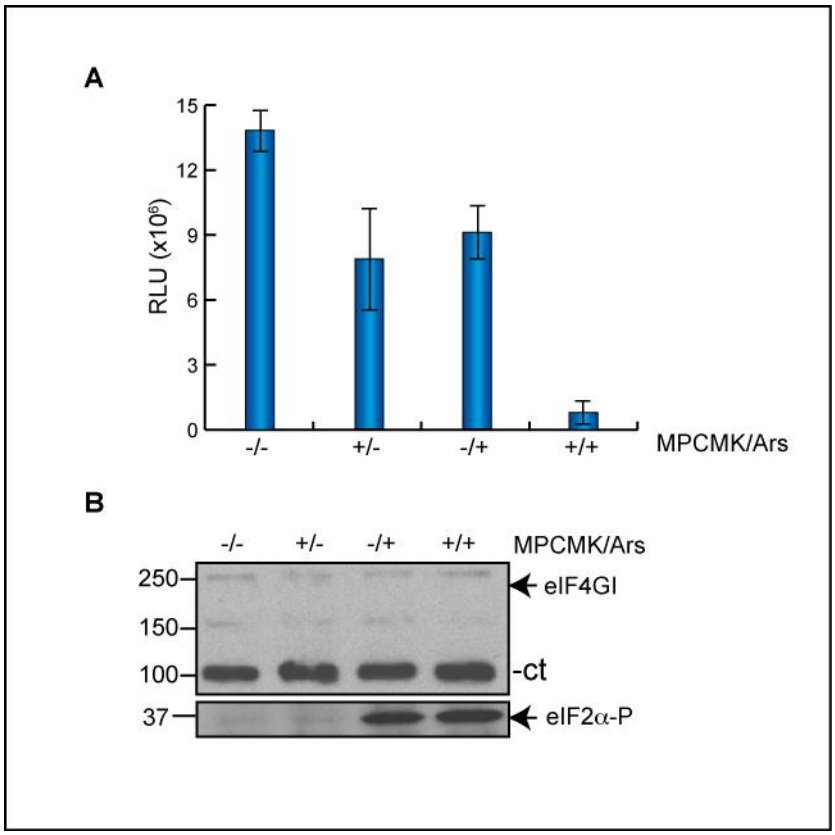

Figura 23. Estudio del efecto de la inhibición de $2A^{pro}$ con MPCMK sobre la traducción eIF2α independiente. A) Se transfectaron células BHK-T7 con pTM1-2A. Después, las células se incubaron con MPCMK durante 1h. Pasado este tiempo, las células se transfectaron con pTM1-luc durante 30 min. A continuación se incubaron las células con 750 μM de MPCMK (+/-), con 200 μM de Ars (-/+) o con ambos inhibidores (+/+) durante 1h. Finalmente las células se procesaron para medir actividad luciferasa. Los valores de luciferasa obtenidos se representan en la gráfica. Las barras de error representan la D.E. B) Las mismas muestras también se utilizaron para detectar los factores eIF4GI y eIF2αP por western blot.

2. ESTUDIO DE LA TRADUCCIÓN DEL IRES DEL VIRUS DE LA HEPATITIS A (HAV) EN PRESENCIA DEL FACTOR eIF4GI CORTADO

Varios estudios han establecido que la traducción dirigida por el IRES de HAV es inhibida por las proteasas de picornavirus $2A^{pro}$ y Lb^{pro}, tanto en sistemas *in vitro* como en células en cultivo [117, 155, 163]. Dicha inhibición de la traducción es causada por el corte del factor eIF4GI, de forma que cuando se suministra el complejo eIF4F intacto, la traducción se restablece. Por tanto, estos resultados marcaban una diferencia con los otros IRES de picornavirus descritos en cuanto al requerimiento de eIFs. Esta característica, junto con otras peculiaridades estructurales, hicieron que al IRES de HAV se le clasificara en un grupo diferente de los descritos hasta la fecha, el grupo III [29, 30].

2.1. Efecto opuesto de la proteasa $2A^{pro}$ de PV y la proteasa Lb^{pro} de FMDV sobre el IRES de HAV

Hemos visto hasta ahora que $2A^{pro}$ es capaz de promover la traducción de los IRES de EMC y PV cuando el factor eIF2α está fosforilado. En cambio, la traducción dirigida por el IRES de HAV se ve fuertemente inhibida en presencia de $2A^{pro}$, esté activo el factor eIF2α o no. Por tanto, quisimos comprobar si la proteasa Lb^{pro} de FMDV (L^{pro}) tenía el mismo efecto que $2A^{pro}$ sobre la traducción dirigida por el IRES de HAV. Para ello utilizamos, por un lado, el plásmido pHAV-luc, que posee el promotor de la polimerasa del fago T7 y la secuencia IRES de HAV seguida de la secuencia del gen luc. Para expresar L^{pro} empleamos un plásmido denominado pFMDV-L que también contiene el promotor de la polimerasa del fago T7, en este caso seguido de la secuencia IRES de FMDV. Utilizamos el mismo sistema empleado hasta el momento, es decir, transfectamos células BHK-T7 con el plásmido pHAV-luc solo o lo co-transfectamos con el plásmido pTM1-2A o con el plásmido pFMDV-L. A las 2 hpt pretratamos las células con Ars y, posteriormente, hicimos un marcaje radiactivo de proteínas en presencia o ausencia del inhibidor. Posteriormente, procesamos las muestras para su análisis mediante SDS-PAGE (Figura 24A). Cuando transfectamos el plásmido pHAV-luc solo o en presencia de $2A^{pro}$, no se observa síntesis de luc, tanto en presencia como en ausencia de Ars; en cambio, cuando se co-expresa con L^{pro}, no sólo se ve claramente luc, sino que además, en presencia de Ars no se observa disminución de la marca radiactiva. Sin embargo, mediante marcaje radiactivo no podemos apreciar claramente la síntesis de L^{pro}. Las mismas muestras se utilizaron para analizar diferentes proteínas por western blot (Fig. 24B). En primer lugar analizamos el corte del factor eIF4GI, estando completamente hidrolizado en presencia de las proteasas. En los siguientes

paneles mostramos el análisis del factor eIF2α, tanto de su forma fosforilada, inducida por el tratamiento de Ars, como del total de eIF2α.

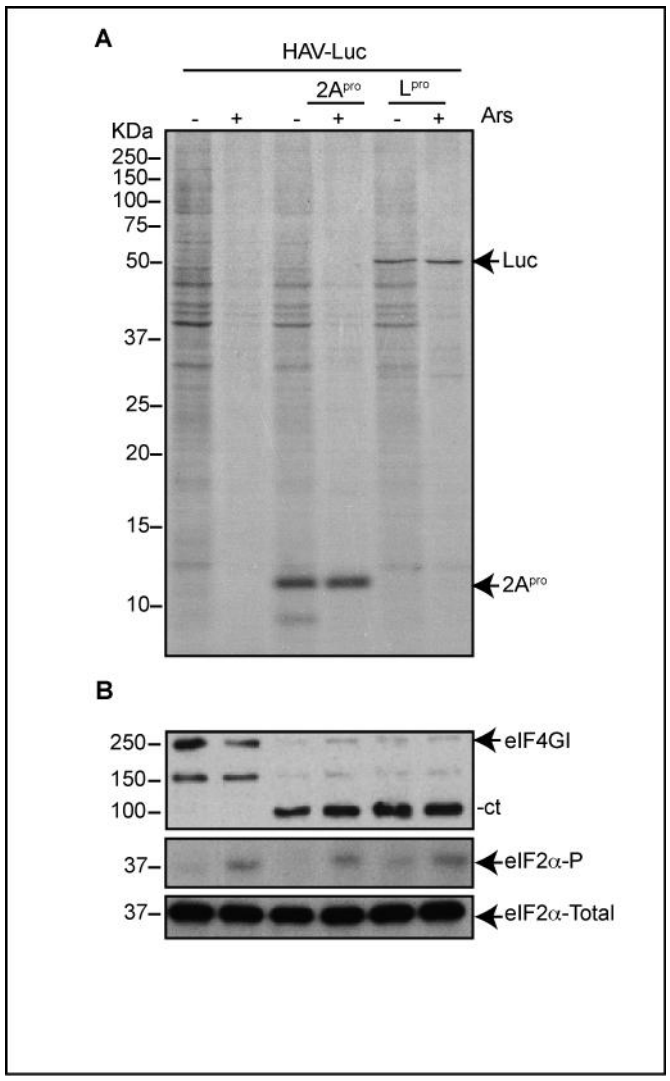

Figura 24. Traducción del IRES de HAV en presencia del factor eIF4GI hidrolizado. Comparación del efecto de $2A^{pro}$ de PV y Lb^{pro} de FMDV. A) Las células BHK-T7 fueron transfectadas con el plásmido pHAV-luc solo o co-transfectado con pTM1-$2A^{pro}$ o pFMDV-Lb^{pro}. A las 2 hpt las células se pretrataron con 200μM de Ars durante 15 min y posteriormente se marcaron con [^{35}S]Met/Cys durante 45 min en presencia o no del inhibidor. Posteriormente las células se procesaron por SDS-PAGE, fluorografía y autorradiografía. B) Las mismas muestras del panel A fueron analizadas por western blot para detectar eIF4GI, eIF2α fosforilado y eIF2αtotal.

Paralelamente, transfectamos células en las mismas condiciones, pero en este caso las muestras fueron procesadas para medir actividad luc. Estudiamos también el efecto en células Huh-T7 para analizar posibles diferencias asociadas con el origen celular. Sin embargo, en ambos casos observamos el mismo efecto, en primer lugar, cuando el plásmido pHAV-luc se expresa solo, la presencia de Ars disminuye la traducción entre un 50-60%. Cuando, por otro lado, se expresa junto con $2A^{pro}$, la traducción se inhibe en más del 80%, ya sea en presencia o ausencia de Ars, y, por último, la presencia de L^{pro} estimula la traducción dirigida por el IRES de HAV más de 10 veces, tanto cuando las células están tratadas con Ars como cuando no lo están (Fig. 25A y 25B). En el caso de las células Huh-T7, también comprobamos el estado de eIF4GI (Fig. 25B, panel inferior), observándose corte cuando están presentes las proteasas.

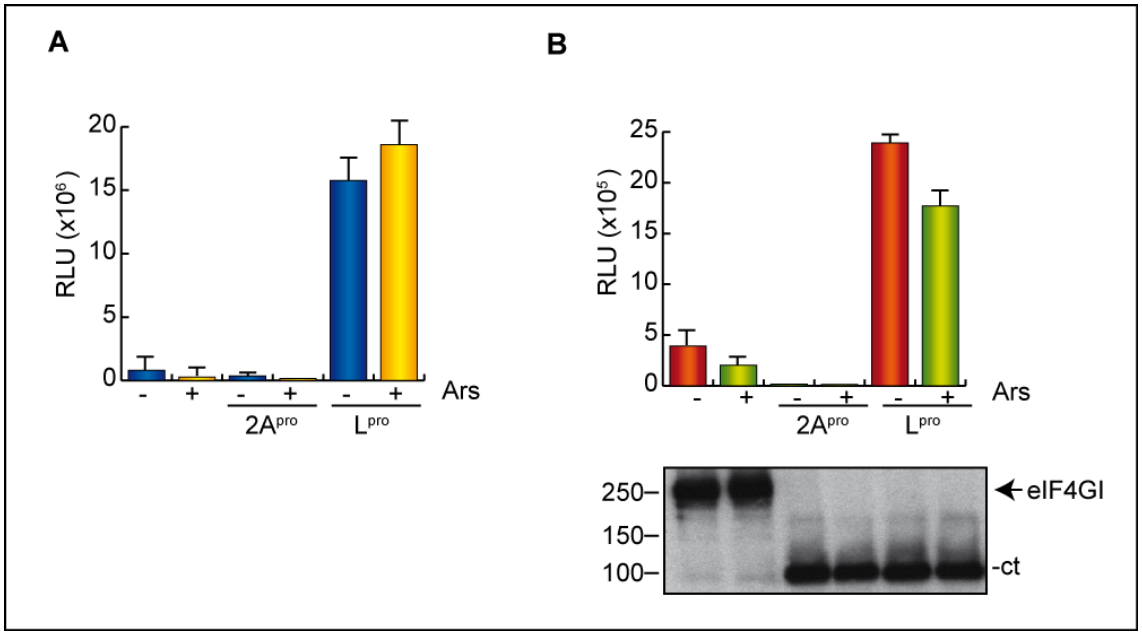

Figura 25. Estudio de la síntesis de luciferasa dirigida por el IRES de HAV en células BHK-T7 y Huh-T7. A) Las células BHK-T7 fueron transfectadas con el plásmido pHAV-luc solo o co-transfectado con pTM1-2A^{pro} o pFMDV-Lb^{pro}. A las 3 hpt las células se trataron con 200μM de Ars durante 1 hora. Pasado este tiempo, las células se recogieron y se lisaron para medir actividad luciferasa. Los valores de luciferasa obtenidos están representados en la gráfica. Las barras de error representan la D.E.. de al menos tres experimentos independientes. B) Las células Huh-T7 fueron transfectadas con el plásmido pHAV-luc solo o co-transfectado con pTM1-2A^{pro} o pFMDV-Lb^{pro}. A las 3 hpt las células se trataron con 200μM de Ars durante 1 hora. Después, las células se procesaron para medir actividad luciferasa. Los valores de luciferasa obtenidos están representados en la gráfica. Las barras de error representan la D.E. de al menos tres experimentos independientes. C) Las mismas muestras utilizadas en B se analizaron por western blot para detectar el corte del factor eIF4GI.

2.2. Estudio de la traducción del IRES de HAV en células Huh-T7 con diferentes concentraciones de L^{pro}

Para seguir estudiando la traducción del IRES de HAV cuando el factor eIF4GI está cortado, llevamos a cabo diferentes experimentos en células Huh-T7. En primer lugar transfectamos el plásmido pHAV-luc solo o lo co-transfectamos con concentraciones crecientes del plásmido pFMDV-L^{pro}. A las 2hpt recogimos las muestras para medir actividad luc.

La figura 26A muestra cómo la traducción de luc dirigida por el IRES de HAV se incrementa conforme va aumentando la cantidad de pFMDV-L^{pro}, de forma que la mayor estimulación se observa cuando la cantidad de pFMDV-L^{pro} transfectado es de 1μg, llegando a ser unas 4 veces más alta que cuando se expresa el plásmido pHAV-luc solo. Paralelamente analizamos el corte de eIF4GI por western blot, apareciendo éste cortado prácticamente por completo cuando se transfecta la cantidad más alta del plásmido (Fig. 26A, panel inferior). A continuación, linearizamos el plásmido pFMDV-L^{pro} y realizamos una transcripción *in vitro* para obtener el mRNA FMDV-L. Una vez purificado y cuantificado el mRNA, transfectamos el plásmido pHAV-luc solo o con cantidades crecientes del mRNA FMDV-L. A las 2 hpt recogimos las

células y medimos actividad luc. Al igual que antes, observamos un incremento en la síntesis de luc conforme aumentamos la cantidad del mRNA FMDV-L (Fig. 26B).

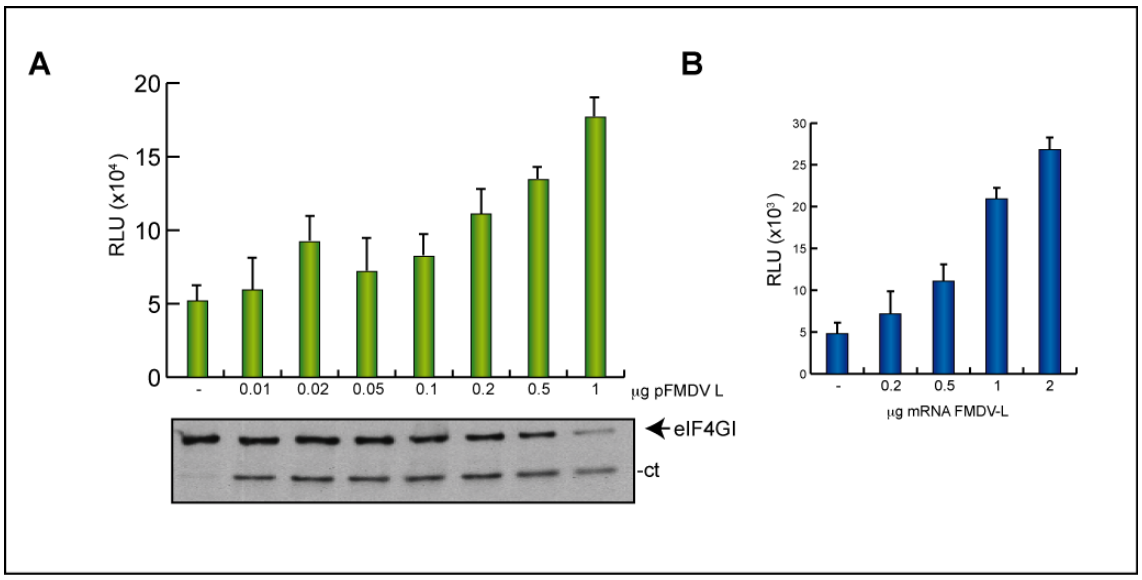

Figura 26. Estudio de la concentración de la proteasa L^{pro} y su efecto en la estimulación del IRES de HAV. A) Las células Huh-T7 fueron transfectadas con el plásmido pHAV solo o con diferentes concentraciones del plásmido pFMDV-Lb^{pro}. A las 3 hpt se procesaron las células para medir actividad luciferasa. Las barras de error representan la D.E.. Paralelamente se analizó el corte del factor eIF4GI por western blot (panel inferior). B) Se linealizó el plásmido pFMDV-Lb^{pro} para obtener el mRNA FMDV-Lb^{pro} por transcripción *in vitro*. A continuación se transfectaron células Huh-T7 con el plásmido pHAV solo o con diferentes concentraciones del mRNA FMDV-L^{pro}. A las 3 hpt se recogieron las células y se midió actividad luciferasa. Las barras de error representan la D.E.

El siguiente experimento que llevamos a cabo consistió en el análisis de la actividad del mRNA EMC-L sobre la traducción del IRES de HAV. Para ello sintetizamos *in vitro* mRNA EMC-L a partir del plásmido pTM1-L. A continuación, transfectamos cantidades crecientes del mRNA junto con el plásmido pHAV-luc. Como control transfectamos pHAV-luc solo. A las 2 hpt se recogieron las muestras y se procesaron para medir actividad luc. En la figura 27A está representada la síntesis de luc, y puede observarse, al igual que en el caso anterior, que esta síntesis se incrementa conforme aumentamos la cantidad de mRNA EMC-L transfectado (Fig. 27B). Se realizó el análisis por western blot para comprobar el estado del factor eIF4GI, el cual aparece progresivamente más hidrolizado conforme se transfectan mayores cantidades de mRNA que codifica para la proteasa (Fig.27B, panel inferior).

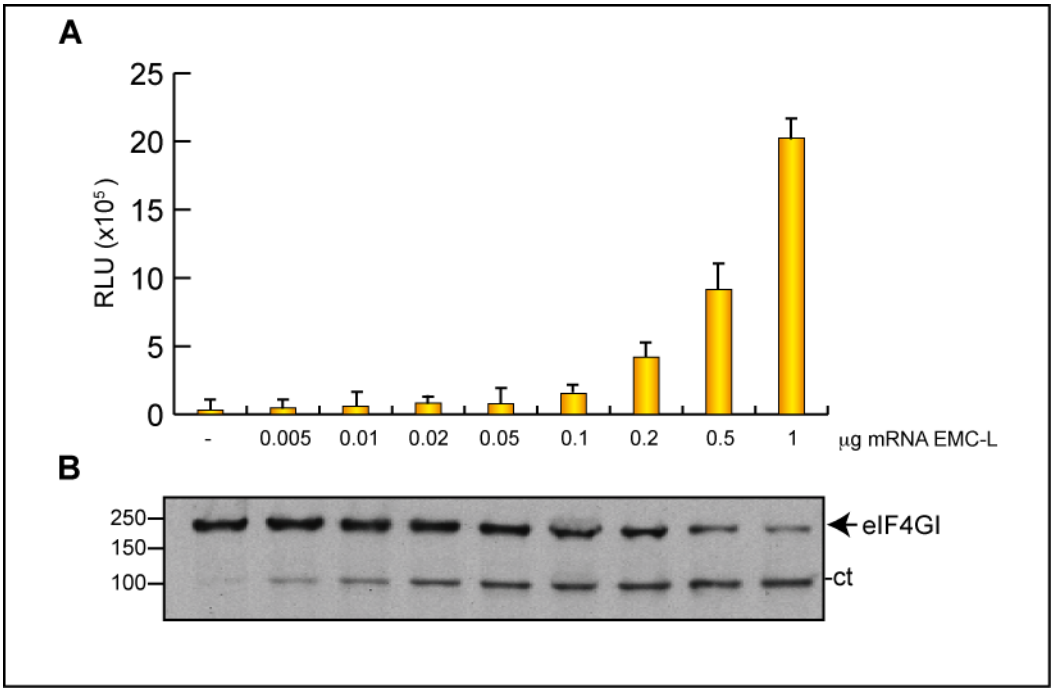

Figura 27. Estudio de la estimulación de la traducción del IRES de HAV mediada por el mRNA EMC-L. A) Se linealizó el plásmido pTM1-L para obtener el mRNA EMC-L por trancripción *in vitro*. A continuación se transfectaron células Huh-T7 con el plásmido pHAV solo o con diferentes concentraciones de mRNA EMC-L. A las 3 hpt se recogieron las células y se midió actividad luciferasa. Las barras de error representan la D.E. B) Mediante western blot se analizó el corte del factor eIF4GI.

Para comprobar que la estimulación observada en la producción de luc no era debida a que L^{pro} estuviera estimulando la etapa de transcripción, generamos el mRNA HAV-luc mediante transcripción *in vitro*. Posteriormente transfectamos el mRNA HAV-luc solo o en combinación con los mRNAs EMC-2A, EMC-L y FMDV-L. Transfectamos 1 µg de cada mRNA y a las 2 hpt recogimos las muestras y analizamos la actividad luc. Como se muestra en la figura 28A, cuando transfectamos el mRNA HAV-luc junto con los mRNAs EMC-L y FMDV-L se estimula la producción de luc, siendo esta estimulación alrededor de unas ocho y seis veces respectivamente, mientras que cuando se cotransfecta con el mRNA EMC-2A la síntesis de luc se ve fuertemente inhibida. Además, al analizar el corte del factor eIF4GI, se puede observar que se encuentra prácticamente hidrolizado por completo en presencia de las proteasas (Figura 28B).

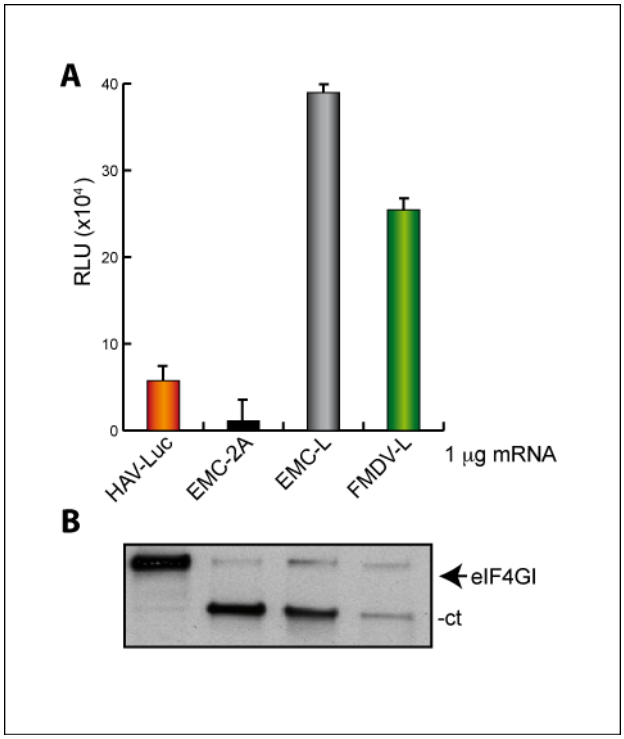

Figura 28. Estudio comparativo del efecto de los mRNAs EMC-2A, EMC-L y FMDV-L sobre la traducción del mRNA HAV-luc. A) Se linearizaron y transcribieron los plásmidos pHAV-luc, pTM1-2A, pTM1-L y pFMDV-L para obtener los mRNAs HAV-luc, EMC-2A^{pro}, EMC-L^{pro} y FMDV-L^{pro} respectivamente. A continuación se transfectó 1µg de mRNA de HAV-luc solo o se co-transfectó en presencia de 1µg de mRNA de EMC-2A^{pro}, FMDV-L^{pro} o EMC-L^{pro}. A las 3 hpt se recogieron las muestras y se lisaron para medir actividad luciferasa. B) Las mismas muestras se utilizaron para detectar el factor eIF4GI por western blot.

Por tanto, de los resultados obtenidos podríamos concluir que el IRES de HAV es capaz de traducirse cuando el factor eIF4GI se encuentra hidrolizado por acción de la proteasa L^{pro}. Además, parece existir correlación con la concentración presente de proteasa, de forma que observamos mayor eficiencia de traducción conforme aumenta el nivel de expresión.

Nuestro siguiente objetivo fue analizar la posibilidad de que al expresar 2A^{pro} se pudiera rescatar la traducción del IRES de HAV en presencia de L^{pro}. Para ello transfectamos 1 µg del mRNA HAV-luc solo o en presencia del mRNA EMC-2A o FMDV-L. Además, el mRNA de HAV-luc se contransfectó con una mezcla de 1 µg EMC-2A más concentraciones crecientes del mRNA de FMDV-L. A las 2 hpt las células se recogieron y se trataron para medir actividad luc. Como esperábamos, la presencia del mRNA EMC-2A inhibe alrededor de 8 veces la síntesis de luc, mientras que la coexpresión del mRNA HAV-luc con el mRNA de FMDV-L estimula la traducción dirigida por el IRES de HAV alrededor de 3 veces.

Sin embargo, cuando ambas proteasas se encuentran presentes, la expresión del mRNA FMDV-Lb^{pro} no es capaz de rescatar la traducción mediada por el IRES de HAV cuando 2A^{pro} está presente (Figura 29). Este resultado nos podría estar indicando la posibilidad de que 2A^{pro} pudiera estar hidrolizando algún factor celular necesario para la traducción dirigida por el IRES de HAV.

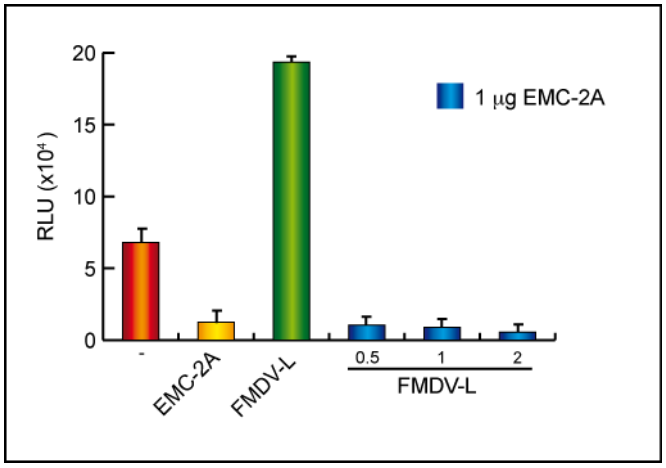

Figura 29. Estudio del rescate de la traducción del mRNA HAV-luc inhibido por el efecto de la proteasa 2A^{pro} de PV. Se transfectaron células Huh-T7 con 1 µg de mRNA HAV-luc solo o en presencia de 1 µg de mRNA EMC-2A o 1 µg de FMDV-Lb. También se transfectó 1 µg de mRNA HAV-luc junto con una mezcla de 1 µg de EMC-2A y diferentes cantidades (0,5, 1 y 2 µg) de mRNA FMDV-Lb^{pro}. A las 3 hpt se recogieron las muestras y se procesaron para medir actividad luciferasa. Las barras de error representan la D.E.

2.3. Estudio de la traducción del mRNA HAV-luc cuando el factor eIF4A está inactivado

En los últimos años, el compuesto hipuristanol ha sido ampliamente utilizado como un inhibidor específico del factor eIF4A [164, 165]. El factor eIF4G entero así como el extremo Ct interaccionan con el IRES de HAV [155]. Además, se sabe que el factor eIF4A interacciona con el extremo Ct del factor eIF4G [3]. Por este motivo, estudiamos la participación del factor eIF4A en la traducción del mRNA HAV-luc cuando el factor eIF4G ha sido hidrolizado por acción de la proteasa L^{pro}. Primeramente analizamos el efecto de cantidades crecientes de hipuristanol sobre la traducción celular.

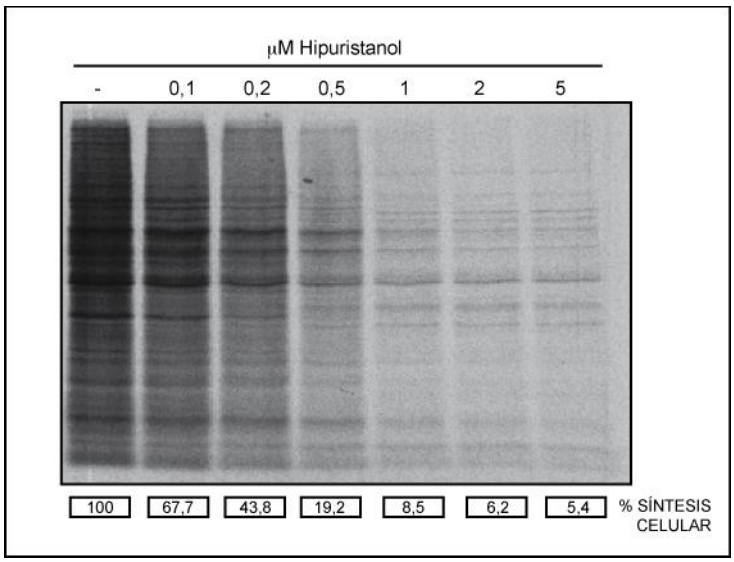

Figura 30. Efecto de la inhibición del factor eIF4A sobre la traducción de las células Huh-T7. Se incubaron células Huh-T7 en presencia de diferentes concentraciones de hipuristanol durante 30´. Pasado este tiempo se añadió medio con [^{35}S]Met/Cys y las mismas concentraciones de inhibidor durante 1h. Después las muestras se procesaron por SDS-PAGE, fluorografía y autorradiografía.

Para ello pretratamos células HuhT7 con cantidades crecientes de hipuristanol (0-5 µM) durante 30 minutos. Posteriormente, las incubamos durante una hora con las mismas concentraciones de compuesto en un medio de marcaje radiactivo de proteínas. Pasado este

tiempo, procesamos las muestras y las analizamos por SDS-PAGE, fluorografía y autorradiografía.

Como esperábamos, la traducción celular disminuye conforme aumentamos las concentraciones de hipuristanol (Fig. 30). Posteriomente analizamos la traducción dirigida por el IRES de HAV en presencia de diferentes concentraciones de hipuristanol.

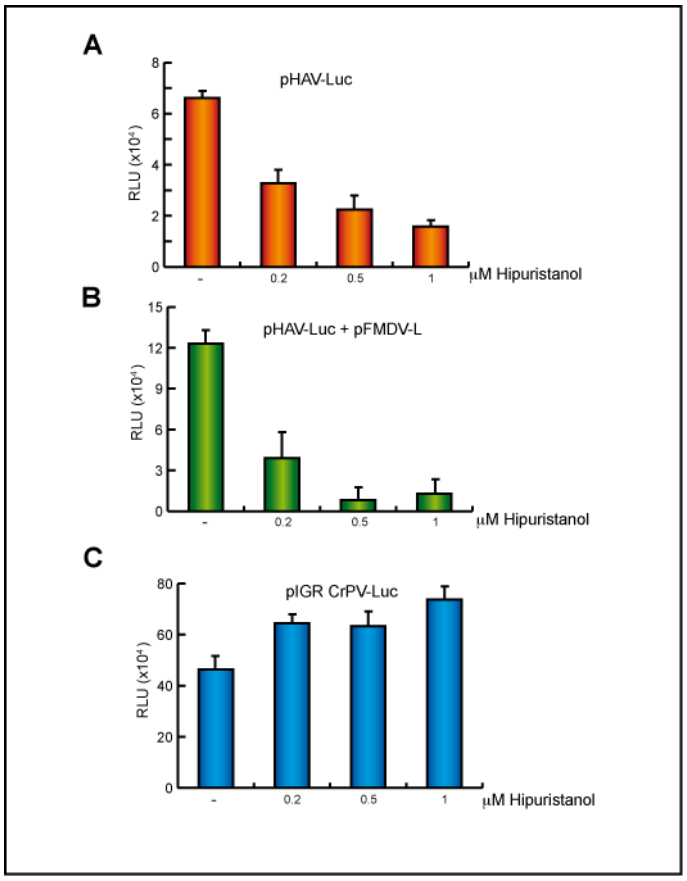

Figura 31. Efecto de la inhibición del factor eIF4A sobre la traducción del IRES de HAV. A)Las células Huh-T7 se transfectaron con el plásmido pHAV-luc..A las 2 hpt se trataron las células con 0,2, 0,5 o 1 μM de hipuristanol durante 1h30min. Después, las células se recogieron y se midió actividad luciferasa,. Las barras de error representan la D.E. obtenida de al menos tres experimentos independientes. B) Las células Huh-T7 se cotransfectaron con los plásmidos pHAV-luc pFMDV-Lb. A las 2 hpt se trataron las células con 0,2, 0,5 o 1 μM de hipuristanol durante 1h30min. Después, las células se recogieron y se midió actividad luciferasa,. Las barras de error representan la D.E. obtenida de al menos tres experimentos independientes. C) Las células Huh-T7 se transfectaron con el plásmido pIGR CrPV-luc. A las 2 hpt se trataron las células con 0,2, 0,5 o 1 μM de hipuristanol durante 1h30min. Después, las células se recogieron y se midió actividad luciferasa,. Las barras de error representan la D.E. obtenida de al menos tres experimentos independientes

En este caso también observamos una fuerte inhibición de la síntesis de luc cuando se transfecta pHAV-luc solo o cuando se cotransfecta con pFMDV-L (Fig. 31A y 31B, respectivamente). Para asegurarnos de la especificidad del compuesto utilizamos como control el plásmido pCrPV IGR-luc. En la figura 31C puede observarse como la presencia del hipuristanol no afecta la traducción dirigida por el IGR de CrPV.

Estos resultados nos indican que posiblemente el factor eIF4A se una al fragmento Ct generado por la proteasa L^{pro}. Además, podría estar indicando de manera indirecta la participación del fragmento Ct en la traducción dirigida por el IRES de HAV.

2.4. Traducción del mRNA HAV-luc en RRL

Estudios previos para esclarecer el requerimiento de los factores necesarios para la traducción dirigida por el IRES de HAV se han realizado, fundamentalmente, en RRL [117, 155]. Por tanto, decidimos utilizar también este sistema para comprobar si el efecto que estábamos observando hasta el momento era reproducible in vitro o, si por el contrario, observábamos alguna diferencia entre el sistema celular y el RRL.

También analizamos el requerimiento del factor eIF2α. Para ello, utilizamos el compuesto poli(I:C) que induce la activación de la quinasa PKR, que a su vez fosforila el factor eIF2α, inactivándolo [166]. Para testar el efecto del poli (I:C) se incubó durante diferentes tiempos con los RRL. Posteriormente analizamos el factor eIF2α fosforilado por western blot. Claramente puede observarse en la figura 32 cómo el compuesto poli (I:C) induce fosforilación de eIF2α.

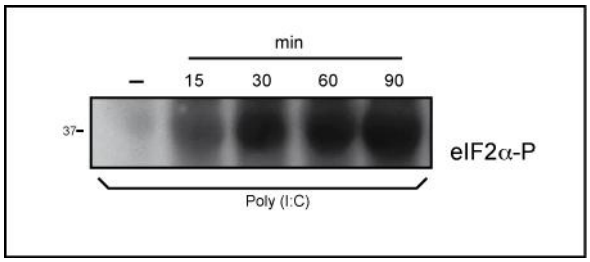

Figura 32. Estudio de la fosforilación de eIF2α inducida por el inhibidor poli (I:C) en RRL. Se trataron RRL con 50 ng de poli (I:C) y se dejaron incubando a 30ºC durante 15, 30, 60 y 90 min. Después se procesaron las muestras y se detectó la forma fosforilada de eIF2α por western blot.

Estudiamos el efecto de L^{pro} sobre el IRES de HAV mediante dos vías. En primer lugar, empleamos el mRNA EMC-Lb^{pro}. Añadimos diferentes concentraciones de este mRNA a los RLL y se incubó durante 1 h para permitir el corte de eIF4G. A continuación añadimos 50 ng de poly (I:C) y se incubó durante 30 min. Por último añadimos a la reacción 100 ng de mRNA HAV-luc durante otra hora. Pasado este tiempo, dividimos las muestras en dos alícuotas para, por un lado, medir actividad luc y, por otro, analizar el corte de eIF4GI por western blot. En la figura 33A están representados los valores de luc. Se puede observar que en este caso, conforme aumentamos la concentración de mRNA EMC-L^{pro} la síntesis de luc va diminuyendo. El efecto del inhibidor poli (I:C), cuando se encuentra el mRNA HAV-luc la inhibición es de más del 50%, mientras que cuando está la proteasa, apenas se observa disminución en la síntesis de luc. Al analizar el factor eIF4GI, éste aparece cortado en todos los casos en los que está presente la proteasa (Fig. 33A, panel inferior). Por otra parte, pensamos que al incubar juntos dos mRNAs diferentes podría estar ocurriendo una competición entre mRNAs por la maquinaria de traducción. Para ensayar este efecto, utilizamos un mRNA control que produjera una proteína sin actividad proteasa. Utilizamos el plásmido pTM1-2C, que da lugar al mRNA EMC-2C. Procedimos de la misma manera, es decir, incubamos los RRLs con concentraciones crecientes de mRNA EMC-2C. A continuación tratamos con poli (I:C) y, por último, incubamos el mRNA

HAV-luc. Como se observa en la figura 33B, en este caso también se produce una disminución en la síntesis de luc conforme aumentamos las cantidades de mRNA EMC-2C. En cuanto al efecto del poli (I:C), los valores disminuyen más del 50% en todos los casos. En la figura 33C está representado el porcentaje de síntesis de luc de los experimentos anteriores, donde el 100% sería la síntesis en ausencia de poli (I:C). Por lo tanto, conforme aumentamos la cantidad de mRNA EMC-L, la traducción de luc es igual tanto en presencia como en ausencia de poli (I:C).

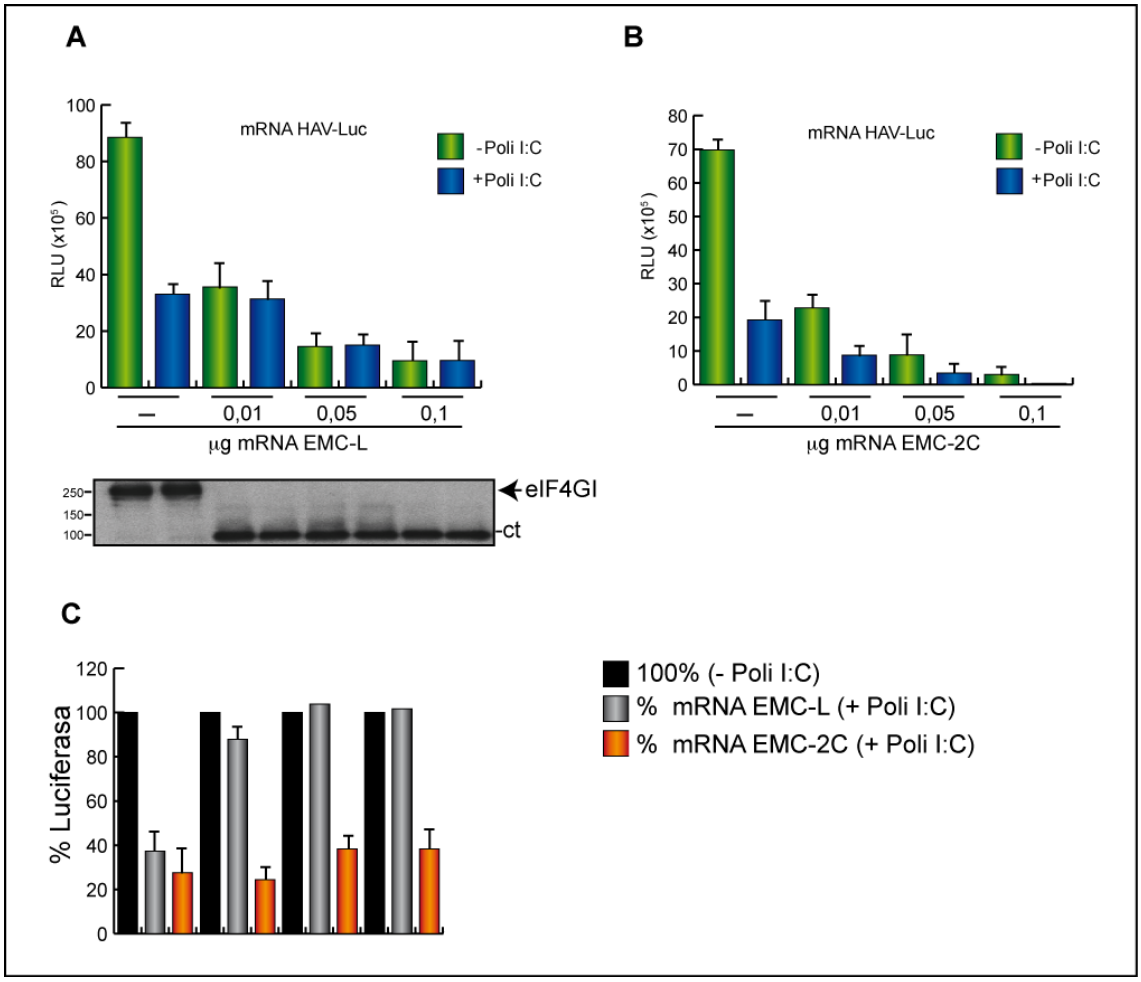

Figura 33. Efecto del mRNA EMC-L en la traducción del mRNA HAV-luc *in vitro*. Se obtuvieron por transcripción *in vitro* los mRNAs HAV-luc, EMC-L y EMC-2C. A continuación, se utilizaron RRL como sistema de traducción in vitro. Se incubaron, en primer lugar, diferentes concentraciones de mRNA EMC-L, por un lado, y mRNA EMC-2C, por otro, durante 1h. A continuación se añadió poli (I:C) durante 30´. Por último se añadió el mRNA HAV-luc y se dejó incubando durante 1h a 30ºC. Pasado este tiempo, las muestras se separaron en dos para mediar actividad luciferasa y analizar el corte del factor eIF4GI por western blot. A) Representación esquemática de la síntesis de luciferasa obtenida del mRNA HAV-Luc en presencia de mRNA EMC-L^{pro} . B) Representación esquemática de la síntesis de luciferasa a partir del mRNA HAV-luc en presencia de mRNA EMC-2C. C) Porcentaje de la síntesis de luciferasa en presencia de EMC-L o EMC-2C y del inhibidor poli (I:C). El 100% representa los valores de síntesis en ausencia de poli (I:C).

Para evitar el problema de la inhibición por competición de mRNAs, utilizamos una L^{pro} purificada cedida amablemente por el Dr. T. Skern (Max F. Perutz Laboratories). En primer lugar se añadió la proteasa a la mezcla de traducción en dos concentraciones diferentes, 10 µM

y 40 μM, e incubamos durante 20 minutos. A continuación añadimos el compuesto poli (I:C) y lo dejamos actuar durante 30 minutos. Por último, añadimos el mRNA HAV-luc y lo incubamos durante una hora. Pasado este tiempo, dividimos la muestra para medir actividad luc y para analizar el corte de eIF4GI. Como se muestra en la figura 34A, cuando añadimos 10 μM de L^{pro}, la síntesis de luc es el doble que cuando el mRNA HAV-luc se encuentra solo. Lo mismo ocurre cuando añadimos 40 μM de proteasa. Ahora bien, la presencia de poli (I:C), como era de esperar, inhibe la traducción del mRNA HAV-luc más del 50%, y lo mismo ocurre cuando añadimos 10 μM de proteasa. En cambio, con 40 μM no se observa disminución en los niveles de luc en presencia de poli (I:C). Claramente se puede ver en la figura 34B que el factor eIF4GI está completamente cortado por L^{pro}. Por tanto, al igual que ocurre en células en cultivo, la traducción en RRL del mRNA HAV-luc tiene lugar cuando el factor eIF4G está hidrolizado por acción de la proteasa L^{pro}. Además, L^{pro} confiere traducibilidad al IRES de HAV cuando el factor eIF2α se encuentra inactivo por acción del poli (I:C).

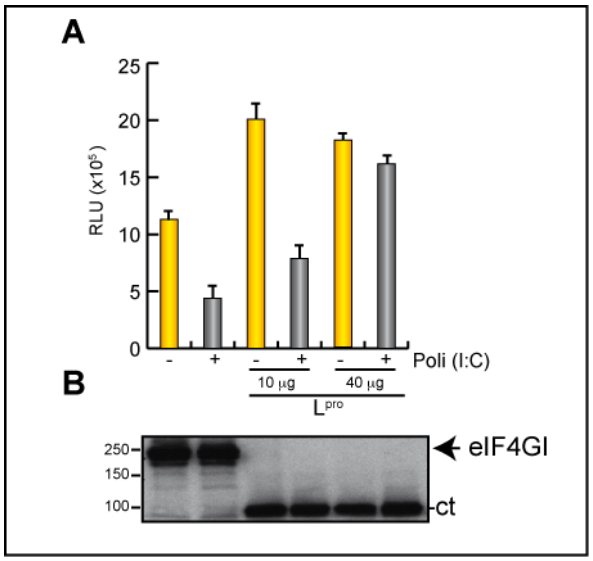

Figura 34. Efecto de L^{pro} purificada en la traducción dirigida por el IRES de HAV *in vitro*. A) Se incubó durante 20 min dos concentraciones diferentes de proteasa (10μM y 40μM). Después se añadió el inhibidor poly (I:C) durante 30´. Por último se incubó el mRNA de HAV-luc durante 1h. A) En la gráfica están representados los valores de luciferasa. Las barras de error representan la D.E.B) Se analizó el corte del factor eIF4GI por western blot.

DISCUSIÓN

1. TRADUCCIÓN DE LOS IRES DE PV Y EMCV PROMOVIDA POR LA PROTEASA 2A DEL VIRUS DE LA POLIO CUANDO EL FACTOR eIF2α ESTÁ FOSFORILADO

A lo largo de su evolución, los virus han desarrollado diferentes estrategias para apoderarse de los factores implicados en el proceso de traducción celular con el fin de favorecer la síntesis de las proteínas virales. En respuesta a la infección, las células han desarrollado diferentes mecanismos de defensa para impedir la replicación del genoma viral. Algunas de estas estrategias están encaminadas a evitar, en última instancia, la unión del mRNA viral a los ribosomas [167].

Los picornavirus poseen proteasas que además de participar en el procesamiento proteolítico de la poliproteína viral también hidrolizan proteínas de la célula hospedadora. Este es el caso de la $3C^{pro}$, presente en todas las especies de picornavirus y de la $2A^{pro}$, presente sólo en algunas especies como PV y RHV [40, 168]. Otras especies como FMDV o ERBV, poseen una proteasa denominada L^{pro}. La $2A^{pro}$ de PV y la L^{pro} de FMDV hidrolizan el factor eIF4G y así bloquean la traducción *cap* dependiente de la mayoría de los mRNAs celulares, mientras la traducción de los mRNAs virales prosigue. Existen algunas excepciones, como es el caso de EMCV, que posee las dos proteasas, L y 2A, pero durante la infección no se produce el corte de eIF4G.

El hecho de que la hidrólisis del factor eIF4G no inhiba la traducción viral se debe a que el genoma de los picornavirus no posee una estructura *cap* en su extremo 5´, en su lugar este mRNA presenta una secuencia altamente estructurada denominada IRES (Internal Ribosome Entry Site) que permite la unión directa de la maquinaria de traducción celular con el RNA viral. Los IRES de los picornavirus se han dividido en cuatro clases en función, principalmente, de su estructura y de los factores de iniciación que requieren para el proceso de la traducción. Así por ejemplo, los IRES de tipo I, representados por los IRES de PV y HRV, y los IRES de tipo II, donde se encuentran los IRES de EMCV y FMDV, no requieren el factor eIF4G para ser funcionales, pero se dividireron en dos grupos distintos ya que comparativamente, sus secuencias son muy diferentes. Al grupo III pertenece el IRES de HAV, cuyas características le sitúan como único representante dentro de este grupo. Por último, el grupo IV, representado por el IRES de PTV-1, posee características similares al IRES de HCV [29, 30].

La inhibición de la traducción es también una respuesta de defensa celular frente a la infección viral. En este caso, la célula dispone de diferentes mecanismos para detectar la presencia del RNA viral en el citoplasma y activar quinasas celulares que inactivan el factor eIF2 mediante la fosforilación de su subunidad alfa, atenuando de forma general la traducción.

En el caso de PV, existen evidencias a favor de que la inactivación progresiva del factor eIF2 por fosforilación tiene lugar conforme avanza la infección [149, 150, 169]. Se propuso que la inactivación del factor eIF2 ocurría en las etapas tardías de la infección, una vez que las proteínas virales han sido sintetizadas, lo que llevó a establecer que este factor era necesario para traducir el RNA viral. Los datos presentados en esta tesis doctoral muestran, sin embargo, que existe una fosforilación significativa del factor eIF2 en células en las que está replicando el replicón de PV y , cuando la síntesis de proteínas virales es máxima (desde aproximadamente las 3 hpt). Además, la adición de Ars, un compuesto que induce la fosforilación de eIF2α a través de la quinasa HRI no afecta significativamente la síntesis de proteínas virales a tiempos tardíos de la infección, mientras que inhibe la traducción de mRNAs celulares. Por otro lado, cuando el tratamiento con Ars comienza previamente a la replicación o infección de PV, el efecto es el contrario y se inhibe la síntesis de proteínas virales. Estos datos en conjunto indican la existencia de un mecansimo dual de traducción del mRNA de PV. Este fenómeno ya ha sido observado en otro virus, el virus Sindbis (SV), un togavirus que posee un mRNA genómico y un mRNA subgenómico denominado mRNA 26S, que codifica principalmente la secuencia de las proteínas estructurales. La traducción del mRNA 26S requiere los factores eIF2 y eIF4G tanto en sistemas *in vitro* como en sistemas celulares, pero puede traducirse sin la participación de estos factores en células infectadas durante la fase tardía de la infección [14]. En el caso de los retrovirus, también se han postulado hipótesis que sostienen que el mRNA viral es capaz de traducirse de una manera dependiente o independiente de la estructura *cap* conforme avanza la infección [29]. Por tanto, en el caso de PV podría estar ocurriendo un fenómeno parecido. En el inicio de la infección, la traducción del RNA de PV requeriría el factor eIF4G intacto, así como el factor eIF2 activo, pero conforme avanzase la infección, el mecanismo de iniciación de la traducción podría estar siendo modificado bajo la influencia de las proteínas virales, y dichos factores podrían ser ahora prescindibles. Además de las proteínas de PV, la participación de otros factores celulares e incluso el propio RNA del virus podrían estar jugando un papel determinante en la iniciación de la traducción durante la fase tardía de la infección. Recientemente este fenómeno de traducción dual de los mRNAs de picornavirus, entre ellos el de PV, ha sido descrito en dos trabajos [16, 32].

Uno de estos trabajos propone que la habilidad para traducir el mRNA viral cuando eIF2α está fosforilado podría ser conferida por la proteasa $3C^{pro}$ mediante el corte del factor eIF5b [32]. Sin embargo, nuestros resultados indican claramente que la única proteína no estructural de PV que permite mantener un elevado nivel de traducción dependiente del IRES cuando eIF2α está fosforilado (tras el tratamiento con Ars) es la $2A^{pro}$. La presencia de $2A^{pro}$ permite todavía el 60% de la síntesis de luciferasa dependiente del IRES de PV cuando se inactiva eIF2α en diferentes células de mamífero (BHK-T7 y Huh-T7). En cambio, se produce una drástica inhibición de la síntesis de luciferasa (> 80%) cuando la proteasa no está presente.

También hemos comprobado que $2A^{pro}$ es capaz de sostener la traducción dirigida por el IRES de EMCV y mantener la síntesis de luciferasa en un 60% cuando eIF2α está fosforilado. . Asimismo , durante el tratamiento con tapsigargina, una droga que induce estrés de retículo y la fosforilación de eIF2α mediante la activación de la quinasa PERK, la traducción celular se inhibe prácticamente por completo, mientras que la síntesis de $2A^{pro}$ a partir del mRNA EMC-2A se mantiene en un 50%. Esto indica que el efecto de $2A^{pro}$ sobre la traducción dirigida por los IRES de picornavirus cuando eIF2α no es activo, tiene lugar independientemente del agente que induce estrés (Ars, medio hipertónico o tapsigargina) y de la quinasa responsable de la fosforilación del eIF2α.

Por tanto, encontramos que algunos IRES de picornavirus, como los IRES de EMCV y PV, poseen características similares a los IRES de flavivirus, ya que ambos pueden traducir sus mRNAs sin utilizar el factor eIF2α [125, 170, 171].

$2A^{pro}$ es una proteasa que desempeña multitud de funciones, que interfieren con diversos procesos celulares, entre ellos, la traducción [40, 107]. . Los resultados presentados en esta tesis indican que la actividad proteolítica de $2A^{pro}$ está estrechamente relacionada con la capacidad de conferir traducibilidad a los IRES de PV y EMCV en condiciones de baja disponibilidad del factor eIF2. Tras comparar el efecto producido por la $2A^{pro}$ activa y una versión de $2A^{pro}$ mutante, que no posee actividad catalítica [79] pudimos confirmar que no solo es necesaria la presencia de la proteína $2A^{pro}$, sino que además tiene que ejercer su actividad proteolítica para llevar a cabo esta función. No obstante, no podemos descartar que la $2A^{pro}$ mutante tenga alterada alguna zona de reconocimiento e interacción con RNA u otras proteínas que sea importante para esta función. Para esclarecer este punto, en futuros experimentos se analizará comparativamente el efecto de diferentes mutantes de la proteasa. . Por tanto, las evidencias presentadas indican que $2A^{pro}$ podría estar ejerciendo un efecto directo en la traducción del RNA [108, 172], lo que implica que la presencia de $2A^{pro}$ y su actividad sobre alguna proteína celular aún no identificada serían necesarias para estimular la traducción dependiente de IRES.

El papel que desempeña $2A^{pro}$ sobre el factor eIF4G ha sido ampliamente estudiado. $2A^{pro}$, proteoliza eIF4G e inhibe, por tanto, la traducción *cap*-dependiente de la gran mayoría de los mRNAs celulares. En contraste, el corte del factor eIF4G correlaciona con un aumento de la síntesis de proteínas de PV [30], aunque existen varias evidencias que indican que esta estimulación no se produce únicamente por el corte del factor eIF4G [108, 161]. El extremo carboxilo de eIF4G, generado tras el corte de las proteasas $2A^{pro}$ de PV y L^{pro} de FMDV, es capaz de reemplazar la función del factor completo en sistemas *in vitro*, permitiendo la unión al ribosoma del IRES de EMCV [173]. Sin embargo, la presencia de este fragmento en células no estimula la traducción mediada por este IRES [108, 161, 174]. Nosotros hemos analizado la

implicación del corte de este factor por $2A^{pro}$, en la capacidad de la proteasa para conferir traducibilidad al IRES de EMCV en condiciones de estrés, en las que el factor eIF2 está fosforilado tras el tratamiento con Ars. En presencia de bajas concentraciones de $2A^{pro}$, y tras obtener un corte completo del factor eIF4G, la traducción del mRNA EMC-luc está fuertemente inhibida en presencia de Ars. Sólo cuando la expresión de $2A^{pro}$ es alta se permite la traducción de la luciferasa. Por tanto, el corte del factor eIF4G no es suficiente , para conferir traducibilidad al IRES de EMCV cuando el factor eIF2 está fosforilado. En cambio, la concentración de $2A^{pro}$ parece ser el factor limitante en este proceso. Además, tras co-expresar cada fragmento Nt ó Ct de eIF4G por separado con el mRNA EMC-luc corroboramos la idea de que el fragmento carboxilo generado tras el corte de la $2A^{pro}$ no es suficiente para estimular la traducción del IRES de EMCV [161]. También observamos que al co-expresar el fragmento carboxilo terminal con elevadas concentraciones del mutante inactivo de $2A^{pro}$ la traducción del IRES de EMCV cuando el factor eIF2 está fosforilado está inhibida.

Por tanto, nuestros datos, en conjunto, apoyan la idea de que la traducción dirigida por los IRES de EMCV o PV cuando el factor eIF2 está fosforilado exije al menos dos requerimientos, uno es la presencia de $2A^{pro}$ y su actividad proteolítica sobre el factor eIF4G (que es importante para la traducción del IRES cuando eIF2 es activo), y otro menos claro implicaría la participación de algún otro componente celular, el cual podría ser hidrolizado o no. Si se inactiva específicamente la actividad catalítica de $2A^{pro}$ con el compuesto MPCMK tras permitir el corte del factor eIF4G ésta ya no es capaz de conferir traducibilidad al IRES con independencia de eIF2. Esta prueba podría indicarnos la participación de otro(s) sustrato(s) en este proceso de traducción. Nuestra hipótesis defiende que en el contexto de la infección podría tener lugar una actividad secuencial de $2A^{pro}$, en la que en primer lugar actuaría sobre el factor eIF4G y, posteriormente, una vez que la traducción celular ha sido inhibida y la célula ha activado sus mecanismos de defensa inhibiendo el factor eIF2, podría actuar sobre otros sustratos celulares (inactivándolos mediante proteolisis) creando un ambiente celular idóneo que permite exclusivamente la traducción del mRNA viral y el progreso del ciclo viral.

Es destacable el hecho de que después de varias décadas estudiando el proceso de traducción de los picornavirus, y siendo PV un modelo importante de estudio, no se haya considerado con anterioridad la posibilidad de que eIF2 no participe en este proceso. De hecho, está ampliamente aceptado que los RNAs de los picornavirus requieren del factor eIF2 para traducirse [23], lo que ha sido respaldado por numerosos estudios en sistemas *in vitro*. Sin embargo, la idea de que el RNA de PV pudiera traducirse sin eIF2 en células infectadas no ha sido estudiada previamente. Los resultados aquí presentados demuestran que $2A^{pro}$ es la única proteína de PV que por sí sola es capaz de conferir traducibilidad al IRES de PV y al IRES de EMCV cuando el factor eIF2 se encuentra fosforilado como resultado del tratamiento con diferentes agentes que inducen estrés celular (Ars, Tg o un medio hipertónico). Podemos

plantear varias posibilidades sobre el papel que podría estar jugando $2A^{pro}$ en esta situación. En el caso del virus Hantaan (HV), un hantavirus (familia *Bunyaviridae*) que no posee estructuras IRES, se ha descrito que una única proteína viral es capaz de sustituir al complejo eIF4F para llevar a cabo la traducción [4]. De forma similar, no podemos descartar que la $2A^{pro}$ estuviera sustituyendo la función de eIF2. Otra posibilidad sería el considerar que la actividad proteolítica de $2A^{pro}$ fuera necesaria para otra función de $2A^{pro}$ desconocida hasta ahora. En este sentido, $2A^{pro}$ podría estar actuando alternativamente como una chaperona, modulando la conformación del IRES y comportándose como un ITAF, lo cual permitiría al RNA viral unirse al ribosoma prescindiendo de eIF2 y eIF4G.

Como está descrito en el caso de la IGR del CrPVes posible que durante la infección, la estructura del IRES sea capaz de encontrar la señal del AUG iniciador sin la ayuda de factores de iniciación de la traducción [175, 176].

Por otro lado, tampoco podemos descartar que algún otro factor celular estuviera sustituyendo al factor eIF2. En el caso de HCV se ha demostrado que en sistemas *in vitro* el factor eIF5b podría reemplazar al factor eIF2 [2, 171]. Por otro lado, otro trabajo también propone que podría ser la Ligatina, conocida también como eIF2D, el factor que podría sustituir la función del eIF2 en el caso del RNA de HCV pero no en el caso de EMCV [171]. Un trabajo más reciente realizado en sistemas celulares, ha demostrado la capacidad del mRNA de HCV de utilizar el factor eIF2A como sustituto de eIF2 en condiciones de estrés en las que existe baja o disponibilidad nula de este factor [126].

Estos nuevos e inesperados resultados abren una nueva área de investigación en el campo de la traducción de los picornavirus. Futuras investigaciones irán encaminadas a elucidar las proteínas celulares implicadas en la traducción del IRES de picornavirus cuando eIF2α es inactivo.

2. ESTUDIO DE LA TRADUCCIÓN DIRIGIDA POR EL IRES DEL VIRUS DE LA HEPATITIS A EN PRESENCIA DEL FACTOR eIF4GI CORTADO

El virus de la hepatitis A es el prototipo del género hepatovirus, dentro de la familia Picornaviridae. Al igual que el resto de los picornavirus, posee una región UTR (Untranslated Region) en su extremo 5´, pero a diferencia de los demás, el IRES de HAV se clasificó en un grupo independiente por su incapacidad para traducirse cuando el factor eIF4G estaba hidrolizado. Esta característica hizo clasificar al IRES de HAV en el grupo III [29, 30].

Sin embargo, en esta tesis se han presentado resultados que indican que la traducción dirigida por el IRES de HAV puede tener lugar cuando el factor eIF4G está hidrolizado por acción de la proteasa L^{pro} de FMDV. Este hecho implica que el IRES de HAV no sería una excepción respecto al mecanismo de traducción del resto de los picornavirus.

Aunque desconocemos la razón de las discrepancias con respecto a los resultados obtenidos por otro grupo [117, 155], los datos presentados en esta tesis confirman claramente que la traducción mediada por el IRES de HAV es independiente del corte de eIF4G En primer lugar hemos estudiado en cultivos celulares cómo la proteasa L^{pro} de FMDV es capaz de estimular la traducción del mRNA HAV-luc cuando el factor eIF4G está totalmente hidrolizado. Además, hemos observado que parece existir cierta correlación entre los niveles de traducción del IRES de HAV y la concentración de L^{pro}. De hecho, comprobamos que cuanto mayor es la concentración de proteasa, mayor es la proporción de eIF4G cortado y mayores son los niveles de traducción del mRNA HAV-luc. En nuestros experimentos hemos empleado construcciones que dan lugar a mRNA monocistrónicos, siendo estos mRNAs más fisiológicos que los obtenidos cuando se utilizan mRNAs dicistrónicos. Aunque estos mRNAs han sido ampliamente utilizados y han representado una herramienta muy útil en el estudio de los IRES, sería mejor utilizar mRNAs monocistrónicos para comprender el funcionamiento de estas estructuras [177, 178].

Es interesante el efecto antagónico que presentan la proteasa $2A^{pro}$ de PV y la proteasa L^{pro} de FMDV sobre la traducción del mRNA HAV-luc. Una posibilidad es que la $2A^{pro}$ estuviera hidrolizando algún factor necesario para la traducción mediada por el IRES de HAV. Aunque en este sentido se ha observado que la adición del complejo eIF4F purificado restablece la inhibición generada por $2A^{pro}$ en la traducción de HAV [155]. Otra posibilidad podría estar relacionada con los fragmentos generados tras el corte del factor eIF4G. En el caso de $2A^{pro}$ el corte se produce entre los aa 681-682, mientras que en el caso de L^{pro}, el corte tiene lugar entre los aa 674-675 [40]. Por tanto, el fragmento generado tras el corte llevado a cabo por L^{pro} es siete residuos más largo que el que se produce con $2A^{pro}$. Sin embargo, esta posibilidad es poco probable.

Lo más factible sería la opción de que $2A^{pro}$ esté cortando algún factor necesario para traducir el mRNA HAV-luc. En este sentido hemos comprobado como al transfectar simultáneamente mRNAs que codifican para ambas proteasas junto con el mRNA HAV-luc, se produce una fuerte inhibición de la síntesis de luciferasa. Por tanto, el efecto inhibitorio de $2A^{pro}$ no se contrarresta al estar presente L^{pro}.

Nuestros resultados también indican que el fragmento Ct generado tras el corte de eIF4G por acción de L^{pro} es necesario para la traducción dirigida por el IRES de HAV. Este fragmento Ct une el factor eIF4A y es necesario para traducir los mRNAs que poseen IRES de picornavirus [3, 173]. Utilizando un inhibidor específico del factor eIF4A hemos observado como la traducción del mRNA HAV-luc se bloquea. En este sentido ocurre igual que con los IRES tipo I y II, ya que también necesitan el factor eIF4A para ser funcionales [30].

Respecto al requerimiento del factor eIF2, hemos aportado evidencias que indican que la proteasa L^{pro} modifica dicho requerimiento para traducir el mRNA HAV-luc. La síntesis de luciferasa que tiene lugar a partir de este mRNA se ve inhibida por Ars en cultivos celulares así como por la adición de poli(I:C) en RRL. Sin embargo esta inhibición no se observa cuando la proteasa L^{pro} está presente.

Por tanto la traducción dirigida por el IRES de HAV tiene lugar no solo cuando el factor eIF4G ha sido hidrolizado por la proteasa L^{pro}, sino también cuando el factor eIF2 está inactivado por fosforilación. Pero en este último caso es necesaria la presencia de altas concentraciones de L^{pro}. Esto indica que el corte de eIF4G por L^{pro} no es suficiente para conferir traducibilidad al IRES de HAV cuando el factor eIF2 no se encuentra disponible. Este resultado coincide con lo observado en el caso de $2A^{pro}$ de PV y los IRES de EMCV y PV.

Muchos estudios se han llevado a cabo para comprender el mecanismo por el cual se traducen los mRNAs de los picornavirus. Aunque se han realizado muchos avances al respecto, continuamente aparecen nuevos e inesperados descubrimientos. De hecho, nuestros resultados indican claramente que el requerimiento de factores del IRES de HAV es más parecido al de los IRES de los grupos I y II de lo que se pensaba anteriormente. Por tanto la clasificación actual necesitaría ser revisada.

Aunque los virus estudiados en esta tesis no suponen un problema de salud en los países desarrollados, existen aún zonas en los que su prevalencia acarrea importantes problemas para la salud pública. Así por ejemplo, según la Organización Mundial de la Salud (OMS), a pesar de los esfuerzos hechos para su erradicación, en 2012 el virus de la poliomielitis está declarado endémico en tres países (Afganistán, Nigeria y Paquistán). Afecta principalmente a niños menores de 5 años, y puede causar una parálisis permanente. Aunque desde 1989 los casos de polio en el mundo han disminuido en más de un 99%, la presencia de un único caso es una

amenaza. De hecho, en los años 2009-2010 se reportaron casos de enfermedad en 23 países declarados libres de polio [179].

El virus de la hepatitis A, por otro lado, es responsable de producir hepatitis agudas en el ser humano, que en algunos casos se convierten en hepatitis fulminantes. En los últimos años, gracias a las mejoras en los sistemas sanitarios, la mortalidad de la hepatitis A ha disminuido, aunque es una importante causa de morbilidad en algunas zonas. Sobre todo en áreas donde la inmunidad es baja o que presentan epidemias intermitentes, han surgido brotes de larga duración y difícil control, que traen consigo los consecuentes problemas económicos y de salud pública [180].

En estas dos infecciones virales, la vacunación así como la información a la población de buenas prácticas higiénico-sanitarias son métodos importantes para prevenir la infección, pero el desarrollo de nuevas opciones de tratamiento son importantes como medida de control de la enfermedad.

El estudio de la traducción viral es un campo en el que continuamente se están realizando nuevos hallazgos. Desde trabajos que muestran la participación o la capacidad de prescindir de determinados factores celulares, hasta el descubrimiento de nuevos sistemas de traducción viral desconocidos previamente. De hecho, se están llevando a cabo estudios muy interesantes que nos hacen comprender mejor la capacidad de los virus para evolucionar y crear estrategias de evasión frente a los mecanismos de defensa de las células a las que infectan. Esto a su vez, nos ayudará a entender mejor los mecanismos de traducción celular en diferentes contextos, como son los procesos de respuesta inmune o la transformación celular. En este último caso, se están haciendo grandes avances en el desarrollo de terapias oncolíticas empleando virus con genoma RNA [181]. Aunque, por otro lado, cada vez son más los tumores cuya aparición se relaciona con la presencia de virus en las células transformadas [182, 183]. Por otro lado, también son cada vez más las enfermedades autoinmunes y degenerativas asociadas a infecciones virales y otros microorganismos [184].

Por tanto la virología molecular y, más concretamente, el estudio de la traducción viral, nos ayudará en última instancia a desarrollar nuevos tratamientos y vacunas. En nuestro caso, experimentos futuros irán encaminados al estudio de la traducción de los mRNAs de los picornavirus y a esclarecer el papel que desempeñan las proteasas $2A^{pro}$ de PV y L^{pro} de FMDV.

CONCLUSIONES

1. El genoma de PV se traduce mediante un mecanismo dual que varía a lo largo de la infección. Tras la entrada del virus y la desencapsidación, la traducción del mRNA viral requiere el factor eIF2α, sin embargo conforme avanza la infección y la síntesis de proteínas virales es máxima, los mRNAs virales se traducen de un modo independiente de eIF2α.

2. La proteasa $2A^{pro}$ es la única proteína no estructural de PV que estimula la traducción de los IRES de PV y EMCV cuando eIF2α está fosforilado. Además, la estimulación que ejerce la proteasa $2A^{pro}$ sobre el IRES de EMCV tiene lugar en diferentes situaciones de estrés que conllevan fosforilación de eIF2α.

3. La actividad proteolítica de $2A^{pro}$ es esencial para conferir independencia del factor eIF2 durante la traducción dependiente de IRES. Además, esta función requiere una alta concentración de la proteasa $2A^{pro}$ y no está relacionada con el corte de eIF4GI. Así, la presencia de una cantidad mínima de $2A^{pro}$ activa que produce el corte completo del factor eIF4G no confiere independencia traduccional del factor eIF2.

4. El fragmento C-terminal de eIF4GI generado tras el corte proteolítico de la proteasa $2A^{pro}$ no es suficiente para estimular la traducción mediada por el IRES de EMCV, ni para conferir independencia del factor eIF2α. La presencia del fragmento C-terminal de eIF4GI y una alta concentración de una proteasa $2A^{pro}$ inactiva tampoco otorga traducibilidad al IRES de EMCV.

5. Las proteasas $2A^{pro}$ de PV y L^{pro} de FMDV tienen efectos opuestos en su capacidad de estimular la traducción mediada por el IRES de HAV en cultivos celulares. La traducción mediada por este IRES tiene lugar en presencia de la proteasa L^{pro} cuando el factor eIF4GI está hidrolizado, mientras que se encuentra inhibida en presencia de la $2A^{pro}$. Además, la L^{pro} es capaz de conferir independencia de eIF2α durante la traducción mediada por el IRES de HAV.

6. La traducción mediada por el IRES de HAV requiere el factor eIF4A activo. El fragmento C-terminal generado tras el corte de L^{pro} podría ser necesario para unirse el factor eIF4A, lo que favorecería la traducción dirigida por el IRES de HAV.

7. En sistemas *in vitro* la proteasa L^{pro} también estimula la traducción mediada por el IRES de HAV cuando el factor eIF4GI está hidrolizado. Asimismo, a altas concentraciones la L^{pro} promueve la traducción del IRES de HAV cuando el eIF2α está fosforilado.

ABREVIATURAS

$2A^{pro}$	Proteasa 2A de PV
$3C^{pro}$	Proteasa 3C de PV
Ars	Arsenito
CHX	Cicloheximida
CrPV IGR	Cricket Paralysis Virus
Ct	Dominio carboxilo-terminal de eIF4G
DMEM	Medio Mínimo de Eagle Modificado por Dulbecco
DNA	ADN, ácido desoxirribonucleio
E.coli	*Escherichia coli*
eIF	Factor de iniciación eucariótico
EMCV	Virus de la encefalomiocarditis
ERBV	Virus de la rinitis equina B
FMDV	Virus de la fiebre aftosa
HAV	Virus de la hepatitis A
HCV	Virus de la hepatitis C
hpe	Horas post-electroporación
hpt	Horas post-transfección
IRES	Sitio de entrada interna del ribosoma
Kb	Kilobase
KDa	Kilodaltons
L^{pro}	Proteasa L de FMDV
Luc	Luciferasa
MCPMK:	Metoxisuccinil-Ala-Ala-Pro-Val-clorometilcetona
Met/Cys	Metionina/cisteína
Met-$tRNA_i$	ARN (*RNA*) mensajero
min	minutos
mRNA	tRNA iniciador unido a metionina
NaCl	Cloruro sódico
Nt	Dominio amino-terminal de eIF4G
PBS	Tampón salino fosfato
PCR	Reacción en cadena de la polimerasa
Poli(A)	Poliadenosina

Poli(I:C)	Ácido poliinosínico:polycitidílico
PV	Virus de la polio
Rep	Replicón
RRL	Lisados de reticulocitos de conejo
SDS-PAGE	Electroforesis en geles de poliacrilamida en presencia de SDS
TBS	Tampón Tris salino
Tg	Tapsigargina
wt	Tipo salvaje o estándar (wild type)

BIBLIOGRAFÍA

1. Lopez-Lastra, M., et al., *Translation initiation of viral mRNAs.* Reviews in medical virology, 2010. **20**(3): p. 177-95.

2. Dmitriev, S.E., et al., *GTP-independent tRNA delivery to the ribosomal P-site by a novel eukaryotic translation factor.* The Journal of biological chemistry, 2010. **285**(35): p. 26779-87.

3. Parsyan, A., et al., *mRNA helicases: the tacticians of translational control.* Nature reviews. Molecular cell biology, 2011. **12**(4): p. 235-45.

4. Mir, M.A. and A.T. Panganiban, *A protein that replaces the entire cellular eIF4F complex.* The EMBO journal, 2008. **27**(23): p. 3129-39.

5. Thomas, M.G., et al., *RNA granules: the good, the bad and the ugly.* Cellular signalling, 2011. **23**(2): p. 324-34.

6. Besse, F. and A. Ephrussi, *Translational control of localized mRNAs: restricting protein synthesis in space and time.* Nature reviews. Molecular cell biology, 2008. **9**(12): p. 971-80.

7. Martin, K.C. and A. Ephrussi, *mRNA localization: gene expression in the spatial dimension.* Cell, 2009. **136**(4): p. 719-30.

8. Haasnoot, J. and B. Berkhout, *RNAi and cellular miRNAs in infections by mammalian viruses.* Methods in molecular biology, 2011. **721**: p. 23-41.

9. Pager, C.T., et al., *MicroRNA-mediated gene silencing.* Progress in molecular biology and translational science, 2009. **90**: p. 187-210.

10. Pearson, C.E., *Repeat associated non-ATG translation initiation: one DNA, two transcripts, seven reading frames, potentially nine toxic entities!* PLoS genetics, 2011. **7**(3): p. e1002018.

11. Zu, T., et al., *Non-ATG-initiated translation directed by microsatellite expansions.* Proceedings of the National Academy of Sciences of the United States of America, 2011. **108**(1): p. 260-5.

12. Wethmar, K., J.J. Smink, and A. Leutz, *Upstream open reading frames: molecular switches in (patho)physiology.* BioEssays : news and reviews in molecular, cellular and developmental biology, 2010. **32**(10): p. 885-93.

13. Castello, A., et al., *Translation of Sindbis virus 26S mRNA does not require intact eukariotic initiation factor 4G.* Journal of molecular biology, 2006. **355**(5): p. 942-56.

14. Sanz, M.A., et al., *Dual mechanism for the translation of subgenomic mRNA from Sindbis virus in infected and uninfected cells.* PloS one, 2009. **4**(3): p. e4772.

15. Ventoso, I., et al., *Translational resistance of late alphavirus mRNA to eIF2alpha phosphorylation: a strategy to overcome the antiviral effect of protein kinase PKR.* Genes & development, 2006. **20**(1): p. 87-100.

16. Welnowska, E., et al., *Translation of Viral mRNA without Active eIF2: The Case of Picornaviruses.* PloS one, 2011. **6**(7): p. e22230.

17. Redondo, N., et al., *Translation without eIF2 Promoted by Poliovirus 2A Protease.* PloS one, 2011. **6**(10): p. e25699.

18. Jackson, R.J., C.U. Hellen, and T.V. Pestova, *The mechanism of eukaryotic translation initiation and principles of its regulation.* Nature reviews. Molecular cell biology, 2010. **11**(2): p. 113-27.

19. Lorsch, J.R. and T.E. Dever, *Molecular view of 43 S complex formation and start site selection in eukaryotic translation initiation.* The Journal of biological chemistry, 2010. **285**(28): p. 21203-7.

20. Sonenberg, N. and A.G. Hinnebusch, *Regulation of translation initiation in eukaryotes: mechanisms and biological targets.* Cell, 2009. **136**(4): p. 731-45.

21. Pestova, T.V., J.R. Lorsch, and C.U. Hellen, *The Mechanism of Translation Initiation in Eukaryotes. Translational Control in Biology and Medicine* 2007, New York: Cold Spring Harbor.

22. Kapp, L.D. and J.R. Lorsch, *The molecular mechanics of eukaryotic translation.* Annual review of biochemistry, 2004. **73**: p. 657-704.

23. Pestova, T.V., et al., *Molecular mechanisms of translation initiation in eukaryotes.* Proceedings of the National Academy of Sciences of the United States of America, 2001. **98**(13): p. 7029-36.

24. Preiss, T. and W.H. M, *Starting the protein synthesis machine: eukaryotic translation initiation.* BioEssays : news and reviews in molecular, cellular and developmental biology, 2003. **25**(12): p. 1201-11.

25. Acker, M.G. and J.R. Lorsch, *Mechanism of ribosomal subunit joining during eukaryotic translation initiation.* Biochemical Society transactions, 2008. **36**(Pt 4): p. 653-7.

26. Sonenberg, N. and T.E. Dever, *Eukaryotic translation initiation factors and regulators.* Current opinion in structural biology, 2003. **13**(1): p. 56-63.

27. Gebauer, F. and M.W. Hentze, *Molecular mechanisms of translational control.* Nature reviews. Molecular cell biology, 2004. **5**(10): p. 827-35.

28. Nomoto, A., Y.F. Lee, and E. Wimmer, *The 5' end of poliovirus mRNA is not capped with m7G(5')ppp(5')Np.* Proceedings of the National Academy of Sciences of the United States of America, 1976. **73**(2): p. 375-80.

29. Balvay, L., et al., *Structural and functional diversity of viral IRESes.* Biochimica et biophysica acta, 2009. **1789**(9-10): p. 542-57.

30. Belsham, G.J., *Divergent picornavirus IRES elements.* Virus research, 2009. **139**(2): p. 183-92.

31. Fitzgerald, K.D. and B.L. Semler, *Bridging IRES elements in mRNAs to the eukaryotic translation apparatus.* Biochimica et biophysica acta, 2009. **1789**(9-10): p. 518-28.

32. White, J.P., L.C. Reineke, and R.E. Lloyd, *Poliovirus switches to an eIF2-independent mode of translation during infection.* Journal of virology, 2011. **85**(17): p. 8884-93.

33. Lin, J.Y., et al., *Viral and host proteins involved in picornavirus life cycle.* Journal of biomedical science, 2009. **16**: p. 103.

34. I. E.C. Leong, C.T.C.a.B.L.S., *processing determinants and functions of cleavage products of picornavirus polyproteins*, in *Molecular biology of Picornaviruses*, B.L. Semler and E. Wimmer, Editors. 2002, ASM Press: Washington, DC, USA. p. 187-198.

35. T. Skern, B.H., A. Guarné et al., *Structure and function of picornavirus proteinases*, in *Molecular Biology of Picornaviruses*, B.L.S.a.E. Wimmer, Editor 2002, ASM Press: Washington, DC, USA. p. 199-212.

36. Lee, C.K. and E. Wimmer, *Proteolytic processing of poliovirus polyprotein: elimination of 2Apro-mediated, alternative cleavage of polypeptide 3CD by in vitro mutagenesis.* Virology, 1988. **166**(2): p. 405-14.

37. Cameron, C.E., D.W. Gohara, and J.J. Arnold, *Poliovirus RNA-dependent RNA polymerase (3Dpol): structure, function and mechanism*, in *Molecular Biology of Picornaviruses*, B.L. Semler and E. Wimmer, Editors. 2002: Washington, DC, USA. p. 255-268.

38. Paul, A.V., *Possible Unifying mechanism of picornavirus genome replication*, in *Molecular Biology of Picornaviruses*, B.L. Semler and E. Wimmer, Editors. 2002: Washington, DC, USA. p. 227-246.

39. Paul, A.V., et al., *Protein-primed RNA synthesis by purified poliovirus RNA polymerase.* Nature, 1998. **393**(6682): p. 280-4.

40. Castello, A., E. Alvarez, and L. Carrasco, *The multifaceted poliovirus 2A protease: regulation of gene expression by picornavirus proteases.* Journal of biomedicine & biotechnology, 2011. **2011**: p. 369648.

41. Lloyd, R.E., *Translational control by viral proteinases.* Virus research, 2006. **119**(1): p. 76-88.

42. Almela, M.J., M.E. Gonzalez, and L. Carrasco, *Inhibitors of poliovirus uncoating efficiently block the early membrane permeabilization induced by virus particles.* Journal of virology, 1991. **65**(5): p. 2572-7.

43. Guinea, R. and L. Carrasco, *Phospholipid biosynthesis and poliovirus genome replication, two coupled phenomena.* The EMBO journal, 1990. **9**(6): p. 2011-6.

44. Carrasco, L., et al., *Effects of viral replication on cellular membrane metabolism and function,* in *Molecular Biology of Picornaviruses*, B.L.S.a.E. Wimmer, Editor 2002, ASM Press: Washington, DC, USA. p. 337-356.

45. Agirre, A., et al., *Viroporin-mediated membrane permeabilization. Pore formation by nonstructural poliovirus 2B protein.* The Journal of biological chemistry, 2002. **277**(43): p. 40434-41.

46. Gonzalez, M.E. and L. Carrasco, *Viroporins.* FEBS letters, 2003. **552**(1): p. 28-34.

47. Madan, V., *Viroporinas de virus animales con genoma RNA*, 2006, Universidad Autónoma de Madrid: Madrid.

48. Hogle, J.M., M. Chow, and D.J. Filman, *Three-dimensional structure of poliovirus at 2.9 A resolution.* Science, 1985. **229**(4720): p. 1358-65.

49. Kitamura, N., et al., *Primary structure, gene organization and polypeptide expression of poliovirus RNA.* Nature, 1981. **291**(5816): p. 547-53.

50. Molla, A., A.V. Paul, and E. Wimmer, *Cell-free, de novo synthesis of poliovirus.* Science, 1991. **254**(5038): p. 1647-51.

51. Pelletier, J. and N. Sonenberg, *Internal initiation of translation of eukaryotic mRNA directed by a sequence derived from poliovirus RNA.* Nature, 1988. **334**(6180): p. 320-5.

52. Wimmer, E., et al., *Synthetic viruses: a new opportunity to understand and prevent viral disease.* Nature biotechnology, 2009. **27**(12): p. 1163-72.

53. Etchison, D., et al., *Inhibition of HeLa cell protein synthesis following poliovirus infection correlates with the proteolysis of a 220,000-dalton polypeptide associated with eucaryotic initiation factor 3 and a cap binding protein complex.* The Journal of biological chemistry, 1982. **257**(24): p. 14806-10.

54. Ryan, M.D. and M. Flint, *Virus-encoded proteinases of the picornavirus super-group.* The Journal of general virology, 1997. **78 (Pt 4)**: p. 699-723.

55. Agol, V.A., *Picornavirus genome: an overview*, in *Molecular Biology of Picornaviruses*, B.L.a.W. Semler, E, Editor 2002: Washington, DC, USA. p. 127-148.

56. Guarne, A., et al., *Structural and biochemical features distinguish the foot-and-mouth disease virus leader proteinase from other papain-like enzymes.* Journal of molecular biology, 2000. **302**(5): p. 1227-40.

57. Guarne, A., et al., *Structure of the foot-and-mouth disease virus leader protease: a papain-like fold adapted for self-processing and eIF4G recognition.* The EMBO journal, 1998. **17**(24): p. 7469-79.

58. Piccone, M.E., et al., *The foot-and-mouth disease virus leader proteinase gene is not required for viral replication.* Journal of virology, 1995. **69**(9): p. 5376-82.

59. de Los Santos, T., et al., *The leader proteinase of foot-and-mouth disease virus inhibits the induction of beta interferon mRNA and blocks the host innate immune response.* Journal of virology, 2006. **80**(4): p. 1906-14.

60. de los Santos, T., et al., *A conserved domain in the leader proteinase of foot-and-mouth disease virus is required for proper subcellular localization and function.* Journal of virology, 2009. **83**(4): p. 1800-10.

61. Hato, S.V., et al., *Differential IFN-alpha/beta production suppressing capacities of the leader proteins of mengovirus and foot-and-mouth disease virus.* Cellular microbiology, 2010. **12**(3): p. 310-7.

62. Devaney, M.A., et al., *Leader protein of foot-and-mouth disease virus is required for cleavage of the p220 component of the cap-binding protein complex.* Journal of virology, 1988. **62**(11): p. 4407-9.

63. Glaser, W. and T. Skern, *Extremely efficient cleavage of eIF4G by picornaviral proteinases L and 2A in vitro.* FEBS letters, 2000. **480**(2-3): p. 151-5.

64. Lloyd, R.E., M.J. Grubman, and E. Ehrenfeld, *Relationship of p220 cleavage during picornavirus infection to 2A proteinase sequencing.* Journal of virology, 1988. **62**(11): p. 4216-23.

65. Donnelly, M.L., et al., *The cleavage activities of aphthovirus and cardiovirus 2A proteins.* The Journal of general virology, 1997. **78 (Pt 1)**: p. 13-21.

66. Konig, H. and B. Rosenwirth, *Purification and partial characterization of poliovirus protease 2A by means of a functional assay.* Journal of virology, 1988. **62**(4): p. 1243-50.

67. Toyoda, H., et al., *A second virus-encoded proteinase involved in proteolytic processing of poliovirus polyprotein.* Cell, 1986. **45**(5): p. 761-70.

68. Ventoso, I., A. Barco, and L. Carrasco, *Genetic selection of poliovirus 2Apro-binding peptides.* Journal of virology, 1999. **73**(1): p. 814-8.

69. Foeger, N., W. Glaser, and T. Skern, *Recognition of eukaryotic initiation factor 4G isoforms by picornaviral proteinases.* The Journal of biological chemistry, 2002. **277**(46): p. 44300-9.

70. Haghighat, A., et al., *The eIF4G-eIF4E complex is the target for direct cleavage by the rhinovirus 2A proteinase.* Journal of virology, 1996. **70**(12): p. 8444-50.

71. Ventoso, I., et al., *Poliovirus 2A proteinase cleaves directly the eIF-4G subunit of eIF-4F complex.* FEBS letters, 1998. **435**(1): p. 79-83.

72. Bovee, M.L., et al., *Direct cleavage of elF4G by poliovirus 2A protease is inefficient in vitro.* Virology, 1998. **245**(2): p. 241-9.

73. Wyckoff, E.E., R.E. Lloyd, and E. Ehrenfeld, *Relationship of eukaryotic initiation factor 3 to poliovirus-induced p220 cleavage activity.* Journal of virology, 1992. **66**(5): p. 2943-51.

74. Zamora, M., W.E. Marissen, and R.E. Lloyd, *Multiple eIF4GI-specific protease activities present in uninfected and poliovirus-infected cells.* Journal of virology, 2002. **76**(1): p. 165-77.

75. Gradi, A., et al., *Proteolysis of human eukaryotic translation initiation factor eIF4GII, but not eIF4GI, coincides with the shutoff of host protein synthesis after poliovirus infection.* Proceedings of the National Academy of Sciences of the United States of America, 1998. **95**(19): p. 11089-94.

76. Irurzun, A., et al., *Monensin and nigericin prevent the inhibition of host translation by poliovirus, without affecting p220 cleavage.* Journal of virology, 1995. **69**(12): p. 7453-60.

77. Perez, L. and L. Carrasco, *Lack of direct correlation between p220 cleavage and the shut-off of host translation after poliovirus infection.* Virology, 1992. **189**(1): p. 178-86.

78. Barco, A., I. Ventoso, and L. Carrasco, *The yeast Saccharomyces cerevisiae as a genetic system for obtaining variants of poliovirus protease 2A.* The Journal of biological chemistry, 1997. **272**(19): p. 12683-91.

79. Ventoso, I., A. Barco, and L. Carrasco, *Mutational analysis of poliovirus 2Apro. Distinct inhibitory functions of 2apro on translation and transcription.* The Journal of biological chemistry, 1998. **273**(43): p. 27960-7.

80. Yu, S.F., et al., *Defective RNA replication by poliovirus mutants deficient in 2A protease cleavage activity.* Journal of virology, 1995. **69**(1): p. 247-52.

81. Teterina, N.L., E.A. Levenson, and E. Ehrenfeld, *Viable polioviruses that encode 2A proteins with fluorescent protein tags.* Journal of virology, 2010. **84**(3): p. 1477-88.

82. Igarashi, H., et al., *2A protease is not a prerequisite for poliovirus replication.* Journal of virology, 2010. **84**(12): p. 5947-57.

83. Morrison, J.M. and V.R. Racaniello, *Proteinase 2Apro is essential for enterovirus replication in type I interferon-treated cells.* Journal of virology, 2009. **83**(9): p. 4412-22.

84. Kuyumcu-Martinez, N.M., M. Joachims, and R.E. Lloyd, *Efficient cleavage of ribosome-associated poly(A)-binding protein by enterovirus 3C protease.* Journal of virology, 2002. **76**(5): p. 2062-74.

85. Belov, G.A., et al., *Bidirectional increase in permeability of nuclear envelope upon poliovirus infection and accompanying alterations of nuclear pores.* Journal of virology, 2004. **78**(18): p. 10166-77.

86. Castello, A., et al., *RNA nuclear export is blocked by poliovirus 2A protease and is concomitant with nucleoporin cleavage.* Journal of cell science, 2009. **122**(Pt 20): p. 3799-809.

87. Sanz, M.A., et al., *Translation driven by picornavirus IRES is hampered from Sindbis virus replicons: rescue by poliovirus 2A protease.* Journal of molecular biology, 2010. **402**(1): p. 101-17.

88. Gorbalenya, A.E., E.V. Koonin, and M.M. Lai, *Putative papain-related thiol proteases of positive-strand RNA viruses. Identification of rubi- and aphthovirus proteases and delineation of a novel conserved domain associated with proteases of rubi-, alpha- and coronaviruses.* FEBS letters, 1991. **288**(1-2): p. 201-5.

89. Gradi, A., et al., *Cleavage of eukaryotic translation initiation factor 4GII within foot-and-mouth disease virus-infected cells: identification of the L-protease cleavage site in vitro.* Journal of virology, 2004. **78**(7): p. 3271-8.

90. Kirchweger, R., et al., *Foot-and-mouth disease virus leader proteinase: purification of the Lb form and determination of its cleavage site on eIF-4 gamma.* Journal of virology, 1994. **68**(9): p. 5677-84.

91. Hinton, T.M., et al., *Conservation of L and 3C proteinase activities across distantly related aphthoviruses.* The Journal of general virology, 2002. **83**(Pt 12): p. 3111-21.

92. Belsham, G.J., *Dual initiation sites of protein synthesis on foot-and-mouth disease virus RNA are selected following internal entry and scanning of ribosomes in vivo.* The EMBO journal, 1992. **11**(3): p. 1105-10.

93. Sangar, D.V., et al., *All foot and mouth disease virus serotypes initiate protein synthesis at two separate AUGs.* Nucleic acids research, 1987. **15**(8): p. 3305-15.

94. Cao, X., et al., *Functional analysis of the two alternative translation initiation sites of foot-and-mouth disease virus.* Journal of virology, 1995. **69**(1): p. 560-3.

95. de Los Santos, T., F. Diaz-San Segundo, and M.J. Grubman, *Degradation of nuclear factor kappa B during foot-and-mouth disease virus infection.* Journal of virology, 2007. **81**(23): p. 12803-15.

96. Chinsangaram, J., M. Koster, and M.J. Grubman, *Inhibition of L-deleted foot-and-mouth disease virus replication by alpha/beta interferon involves double-stranded RNA-dependent protein kinase.* Journal of virology, 2001. **75**(12): p. 5498-503.

97. Chinsangaram, J., M.E. Piccone, and M.J. Grubman, *Ability of foot-and-mouth disease virus to form plaques in cell culture is associated with suppression of alpha/beta interferon.* Journal of virology, 1999. **73**(12): p. 9891-8.

98. Wang, D., et al., *The leader proteinase of foot-and-mouth disease virus negatively regulates the type I interferon pathway by acting as a viral deubiquitinase.* Journal of virology, 2011. **85**(8): p. 3758-66.

99. Yu, Y., et al., *The mechanism of translation initiation on Aichivirus RNA mediated by a novel type of picornavirus IRES.* The EMBO journal, 2011. **30**(21): p. 4423-36.

100. Belsham, G.J. and R.J. Jackson, *Translation initiation on picornavirus RNA*, in *Translational Control of Gene Expression*, N. Sonenberg, J.W. Hershey, and M.B. Mathews, Editors. 2000, Cold Spring Harbor: New York.

101. Doudna, J. and P. Sarnow, *Translation Initiation by viral internal ribosome entry sites.*, in *Translational Control in Biology an Medicine*2007, CSHL. p. 129-153.

102. Dorner, A.J., et al., *In vitro translation of poliovirus RNA: utilization of internal initiation sites in reticulocyte lysate.* Journal of virology, 1984. **50**(2): p. 507-14.

103. Svitkin, Y.V., et al., *The requirement for eukaryotic initiation factor 4A (elF4A) in translation is in direct proportion to the degree of mRNA 5' secondary structure.* RNA, 2001. **7**(3): p. 382-94.

104. Bordeleau, M.E., et al., *Functional characterization of IRESes by an inhibitor of the RNA helicase eIF4A.* Nature chemical biology, 2006. **2**(4): p. 213-20.

105. Borman, A.M., et al., *Comparison of picornaviral IRES-driven internal initiation of translation in cultured cells of different origins.* Nucleic acids research, 1997. **25**(5): p. 925-32.

106. Dobrikova, E.Y., et al., *Competitive translation efficiency at the picornavirus type 1 internal ribosome entry site facilitated by viral cis and trans factors.* Journal of virology, 2006. **80**(7): p. 3310-21.

107. Hambidge, S.J. and P. Sarnow, *Translational enhancement of the poliovirus 5' noncoding region mediated by virus-encoded polypeptide 2A.* Proceedings of the National Academy of Sciences of the United States of America, 1992. **89**(21): p. 10272-6.

108. Roberts, L.O., R.A. Seamons, and G.J. Belsham, *Recognition of picornavirus internal ribosome entry sites within cells; influence of cellular and viral proteins.* RNA, 1998. **4**(5): p. 520-9.

109. Ziegler, E., et al., *Picornavirus 2A proteinase-mediated stimulation of internal initiation of translation is dependent on enzymatic activity and the cleavage products of cellular proteins.* Virology, 1995. **213**(2): p. 549-57.

110. Pestova, T.V., C.U. Hellen, and I.N. Shatsky, *Canonical eukaryotic initiation factors determine initiation of translation by internal ribosomal entry.* Molecular and cellular biology, 1996. **16**(12): p. 6859-69.

111. Pilipenko, E.V., et al., *A cell cycle-dependent protein serves as a template-specific translation initiation factor.* Genes & development, 2000. **14**(16): p. 2028-45.

112. Monie, T.P., et al., *Structural insights into the transcriptional and translational roles of Ebp1.* The EMBO journal, 2007. **26**(17): p. 3936-44.

113. Chard, L.S., et al., *Hepatitis C virus-related internal ribosome entry sites are found in multiple genera of the family Picornaviridae.* The Journal of general virology, 2006. **87**(Pt 4): p. 927-36.

114. Brown, E.A., A.J. Zajac, and S.M. Lemon, *In vitro characterization of an internal ribosomal entry site (IRES) present within the 5' nontranslated region of hepatitis A virus RNA: comparison with the IRES of encephalomyocarditis virus.* Journal of virology, 1994. **68**(2): p. 1066-74.

115. Glass, M.J., X.Y. Jia, and D.F. Summers, *Identification of the hepatitis A virus internal ribosome entry site: in vivo and in vitro analysis of bicistronic RNAs containing the HAV 5' noncoding region.* Virology, 1993. **193**(2): p. 842-52.

116. Ali, I.K., et al., *Activity of the hepatitis A virus IRES requires association between the cap-binding translation initiation factor (eIF4E) and eIF4G.* Journal of virology, 2001. **75**(17): p. 7854-63.

117. Borman, A.M. and K.M. Kean, *Intact eukaryotic initiation factor 4G is required for hepatitis A virus internal initiation of translation.* Virology, 1997. **237**(1): p. 129-36.

118. Whetter, L.E., et al., *Low efficiency of the 5' nontranslated region of hepatitis A virus RNA in directing cap-independent translation in permissive monkey kidney cells.* Journal of virology, 1994. **68**(8): p. 5253-63.

119. Schultz, D.E., C.C. Hardin, and S.M. Lemon, *Specific interaction of glyceraldehyde 3-phosphate dehydrogenase with the 5'-nontranslated RNA of hepatitis A virus.* The Journal of biological chemistry, 1996. **271**(24): p. 14134-42.

120. Zell, R., et al., *Porcine teschoviruses comprise at least eleven distinct serotypes: molecular and evolutionary aspects.* Journal of virology, 2001. **75**(4): p. 1620-31.

121. Witwer, C., et al., *Conserved RNA secondary structures in Picornaviridae genomes.* Nucleic acids research, 2001. **29**(24): p. 5079-89.

122. Pisarev, A.V., et al., *Functional and structural similarities between the internal ribosome entry sites of hepatitis C virus and porcine teschovirus, a picornavirus.* Journal of virology, 2004. **78**(9): p. 4487-97.

123. Pestova, T.V. and C.U. Hellen, *Internal initiation of translation of bovine viral diarrhea virus RNA.* Virology, 1999. **258**(2): p. 249-56.

124. Pestova, T.V., et al., *A prokaryotic-like mode of cytoplasmic eukaryotic ribosome binding to the initiation codon during internal translation initiation of hepatitis C and classical swine fever virus RNAs.* Genes & development, 1998. **12**(1): p. 67-83.

125. Terenin, I.M., et al., *Eukaryotic translation initiation machinery can operate in a bacterial-like mode without eIF2.* Nature structural & molecular biology, 2008. **15**(8): p. 836-41.

126. Kim, J.H., et al., *eIF2A mediates translation of hepatitis C viral mRNA under stress conditions.* The EMBO journal, 2011. **30**(12): p. 2454-64.

127. Lancaster, A.M., E. Jan, and P. Sarnow, *Initiation factor-independent translation mediated by the hepatitis C virus internal ribosome entry site.* RNA, 2006. **12**(5): p. 894-902.

128. Roberts, L.O. and E. Groppelli, *An atypical IRES within the 5' UTR of a dicistrovirus genome.* Virus research, 2009. **139**(2): p. 157-65.

129. Garrey, J.L., et al., *Host and viral translational mechanisms during cricket paralysis virus infection.* Journal of virology, 2010. **84**(2): p. 1124-38.

130. Pyronnet, S., L. Pradayrol, and N. Sonenberg, *A cell cycle-dependent internal ribosome entry site.* Molecular cell, 2000. **5**(4): p. 607-16.

131. Goh, W.C., et al., *HIV-1 Vpr increases viral expression by manipulation of the cell cycle: a mechanism for selection of Vpr in vivo.* Nature medicine, 1998. **4**(1): p. 65-71.

132. Alvarez, E., et al., *HIV protease cleaves poly(A)-binding protein.* The Biochemical journal, 2006. **396**(2): p. 219-26.

133. Alvarez, E., L. Menendez-Arias, and L. Carrasco, *The eukaryotic translation initiation factor 4GI is cleaved by different retroviral proteases.* Journal of virology, 2003. **77**(23): p. 12392-400.

134. Ventoso, I., et al., *HIV-1 protease cleaves eukaryotic initiation factor 4G and inhibits cap-dependent translation.* Proceedings of the National Academy of Sciences of the United States of America, 2001. **98**(23): p. 12966-71.

135. Buchholz, U.J., S. Finke, and K.K. Conzelmann, *Generation of bovine respiratory syncytial virus (BRSV) from cDNA: BRSV NS2 is not essential for virus replication in tissue culture, and the human RSV leader region acts as a functional BRSV genome promoter.* Journal of virology, 1999. **73**(1): p. 251-9.

136. Hanahan, D., *Studies on transformation of Escherichia coli with plasmids.* J Mol Biol, 1983. **166**(4): p. 557-80.

137. Studier, F.W. and B.A. Moffatt, *Use of bacteriophage T7 RNA polymerase to direct selective high-level expression of cloned genes.* J Mol Biol, 1986. **189**(1): p. 113-30.

138. Studier, F.W., et al., *Use of T7 RNA polymerase to direct expression of cloned genes.* Methods Enzymol, 1990. **185**: p. 60-89.

139. Aldabe, R., *Modificaciones celulares inducidas por proteínas del virus de la polio*, 1995, Universidad Autónoma de Madrid: Madrid.

140. Aldabe, R., et al., *Expression of poliovirus 2Apro in mammalian cells: effects on translation.* FEBS letters, 1995. **377**(1): p. 1-5.

141. Aldabe, R., A. Barco, and L. Carrasco, *Membrane permeabilization by poliovirus proteins 2B and 2BC.* The Journal of biological chemistry, 1996. **271**(38): p. 23134-7.

142. Aldabe, R. and L. Carrasco, *Induction of membrane proliferation by poliovirus proteins 2C and 2BC.* Biochemical and biophysical research communications, 1995. **206**(1): p. 64-76.

143. Andino, R., et al., *Poliovirus RNA synthesis utilizes an RNP complex formed around the 5'-end of viral RNA.* The EMBO journal, 1993. **12**(9): p. 3587-98.

144. Novoa, I., *Efecto de la proteasa 2A del virus de la polio sobre la traducción de ARNm*, 1996, Universidad Autónoma de Madrid: Madrid.

145. Sambrook, J., Fritsch, E.R. y Maniatis, T., *Molecular Cloning: A Laboratory Manual*2001, New York, NY: Cold Spring Harbor Laboratory Press.

146. Dulbecco, R. and G. Freeman, *Plaque production by the polyoma virus.* Virology, 1959. **8**(3): p. 396-7.

147. Liljestrom, P. and H. Garoff, *Internally located cleavable signal sequences direct the formation of Semliki Forest virus membrane proteins from a polyprotein precursor.* J Virol, 1991. **65**(1): p. 147-54.

148. Pestova, T.V., et al., *eIF2-dependent and eIF2-independent modes of initiation on the CSFV IRES: a common role of domain II.* The EMBO journal, 2008. **27**(7): p. 1060-72.

149. Neznanov, N., et al., *Different effect of proteasome inhibition on vesicular stomatitis virus and poliovirus replication.* PloS one, 2008. **3**(4): p. e1887.

150. O'Neill, R.E. and V.R. Racaniello, *Inhibition of translation in cells infected with a poliovirus 2Apro mutant correlates with phosphorylation of the alpha subunit of eucaryotic initiation factor 2.* Journal of virology, 1989. **63**(12): p. 5069-75.

151. Fernandez, J., et al., *Regulation of internal ribosomal entry site-mediated translation by phosphorylation of the translation initiation factor eIF2alpha.* The Journal of biological chemistry, 2002. **277**(21): p. 19198-205.

152. Wehner, K.A., S. Schutz, and P. Sarnow, *OGFOD1, a novel modulator of eukaryotic translation initiation factor 2alpha phosphorylation and the cellular response to stress.* Molecular and cellular biology, 2010. **30**(8): p. 2006-16.

153. Black, T.L., et al., *The cellular 68,000-Mr protein kinase is highly autophosphorylated and activated yet significantly degraded during poliovirus infection: implications for translational regulation.* Journal of virology, 1989. **63**(5): p. 2244-51.

154. Black, T.L., G.N. Barber, and M.G. Katze, *Degradation of the interferon-induced 68,000-M(r) protein kinase by poliovirus requires RNA.* Journal of virology, 1993. **67**(2): p. 791-800.

155. Borman, A.M., Y.M. Michel, and K.M. Kean, *Detailed analysis of the requirements of hepatitis A virus internal ribosome entry segment for the eukaryotic initiation factor complex eIF4F.* Journal of virology, 2001. **75**(17): p. 7864-71.

156. Rojas, M., C.F. Arias, and S. Lopez, *Protein kinase R is responsible for the phosphorylation of eIF2alpha in rotavirus infection.* Journal of virology, 2010. **84**(20): p. 10457-66.

157. Hamanaka, R.B., et al., *PERK and GCN2 contribute to eIF2alpha phosphorylation and cell cycle arrest after activation of the unfolded protein response pathway.* Molecular biology of the cell, 2005. **16**(12): p. 5493-501.

158. Goossens, A., et al., *The protein kinase Gcn2p mediates sodium toxicity in yeast.* The Journal of biological chemistry, 2001. **276**(33): p. 30753-60.

159. Bevilacqua, E., et al., *eIF2alpha phosphorylation tips the balance to apoptosis during osmotic stress.* The Journal of biological chemistry, 2010. **285**(22): p. 17098-111.

160. Novoa, I., et al., *Feedback inhibition of the unfolded protein response by GADD34-mediated dephosphorylation of eIF2alpha.* The Journal of cell biology, 2001. **153**(5): p. 1011-22.

161. Kaiser, C., et al., *Activation of cap-independent translation by variant eukaryotic initiation factor 4G in vivo.* RNA, 2008. **14**(10): p. 2170-82.

162. Molla, A., C.U. Hellen, and E. Wimmer, *Inhibition of proteolytic activity of poliovirus and rhinovirus 2A proteinases by elastase-specific inhibitors.* Journal of virology, 1993. **67**(8): p. 4688-95.

163. Whetter, L.E., et al., *Analysis of hepatitis A virus translation in a T7 polymerase-expressing cell line.* Archives of virology. Supplementum, 1994. **9**: p. 291-8.

164. Lindqvist, L., et al., *Selective pharmacological targeting of a DEAD box RNA helicase.* PloS one, 2008. **3**(2): p. e1583.

165. Lindqvist, L. and J. Pelletier, *Inhibitors of translation initiation as cancer therapeutics.* Future medicinal chemistry, 2009. **1**(9): p. 1709-22.

166. Berlanga, J.J., et al., *Antiviral effect of the mammalian translation initiation factor 2alpha kinase GCN2 against RNA viruses.* The EMBO journal, 2006. **25**(8): p. 1730-40.

167. Mohr, I.J., T. Peery, and M.B. Mathews, *Protein synthesis and translational control during viral infection*, in *Translation Control in Biology and Medicine*, C.S.H.L., Editor 2007: New York. p. 545-599.

168. Kuyumcu-Martinez, N.M., et al., *Cleavage of poly(A)-binding protein by poliovirus 3C protease inhibits host cell translation: a novel mechanism for host translation shutoff.* Molecular and cellular biology, 2004. **24**(4): p. 1779-90.

169. Ransone, L.J. and A. Dasgupta, *A heat-sensitive inhibitor in poliovirus-infected cells which selectively blocks phosphorylation of the alpha subunit of eucaryotic initiation factor 2 by the double-stranded RNA-activated protein kinase.* Journal of virology, 1988. **62**(10): p. 3551-7.

170. Lukavsky, P.J., *Structure and function of HCV IRES domains.* Virus research, 2009. **139**(2): p. 166-71.

171. Skabkin, M.A., et al., *Activities of Ligatin and MCT-1/DENR in eukaryotic translation initiation and ribosomal recycling.* Genes & development, 2010. **24**(16): p. 1787-801.

172. Macadam, A.J., et al., *Role for poliovirus protease 2A in cap independent translation.* The EMBO journal, 1994. **13**(4): p. 924-7.

173. Lomakin, I.B., C.U. Hellen, and T.V. Pestova, *Physical association of eukaryotic initiation factor 4G (eIF4G) with eIF4A strongly enhances binding of eIF4G to the internal ribosomal entry site of encephalomyocarditis virus and is required for internal initiation of translation.* Molecular and cellular biology, 2000. **20**(16): p. 6019-29.

174. De Gregorio, E., T. Preiss, and M.W. Hentze, *Translation driven by an eIF4G core domain in vivo.* The EMBO journal, 1999. **18**(17): p. 4865-74.

175. Deniz, N., et al., *Translation initiation factors are not required for Dicistroviridae IRES function in vivo.* RNA, 2009. **15**(5): p. 932-46.

176. Wilson, J.E., et al., *Naturally occurring dicistronic cricket paralysis virus RNA is regulated by two internal ribosome entry sites.* Molecular and cellular biology, 2000. **20**(14): p. 4990-9.

177. Junemann, C., et al., *Picornavirus internal ribosome entry site elements can stimulate translation of upstream genes.* The Journal of biological chemistry, 2007. **282**(1): p. 132-41.

178. Niepmann, M., *Internal translation initiation of picornaviruses and hepatitis C virus.* Biochimica et biophysica acta, 2009. **1789**(9-10): p. 529-41.

179. WHO. http://www.who.int/topics/poliomyelitis/en/.

180. FitzSimons, D., et al., *Hepatitis A and E: update on prevention and epidemiology.* Vaccine, 2010. **28**(3): p. 583-8.

181. Russell, S.J., *RNA viruses as virotherapy agents.* Cancer gene therapy, 2002. **9**(12): p. 961-6.

182. Nikitin, P.A. and M.A. Luftig, *The DNA damage response in viral-induced cellular transformation.* British journal of cancer, 2012. **106**(3): p. 429-35.

183. Hippocrate, A., L. Oussaief, and I. Joab, *Possible role of EBV in breast cancer and other unusually EBV-associated cancers.* Cancer letters, 2011. **305**(2): p. 144-9.

184. Pordeus, V., et al., *Infections and autoimmunity: a panorama.* Clinical reviews in allergy & immunology, 2008. **34**(3): p. 283-99.

Cellular Microbiology (2010) **12**(8), 1144–1157
doi:10.1111/j.1462-5822.2010.01460.x
First published online 22 April 2010

Cell permeabilization by poliovirus 2B viroporin triggers bystander permeabilization in neighbouring cells through a mechanism involving gap junctions

Vanesa Madan,*† Natalia Redondo and Luis Carrasco
Centro de Biología Molecular 'Severo Ochoa' (CSIC-UAM), C/Nicolás Cabrera 1, Universidad Autónoma de Madrid, Canto Blanco, 28049 Madrid, Spain.

Summary

Poliovirus 2B protein is a well-known viroporin implicated in plasma membrane permeabilization to ions and low-molecular-weight compounds during infection. Translation in mammalian cells expressing 2B protein is inhibited by hygromycin B (HB) but remains unaffected in mock cells, which are not permeable to the inhibitor. Here we describe a previously unreported bystander effect in which healthy baby hamster kidney (BHK) cells become sensitive to HB when co-cultured with a low proportion of cells expressing poliovirus 2B. Viroporins E from mouse hepatitis virus, 6K from Sindbis virus and NS4A protein from hepatitis C virus were also able to permeabilize neighbouring cells to different extents. Expression of 2B induced permeabilization of neighbouring cell lines other than BHK. We found that gap junctions are responsible mediating the observed bystander permeabilization. Gap junctional communication was confirmed in 2B-expressing co-cultures by fluorescent dye transfer. Moreover, the presence of connexin 43 was confirmed in both mock and 2B-transfected cells. Finally, inhibition of HB entry to neighbouring cells was observed with 18α-glycyrrhethinic acid, an inhibitor of gap junctions. Taken together, these findings support a mechanism involving gap junctional intercellular communication in the bystander permeabilization effect observed in healthy cells co-cultured with poliovirus 2B-expressing cells.

Received 22 November, 2009; revised 21 February, 2010; accepted 10 March, 2010. *For correspondence. E-mail Vanesa_Madan@med.uni-heidelberg.de; Tel. (+49) 6221 56 4834; Fax (+49) 6221 56 4570.
†Present address: Department of Infectious Diseases, Molecular Virology, University of Heidelberg, D-69120 Heidelberg, Germany.

Introduction

Poliovirus (PV) infection leads to plasma membrane permeabilization and proliferation of intracellular vesicles in which viral replication complexes are assembled (Bienz *et al.*, 1992; Schlegel *et al.*, 1996). PV 2B protein and its precursor 2BC are the main effectors of membrane leakiness, and together with 3A protein, they induce a significant rearrangement of internal cellular membranes (Aldabe and Carrasco, 1995; Suhy *et al.*, 2000; Choe *et al.*, 2005). PV 2B has been previously described as a genuine member of the viroporin family that is able to permeabilize bacteria, yeast and mammalian cells to ions and small molecules (Aldabe *et al.*, 1996; van Kuppeveld *et al.*, 1997; Agirre *et al.*, 2002). Viroporins are small proteins encoded by animal viruses and contain at least one membrane-spanning domain (Gonzalez and Carrasco, 1998; Ye and Hogue, 2007; Gan *et al.*, 2008). The main function of these very hydrophobic proteins during the viral life cycle is to facilitate the release of viral particles from cells (Klimkait *et al.*, 1990; van Kuppeveld *et al.*, 1997; Sanz *et al.*, 2003). Viroporins assemble in homopolymers to form ion channels in cellular membranes and they constitute a target for antiviral drug development (Pinto *et al.*, 1992; Ewart *et al.*, 1996; Melton *et al.*, 2002; Pavlovic *et al.*, 2003; Wilson *et al.*, 2004; Madan *et al.*, 2007; Griffin *et al.*, 2008; Pielak *et al.*, 2009). Recently, the three-dimensional structure of a viroporin has been unravelled (Luik *et al.*, 2009). Electron microscopy studies revealed that hexamers of the hepatitis C virus (HCV) p7 viroporin assemble to form a flower-shaped structure with protruding petals oriented towards the ER lumen. These studies are not only of fundamental interest to understand viroporin architecture, but may also aid in the design of antiviral compounds against p7 protein. Indeed, HCV p7 is a key target to develop compounds that block HCV infection (Pavlovic *et al.*, 2003; Griffin *et al.*, 2008). Apart from HCV p7, picornavirus 2B is one of the best-characterized viroporins (van Kuppeveld *et al.*, 1997; Agirre *et al.*, 2002). We recently reported that an amphipathic peptide spanning 2B residues 35–55 effectively allows diffusion of solutes with a molecular weight under 1 kDa both in mammalian cells and in boundary liposomes (Madan *et al.*, 2007). In that study, addition of the peptide to patch-clamped natural plasma

membrane induced ion channel activity, indicating that this region of 2B is endowed with pore-forming activity. In a comparative study of the ability of different viroporins to permeabilize the plasma membrane of baby hamster kidney (BHK) cells, PV 2B together with E protein from mouse hepatitis virus powerfully and rapidly induced permeabilization, whereas other viroporins such as HCV p7, influenza A virus M2 or 6K from Sindbis virus (SV) were less effective or required longer expression to achieve similar membrane alterations in BHK cells (Madan, 2008). To date, a combination of electrophysiological measurements and studies involving entry of unpermeant translation inhibitors, such as hygromycin B (HB), in cells expressing a specific viral product has allowed pore-forming proteins to be distinguished from other viral proteins with cytotoxic properties, both in prokaryotic and in eukaryotic cells (Guinea and Carrasco, 1994; Wang *et al*., 1994; Ewart *et al*., 1996; Barco and Carrasco, 1998; Gonzalez and Carrasco, 1998; Wilson *et al*., 2004; Madan *et al*., 2005). In the last few years, certain viral proteins such as E and 3a from coronavirus and Vpr from HIV-1 have been reported to be released from mammalian cells to the extracellular medium (Maeda *et al*., 1999; Huang *et al*., 2006; Xiao *et al*., 2008). However, their function either as soluble or integral membrane proteins in secreted lipid vesicles is still largely unknown. Extracellular Vpr has been shown to deregulate expression of various cytokines and inflammatory proteins, as well as to induce cell death in uninfected bystander cells (Huang *et al*., 2000; Moon and Yang, 2006; Xiao *et al*., 2008). Here, we investigate whether 2B protein is released from transfected cells to the extracellular medium and whether it permeabilizes non-transfected neighbouring cells. Our findings reveal that 2B expression in a small proportion of BHK cells induces substantial permeabilization to HB in healthy neighbouring cells. We provide compelling evidence to support the hypothesis that 2B-mediated bystander permeabilization of neighbouring cells takes place via HB passage through connexin gap junctions.

Results

Expression of PV 2B protein in BHK cells induces membrane permeabilization of neighbouring cells

Expression of PV 2B induces membrane permeabilization to ions and small molecules (e.g. nucleotides, Ca^{2+} ions or antibiotics such as HB) in mammalian cells to a similar extent as in the mid-phase of virus infection (van Kuppeveld *et al*., 1997). In previous works we noted that even though a low percentage of BHK cells was transfected with SV-derived replicons coding for 2B, the whole cell culture was almost entirely permeabilized. To assess membrane permeabilization to the translation inhibitor HB in cells neighbouring 2B-expressing cells, decreasing proportions of 2B-transfected cells were co-cultured with non-transfected cells. Membrane permeabilization was assayed by protein labelling with [^{35}S] Met/Cys at different time points. In the presence of HB, protein synthesis is expected to occur only in non-transfected neighbouring cells, while those that express 2B are permeable to the inhibitor and do not synthesize cellular proteins. We found that neighbouring cells were powerfully permeabilized to HB (~50% translation inhibition) from 5 h post electroporation (hpe) when cultured with 2B-expressing cells at ratios as low as 1:8 (Fig. 1A and C). By 8 hpe, translation of healthy cells was reduced to 20% compared with controls, indicating increased entry of HB (see right graph in Fig. 1C). Increasing proportions of viroporin-expressing cells (from 1/4 or 25%) led to an almost complete permeabilization of neighbouring cells to HB from 5 hpe. Simultaneously, immunofluorescence assays using specific antibodies against 2B protein were performed in order to visualize the presence of the viral protein in these co-cultures (Fig. 1B). PV 2B was not detected in the majority of cultured cells, with only an estimated 25% of cells displaying 2B protein specific fluorescence.

Similar results were obtained in permeabilization assays using untransfected cells and BHK cells expressing the 2B precursor 2BC (Fig. 1C, dark grey bars, and Fig. S1). These findings support the notion that healthy cells were permeable to HB when co-cultured with cells that express PV 2B or 2BC. Moreover, the extent of permeabilization to HB in neighbouring cells was directly dependent on the proportion of 2B-expressing cells that were co-cultured as well as on the length of incubation. However, at 19 hpe, when signs of apoptosis are evident and cell death occurs in a high proportion of cells that express 2B (Madan *et al*., 2008), permeabilization of healthy counterparts was found to be significantly lower than that seen at earlier time points (data not shown). These differences strongly suggest that the permeabilization of healthy cells requires the 2B-expressing cells to still be alive.

Several viroporins induce different degrees of permeabilization to HB in neighbouring cells

A comparative analysis was carried out using E protein from MHV-A59 and 6K from SV to study whether other viroporins can permeabilize healthy neighbouring cells. PV 2B and coronavirus E proteins have been described to induce a rapid and efficient permeabilization of BHK cells, whereas SV 6K required a longer period of expression to permeabilize the plasma membrane extensively. In addition, a small and cytotoxic protein from HCV, NS4A, exhibited viroporin-like activity several hours after its

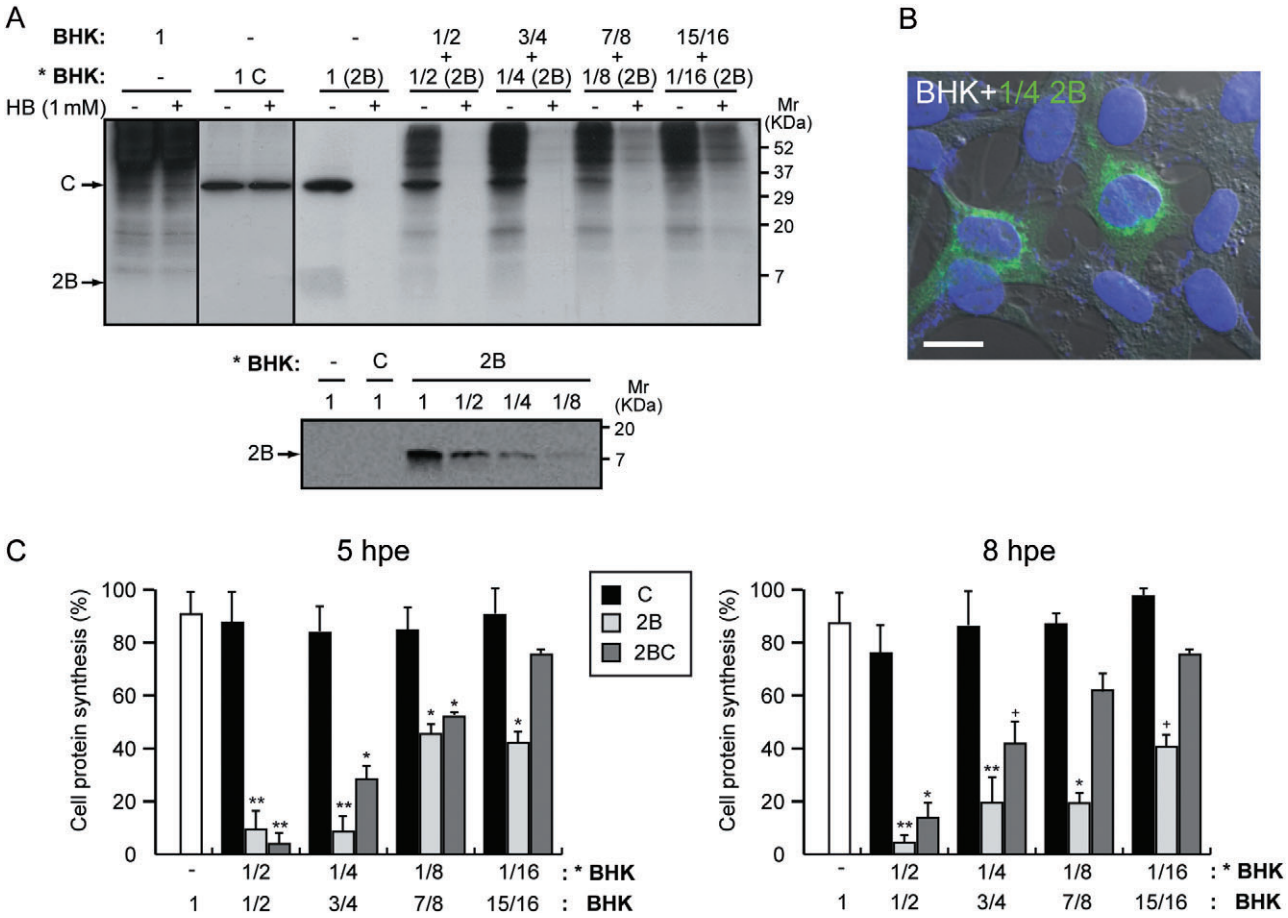

Fig. 1. Expression of PV 2B protein in BHK cells induces permeabilization of neighbouring cells to HB. BHK cells were electroporated with *in vitro* synthesized RNA from the plasmids pT7 repC+2B or pT7 repC+2BC. Different proportions of electroporated cells (as indicate in the figure, * BHK) were mixed with mock BHK cells and seeded in 24-well plates. Cell density (ρ) in each well was approximately 1.9×10^5 cells cm^{-2}. At different times after transfection, proteins were labelled with [^{35}S] Met/Cys in the absence (–) or presence (+) of 1 mM HB for 40 min. Samples were processed by SDS-PAGE (17.5%) followed by fluorography and autoradiography.

A. Membrane permeabilization of neighbouring cells (mock cells) assayed by the inhibition of translation as a result of HB entry induced by 2B protein at 8 h post electroporation (hpe) (a representative experiment). All of the cells expressing 2B are permeable to HB (proportion 1; cell $\rho = 1.9 \times 105$ cells cm^{-2}). A Western blot using polyclonal antibodies against 2B protein was performed to show 2B expression and its proportional decrease with dilutions of transfected cells (lower panel).

B. Immunofluorescence staining at 8 hpe in a sample in which only 25% of BHK cells expressed 2B protein. Cells were fixed, permeabilized and double stained with anti-2B antibodies (green) and DAPI (nuclei labelling, blue). The panel shows merged immunofluorescence and phase-contrast images. Scale bar, 10 μM.

C. Statistical analysis of membrane permeabilization of neighbouring cells caused by 2B and its precursor, 2BC, at 5 (left graph) and 8 hpe (right graph). Each bar represents the percentage of cellular protein synthesis in HB-treated cells compared with untreated cells. Cellular proteins bands were quantified by densitometry. All data are shown as the mean ± SD of at least three independent experiments. (5 hpe; $^{**}P < 0.01$, $^{*}P < 0.05$, 8 hpe; $^{**}P < 0.001$, $^{*}P < 0.01$, $^{+}P < 0.05$).

expression in BHK cells (Madan *et al*., 2008). To analyse membrane permeabilization of healthy cells to HB at different times by several viroporin-expressing cells, we carried out assays using the co-culture system. BHK cells were electroporated with the corresponding SV-derived replicons (RNAs) coding for either SV C alone, 2B, E, NS4A or 6K. Equal proportions of transfected and non-tranfected cells were mixed and seeded, and translation inhibition by HB was quantified at 8 hpe (C, 2B, E and NS4A) or 16 hpe (6K). Figure 2 shows a representative PAGE analysis in which C protein and viroporin synthesis was detected by metabolic protein labelling. The presence of NS4A was also confirmed by Western blotting, using a specific monoclonal antibody (data not shown). Expression of coronavirus E protein permeabilized transfected cells and also resulted in HB entry in neighbouring cells to a slightly lesser extent than observed in PV 2B co-cultures. The permeabilization activity induced by HCV NS4A expression was delayed compared with that seen upon 2B or E protein expression (Madan *et al*., 2008). Consequently, HB entry in non-transfected cells was notably impaired, as occurred in co-cultures expressing

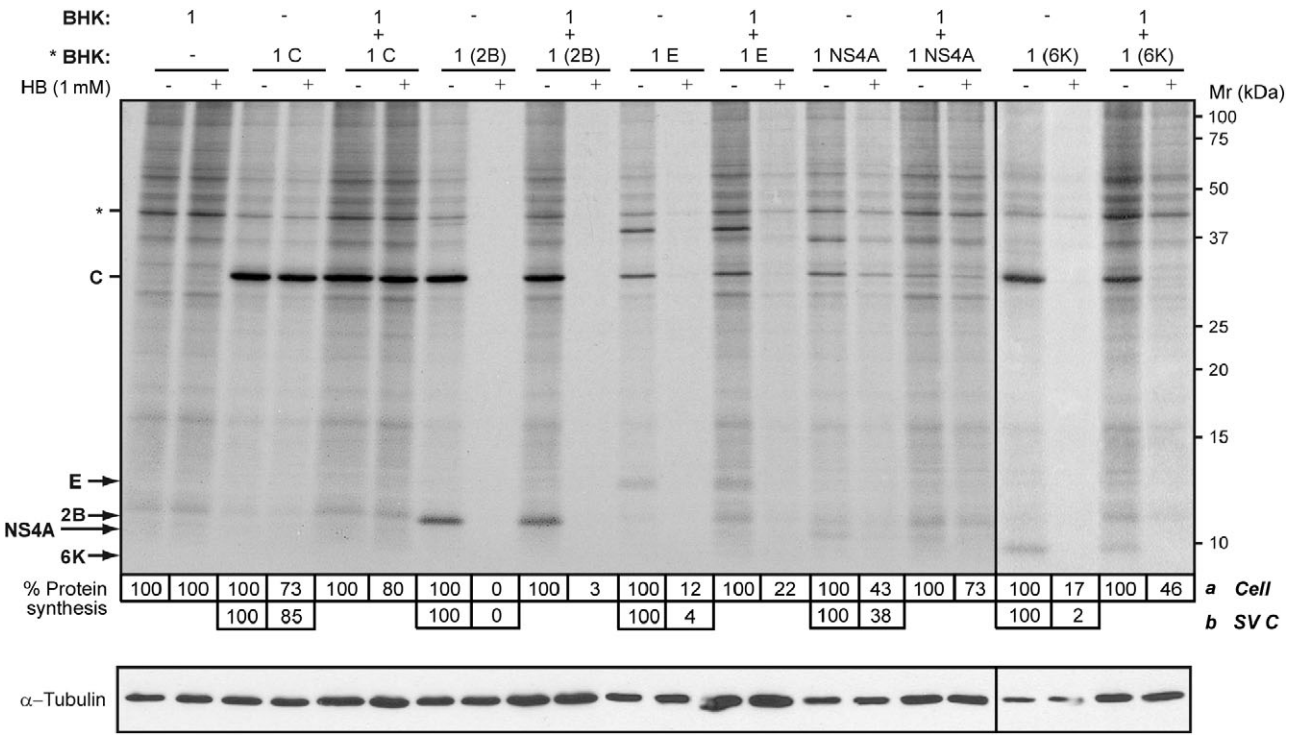

Fig. 2. Expression of different viroporins induces permeabilization of neighbouring cells to HB to different extents. BHK cells were electroporated with *in vitro* synthesized RNA from the plasmids pT7 repC+2B, pT7 repC+E, pT7 repC+NS4A or pT7 repC+6K. Transfected cells (* BHK) were mixed with mock cells in equal proportions (ratio 1:1; total cell $\rho = 1.9 \times 10^5$ cells cm^{-2}) or seeded separately (proportion 1; total cell $\rho = 8 \times 10^4$ cells cm^{-2}) in 24-well plates. As a negative control, cells were transfected with RNA from pT7 repC (encoding Sindbis virus capsid protein). At 8 h post electroporation (hpe) (cells expressing only C protein, 2B, E or NS4A protein co-cultured with mock cells) or 16 hpe (cells expressing 6K co-cultured with mock cells), proteins were metabolically labelled in the absence (–) or presence (+) of 1 mM HB for 40 min. Samples were processed by SDS-PAGE (17.5%). To measure membrane permeabilization of neighbouring cells, protein synthesis in those cells was quantified by densitometry of bands corresponding to actin, * (a). Permeabilization of cells expressing either C protein or viroporins is represented as the decrease in protein synthesis which was quantified by densitometry of bands corresponding to C protein (b). Numbers below the gel indicate the percentage of cell protein synthesis in HB-treated cells compared with untreated cells. Most cells expressing viroporins 2B, E or 6K were permeable to HB. A Western blot using monoclonal antibodies against α-tubulin was performed as a control for protein load (lower panel).

the non-permeabilizing C protein from SV. In contrast, permeabilization of healthy cells that were co-cultured with 6K-expressing cells for 16 h was unexpectedly lower than that seen in the 2B or E co-cultures, even though 6K-expressing cells were entirely permeabilized (Fig. 2, right panel). These findings reveal the different capabilities of the viroporins tested to promote permeabilization of neighbouring cells. Moreover, this may reflect the different viroporin activity of each viral protein.

Expression of 2B viroporin in BHK cells promotes translation inhibition by HB in other cell lines

To address the importance of this secondary permeabilization effect mediated by 2B on co-cultured non-transfected cells, two additional cell lines were assayed. Huh-7 and HeLa tumour cell lines were mixed with 2B-transfected BHK cells at different ratios (a total of 3×10^5 cells), and entry of HB was assayed at 8 hpe. Significant permeabilization of Huh-7 cells (~55% translation inhibition by HB) was accomplished when at least 75% of the mixed cell population were transfected BHK cells (Fig. 3 and Fig. S3). Assays using BHK/HeLa cell co-cultures revealed that 50% 2B-expressing BHK cells was sufficient to induce the same extent of permeabilization in HeLa cells as in Huh-7 cells (Fig. S3-1). In contrast to the results obtained with co-cultures only composed of BHK cells (Fig. 1), co-cultures containing less than 50% or 75% transfected BHK cells did not result in substantial permeabilization of neighbouring tumour cells. These results suggest that in addition to the viroporin activity of 2B, permeabilization to HB of non-transfected cells is also influenced by the neighbouring cell line.

Next, we explored the possibility that permeabilization of healthy cells was only increased when both transfected and non-transfected cells belonged to the same cell line. To this end, Huh-7 cells were electroporated with SV-derived replicon coding for 2B (Rep C+2B) and co-cultured with healthy Huh-7 cells at ratios from 1:4 to 1:2. As shown in Fig. 4, although transfected Huh-7 cells

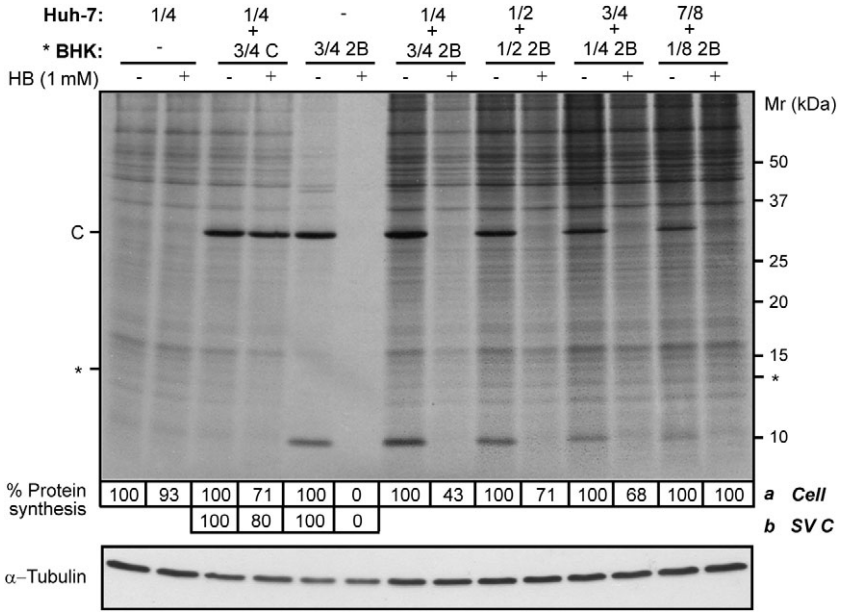

Fig. 3. Expression of 2B viroporin in BHK cells promotes translation inhibition by HB in other cell lines. Different proportions of BHK cells, transfected with RNA from SV replicon encoding 2B protein or C (* BHK), and Huh-7 cells (mock cells) were mixed (total cell $\rho = 1.9 \times 10^5$ cells cm^{-2}). Permeabilization of neighbouring Huh-7 cells to HB was analysed at 8 h post electroporation (hpe) by metabolic labelling of proteins in the absence (–) or presence (+) of 1 mM HB for 40 min. Protein synthesis in Huh-7 cells (a) was quantified by densitometry of bands corresponding to a specific protein of Huh-7 cells (*). As a negative control, a high proportion of BHK cells expressing SV C protein were mixed with mock Huh-7 cells (3 BHK:1 Huh-7). Permeabilization of BHK cells expressing 2B was quantified by densitometry of the SV C protein band (b). Numbers below the gel indicate the percentage of protein synthesis in HB-treated cells compared with untreated cells. A Western blot using monoclonal antibodies against α-tubulin was performed as a control for protein load (lower panel).

were powerfully permeabilized at 8 hpe, the neighbouring cells exhibited little permeabilization to HB. In this case, 2B protein synthesized from 50% transfected cells only promoted a weak permeabilization of the non-transfected counterparts, leading to a translation inhibition of about 40%. However, in BHK-cell co-cultures, equal and even lower ratios of 2B-expressing BHK cells gave rise to almost total permeabilization of neighbouring cells. Co-cultures of HeLa cells cannot be assayed, since this cell line is not permissive for SV or its replicons. Taken together these observations strongly suggest that cellular factors might be involved both in the enhancement and resistance to HB permeabilization of non-transfected cells.

Permeabilization of neighbouring cells to HB is dependent on cell–cell contact

To examine whether cell contact is involved in mediating the transfer of HB from cells expressing 2B protein to bystander cells, we co-cultured mixtures of BHK cells at various densities. Co-cultures including a fixed proportion

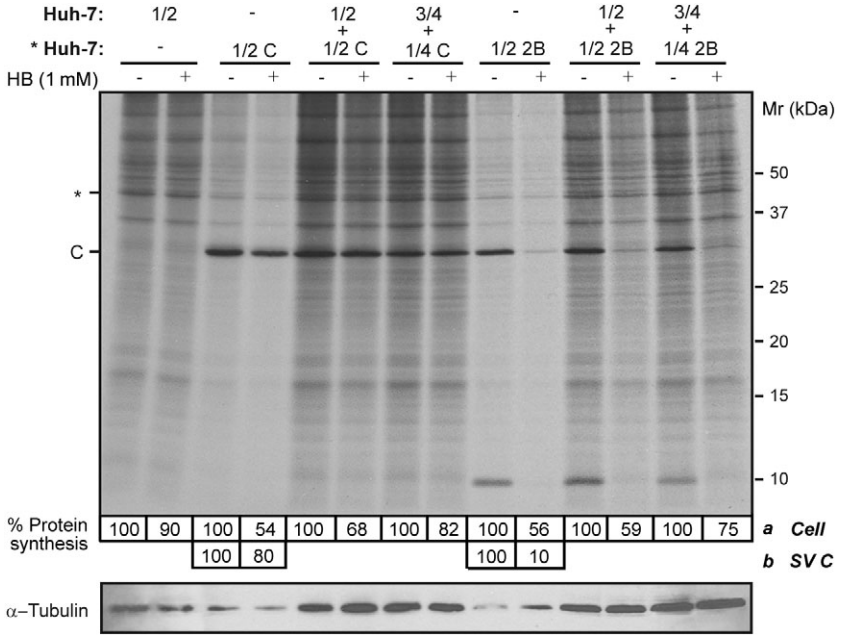

Fig. 4. Permeabilization of neighbouring cells to HB depends on the cell line that expresses 2B. Huh-7 cells were electroporated with SV-derived replicons encoding C+2B or only C protein (negative control) as described in *Experimental procedures*. Different proportions of transfected cells (* Huh-7) were mixed with mock Huh-7 cells (total cell $\rho = 1.9 \times 10^5$ cells cm^{-2}) or seeded separately (proportion 1/2; total cell $\rho = 8 \times 10^4$ cells cm^{-2}). At 8 h post electroporation (hpe), permeabilization of neighbouring Huh-7 cells was assayed by the inhibition of translation as a result of HB entry induced by 2B protein. Protein synthesis in Huh-7 cells (a) was quantified by densitometry of bands corresponding to actin (*). Permeabilization of Huh-7 cells expressing 2B was quantified by densitometry of SV C protein band (b). Numbers below the gel indicate the percentage of protein synthesis in HB-treated cells compared with untreated cells. A Western blot using monoclonal antibodies against α-tubulin was performed as a control for protein load (lower panel).

of 25% 2B-expressing cells and 75% healthy cells were seeded on plates with different growth areas. As shown in Fig. 5A, the permeabilization of neighbouring cells by 2B at 8 hpe proved to be directly proportional to the cell density (confluency) of the co-cultures. This finding suggests that contact between cells that express 2B and non-transfected cells is important for the bystander permeabilization effect to occur. To further assess the significance of intercellular communication in cell permeabilization, we used similar co-cultures in which there was no direct contact between the two cell populations (see schemes in Fig. 5B). Although both cell types shared the same culture medium, when HB entry was evaluated at 8 hpe only the cells expressing 2B protein were permeabilized (Fig. 5B). This finding makes it unlikely that permeabilization of cultured cells is mediated by release of 2B alone or 2B-containing vesicles into the culture medium. Moreover, 2B was not detected in the supernatant obtained from the culture medium of transfected cells at 8 hpe (Fig. 5C). Under these experimental conditions, no cell lysis was observed after expression of viral proteins, as both C protein and α-tubulin were absent in the supernatants. Detection of E protein from MHV in the culture medium served as a positive control to confirm that proteins can be released from E-expressing cells (Maeda *et al*., 1999).

GAP junctional communication in BHK cells expressing PV 2B protein

Once it was established that permeabilization of neighbouring cells by 2B-expressing cells was not mediated by the release of 2B to the medium and required cell–cell contact, we explored the possibility that HB transfer occurred through gap junctions. In order to study gap junctional communication, BHK cells were labelled with two fluorescent probes, DiI and calcein AM (acetomethyl ester). DiI is a hydrophobic dye that labels cell membranes and does not diffuse through gap junctions. Calcein AM is a colourless uncharged molecule that freely enters cells and is hydrolysed by endogenous esterases to generate calcein, the charged fluorescent form. Calcein cannot diffuse through the plasma membrane but is able to pass across gap junctions. Therefore, the transfer of calcein from cell to cell is a suitable indicator of gap junctional communication. First, BHK cells transfected with 2B replicon or control cells (transfection with C replicon) were double labelled and washed before being mixed with unlabelled cells (1:3). Non-transfected co-cultures established functional contacts as assessed by transfer of intracellular green fluorescent calcein to the cytoplasm of neighbouring DiI-negative cells (Fig. 6A). Similarly, calcein transfer from 2B-expressing cells to healthy cells was also observed at 8 hpe (Fig. 6C). Furthermore, we noted that the number of neighbouring cells which received calcein was comparable both in 2B and C protein co-cultures, although it was slightly lower than that obtained for non-transfected co-cultures (Fig. 5B and C and data not shown). This difference could be accounted for by the shut off induced by the SV-derived replicons (Sanz *et al*., 2007). To gain further insights into the significance of these results, connexion 43 (Cx 43) level was examined by immunoblotting in cells that express the viral products and in healthy cells. Cx 43 is widely expressed in different types of mammalian cells and assembles gap junction channels. Although Cx 43 expression in BHK cells has been previously reported, other investigators described them as communication-deficient cells since they detected endogenous Cx 43 retained in the Golgi (Udawatte and Ripps, 2005). We found the expression of Cx 43 in BHK cells as well as two products which migrate above Cx 43, corresponding to phosphorylated forms of the protein (Asklund *et al*., 2003). Although the amount of Cx 43 was similar in both transfected and untransfected cells, a slight reduction in accumulated connexin was observed after synthesis of the viral proteins (Fig. 6D). In order to examine the subcellular localization of Cx 43 in BHK cells, an immunofluorescence assay was performed using specific antibodies. An intracellular Cx 43 staining pattern, probably resulting from the association of connexin with the Golgi complex, was observed, consistent with previous studies (Udawatte and Ripps, 2005). Unexpectedly, Cx 43 was also clearly observed at the plasma membrane. Moreover, punctate Cx 43 staining was concentrated at cell–cell contact areas corresponding to bona fide gap junctions (Fig. 6E). It is important to mention that this localization pattern of Cx 43 was not altered after expression of SV C or PV 2B proteins at 8 hpe and, furthermore, Cx 43 was detected at contacts between transfected and healthy non-transfected BHK cells (Fig. 6F). Nevertheless, a very low proportion of 2B-expressing cells exhibited a reduced level of Cx 43-associated fluorescence. This observation is consistent with the slight reduction reported above. Taken together, these findings support the notion that gap junctions assembled by Cx 43 are functional both in healthy and in 2B-expressing BHK cells and could mediate the transfer of HB from permeabilized 2B-expressing cells to neighbouring cells, as occurs with the calcein dye-coupling assay.

Blocking gap junctional intercellular communication inhibits permeabilization of neighbouring cells

To further investigate whether permeabilization of neighbouring cells to HB is mediated by gap junctional communication, we assessed the effect of 18α-glycyrrhethinic acid (18-α-GA), a selective inhibitor of gap junctions.

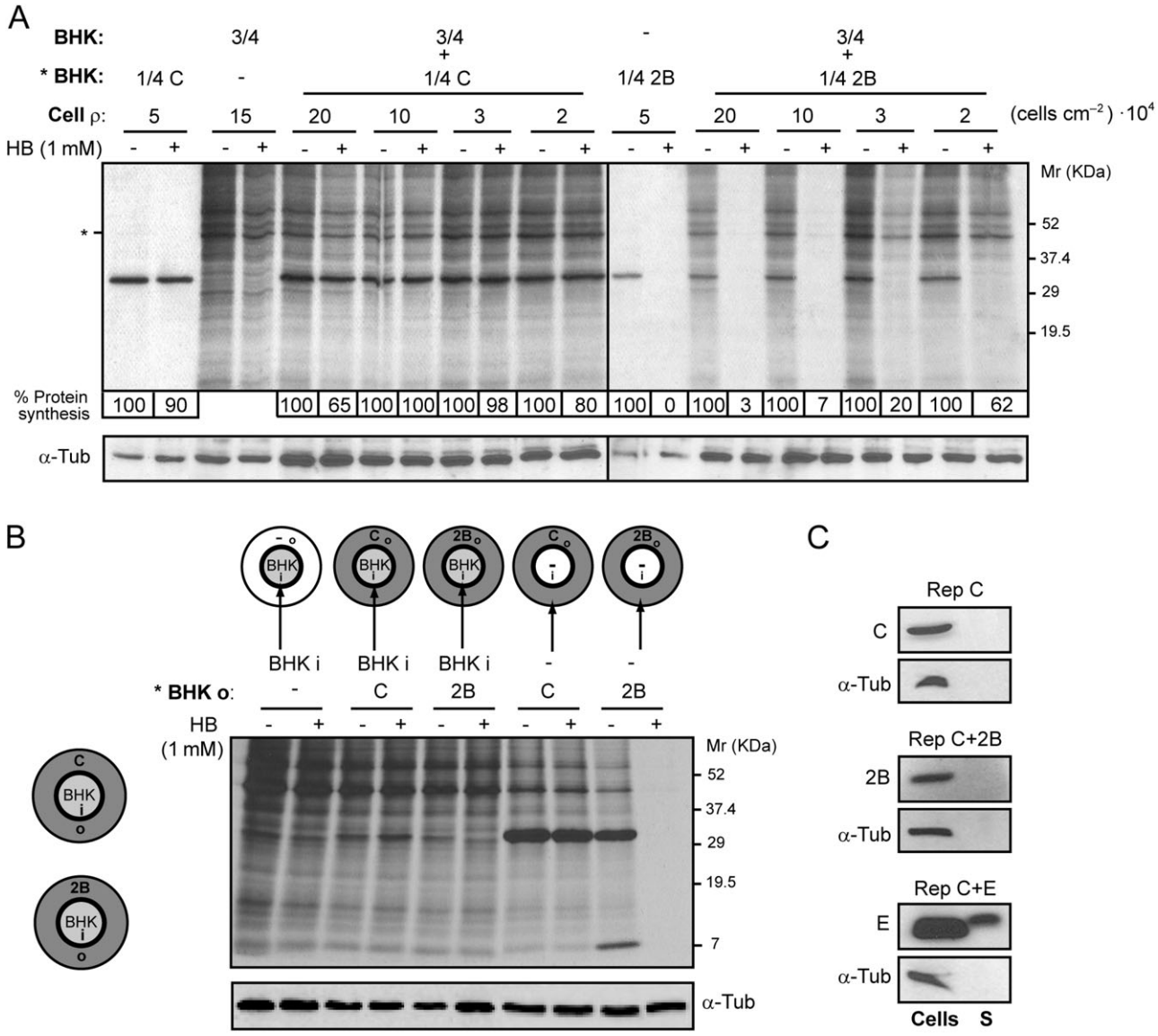

Fig. 5. Permeabilization of neighbouring cells to HB is dependent on cell–cell contact.
A. A fixed proportion of transfected (with replicons encoding C+2B or C alone; * BHK) and mock cells (*BHK : BHK, 1:3; total number of cells = 4×10^5; cell ρ at maximum confluence = 20×10^4 cells cm^{-2}) was seeded on plates with different growth areas (2, 3.8, 11.8 and 19.5 cm^2). At 8 h post electroporation (hpe), permeabilization of mock cells was assayed by the inhibition of translation as a result of HB entry induced by 2B protein. Protein synthesis in mock cells was quantified by densitometry of bands corresponding to actin (*). Numbers below the gel indicate the percentage of protein synthesis in HB-treated cells compared with untreated cells. As a control for protein load, α-tubulin was detected by Western blotting (lower panel).
B. Permeabilization of BHK cells is not induced when cell contact with 2B-expressing cells is not established. Schematic drawings of culture plates (growth area = 11.8 cm^2) containing a central ring that divides the plate into an independent inner (i) chamber (growth area ≈ 2 cm^2) and an outer (o) concentric region (left). Cells transfected with replicons encoding C+2B or C alone were seeded on the outer region of the plate (grey) and mock cells were independently seeded into the central chamber (white). Once cells were settled, the central ring was removed in such a way that all cells shared the same culture medium. At 8 hpe, cells were metabolically labelled for 40 min in the absence (–) or presence (+) of 1 mM HB. Transfected and mock cells were independently collected in loading buffer by first replacing the central ring the culture plate. Mock cells (from the central chamber) and transfected cells (outer region) expressing C+2B or C (negative control) were loaded separately, as indicated in the figure (right panel), and processed by SDS-PAGE. It can be observed that only cells that express 2B protein are permeable to HB. As a protein loading control, α-tubulin was detected by Western blotting (lower panel).
C. 2B protein is not released into the culture medium. Cells expressing C alone, 2B or E protein from MHV-A59 (positive control) and their respective culture media were collected separately at 8 hpe. Cells were resuspended in loading buffer while culture media were centrifuged and proteins from supernatants (S) were precipitated using trichloroacetic acid (see *Experimental procedures*) and resuspended in loading buffer. The presence of viral proteins in cells and supernatants was analysed by Western blotting using rabbit polyclonal antibodies directed against C, 2B and E. The absence of cellular proteins in supernatant was confirmed by Western blotting using monoclonal antibodies specific for α-tubulin.

Co-cultures composed of 25% 2B-expressing cells and 75% healthy cells were employed. HB treatment was carried out in the presence or absence of 25 μM or 50 μM 18-α-GA, to analyse possible changes in protein synthesis occurring in healthy cells (Davidson *et al*., 1986). Figure 7A shows that blockade of gap junctions by 18-α-GA prevented the entry of HB into neighbouring cells. As a consequence, protein synthesis in these cells was not inhibited by the presence of HB.

Notably, the inhibition of bystander permeabilization mediated by 18-α-GA was dose dependent and the maximum effect was observed at a concentration of 50 μM (Fig. 7B and C). Moreover, 18-α-GA had no apparent effect on permeabilization of 2B-expressing cells to HB. Indeed, the weak signal of protein synthesis detected in the presence of both HB and 18-α-GA is likely to have come from a small proportion of cells that were not transfected during the electroporation process. These results are consistent with the hypothesis that permeabilization of healthy cells in co-culture with 2B-expressing cells is mediated exclusively by Cx 43 gap junctional intercellular communication.

Discussion

Viroporins are integral membrane proteins that permeabilize the cells in which they are synthesized to ions and small molecules (Gonzalez and Carrasco, 1998). To date, the permeabilizing activity of PV 2B protein to small molecules and ions had only been described to occur cell autonomously (de Jong *et al*., 2006; Madan *et al*., 2007). In this study, we have provided evidence that permeabilization of cells to the translation inhibitor HB by PV 2B viroporin promotes a bystander inhibition of protein synthesis in non-transfected cells. This is the first report of a bystander permeabilization effect triggered by a viroporin. Permeabilization assays carried out using co-cultures of 2B-expressing cells with non-transfected cells revealed that the entry of HB takes place efficiently in both healthy and transfected BHK cells at early time points after transfection, when the 2B permeabilizing activity is maximal. Moreover, the observation of a reduced bystander effect at later time points, when most 2B-expressing cells exhibit clear signs of apoptosis, suggests that this phenomenon is primarily triggered by the synthesis of 2B protein.

The ability of other viroporins (MHV E and SV 6K) and the cytotoxic HCV NS4A protein to permeabilize healthy neighbouring cells was tested in co-cultures containing equal proportions of transfected and non-transfected BHK cells. Our present findings indicate that MHV E and SV 6K proteins also induce the entry of HB into surrounding non-transfected cells. However, the extent of this effect depended on the viroporin tested and its permeabilization kinetics. The coronavirus E protein induced a rapid and powerful permeabilization of the plasma membrane soon after its synthesis, as observed in cells expressing 2B (Madan *et al*., 2005; 2008). The bystander effect in co-cultures expressing E was also comparable to that promoted by PV 2B. In contrast, SV 6K protein requires longer times of expression to efficiently permeabilize cells. Although 6K-expressing cells were entirely permeabilized at 16 hpe in this case, the entry of HB in healthy neighbouring cells was only moderate. As a consequence of the slow permeabilization kinetics of 6K, the shut-off induced by the SV replicon for a longer period of time might have interfered with the function of other essential cellular factors required for the permeabilization of healthy cells. The expression of NS4A caused cytotoxicity in BHK cells but did not permeabilize them efficiently. Therefore, protein synthesis of non-transfected cells remained unaltered. Previously, we reported that the viroporins included in this work induce caspase-dependent apoptosis (Madan *et al*., 2008). However, since permeabilization already occurs soon after transfection, when no signs of cell death are apparent, it is unlikely that permeabilization of healthy cells to HB occurs as a result of cytotoxicity arising from the presence of apoptotic transfected cells. Moreover, in the case of NS4A, apoptosis can be detected in transfected cells at early time points after its expression but no bystander permeabilization was found (data not shown) (Madan *et al*., 2008).

The co-culture experiments described here allowed us to establish that at least two parameters are also essential for powerful bystander permeabilization to occur: (i) an adequate proportion of BHK cells that express 2B protein (Fig. 1) and (ii) cell–cell contact between healthy and 2B-expressing cells (Fig. 5A and B). Possible mechanisms underlying this phenomenon include endocytosis of toxic cell debris arising from viroporin-expressing cells, exposure to secreted soluble viroporins or cell–cell transfer of HB (through gap junctions). We can rule out the two first possibilities, as healthy cells incubated for different periods of time with the medium obtained from cultures of 2B-expressing cells were not permeabilized (data not shown). Furthermore, no 2B protein was found in the protein precipitate from the extracellular medium (Fig. 5C). The E protein from MHV-A59 is released in vesicles from transfected cells to the extracellular medium (Maeda *et al*., 1999). Here, we have shown that E protein is able to induce a bystander permeabilization to HB in neighbouring cells similar to that exerted by 2B, but only the E protein is detected in the culture medium of transfected cells (Figs 2 and 5C). Further studies will be needed to define a possible role of extracellular E viroporin in mediating the bystander effect in neighbouring non-transfected cells.

Our work provides evidence to support the hypothesis that 2B permeabilizes neighbouring cells through gap

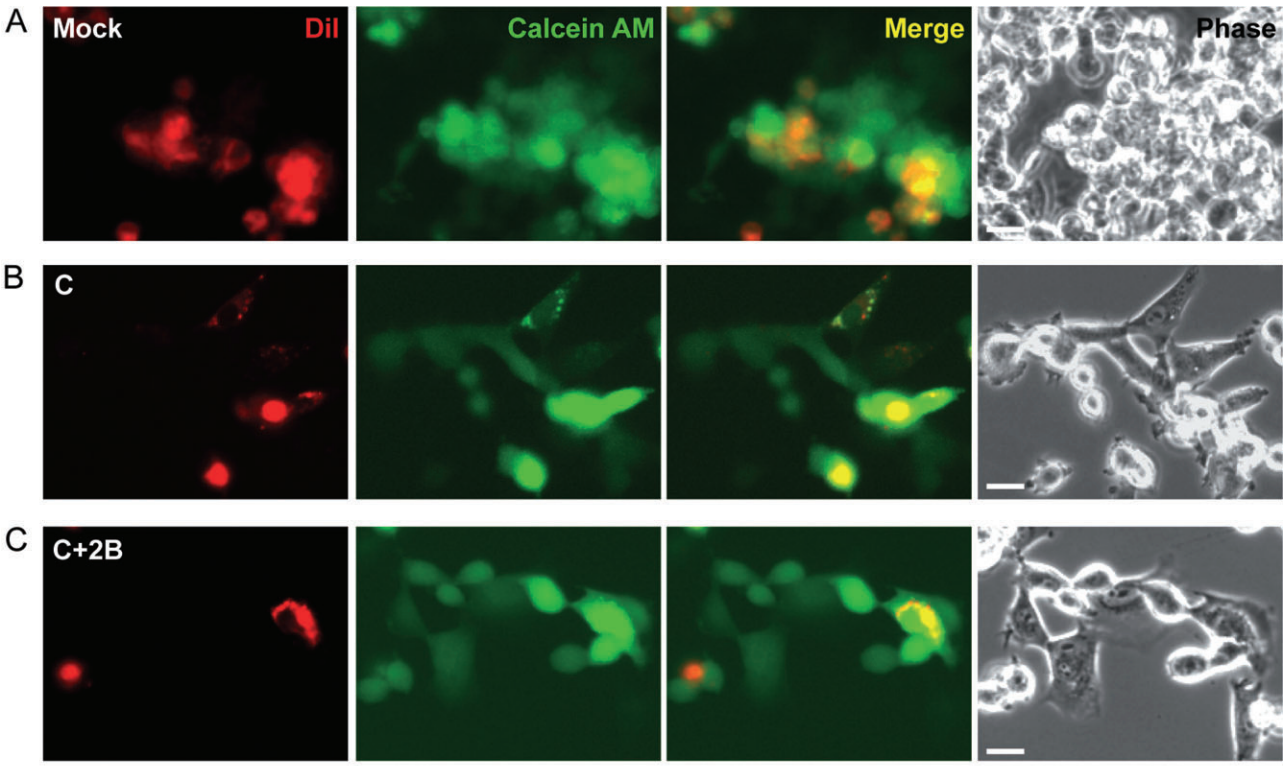
A
Mock
DiI
Calcein AM
Merge
Phase
B
C
C
C+2B

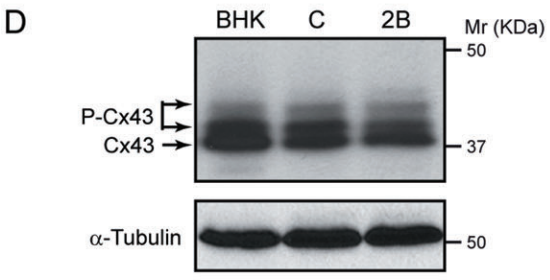
D
BHK
C
2B
Mr (KDa)
50
37
50
P-Cx43
Cx43
α-Tubulin

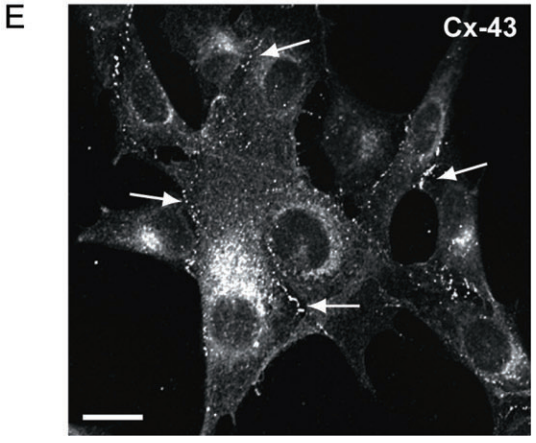
E
Cx-43

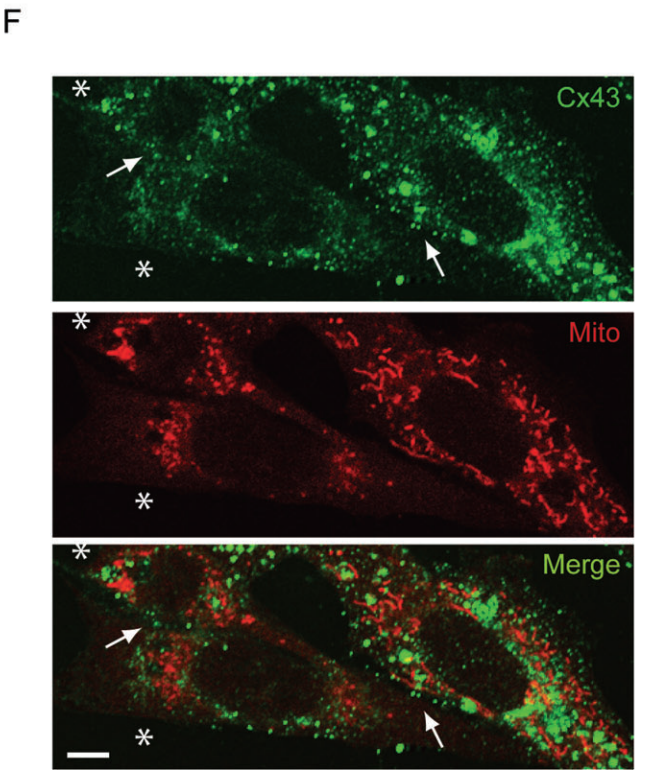
F
Cx43
Mito
Merge

Fig. 6. Gap junction-mediated fluorescent dye transfer.
A–C. Mock BHK cells (A) or cells electroporated with SV replicon encoding C (B) or C+2B proteins (C) were preloaded with DiI and calcein AM fluorescent probes and mixed with unlabelled non-transfected cells as indicated in *Experimental procedures*. Diffusion of calcein was analysed at 8 h post electroporation (hpe) in living cells. Calcein spread to DiI-negative cells, indicating the presence of intercellular coupling (A–C, merged panels), while DiI was retained in the preloaded cells (A–C, left panels). The right-hand panels show phase-contrast images of these cells. Bars, 10 μm.
D. Cx 43 levels in transfected cells. Expression of Cx 43 in non-transfected cells and cells expressing C or C+2B was analysed by Western blotting using a rabbit anti-Cx 43 antibody. Detection of α-tubulin served as a loading control. P-Cx43, phosphorylated forms of Cx 43.
E and F. Cx 43 distribution in BHK cells. Immunofluorescence of non-transfected cells (E) using a rabbit anti-Cx 43 antibody reveals Cx 43 staining of intracellular and plasma membranes (arrows). Bar, 10 μm. Immunofluorescence staining at 8 hpe in a sample in which only 25% of BHK cells expressed 2B protein (F). To detect the 2B-expressing cells (labelled with a white asterisk, *), 'mitotracker', a vital marker of mitochondria, was used. 2B expression induces a perinuclear redistribution of mitochondria that allows us to discriminate the transfected from the non-transfected cells, which show a normal mitochondrial pattern (Madan *et al.*, 2008). Bar, 5 μm.

junctions. The observation that entry of HB into neighbouring cells is directly proportional to the cell density and requires contact between healthy and 2B-expressing cells supports a requirement for additional cellular factors besides 2B synthesis for the bystander effect to occur (Fig. 5A and B). Our findings strongly support a role for gap junctions in the bystander permeabilization effect. Gap junctions mediate communication by means of cell coupling between neighbouring cells, allowing ions and water-soluble substances to pass from one cell to another (Kumar and Gilula, 1996; Rose and Ransom, 1997). Gap junctional intercellular communication mediates a bystander effect and it is a natural amplifier of the therapeutic effect in herpes simplex virus-thymidine kinase/ganciclovir (HSV-tk/GCV) gene therapy (Dilber *et al.*, 1997; Asklund *et al.*, 2003). Gap junctional intercellular communication is often downregulated in cancer cells (Yamasaki, 1990; Zhang *et al.*, 2007). Consistent with

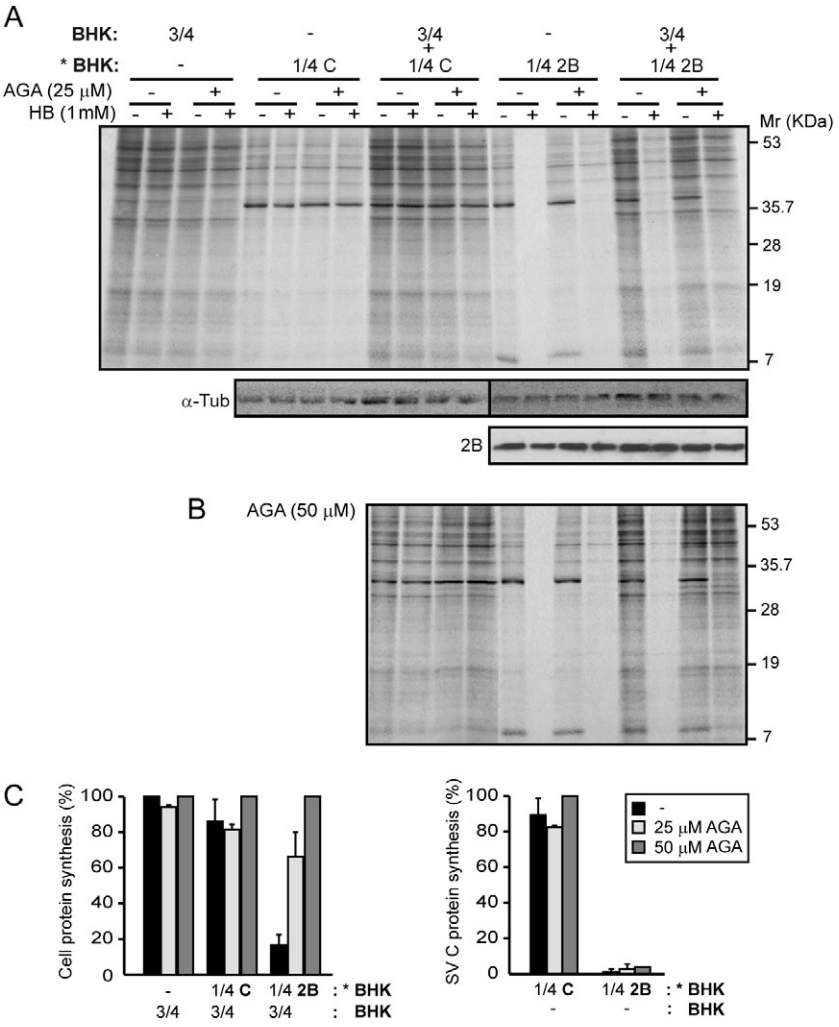

Fig. 7. Permeabilization of neighbouring cells to HB is inhibited by 18α-glycyrrhetinic acid.
A and B. A fixed proportion of transfected cells (with replicons encoding C+2B or C alone; * BHK) and mock cells (BHK) was mixed (*BHK : BHK, 1:3; total cell $\rho = 1.95 \times 10^5$ cells cm^{-2}) or seeded separately (proportion 3/4 BHK; total cell $\rho = 1.46 \times 10^5$ cells cm^{-2} and 1/4 *BHK; total cell $\rho = 4.8 \times 10^4$ cells cm^{-2}) in 24-well plates in the absence or presence of 25 μM (A) or 50 μM (B) 18α-glycyrrhetinic acid (18-α-GA). At 7 h post electroporation (hpe), proteins were metabolically labelled in the absence (–) or presence (+) of 1 mM HB and 18-α-GA for 40 min. As protein loading controls, α-tubulin and 2B protein from 2B-expressing cells or co-cultured cells were detected by Western blotting (A, lower panel).
C. Membrane permeabilization inhibition of neighbouring cells (BHK) by 18-α-GA at 8 hpe (left graph). Each bar represents the percentage of protein synthesis in HB-treated cells compared with untreated cells. Cellular protein bands were quantified by densitometry. The effect of 18-α-GA on membrane permeabilization in 2B-expressing BHK cells is shown in the right-hand graph. C protein bands were quantified by densitometry. All data are represented as the mean ± SD of at least three independent experiments.

these observations, the bystander permeabilization to HB in two tumour cell lines, Huh-7 and HeLa cells, that were co-cultured with BHK or Huh-7 cells expressing 2B protein, was significantly reduced in comparison with that reported for co-cultures of transfected and healthy BHK cells. This observation is consistent with a recent study implicating Cx 43 in the reduction of gap junctional intercellular communication in Huh-7 cells via downregulation of Cx 32 expression (Zhang *et al*., 2007). We have confirmed the presence of Cx 43 protein in non-transfected and 2B-expressing BHK cells and its distribution at the plasma membrane in areas of contact between adjacent cells (Fig. 6D–F). Cx 43 was also detected in Huh-7 cells, although as a consequence of transfection of replicons encoding either C or C+2B protein, its amount was even more reduced than that observed in non-transfected cells (Fig. S6). In our experiments, we still detected a bystander effect when co-cultures include a high proportion of 2B-expressing Huh-7 cells. Moreover, we confirmed the functional status of gap junction channels in BHK cells with the ability to establish new cell–cell contacts and to mediate fluorescent dye transfer between healthy and 2B-expressing cells (Fig. 6A–C).

Finally, the inhibition of Cx 43-mediated gap junctional communication by 18-α-GA abolished the bystander entry of HB in healthy BHK cells co-cultured with 2B-expressing cells. This finding supports the hypothesis that the bystander phenomenon involves cell–cell transfer of HB via gap junctions (Fig. 7). We propose a model in which HB first enters 2B-permeable cells passing through viral (a) or cellular pores at the plasma membrane (b) or via an as yet undefined pathway (c). Once inside cells, HB inhibits translation in 2B-expressing cells and is simultaneously transferred to neighbouring cells through gap junctions (Fig. 8), leading to inhibition of protein synthesis in those healthy cells. Thus, the effect of HB on neighbouring cells would depend on the gap junctional intercellular communication and the proportion of cells that express 2B protein, which would act as the trigger for the bystander effect. In addition, the present findings suggest that cytotoxic drugs, having membrane permeability properties similar to HB, can enter viroporin-expressing cells and subsequently may kill adjacent tumour cells.

Experimental procedures

Cell culture

BHK-21 and Huh-7 cells were routinely cultured at 37°C in Dulbecco's modified Eagle's medium (DMEM) supplemented with 5% and 10% fetal calf serum (FCS), respectively, non-essential amino acids, antibiotics and antimycotics. Imaging was performed in glass-bottomed dishes (MatTek) in DMEM lacking phenol red, FCS and antibiotics but containing L-glutamine and non-essential amino acids.

SV replicons

Sindbis virus-derived replicons containing sequences encoding 2B (pT7 repC+2B) and 2BC (pT7 repC+2BC) proteins from PV (strain Mahoney-1), 6K protein (pT7 repC+6K) from SV, E protein (pT7 repC+E) from MHV-A59, NS4A protein (pT7 repC+NS4A) from HCV type b or only SV C (pT7 repC) protein have been described elsewhere (Sanz *et al*., 2003; Madan *et al*., 2008).

Transfection of BHK-21 cells

BHK-21 and Huh-7 cells were electroporated with *in vitro* synthesized mRNAs. Transcription reactions were carried out with T7 RNA polymerase (Promega) and the corresponding plasmids as templates, according to the manufacturer's instructions. Subconfluent BHK-21 and Huh-7 cells were harvested, washed with ice-cold phosphate-buffered saline (PBS) and cytomix buffer (van den Hoff *et al*., 1992), respectively, and resuspended in PBS or cytomix at a density of approximately 2.5×10^6 cells ml^{-1}. To electroporate BHK-21 cells, an aliquot (50 ml) of the transcription mixture containing 15 mg of RNA from each of the different DNA replicons was added to 0.4 ml of cell suspension and transferred to a 2 mm electroporation cuvette (Bio-Rad). In the case of Huh-7 cells, two aliquots of the transcription mixture were added to 0.8 ml of cell suspension and transferred to a 4 mm electroporation cuvette (Bio-Rad). Electroporation of BHK-21 cells was performed at room temperature (RT) by generating two consecutive 1.5 kV, 25 mF pulses using a Gene Pulser apparatus (Bio-Rad), as previously described (Liljestrom and Garoff, 1991). Electroporation of Huh-7 cells was performed at RT by generating one 270 V, 960 mF pulse using a Gene Pulser II apparatus (Bio-Rad). Finally, cells were diluted in DMEM supplemented with 10% FCS and seeded onto culture plates.

Permeabilization of neighbouring cells to HB

BHK-21 or Huh-7 cells were electroporated with the corresponding RNA synthesized *in vitro* from the different constructs and

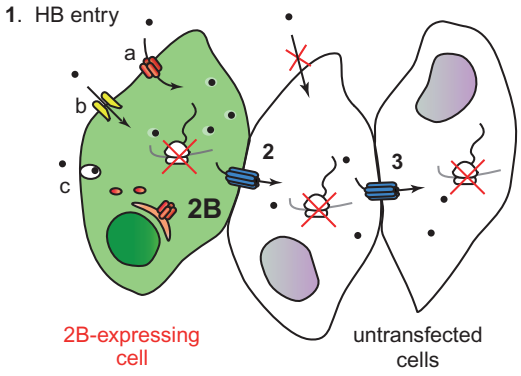

Fig. 8. Model of bystander permeabilization to HB. Model illustrating that 2B-expressing cells trigger HB entry in untransfected cells. 1. First, impermeable HB enters cells permeabilized by 2B protein and inhibits translation (see *Discussion*). 2. HB diffuses through gap junctions to non-transfected cells in close contact with 2B-expressing cells, resulting in inhibition of protein synthesis of these cells. 3. HB is transferred to a larger number of neighbouring cells.

counted using a Neubauer chamber. Different proportions of electroporated cells were mixed with non-electroporated BHK-21 or Huh-7 cells (mock cells) and then seeded in wells of L-24 plates (95–100% confluence). At different time points, cells were pre-treated with 1 mM HB (Clontech) for 15 min at 37°C, or left untreated. Next, proteins were radiolabelled for 40 min with 10 mCi [^{35}S] Met/Cys (Promix; Amersham Pharmacia) in methionine/cysteine-free DMEM in the presence or absence of 1 mM HB. Finally, cells were collected in sample buffer, boiled for 4 min and analysed by SDS-PAGE (17.5%) and fluorography. Protein synthesis was quantified by densitometry using a GS-710 calibrated Imaging Densitometer (Bio-Rad) and calculated by dividing the values obtained for samples treated with HB by the corresponding values obtained from untreated cells. Viral and cellular protein synthesis was quantified by densitometry of the C protein band or a cellular protein band (actin) respectively.

To study the permeabilization of non-transfected cells co-cultured with cells expressing 2B protein in the absence of cell–cell contact, cells were seeded separately in a p35 culture plate containing an independent central chamber. To create an independent central well (growth area ≈ 2 cm^2), a methacrylate ring was reversibly fixed on the centre of the culture plate with 1.8% agarose. Non-transfected cells were seeded into the central well and transfected cells were seeded on the outer region of the plate. After cell attachment, culture medium was carefully removed from the central area before removing the ring separating the regions. Cells were then cultured at 37°C in the medium initially added to the outer region. At the indicated time, cells were pre-treated with HB and radiolabelled in the absence or presence of this translation inhibitor. The ring was placed back in the plate in order to collect the non-transfected and transfected cells independently.

To study the effect of the gap junctional communication inhibitor 18-α-GA (Sigma) on permeabilization of neighbouring cells to HB, transfected and mock cell mixtures were seeded in the absence or presence of 25 μM or 50 μM 18-α-GA. Cells were radiolabelled at 7 hpe before pre-treatment, in the absence or presence of HB and 18-α-GA, and processed as indicated above.

Precipitation of proteins with trichloroacetic acid

The culture medium from transfected cells was centrifuged at 2000 r.p.m. for 4 min to remove detached cells. Trichloroacetic acid was added to supernatants at a final concentration of 3% (at RT). Then supernatants were incubated at 65°C for 5 min, on ice for 5 min and centrifuged at 8000 r.p.m. for 10 min. The protein pellets were washed twice with cold acetone (–20°C), dried and resuspended in loading buffer. Samples were boiled and processed by SDS-PAGE.

Western blotting

Electroporated cells expressing the different viral proteins, mock cells or co-cultured cells (as indicated in the figures) were collected in sample buffer, boiled and processed by SDS-PAGE. After electrophoresis, proteins were transferred to a nitrocellulose membrane as described previously (Barco and Carrasco, 1995). Mouse monoclonal anti-α-tubulin antibodies (Sigma) were used at a 1:5000 dilution to evaluate protein loading. To detect PV 2B and SV C proteins, specific rabbit polyclonal antibodies (Barco and Carrasco, 1995; Madan *et al*., 2005) were used at dilutions of 1:1000 and 1:10 000 respectively. Polyclonal rabbit antibodies against E protein from MHV-A59 were generously provided by S. Makino (University of Texas Medical Branch at Galveston, Texas) and used at a 1:1000 dilution. Polyclonal anti-connexin 43 (Cx 43) antibodies (Sigma) were used at a 1:1000 dilution. Incubation with primary antibodies was performed for 2 h at RT, and then the membrane was washed three times with PBS containing 0.2% Tween-20 and incubated for 1 h with horseradish peroxidase-conjugated anti-mouse (Promega) or anti-rabbit IgG antibodies (Amersham) at a 1:10 000 dilution. After washing three times, protein bands were visualized with the ECL detection system (Amersham).

Immunofluorescence microscopy

BHK cells electroporated with RepC+2B and non-transfected cells were mixed and seeded on coverslips, fixed in 4% paraformaldehyde for 15 min, washed twice in PBS, and then permeabilized for 10 min with 0.2% Triton X-100 in PBS. Cells were incubated with specific rabbit polyclonal antibodies against the PV 2B protein for 1 h in PBS containing 0.1% FCS and 0.1% Triton X-100. Polyclonal anti-Cx 43 antibodies (Sigma) were used at a 1:400 dilution to detect gap junctions. Coverslips were washed three times with PBS and then incubated with a mix of Alexa 488-conjugated anti-rabbit IgG (Molecular Probes) and To-Pro-3 (Invitrogen), both at a dilution of 1:500. Coverslips were mounted in ProLong Gold antifade reagent (Invitrogen) and examined with a Radiance 2000 (Bio-Rad/Zeiss) confocal laser scanning microscope. For mitochondria staining, cells were incubated with 2 μM Mitotracker Red CMH2Ros (Molecular Probes) for 45 min before fixation.

Fluorescent dye transfer

BHK-21 cells (1×10^6 cells) electroporated with SV replicon encoding C or C+2B proteins were labelled with 5 μM calcein-AM (acetomethyl ester) and 10 μM DiI (Molecular Probes) diluted in serum-free medium for 20 min at 37°C. Cells were washed twice in PBS and twice in serum-free DMEM. Cells were resuspended in an adequate volume of fresh serum-free medium. Next, ~2×10^5 labelled cells were mixed with unlabelled non-transfected cells (1:3) and transferred to a glass-bottomed dish, allowing the cells to settle. Diffusion of calcein-AM from transfected cells to non-transfected cells was monitored under an Axiovert 200 (Zeiss) inverted microscope (20× objective). Images were recorded with a digital CCD camera (Hamamatsu).

Statistical analysis

Data are presented as mean values ± SD. Differences were tested for significance by Student's *t*-test. The effect of viroporins on neighbouring cells was compared with controls (transfection of repC). The cut-off for statistical significance was set at $P < 0.05$.

Acknowledgements

This study was supported by a DGICYT Grant (BFU 2006-02182) and an Institutional Grant awarded to the Centro de Biología Molecular 'Severo Ochoa' by the Fundación Ramón Areces.

References

Agirre, A., Barco, A., Carrasco, L., and Nieva, J.L. (2002) Viroporin-mediated membrane permeabilization. Pore formation by nonstructural poliovirus 2B protein. *J Biol Chem* **277:** 40434–40441.

Aldabe, R., and Carrasco, L. (1995) Induction of membrane proliferation by poliovirus proteins 2C and 2BC. *Biochem Biophys Res Commun* **206:** 64–76.

Aldabe, R., Barco, A., and Carrasco, L. (1996) Membrane permeabilization by poliovirus proteins 2B and 2 BC. *J Biol Chem* **271:** 23134–23137.

Asklund, T., Appelskog, I.B., Ammerpohl, O., Langmoen, I.A., Dilber, M.S., Aints, A., *et al.* (2003) Gap junction-mediated bystander effect in primary cultures of human malignant gliomas with recombinant expression of the HSVtk gene. *Exp Cell Res* **284:** 185–195.

Barco, A., and Carrasco, L. (1995) A human virus protein, poliovirus protein 2 BC, induces membrane proliferation and blocks the exocytic pathway in the yeast *Saccharomyces cerevisiae*. *EMBO J* **14:** 3349–3364.

Barco, A., and Carrasco, L. (1998) Identification of regions of poliovirus 2 BC protein that are involved in cytotoxicity. *J Virol* **72:** 3560–3570.

Bienz, K., Egger, D., Pfister, T., and Troxler, M. (1992) Structural and functional characterization of the poliovirus replication complex. *J Virol* **66:** 2740–2747.

Choe, S.S., Dodd, D.A., and Kirkegaard, K. (2005) Inhibition of cellular protein secretion by picornaviral 3A proteins. *Virology* **337:** 18–29.

Davidson, J.S., Baumgarten, I.M., and Harley, E.H. (1986) Reversible inhibition of intercellular junctional communication by glycyrrhetinic acid. *Biochem Biophys Res Commun* **134:** 29–36.

Dilber, M.S., Abedi, M.R., Christensson, B., Bjorkstrand, B., Kidder, G.M., Naus, C.C., *et al.* (1997) Gap junctions promote the bystander effect of herpes simplex virus thymidine kinase *in vivo*. *Cancer Res* **57:** 1523–1528.

Ewart, G.D., Sutherland, T., Gage, P.W., and Cox, G.B. (1996) The Vpu protein of human immunodeficiency virus type 1 forms cation-selective ion channels. *J Virol* **70:** 7108–7115.

Gan, S.W., Ng, L., Lin, X., Gong, X., and Torres, J. (2008) Structure and ion channel activity of the human respiratory syncytial virus (hRSV) small hydrophobic protein transmembrane domain. *Protein Sci* **17:** 813–820.

Gonzalez, M.E., and Carrasco, L. (1998) The human immunodeficiency virus type 1 Vpu protein enhances membrane permeability. *Biochemistry* **37:** 13710–13719.

Griffin, S., Stgelais, C., Owsianka, A.M., Patel, A.H., Rowlands, D., and Harris, M. (2008) Genotype-dependent sensitivity of hepatitis C virus to inhibitors of the p7 ion channel. *Hepatology* **48:** 1779–1790.

Guinea, R., and Carrasco, L. (1994) Influenza virus M2 protein modifies membrane permeability in *E. coli* cells. *FEBS Lett* **343:** 242–246.

van den Hoff, M.J., Moorman, A.F., and Lamers, W.H. (1992) Electroporation in 'intracellular' buffer increases cell survival. *Nucleic Acids Res* **20:** 2902.

Huang, C., Narayanan, K., Ito, N., Peters, C.J., and Makino, S. (2006) Severe acute respiratory syndrome coronavirus 3a protein is released in membranous structures from 3a protein-expressing cells and infected cells. *J Virol* **80:** 210–217.

Huang, M.B., Weeks, O., Zhao, L.J., Saltarelli, M., and Bond, V.C. (2000) Effects of extracellular human immunodeficiency virus type 1 vpr protein in primary rat cortical cell cultures. *J Neurovirol* **6:** 202–220.

de Jong, A.S., Visch, H.J., de Mattia, F., van Dommelen, M.M., Swarts, H.G., Luyten, T., *et al.* (2006) The coxsackievirus 2B protein increases efflux of ions from the endoplasmic reticulum and Golgi, thereby inhibiting protein trafficking through the Golgi. *J Biol Chem* **281:** 14144–14150.

Klimkait, T., Strebel, K., Hoggan, M.D., Martin, M.A., and Orenstein, J.M. (1990) The human immunodeficiency virus type 1-specific protein vpu is required for efficient virus maturation and release. *J Virol* **64:** 621–629.

Kumar, N.M., and Gilula, N.B. (1996) The gap junction communication channel. *Cell* **84:** 381–388.

van Kuppeveld, F.J., Hoenderop, J.G., Smeets, R.L., Willems, P.H., Dijkman, H.B., Galama, J.M., and Melchers, W.J. (1997) Coxsackievirus protein 2B modifies endoplasmic reticulum membrane and plasma membrane permeability and facilitates virus release. *EMBO J* **16:** 3519–3532.

Liljestrom, P., and Garoff, H. (1991) Internally located cleavable signal sequences direct the formation of Semliki Forest virus membrane proteins from a polyprotein precursor. *J Virol* **65:** 147–154.

Luik, P., Chew, C., Aittoniemi, J., Chang, J., Wentworth, P., Jr, Dwek, R.A., *et al.* (2009) The 3-dimensional structure of a hepatitis C virus p7 ion channel by electron microscopy. *Proc Natl Acad Sci USA* **106:** 12712–12716.

Madan, V., Garcia Mde, J., Sanz, M.A., and Carrasco, L. (2005) Viroporin activity of murine hepatitis virus E protein. *FEBS Lett* **579:** 3607–3612.

Madan, V., Sanchez-Martinez, S., Vedovato, N., Rispoli, G., Carrasco, L., and Nieva, J.L. (2007) Plasma membrane-porating domain in poliovirus 2B protein. A short peptide mimics viroporin activity. *J Mol Biol* **374:** 951–964.

Madan, V., Castello, A., and Carrasco, L. (2008) Viroporins from RNA viruses induce caspase-dependent apoptosis. *Cell Microbiol* **10:** 437–451.

Maeda, J., Maeda, A., and Makino, S. (1999) Release of coronavirus E protein in membrane vesicles from virus-infected cells and E protein-expressing cells. *Virology* **263:** 265–272.

Melton, J.V., Ewart, G.D., Weir, R.C., Board, P.G., Lee, E., and Gage, P.W. (2002) Alphavirus 6K proteins form ion channels. *J Biol Chem* **277:** 46923–46931.

Moon, H., and Yang, J. (2006) Role of HIV Vpr as a regulator of apoptosis and an effector on bystander cells. *Mol Cells* **21:** 7–20.

Pavlovic, D., Neville, D.C., Argaud, O., Blumberg, B., Dwek, R.A., Fischer, W.B., and Zitzmann, N. (2003) The hepatitis C virus p7 protein forms an ion channel that is inhibited by long-alkyl-chain iminosugar derivatives. *Proc Natl Acad Sci USA* **100:** 6104–6108.

Pielak, R.M., Schnell, J.R., and Chou, J.J. (2009) Mechanism of drug inhibition and drug resistance of influenza A M2 channel. *Proc Natl Acad Sci USA* **106:** 7379–7384.

Pinto, L.H., Holsinger, L.J., and Lamb, R.A. (1992) Influenza virus M2 protein has ion channel activity. *Cell* **69:** 517–528.
Rose, C.R., and Ransom, B.R. (1997) Gap junctions equalize intracellular Na+ concentration in astrocytes. *Glia* **20:** 299–307.
Sanz, M.A., Madan, V., Carrasco, L., and Nieva, J.L. (2003) Interfacial domains in Sindbis virus 6K protein. Detection and functional characterization. *J Biol Chem* **278:** 2051–2057.
Sanz, M.A., Castello, A., and Carrasco, L. (2007) Viral translation is coupled to transcription in Sindbis virus-infected cells. *J Virol* **81:** 7061–7068.
Schlegel, A., Giddings, T.H., Jr, Ladinsky, M.S., and Kirkegaard, K. (1996) Cellular origin and ultrastructure of membranes induced during poliovirus infection. *J Virol* **70:** 6576–6588.
Suhy, D.A., Giddings, T.H., Jr, and Kirkegaard, K. (2000) Remodeling the endoplasmic reticulum by poliovirus infection and by individual viral proteins: an autophagy-like origin for virus-induced vesicles. *J Virol* **74:** 8953–8965.
Udawatte, C., and Ripps, H. (2005) The spread of apoptosis through gap-junctional channels in BHK cells transfected with Cx32. *Apoptosis* **10:** 1019–1029.
Wang, C., Lamb, R.A., and Pinto, L.H. (1994) Direct measurement of the influenza A virus M2 protein ion channel activity in mammalian cells. *Virology* **205:** 133–140.
Wilson, L., McKinlay, C., Gage, P., and Ewart, G. (2004) SARS coronavirus E protein forms cation-selective ion channels. *Virology* **330:** 322–331.
Xiao, Y., Chen, G., Richard, J., Rougeau, N., Li, H., Seidah, N.G., and Cohen, E.A. (2008) Cell-surface processing of extracellular human immunodeficiency virus type 1 Vpr by proprotein convertases. *Virology* **372:** 384–397.
Yamasaki, H. (1990) Gap junctional intercellular communication and carcinogenesis. *Carcinogenesis* **11:** 1051–1058.
Ye, Y., and Hogue, B.G. (2007) Role of the coronavirus E viroporin protein transmembrane domain in virus assembly. *J Virol* **81:** 3597–3607.
Zhang, D., Kaneda, M., Nakahama, K., Arii, S., and Morita, I. (2007) Connexin 43 expression promotes malignancy of HuH7 hepatocellular carcinoma cells via the inhibition of cell–cell communication. *Cancer Lett* **252:** 208–215.

Supporting information

Additional Supporting Information may be found in the online version of this article:

Fig. S1. Expression of poliovirus 2 BC protein in BHK cells induces permeabilization of neighbouring cells to HB. Membrane permeabilization of neighbouring cells (mock cells) assayed by the inhibition of translation as a result of HB entry induced by 2 BC protein at 8 h post electroporation (a representative experiment). It can be observed that all cells expressing 2 BC are permeable to HB (proportion 1:1; total cell $\rho = 1.9 \times 10^5$ cells cm^{-2}).
Fig. S3. Protein expression in Huh-7 cells. Different proportions of Huh-7 mock cells (input of experiment in Fig. 3) were seeded and protein expression was analysed by metabolic labelling of proteins in the absence (–) or presence (+) of 1 mM HB for 40 min. Protein synthesis in Huh-7 cells was quantified by densitometry of bands corresponding to actin (*). Numbers below the gel indicate the percentage of protein synthesis in HB-treated cells compared with untreated cells.
Fig. S3-1. Expression of 2B viroporin in BHK cells induces HB entry in HeLa cells. Different proportions of BHK cells, transfected with RNA from SV replicon encoding 2B protein, and HeLa cells (mock cells) were mixed (total cell $\rho = 1.9 \times 10^5$ cells cm^{-2}). Permeabilization of HeLa cells to HB was analysed at 8 h post electroporation by metabolic labelling of proteins in the absence (–) or presence (+) of 1 mM HB for 40 min. Protein synthesis in HeLa cells (a) was quantified by densitometry of bands corresponding to cellular proteins. As a negative control, BHK cells expressing SV C protein and mock HeLa cells were mixed in equal proportions. Permeabilization of BHK cells expressing 2B was quantified by densitometry of the SV C protein band (b). Numbers below the gel indicate the percentage of protein synthesis in HB-treated cells compared with untreated cells.
Fig. S6. Cx 43 levels in Huh-7 cells. Expression of Cx 43 in non-transfected cells and cells expressing C or C+2B was analysed by Western blotting using a rabbit anti-Cx 43 antibody. Detection of α-tubulin served as a loading control. P-Cx43, phosphorylated form of Cx 43.

Please note: Wiley-Blackwell are not responsible for the content or functionality of any supporting materials supplied by the authors. Any queries (other than missing material) should be directed to the corresponding author for the article.

doi:10.1016/j.jmb.2010.07.014 J. Mol. Biol. (2010) 402, 101–117

JMB

Available online at www.sciencedirect.com

ScienceDirect

ELSEVIER

Translation Driven by Picornavirus IRES Is Hampered from Sindbis Virus Replicons: Rescue by Poliovirus 2A Protease

Miguel Angel Sanz*, Ewelina Welnowska, Natalia Redondo and Luis Carrasco

Centro de Biología Molecular "Severo Ochoa", CSIC-UAM, C/Nicolás Cabrera, 1, Universidad Autónoma, Cantoblanco, 28049 Madrid, Spain

Received 5 May 2010; received in revised form 6 July 2010; accepted 12 July 2010
Available online 17 July 2010

Alphavirus replicons are very useful for analyzing different aspects of viral molecular biology. They are also useful tools in the development of new vaccines and highly efficient expression of heterologous genes. We have investigated the translatability of Sindbis virus (SV) subgenomic mRNA bearing different 5′-untranslated regions, including several viral internal ribosome entry sites (IRESs) from picornaviruses, hepatitis C virus, and cricket paralysis virus. Our findings indicate that all these IRES-containing mRNAs are initially translated in culture cells transfected with the corresponding SV replicon but their translation is inhibited in the late phase of SV replication. Notably, co-expression of different poliovirus (PV) non-structural genes reveals that the protease 2A ($2A^{pro}$) is able to increase translation of subgenomic mRNAs containing the PV or encephalomyocarditis virus IRESs but not of those of hepatitis C virus or cricket paralysis virus. A PV $2A^{pro}$ variant deficient in eukaryotic initiation factor (eIF) 4GI cleavage or PV protease 3C, neither of which cleaves eIF4GI, does not increase picornavirus IRES-driven translation, whereas L protease from foot-and-mouth disease virus also rescues translation. These findings suggest that the replicative foci of SV-infected cells where translation takes place are deficient in components necessary to translate IRES-containing mRNAs. In the case of picornavirus IRESs, cleavage of eIF4GI accomplished by PV $2A^{pro}$ or foot-and-mouth disease virus protease L rescues this inhibition. eIF4GI co-localizes with ribosomes both in cells electroporated with SV replicons bearing the picornavirus IRES and in cells co-electroporated with replicons that express PV $2A^{pro}$. These findings support the idea that eIF4GI cleavage is necessary to rescue the translation driven by picornavirus IRESs in baby hamster kidney cells that express SV replicons.

Keywords: Sindbis replicon; picornavirus IRES; poliovirus 2A; eIF4G; regulation of translation

Edited by J. Karn

*Corresponding author. E-mail address: masanz@cbm.uam.es.

Abbreviations used: SV, Sindbis virus; PV, poliovirus; EMCV, encephalomyocarditis virus; HCV, hepatitis C virus; CrPV, cricket paralysis virus; FMDV, foot-and-mouth disease virus; SFV, Semliki Forest virus; VEEV, Venezuelan equine encephalitis virus; sgmRNA, subgenomic mRNA; UTR, untranslated region; IRES, internal ribosome entry site; eIF, eukaryotic initiation factor; $2A^{pro}$, protease 2A; L^{pro}, protease L; ORF, open reading frame; nsP, non-structural proteins; luc, luciferase; SG, stress granule; BHK, baby hamster kidney; hpe, hours post-electroporation; IGR, intergenic region; DMEM, Dulbecco's modified Eagle's medium; PBS, phosphate-buffered saline.

Introduction

Eukaryotic mRNAs contain sequences upstream of the AUG initiation codon known as 5′-untranslated region (UTR), which dictate the translation mechanism of these mRNAs. Two major mechanisms for the initiation of mRNA translation are known in eukaryotic cells: cap-dependent and internal ribosome entry promoted by internal ribosome entry site (IRES) elements.[1–4] Cap-dependent translation is the mechanism followed by the vast majority of eukaryotic mRNAs. It involves recognition of the cap structure by eIF4E bound to the other two components of the eIF4F complex (eIF4G and eIF4A).[4,5] This canonical mechanism of initiation also requires the participation of other eukaryotic initiation factors (eIFs) such as eIF1, eIF1A, eIF2, eIF3, eIF4B, eIF5A, and eIF5B.[5] These eIFs, in conjunction with the 40S and 60S ribosomal subunits, lead to the formation of the initiation complex, which is the 80S ribosome containing Met-tRNA$_i$ bound to the P site and interacting with the AUG initiation codon.[1–4] Several IRES elements have been described both in cellular and in viral mRNAs.[6–8] In the case of animal viruses, four major groups are known to encode for mRNAs bearing IRES elements: picornaviruses, flaviviruses, pestiviruses, and retroviruses.[7,9,10] Based on their structure and function, these IRESs have been classified into several groups. Up to four groups may be present in picornaviruses, although there are two that are more representative. IRES type I is typical of entero/rhinoviruses, with poliovirus (PV) as the prototype, while type II is present in cardio/aphthoviruses, the prototype being encephalomyocarditis virus (EMCV).[9,11] As regards their shape, IRESs contain a rich secondary structure with several stem–loops, which are crucial for their activity. Most IRES elements bear a tRNA-like motif that is involved in binding to ribosomes.[12,13] In addition, downstream of this tRNA-like sequence, picornavirus IRESs have a polypyrimidine tract that is also crucial for its correct functioning.[14,15] On the other hand, the requirements for eIFs vary according to the IRES analyzed; thus, picornavirus types I and II do not require eIF4E and can be translated when eIF4G is cleaved by PV protease 2A (2A^{pro}).[16,17] By contrast, hepatitis A virus IRES requires eIF4E and an intact eIF4G.[11,18] Notably, hepatitis C virus (HCV) mRNA can be translated without eIF4F complex and even in the absence of eIF2.[13,19] Most strikingly, cricket paralysis virus (CrPV) mRNA directs protein synthesis in the absence of all known initiation factors.[3,10,20–22] Apart from eIFs, a number of cellular proteins exhibit the ability to interact directly with IRESs, modulating their activity.[9–11,13]

Several species of the alphavirus genus, including Sindbis virus (SV), Semliki Forest virus (SFV), and Venezuelan equine encephalitis virus (VEEV), have been employed to develop expression vectors in mammalian and invertebrate cells.[23–26] The modular structure of the alphavirus genome, as well as their mode of gene expression, makes these viruses well suited to the development of cloning vectors for high-level expression of heterologous genes.[27,28] Apart from their applicability to analysis of particular aspects of molecular virology, alphavirus vectors are of interest in the development of new vaccines, as oncolytic viruses, as vectors for gene therapy, and for specific protein expression in some organs or tissues.[25,29–31] Alphaviruses possess a single-stranded RNA genome of positive polarity of about 12 kb, which contains two open reading frames (ORFs).[27,28] The first located close to the 5′ end encompasses about two-thirds of the genome, encoding the four non-structural proteins (nsPs), while the second ORF encodes the structural proteins (C, E3, E2, 6K, and E1). The sequence located between these two ORFs on the negative-strand RNA constitutes an internal promoter that directs the transcription of the subgenomic mRNA (sgmRNA).[32] The alphavirus lytic cycle is divided into two distinct phases. During the early phase, nsP1–4 proteins necessary for negative-strand RNA synthesis and for the generation of large amounts of sgmRNA are synthesized. At about 2–3 h post-infection, the late phase commences, giving rise to the synthesis of large amounts of structural proteins directed by translation of sgmRNA. At that time, cellular translation has been abrogated and the alphavirus-infected cells only synthesize viral proteins.[33] Several alphavirus vectors have been developed; some of them replace the ORF for the structural proteins with heterologous gene sequences. This type of vector usually synthesizes the heterologous protein very efficiently, particularly when the initial coding sequence for C protein is included.[34] However, these vectors are defective and do not produce new virus particles unless a helper vector encoding the structural proteins is provided.[35] Another type of alphavirus vectors contains a duplicate internal promoter, under which the heterologous gene is cloned, maintaining the two ORFs intact. These vectors are non-defective and can be encapsidated in new virus particles, although the length and the potential toxicity of the cloned genes make them unstable.[24] Picornavirus IRESs have been employed in many different types of virus vectors, including SFV and VEEV vectors. Controversial findings have been published about the efficacy of expression of genes cloned downstream from picornavirus IRESs in alphavirus vectors. Some researchers claimed that these genes are expressed efficiently,[31,36,37] but this has subsequently been questioned.[38] In the present work, we have tested the efficacy of several IRES elements for directing translation of SV replicons. Our present results indicate that IRESs from several animal

viruses, including picornaviruses, are almost nonfunctional in cells transfected with SV replicons. Of interest, PV $2A^{pro}$ is able to confer high translatability on picornavirus IRESs when these are transcribed from SV replicons.

Results

Efficacy of translation of SV sgmRNA containing different leader sequences

The SV sgmRNA is efficiently translated in baby hamster kidney (BHK) cells transfected with an SV replicon, particularly when both the subgenomic leader sequence and the translational enhancer element are present.[33] The enhancer element is a hairpin structure that starts at nucleotide 28 downstream of the AUG initiation codon. This motif encompasses nucleotides 77–139 of the sgmRNA, containing an extensive G–C pairing stretch that could form a very stable structure within the coding region for the capsid protein.[34,39] In addition, there are many viral mRNA leader sequences, such as picornavirus IRESs that promote efficacious translation in virus-infected cells or upon transfection in uninfected cells. To analyze the efficiency at promoting the translation of different leader sequences present in SV sgmRNAs, we engineered a number of SV replicons. In these replicons, the genuine leader sequence of sgmRNA from SV was replaced by different leader sequences. In all cases, the first 11 nucleotides of SV sgmRNA were retained to ensure efficient transcription from the internal SV promoter.[40] A schematic representation of the replicons used in this respect is shown in Fig. 1a. The replicon rep C+luciferase (luc) was utilized to produce genuine SV sgmRNA because it bears the complete sgmRNA leader sequence (L26S) and the translation-enhancing motif.[33] The replicon rep L26S-luc only contains the SV sgmRNA leader sequence of 49 nucleotides before the AUG initiation codon that precedes the luc gene. The replicon rep Lluc-luc bears luc leader sequence and finally the replicon rep LPol-luc contains the PV IRES element before the luc gene. Plasmids encoding the above-described SV replicons were linearized by digestion with XhoI and transcribed *in vitro* with T7 RNA polymerase. Equal quantities of replicons prepared *in vitro* were electroporated into BHK cells, and at 5 hours post-electroporation (hpe), protein synthesis was analyzed by radioactive labeling (Fig. 1b, upper panel). BHK cells electroporated with rep C+luc efficiently synthesize C+luc, which is processed to C and luc products by the protease activity of C protein. Electroporation of rep L26S-luc gives rise to an appreciable but lower amount (68% inhibition) of luc as compared to rep C+luc. Most probably, the lower translation of rep L26S-luc sgmRNA is due to the absence of the translation-enhancing motif. The synthesis of luc decreases drastically when the L26S sequence is replaced by the luc leader sequence. This result indicates that the sgmRNA generated in this case containing a cellular leader sequence is very poorly recognized by the translation machinery, even though it is synthesized by viral transcription. Notably, the presence of PV IRES in sgmRNA renders it very inefficient for translation in SV-replicating cells. In both cases, luc cannot be detected by radioactive labeling. In these two cases, accumulation of luc during the first 5 h of replication is only barely evidenced by Western blot analysis using specific anti-luc antibodies (Fig. 1b, lower panel), whereas a clear band corresponding to luc production is apparent in rep C+luc electroporated cells.

Luc production was also analyzed by measuring luc activity at different times after electroporation (Fig. 1c). This activity increased exponentially from 3 to 7 hpe for BHK cells electroporated with rep C+Luc, while rep L26-luc gives rise to lower values. Remarkably, a low increase of luc activity was observed with rep Lluc-luc and rep LPol-luc. In this last case, the values obtained for luc activity at 7 hpe are 2 orders of magnitude lower than those found for rep C+luc. This finding was unexpected since picornavirus IRES elements are being employed for gene expression in alphavirus vectors.[31,36,37]

To determine the amount of each mRNA produced from the different replicons utilized in Fig. 1a, we tested viral transcription in parallel. To this end, 2.5 μg/ml actinomycin D was added from 1 hpe, and further, cells were incubated from 3 hpe with [^{3}H]uridine. At 5 1/2 hpe, total mRNA was extracted and analyzed by agarose denatured gels (Fig. 1d). Actinomycin D efficiently blocked cellular transcription and no incorporation of [^{3}H] uridine in RNA was detected in mock-electroporated cells. However, cells expressing the different replicons exhibited a good incorporation of [^{3}H] uridine, leading to the detection of both genomic and subgenomic SV mRNAs (Fig. 1d). The amount of these mRNAs varies slightly among the different replicons analyzed, but this small variation did not explain the differences observed in the amount of luc synthesized. Of particular interest is the case of rep LPol-Luc, which contains one IRES sequence both in genomic and in sgmRNA that, in principle, would permit luc translation from both RNAs. Despite the presence of these mRNAs at control levels, the amount of luc synthesized in BHK cells transfected with rep LPol-Luc was very low. Therefore, we conclude that PV IRES poorly directs translation in BHK cells that replicate rep LPol-Luc.

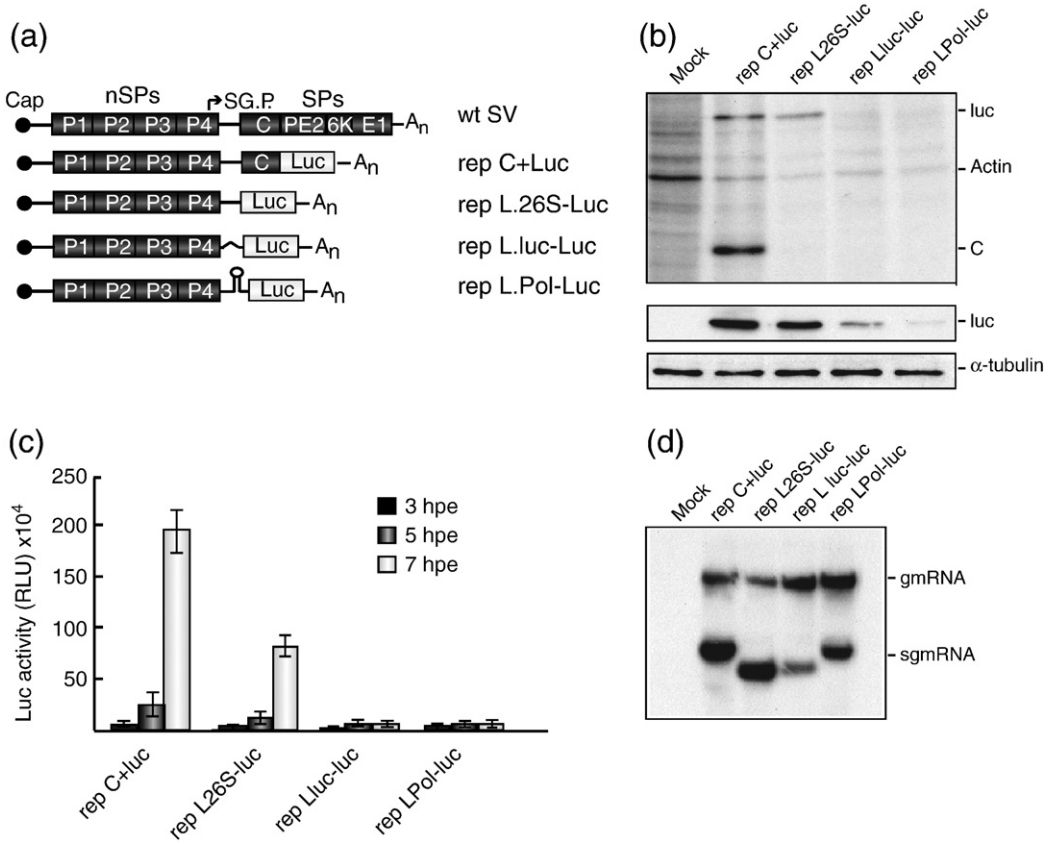

Fig. 1. Luc synthesis from different SV replicons bearing foreign leader sequences in sgmRNAs. (a) Schematic representation of the SV genome and the different replicons employed. The lines or symbols drawn behind the subgenomic promoter (SG.P.) represent the different leader sequences cloned. (b) BHK cells were electroporated with transcription buffer as control or with *in vitro* transcribed RNAs from the different plasmids, and at 5 hpe, protein synthesis was analyzed by incorporation of [^{35}S]Met,Cys as is indicated in Materials and Methods. Cell monolayers were resuspended in sample buffer, loaded onto a 15% polyacrylamide gel, and analyzed by SDS-PAGE followed by fluorography and autoradiography (upper panel). In parallel, an aliquot of these samples was transferred to a nitrocellulose membrane and analyzed by Western blot using anti-luc or anti-α-tubulin antibodies. The amount of α-tubulin present in samples was used as a loading control (lower panel). (c) BHK cells electroporated with the different replicons were collected at different times after electroporation and luc activity was determined. Luc activity values are means±SD of three representative experiments performed in triplicate. (d) BHK cells were electroporated as in (b) and treated with 2.5 μg/ml actinomycin D from 1 hpe and 30 μCi/ml [^{3}H]uridine (740 Gbq/mmol) from 3 hpe. At 5 1/2 hpe, total RNA from cells was extracted and analyzed in 0.8% agarose gels and then subjected to fluorography and autoradiography. C, capsid; luc, luciferase; gmRNA, genomic mRNA; sgmRNA, subgenomic mRNA; hpe, hours post-electroporation.

Translation of SV sgmRNAs bearing different viral IRESs

It is usually thought that mRNAs containing viral IRESs are quite efficacious at directing translation both in uninfected and in virus-infected cells. In fact, years ago, we found that togavirus-infected cells efficiently translate picornavirus mRNAs when cells are doubly infected with SFV and PV or EMCV.[41,42] Therefore, it was unexpected to find that sgmRNAs containing PV IRES were inefficiently translated when synthesized by the SV replication machinery. To investigate whether this phenomenon only occurs with PV IRES or whether this failure to direct translation also occurs in other viral IRESs, we constructed new SV replicons containing different classes of viral IRESs. Thus, IRES sequences from EMCV, HCV, and the intergenic region (IGR) IRES of CrPV were cloned by replacing the leader sequence of SV sgmRNA. BHK cells were electroporated with these replicons, and protein synthesis was analyzed at 7 hpe (Fig. 2b, upper panel). Luc synthesis could not be detected by radioactive labeling with any of the new replicons tested, as observed with rep LPol-luc. However, Western blot analyses showed that a very low amount of luc had

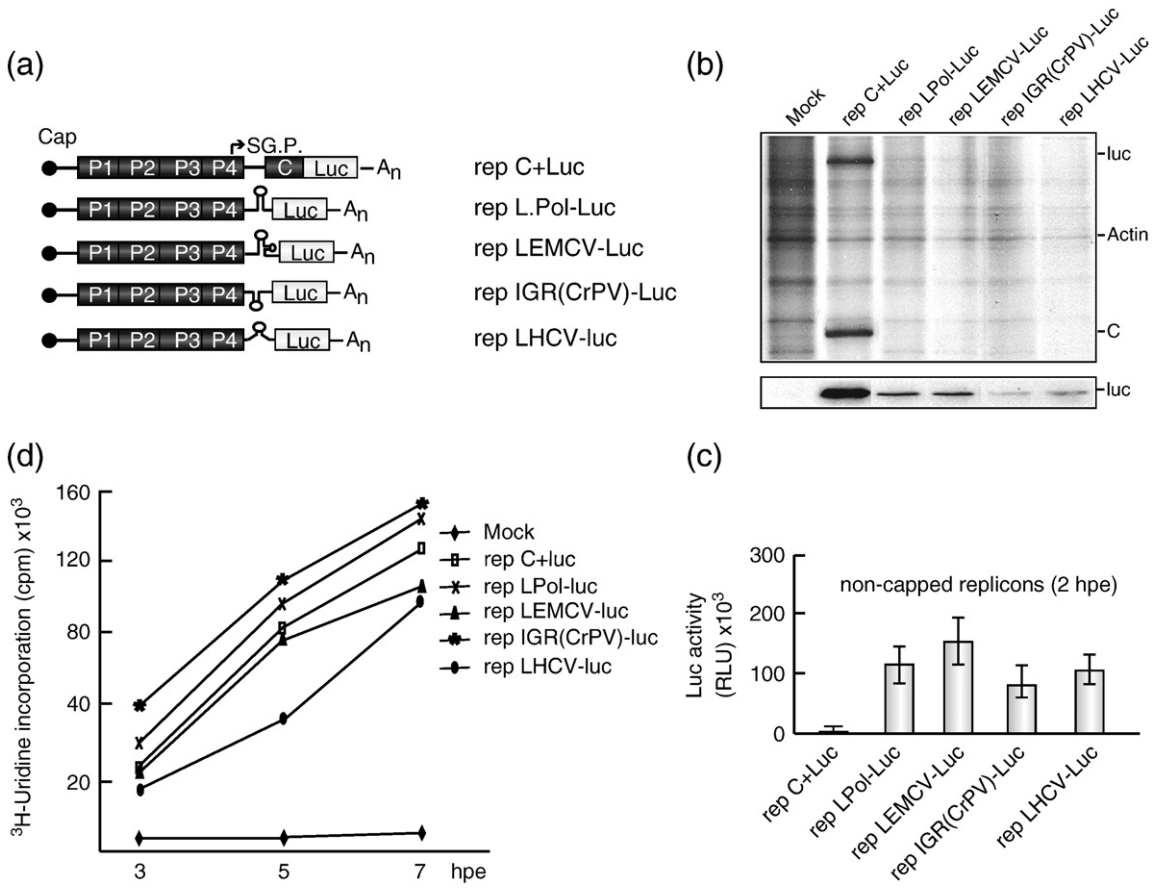

Fig. 2. Luc production from SV replicons encoding several IRES sequences. (a) Schematic representation of the replicons. (b) BHK cells were electroporated with transcription buffer as control or with *in vitro* transcribed replicons, and at 7 hpe, protein synthesis was analyzed by incorporation of [^{35}S]Met,Cys, SDS-PAGE, fluorography, and autoradiography (upper panel). A duplicate of these samples was transferred to nitrocellulose and analyzed by Western blot with anti-luc antibodies (lower panel). (c) BHK cells were electroporated with *in vitro* non-capped replicons and, at 2 hpe, were collected, and luc activity was determined. Luc activity results are means±SD of two representative experiments performed in triplicate. (d) BHK cells electroporated with different replicons were fixed at different times after electroporation as indicated in Materials and Methods and then harvested to measure [^{3}H]uridine incorporation in a liquid scintillation spectrometer. Cpm values are means±SD of two representative experiments performed in triplicate.

accumulated during 7 h of replication (Fig. 2b, lower panel). Our conclusion is therefore that the different viral IRESs tested were all very inefficiently translated in cells electroporated with SV replicons. Once again, this finding was surprising because IRES-driven translation has a low requirement for some eIFs, particularly the HCV and IGR of CrPV IRESs.

Uncapped RNA replicons were electroporated in BHK cells and luc activity was estimated at 2 hpe to assess whether the viral IRESs assayed were operative when forming part of the SV genomic RNA. Translation of the first cistron from uncapped replicons that gives rise to SV nsPs is very inefficient, and therefore, viral replication and transcription do not operate under these conditions at this early time. This was corroborated by transfection of uncapped rep C+luc to render no luc activity at all, indicating that no sgmRNA is produced under these conditions. By contrast, the presence of IRES inside those replicons should permit translation of the input mRNAs and give rise to luc activity. Indeed, this was the case, as luc activity was detected in cells electroporated with replicons bearing the different viral IRESs (Fig. 2c). These findings reflect that IRES sequences can direct translation from genomic RNA in BHK cells, while only the sgmRNA from rep C+luc can be translated. Of note was that the IRES elements analyzed could be recognized in BHK cells before SV replication. By contrast, these IRESs seem to be non-functional in the late phase of SV replication, suggesting that the conditions for mRNAs translation have been modified.

To measure the replication of constructs bearing the different viral IRESs, we estimated [^{3}H]uridine

incorporation at different times in actinomycin-D-treated cells. BHK cells were electroporated with the different replicons and, at the times indicated, RNA synthesis was measured (Fig. 2d). No RNA synthesis was observed in mock-electroporated cells, whereas viral RNA synthesis increased to a similar extent in all replicons examined, including those containing viral IRESs. It must be taken into account that, in principle, with the constructs bearing viral IRESs, both genomic and sgmRNAs can direct the synthesis of luc. Therefore, after 2–3 hpe, the luc activity estimated may come from the translation of both genomic and sgmRNAs. Our present findings reveal that total SV mRNA production does not vary significantly with the different replicons assayed. Thus, it seems clear that both genomic and sgmRNAs bearing the different viral IRESs are poorly translated in BHK cells at late replication times.

EMCV IRES is inactive even when SV sgmRNAs are engaged in translation

In SV-infected cells, translation of sgmRNAs is coupled to its transcription.[43] Two factors determine the engagement of this sgmRNA in the translation machinery: (1) The structure of sgmRNA and (2) its transcription by SV nsPs. We reasoned that the IRES sequence was unable to associate with the translation components after viral transcription, but perhaps IRES could promote translation once the sgmRNA had been recognized by ribosomes and was already engaged in translation. To test this possibility, we designed a new SV replicon encoding a bicistronic sgmRNA. This sgmRNA contains the canonical leader sequence of 26S mRNA, as well as the entire C sequence, which is followed by EMCV IRES and luc gene, rep C+LEMCV-luc (see Fig. 3a). BHK cells were electroporated with the new replicon and also with rep C+luc and rep LEMCV-luc as controls. Protein synthesis was analyzed at different times after electroporation by radioactive labeling (Fig. 3b, upper panel) and by Western blot with anti-luc antibodies (Fig. 3b, lower panel). Synthesis of C protein from rep C+LEMC-luc, which is directed by the first cistron of sgmRNA, is very efficient and similar to control rep C+luc (Fig. 3b, upper panel). However, luc production, which should be directed by the EMCV IRES located as a second cistron in the same mRNA, is very low. Luc production from rep C+LEMC-luc is similar to that obtained from rep LEMCV-luc (Fig. 3b, lower panel) where the IRES sequence is in the beginning of sgmRNA. This result is consistent with the idea that even though the sgmRNA is being translated by ribosomes and other translation components, they run off upon translation of the first cistron. Most probably, a crucial component necessary to start IRES-driven translation is absent in this environment.

For comparative reasons, we have also examined the capacity of the subgenomic leader sequence together with the enhancing motif to promote internal translation in cells transfected with an SV

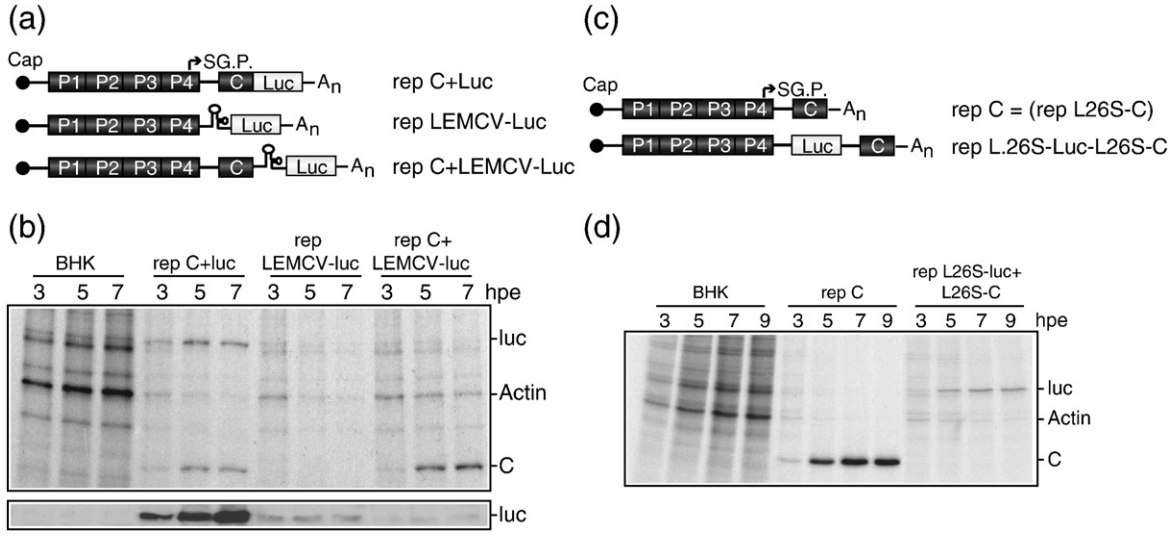

Fig. 3. Inactive IRES elements present in sgmRNAs. (a) Schematic representation of replicons used in (b). (b) Cells were electroporated with the different replicons, and at the times indicated, protein synthesis was analyzed by incorporation of [^{35}S]Met,Cys, SDS-PAGE, fluorography, and autoradiography (upper panel) or transferred to nitrocellulose and analyzed by Western blot with anti-luc antibodies (lower panel). (c) Schematic representation of replicons used in (d). (d) Cells were electroporated with the different replicons, and at the times indicated, protein synthesis was analyzed by incorporation of [^{35}S]Met,Cys, SDS-PAGE, fluorography, and autoradiography.

replicon. Previously, it has been described that these sequences, when placed in a bicistronic mRNA, do not drive internal translation.[39] We now wanted to test whether these sequences could promote internal translation when present in an SV sgmRNA at late times of infection, when the translation requirements have been modified. Thus, a replicon was constructed encoding sgmRNA, in turn encoding L26S-luc followed by L26S-C sequences (see scheme in Fig. 3c). Upon electroporation, this replicon leads to luc synthesis, while the production of C was absent (Fig. 3d). By contrast, BHK cells, electroporated with rep C (see scheme in Fig. 3c), rendered high levels of C protein (Fig. 3d). However, the same subgenomic leader sequence together with the enhancing motif located internally in the sgmRNA does not promote translation despite the fact that it was produced by the SV transcription machinery at times when viral translation exhibits a low requirement for eIFs. This finding strongly supports the conclusion that there are at least three features that should be met by the structure of sgmRNA to be efficiently translated: (i) the leader sequence, (ii) the enhancing element, and (iii) the capped 5′ end.

Rescue of picornavirus IRES-driven translation by co-expression of PV nsPs

Next, we wanted to test whether any of the PV nsPs could rescue the inability of PV IRES to direct translation in SV-replicon-transfected cells. The rationale of this experiment is based on the fact that individual viral proteins can replace, in some instances, particular initiation factors as occurs with influenza virus, rotavirus, or hantavirus.[44–46] The PV non-structural genes were cloned after the SV C sequence to obtain replicons rep C+"PV protein". In particular, the PV genes 2A, 2B, 2BC, 2C, 3A, 3AB, and 3C were cloned in this manner (Fig. 4a). As shown in Fig. 4b, the synthesis of these PV proteins was detected by radioactive labeling. Although the PV proteins are initially synthesized as a fusion polypeptide between SV C and the corresponding PV protein, the proteolytic activity of C at its carboxy terminus liberates the genuine PV protein (Fig. 4b). Therefore, both SV C and the PV protein are produced in equimolar amounts. The majority of PV proteins are synthesized to high levels, although some of them, particularly the two PV proteases and viroporin 2B, exhibit a detrimental effect on SV gene

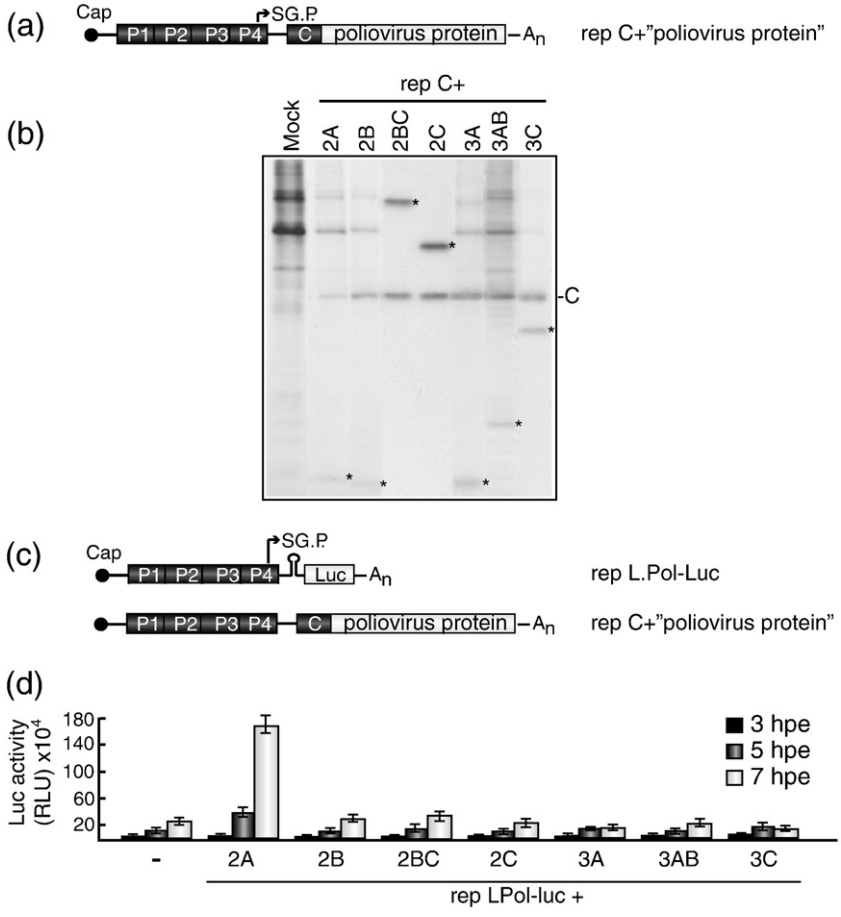

Fig. 4. Transactivation of PV IRES by PV nsPs. (a) Schematic representation of the replicons used in the experiment described in (b). (b) Expression of the different nsPs from PV by the system rep C+"poliovirus protein" was analyzed at 7 hpe by incorporation of [^{35}S]Met,Cys, SDS-PAGE, fluorography, and autoradiography. PV proteins are indicated by an asterisk. (c) Schematic representation of replicons used in the experiment described in (d). (d) Cells were co-electroporated with a mixture of *in vitro* synthesized rep LPol-Luc and each different replicon rep C+"poliovirus protein". At different times, cells were harvested and luc activity was determined. Luc activity results are means±SD of three representative experiments performed in triplicate.

expression. To test whether any PV protein could rescue the translation of mRNAs containing the PV IRES, co-expression of rep LPol-luc with replicons encoding each one of the PV genes was carried out. To this end, *in vitro* transcribed rep LPol-luc were electroporated with each rep C+"PV protein" and luc activity was measured at different times after co-electroporation. Remarkably, expression of PV $2A^{pro}$ very much enhanced luc production at all times measured (Fig. 4d). By contrast, none of the other PV nsPs examined increased luc activity. The stimulation of luc activity by PV $2A^{pro}$ at 7 hpe was greater than 7.5-fold.

Transactivation activity on picornavirus IRESs of different proteases

Since $2A^{pro}$ is a well-known protease that cleaves eIF4GI,[47] it was of interest to study whether this proteolytic activity was necessary for the enhancing effect observed above. Thus, we analyzed the expression of a 2A variant previously described as proteolytically inactive, 2A(G60R),[48] and another picornaviral protease, protease L (L^{pro}) from foot-and-mouth disease virus (FMDV), also known to hydrolyze eIF4GI.[49] Two new SV replicons containing the PV 2A variant and FMDV L^{pro} were constructed and co-electroporated with rep LPol-luc (Fig. 5a). At 7 hpe, which corresponds with the highest transactivation effect, protein synthesis, eIF4GI proteolysis, and luc activity were examined (Fig. 5b–d). Decreased gene expression was observed in cells that synthesize $2A^{pro}$ or L^{pro}, as compared to the ones that express inactive 2A (G60R) (Fig. 5b). Notably, luc activity was much higher in cells expressing PV $2A^{pro}$ or FMDV L^{pro} as compared to the PV 2A(G60R) variant (Fig. 5d). As expected, eIF4GI, which is detected as two proteins of ~220 and ~150 kDa in BHK cells,[50,51] was cleaved in cells expressing $2A^{pro}$ or L^{pro} but remained intact in cells synthesizing 2A(G60R) (Fig. 5c). It therefore seems clear that eIF4GI

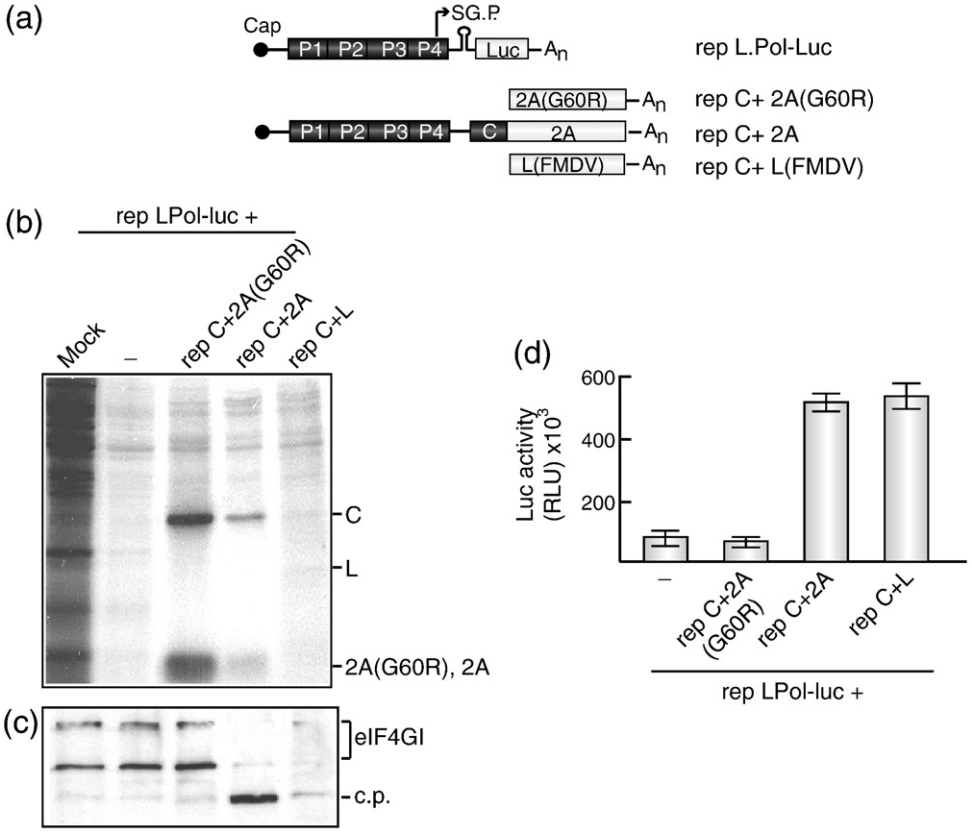

Fig. 5. Activity of different picornavirus proteases on IRES-driven translation. (a) Schematic representation of replicons used in (b)–(d). (b) Cells were co-electroporated with rep LPol-luc and each different replicon indicated in the figure or transcription buffer as control and at 7 hpe protein synthesis was analyzed by incorporation of [^{35}S]Met,Cys, SDS-PAGE, fluorography, and autoradiography. (c) Integrity of eIF4GI was analyzed in parallel by Western blot with anti-eIF4GI antibodies. (d) Luc activity was also determined at this time, and the results are means±SD of one experiment performed in triplicate. c.p., cleavage product.

proteolysis is crucial for the activating activity of picornavirus IRES translation in the SV replicon system.

EMCV infection does not lead to proteolysis of eIF4GI, although its IRES element can be activated by FMDV L^{pro}.[52] We considered it of interest to analyze the potential activation of EMCV IRES by different picornavirus proteins using SV replicons. To this end, co-electroporation of rep LEMCV-luc with the replicons indicated in Fig. 6a was carried out. We tested the transactivation effect of PV $2A^{pro}$, its variant 2A(G60R), FMDV L^{pro}, and EMCV 2A, which has no proteolytic activity. Synthesis of luc assayed by radioactive labeling can only be clearly detected in cells co-electroporated with rep LEMCV-luc and rep C+2A at 7 hpe (Fig. 6b, upper panel). In agreement with this result, a notable increase in luc accumulation is observed in the corresponding Western blot analysis (Fig. 6b, lower panel). Like PV 2A, expression of FMDV L^{pro} diminished gene expression from SV replicons and its synthesis decreased with time (Fig. 6b, upper panel). By contrast, luc production, measured by Western blot with anti-luc antibodies, increased over time as occurs on expression of PV $2A^{pro}$. Two products of luc with different mobility were detected by Western blot in L^{pro}-expressing cells, probably due to its proteolytic cleavage by FMDV protease (Fig. 6b, lower panel). However, expression of the inactive $2A^{pro}$ (G60R) or EMCV 2A does not transactivate luc translation. The synthesis of these proteins increases with time during the experiment (Fig. 6b, upper panel), but the production of luc does not (Fig. 6b, lower panel). In summary, transactivation of PV or EMCV IRESs is observed when proteases that cleave eIF4GI are co-expressed.

Transactivation activity of PV $2A^{pro}$ on several viral IRESs

Our next goal was to analyze the activity of PV $2A^{pro}$ on luc synthesis directed by mRNAs containing different viral IRES elements. Thus, BHK cells were co-electroporated with the following replicons

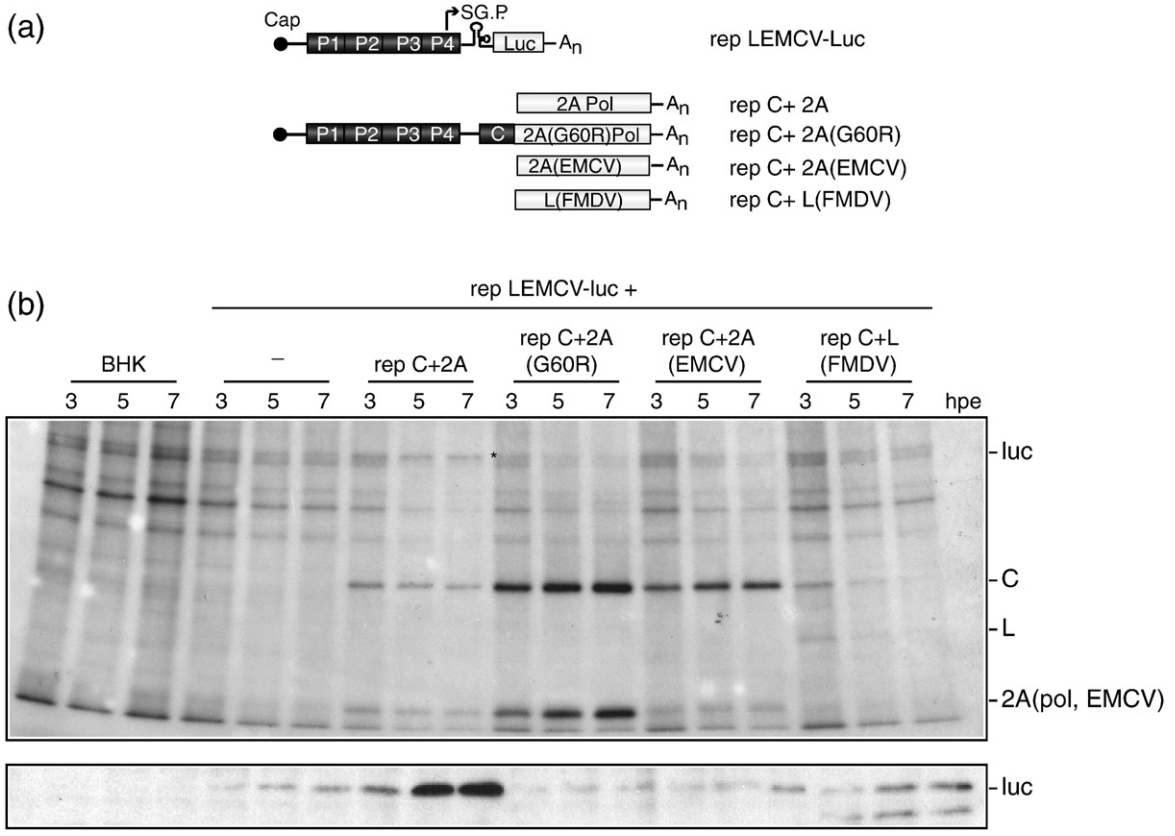

Fig. 6. Transactivation of translation of EMCV IRES. (a) Schematic representation of replicons used in (b). (b) Cells were co-electroporated with rep LEMCV-luc and each different replicon indicated in the figure or transcription buffer as control. At different hpe, protein synthesis was analyzed by incorporation of [^{35}S]Met,Cys, followed by SDS-PAGE, fluorography, and autoradiography (upper panel) or transferred to nitrocellulose and analyzed by Western blot with anti-luc antibodies (lower panel).

prepared *in vitro*: rep C+luc, rep LPol-luc, rep LEMCV-luc, rep IGR(CrPV)-luc or rep LHCV-luc and rep C+2A or rep C+2A(G60R) as control (Fig. 7a). At 7 hpe, luc activity was determined, as well as the total amount of luc synthesized by Western blot with anti-luc antibodies (Fig. 7b and c). Consistent with the above findings, luc production is clearly enhanced in cells co-electroporated with rep LPol-luc or rep LEMC-luc and rep C+2A as compared to cells co-electroporated with rep C+2A(G60R) when determined by both luc activity and by Western blot with anti-luc antibodies (Fig. 7b and c). However, expression of 2A *versus* 2A(G60R) only produces a slight stimulation of luc on rep C+Luc and was even detrimental for rep IGR(CrPV)-luc and rep LHCV-luc (Fig. 7b and c). In conclusion, rescue of translation of viral IRESs by PV $2A^{pro}$ in this system seems to be restricted to picornavirus IRESs, while this protease diminished luc synthesis driven by HCV or IGR of CrPV IRESs.

Immunolocalization of eIF4GI in BHK cells electroporated with SV replicons

Previously, we have reported that eIF4GI is located in stress granules (SGs) in SV-infected cells.[53] This factor is also found in SG at early times in PV-infected cells, although as infection progresses, eIF4GI is redistributed and does not appear in SG.[54] We reasoned that perhaps the lack of translation of sgmRNAs bearing picornavirus IRESs was due to the sequestration of eIF4GI in SG. The cleavage of eIF4GI would permit the redistribution of the carboxy terminus of this factor in order to participate in IRES-driven translation. To test this hypothesis, we analyzed the cellular localization of

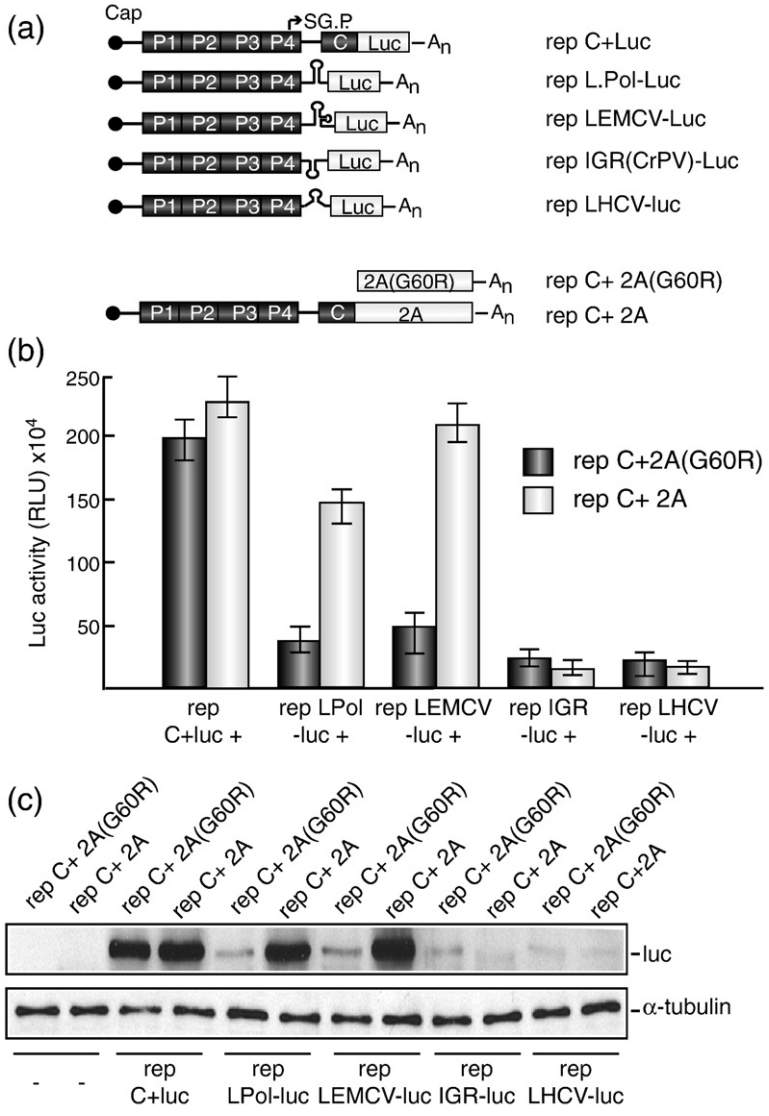

Fig. 7. Transactivation activity of PV $2A^{pro}$ on different viral IRES elements. (a) Schematic representation of replicons employed. (b) BHK cells were co-electroporated with the different replicons rep "IRES-luc" indicated in the figure plus rep C+2A or rep C+2A(G60R) and, at 7 hpe, harvested to measure luc activity (b) and to analyze luc production by Western blot with anti-luc antibodies (c). Western blot with anti-α-tubulin was made as a quantity control (c). Luc activity results are means±SD of three measurements of the same experiment.

eIF4GI and the formation of SG by confocal microscopy using antibodies against the SG marker TIA-1 and against eIF4GI (Supplementary Data). Cells were electroporated with transcription buffer or with rep LEMCV-luc or co-electroporated with rep LEMC-luc and rep C+2A. Induction of SG containing eIF4GI and TIA-1 was clearly apparent in SV-infected cells. By contrast, SG formation was not found in cells electroporated with transcription buffer. In these cells, TIA-1 can be detected in both nucleus and cytoplasm, whereas eIF4GI is mainly located at the cytoplasm. Surprisingly, cells electroporated with rep LEMC-luc do not contain SG, despite the fact that in this case TIA-1 appears redistributed in the cytoplasm as occurs with eIF4GI. Thus, it seems that electroporation blocks the induction of SG that is evident in SV-infected cells. Expression of PV $2A^{pro}$ leads to cell rounding, but also in this case, no SG formation was observed, and both TIA-1 and eIF4GI are evenly distributed in the cytoplasm. Ribosomes co-localize with eIF4GI when cells are electroporated with rep LEMC-luc both in the absence and in the presence of PV $2A^{pro}$. Using the ImageJ program with the Just Another Co-localization Plugin,[55] the co-localization factor (Pearson's coefficient) rate for eIF4GI and ribosomes was 0.74 on a scale of 0 to 1 (0–0.5 indicates no co-localization and 0.5–1 indicates co-localization) for cells electroporated with rep LEMC-luc and 0.83 for those that co-express PV $2A^{pro}$. In conclusion, the translational rescue of mRNAs with IRES from rep LEMCV-luc conferred by $2A^{pro}$ cannot be attributed to the release of eIF4GI from SG and to its redistribution. Instead, cleavage of eIF4GI is the event necessary to rescue picornavirus IRES-driven translation in BHK cells that express SV replicons.

Discussion

Mammalian cells infected by cytolytic viruses usually undergo profound modifications in the pattern of translation,[56,57] and this is indeed the case for alphavirus-infected cells, where cellular protein synthesis is abrogated soon after infection, while 26S sgmRNA is still translated.[28] For a long time, it was thought that the structure of viral mRNAs determined their translatability under infection conditions. However, we found that SV sgmRNA transfected at late times of infection in SV-infected cells was excluded from translation.[43] Similar results were found when mRNAs containing EMCV IRES were transfected in EMC-, SV-, or VSV-infected cells. Therefore, in addition to the structural features required by a viral mRNA for efficient translation in virus-infected cells, it must be synthesized by the viral transcriptional apparatus. Moreover, the origin of sgmRNA dictates the mode of translation and eIF requirements for translation. SV sgmRNAs directly electroporated in BHK cells are translated by a canonical mechanism, while those produced by viral transcription do not require eIF4G.[53] These observations suggest a dual mode for the translation of these viral mRNAs. Initially, viral mRNAs are translated using the canonical set of eIFs, while at late times of SV replication, a switch to a different mode of translation takes place. This new mechanism of protein synthesis involves the exclusive use of newly synthesized viral mRNAs, which do not require some eIFs, such as eIF4G. In the present work, we found that only genuine mRNAs from SV are efficiently translated, while sgmRNAs containing foreign leader sequences are poor substrates for translation, despite similar levels of mRNA transcription. Therefore, as shown in Fig. 1, for the efficient translation of sgmRNA, both requirements are necessary: the 5′-UTR of sgmRNA must contain the adequate structure and this mRNA should be transcribed from the replicon.

In principle, mRNAs containing picornavirus IRESs have lower requirements for some eIFs to direct protein synthesis.[1,16] For this reason, it was of interest to explore the efficacy of translation of mRNAs containing picornavirus IRESs that are produced from SV replicons by the viral transcriptional machinery. Our present findings indicate that these mRNAs are initially translated in electroporated cells. However, their translation is inhibited when viral replication progresses, despite the fact that these mRNAs are being synthesized by the SV replication machinery. It seems that at least one important component of the protein-synthesizing machinery fundamental for picornavirus IRES-driven translation is not available in SV replicative foci. Somehow, genuine SV mRNAs are efficiently directed to the translation machinery, probably by the participation of a viral protein that recognizes a specific structure or sequence in SV sgmRNA. In this regard, the N protein from hantavirus is able to replace the entire eIF4F complex during viral translation.[46] Probably, there are more viral proteins that enhance translation of their corresponding viral mRNAs and modify the eIF requirements.

Notably, co-expression of PV $2A^{pro}$ largely restores the translatability of picornavirus IRES mRNAs under SV infection conditions. The fact that PV $2A^{pro}$ cleaves eIF4G[51,58] points to the idea that this event is the one responsible for rescuing IRES mRNA translatability under these conditions. At least two findings support this notion: one is that none of the PV nsPs, apart from PV $2A^{pro}$, exhibited this activity; the other observation is that a $2A^{pro}$ variant unable to cleave eIF4G[48] failed to rescue picornavirus IRES mRNA for translation. In addition, another picornavirus protease that cleaves eIF4G and FMDV L^{pro}, which is unrelated to PV $2A^{pro}$, also enhanced IRES-driven translation from SV replicons. Recently, we found that eIF4G may

not be utilized to translate SV sgmRNAs[50] and co-localizes with TIA-1 in SG in SV-infected cells.[53] Remarkably, in electroporated BHK cells, the formation of SG is hampered and eIF4GI co-localizes with ribosomes both in cells replicating rep LEMC-luc and in cells that co-express PV $2A^{pro}$. Therefore, the inability of picornavirus IRES to direct translation in SV-replicating cells cannot be ascribed to the sequestration of eIF4GI in SG. Our conclusion is that cleavage of eIF4GI by PV $2A^{pro}$ could provide the C-terminal fragment of this factor that is then able to participate in translation of picornavirus IRES mRNAs synthesized by the SV transcriptional machinery. However, the possibility that other cellular proteins targeted by PV $2A^{pro}$ are responsible for this phenomenon is still open.

Of particular interest is the failure of HCV IRES to be translated under these conditions. The current model for HCV mRNA translation is that it does not require the eIF4F complex[7,17] or even eIF2.[19] Thus, at present, it is unknown why HCV IRES-driven translation from SV replicons is so inefficient. One possibility is that this mRNA requires a micro-RNA (MIR-122) for its efficient translation[59–61] and perhaps, this micro-RNA is absent from BHK cells. However, HCV-luc is well translated when directly transfected in BHK cells (see Fig. 2d). Therefore, a crucial component for HCV translation may be absent in SV replicative foci. This component seems to be specific for HCV-luc mRNA, since SV sgmRNA is efficiently translated at these replicative sites. Moreover, HCV translation is not rescued by PV $2A^{pro}$ pointing to the specificity of this protease on the stimulation of picornavirus IRESs. Another case of interest is the relatively low translatability of CrPV IGR-luc mRNA. This was unexpected because this mRNA is not thought to require any eIF to direct translation.[20,62] Still, it could be possible that the presence of a given CrPV protein may enhance the translatability of each mRNA. Consistent with this idea, CrPV mRNA can be translated by a canonical mechanism at the beginning of infection, while at late times, it follows an eIF-independent mechanism.[63] Most probably, IRES-containing mRNAs can exhibit a dual mechanism of translation, as occurs with SV sgmRNA.[53] Such a mechanism takes place in cell-free systems or in transfected cells, while the eIF requirements vary in the context of infection. Therefore, the sgmRNAs bearing an IRES element described in this work are generated in a microenvironment different from their own infections. Obviously, in the context of their infections, these mRNAs will be preferentially translated.

It is well established that EMCV and PV IRESs are stimulated by L^{pro} or $2A^{pro}$, both in transfected cells and in cell-free systems.[52,64–66] The generation of the carboxy-terminal fragment of eIF4GI is responsible for this stimulation.[49,64,67] Interestingly, EMCV infection does not lead to eIF4G cleavage, making it difficult to explain why such IRES is stimulated upon eIF4GI cleavage. Perhaps, an EMCV protein is able to stimulate its own IRES element. However, the rescue of EMCV IRES in SV replicons was not achieved with EMCV 2A (see Fig. 6) or with the L protein (data not shown). The inability of picornavirus IRES to be translated in SV-infected cells is not observed when cells are doubly infected with picornaviruses and alphaviruses.[41,42] In those cells, viral translation is coupled to transcription in each type of viral replicative foci. In the case of SV replicons containing IRES, translation is not coupled to transcription, probably due to the absence of one or more viral proteins necessary to enhance translation of IRES-containing mRNAs.

Finally, several reports have suggested that translation driven by picornavirus IRESs can take place from SFV or VEEV replicons.[31,36,37] Although differences may exist among different alphavirus species in this respect, our present results reveal that the viral IRESs analyzed are inefficiently used for translation when they are transcribed by SV replicons.

Materials and Methods

Cell line and viruses

BHK-21 cells and SV were used to perform the experiments. SV virus stock was prepared from a pT7 SVwt infective cDNA clone (where wt is wild type).[68] Viral infection of BHK cells was carried out in Dulbecco's modified Eagle's medium (DMEM) without serum for 40 min to permit virus attachment. This medium was then removed and infection continued in DMEM with 10% fetal calf serum.

Plasmids and recombinant DNA procedures

Plasmids rep C and rep C+luc[43] or rep C+2A and rep C+2C[50] have been described previously. Mutation G60R in 2A has also been previously described.[48] Plasmids rep C+"poliovirus protein" were made in several stages. A shuttle vector, pH3′2J-"C" was first made to insert the sequence of "C" from the AatII site until the end of the gene plus an NdeI restriction site between AccI and XbaI sites in pH3′2J.[69] Oligonucleotides 5′pH3-"C" and 3′PH3-"C" were used to obtain "C" by PCR. Next, PV genes were obtained by PCR from pT7XLD[70] using the forward and reverse oligonucleotides listed at Table 1. These genes were cloned at the NdeI site or between the NdeI and BamHI sites in pH3′2J-"C" to obtain plasmids pH3′2J-"C+.poliovirus protein". Finally, each plasmid pH3′2J-"C+.poliovirus protein" was digested with AatII/XhoI and cloned at the same sites of pT7 SVwt[68] to generate the different plasmids rep C+"poliovirus protein". The same strategy was employed to construct the plasmids rep C+2A (EMCV) and rep C+L(FMDV). Gene 2A from EMCV derived from plasmid pEBal 2 was a kind gift from Palmenberg AC (Institute for Molecular Virology and Department of Biochemistry, University of Wisconsin-

Table 1. Oligonucleotide sequences

Name	Sequence (5′–3′)
5′pH3-"C"	GGGCCCGTAGACGACGTCAAGAAGGAGGAGGC
3′PH3-"C"	GGTCTAGACATATGTGCGGACCACTCTTCGGTACCTTC
5′2B	CCCGGGCATATGGGCATCACCAATTACATAGAG
3′2B	GGCCCGGATCCTTATTATTGCTTGATGACATAAGGTA
5′2C	CCCGGGCATATGGGTGACAGTTGGTTGAAGAAG
3′2C	GGCCCATATGTTATTGAAAACAAAGCCTCCATACA
5′3A	CCCGGGCATATGGGACCACTCCAGTATAAAGAC
3′3A	GGGCCCTGATCATTACTGGTGTCCAGCAAACAGTT
3′3B	GGGCCCTGATCATTATTGTACCTTTGCTGTCCGAAT
5′3C	GGCCCCATATGGGACCAGGGTTCGATTACGCA
3′3C	TGGGGGATCCTATCAATATGTGTCGAGCAGTTTTTG
5′2A(EMCV)	CCGGGCATATGAGTCCAAATGCCCTAGAC
3′2A(EMCV)	GGCCCGGATCCTTACCCTGGATTTGTCTCAATG
5′L(FMDV)	CCGGCATATGAATACAACTGACTG
3′L(FMDV)	GGCCCGGATCCTTACTTGAGCTTTCGCTGAAC
5′SV HpaI	CTATGGCGTTAACCGGTCTGATGATC
3′Luc SphI	CCCGGGGCATGCGAGAATCTGACGCAG
5′Nexo SV-LPol	CTAAATAGTCAGCATTAAAACAGCTC
3′Nexo SV-LPol	GAGCTGTTTTAATGCTGACTATTTAG
5′Nco Luc	GGGGCCCCATGGAAGACGCCAAAAAC
3′BamHI luc	ACGCGCGCATCCTTACAATTTGGACTTTCC
5′Nexo SV-LEMCV	CCTAAATAGTCAGCATGGGAGACCACAACGGTTTCC
3′Nexo SV-LEMCV	GGAAACCGTTGTGGTCTCCCATGCTGACTATTTAGG
5′Nexo SV-IGR	CCTAAATAGTCAGCAAGCAAAAATGTGATCTTGCTTGT
3′Nexo SV-IGR	ACAAGCAAGATCACATTTTTGCTTGCTGACTATTTAGG
5′Nexo SV-LHCV	CCTAAATAGTCAGCCAGCCCCCG
3′Nexo SV-LHCV	CGGGGGCTGGCTGACTATTTAG
5′Nexo SV-LLuc	CCTAAATAGTCAGCATTGTCGCTCGCAGTGAC
3′Nexo SV-LLuc	GTCACTGCGAGCGACAATGCTGACTATTTAGG
5′AatII C	ATTGTTCGACGTCAAGAAC
5′Nexo C-LEMCV	AGAGTGGTCCGCACATATGGGAGACCACAACGGTTTC
3′Nexo C-LEMCV	GAAACCGTTGTGGTCTCCCATATGTGCGGACCACTCT
5′ApaI L26S	GCGCGCGGGCCCCAGCATAGTACATTTCAT
3′XhoI 3UTR	ATTAATTCCCCTCGAGGAATTCC

Madison). Gene L from FMDV was derived from plasmid PMT28.[71]

The plasmids where the sgmRNA-leader sequence (L26S) was replaced by different leader sequences were made including a product obtained after two consecutive PCRs between HpaI and SphI sites in rep C+luc. The first PCR was made on rep C+luc using 5′ SV HpaI as forward primer and using as reverse primer each different 3′Nexo SV-"leader sequence" listed at Table 1. The second PCR employed each 5′Nexo SV"leader sequence", which has the reverse and complementary sequence of 3′ oligonucleotide used before, and as 3′oligonucleotide 3′Luc SphI; plasmids with different leader-luc sequences were used as DNA templates. The partner products were then mixed to be used as templates in a new PCR with the oligonucleotides 5′SV HpaI and 3′Luc SphI. Plasmid pT75NCpolioLUC[72] was used as a template to obtain the LPol-luc sequence. To make pTM1-luc, we cloned the luc sequence obtained with the oligonucleotides 5′NcoI-Luc and 3′BamHI-Luc in NcoI/BamHI sites from pTM1.[73] Subsequently, pTM1-luc was used as a template to obtain the LEMCV-luc sequence. The template to obtain the IGR-luc sequence was the plasmid T7 Rluc ΔEMCV IGR-Fluc.[20] Plasmid pT733coreHCVLuc, which has the leader sequence from HCV plus the first 33 nucleotides of the capsid gene before the luc sequence, was used to obtain the LHCV-luc sequence. This plasmid was a kind gift from Takashi Shimoike (National Institute of Infectious Diseases, Musashi-murayama, Tokio).

Plasmid rep C+LEMC-luc was prepared with a product obtained after two consecutive PCRs between AatII and SphI sites in rep C+luc. In the first PCR, oligonucleotides 5′AatII C and 3′Nexo C-LEMCV plus rep C were used as DNA template. The other PCR product was obtained using 5′Nexo C-LEMCV and 3′Luc SphI oligonucleotides plus rep LEMCV-luc as DNA template. Oligonucleotides 5′AatII C and 3′Luc SphI with a mixture of the above products as DNA template were employed in the next PCR.

Plasmid rep L26S-luc-L26S-C was prepared by cloning the PCR product obtained with the oligonucleotides 5′ ApaI L26S and 3′XhoI 3UTR plus rep C as DNA template in the ApaI/XhoI sites from rep L26S-luc.

In vitro transcription and transfection

Plasmids digested with XhoI enzyme were used as templates for *in vitro* RNA transcription with T7 RNA polymerase (Promega). The transcription mixture always contained an $m^7G(5')ppp(5')G$ cap analog except in the experiment where translation driven by IRES was assayed. For transfection, subconfluent BHK cells were harvested, washed with ice-cold phosphate-buffered saline (PBS), and resuspended at a density of approximately 2.5×10^6 cells/ml in the same buffer. Subsequently, 20 μg of *in vitro* transcribed RNA were added to 0.4 ml cell suspension and the mixture was transferred to a 2-mm

cuvette. Electroporation was carried out at room temperature by generating two consecutive 1.5-kV, 25-mF pulses with a Gene Pulser apparatus (Bio-Rad), as previously described.[74]

Analysis of protein synthesis by radioactive labeling

Protein synthesis was analyzed by replacing the growth media for half hour with 0.2 ml DMEM without methionine–cysteine supplemented with 2 μl EasyTag™ EXPRESS ^{35}S Protein Labeling mix, [^{35}S]Met-Cys (11 mCi/ml, 37.0 Tbq/mmol; Perkin Elmer) per well of an L-24 plate. The cells were then collected in the appropriate gel loading buffer (62.5 mM Tris–HCl, pH 6.8, 2% SDS, 0.1 M dithiothreitol, 17% glycerol, and 0.024% bromophenol blue) and analyzed by autoradiography of SDS-polyacrylamide gels.

Analysis of the viral RNA synthesis by radioactive labeling

Uridine [5-^{3}H] incorporation in cells treated with actinomycin D (2.5 μg/ml) was employed to detect viral RNA synthesis by agarose gel electrophoresis of labeled RNA or by measuring radioactivity in a scintillation counter. For electrophoretic analysis, total RNA from approximately 2.5×10^{6} cells treated with actinomycin D from 1 h after electroporation and with [^{3}H]uridine (740 GBq/mmol, 30 μCi/ml, final concentration) from 3 hpe was extracted at 5 1/2 hpe using the RNAeasy mini Kit (Qiagen) and resuspended in 40 μl water. Samples (20 μl) were denatured by treatment with glyoxal and dimethyl sulfoxide and separated by electrophoresis in 0.8% agarose gels containing 10 mM phosphate buffer as indicated by Sambrook *et al.* in their laboratory manual.[75] Geles were treated with the autoradiography enhancer EN^{3}HANCE (PerkinElmer), dried, and exposed to X-ray film at −70 °C. To measure [^{3}H]uridine incorporation by a scintillation counter, we treated approximately 6×10^{5} cells with actinomycin D (2.5 μg/ml) from 1 hpe and with [^{3}H]uridine (30 μCi/ml, final concentration) from 2 hpe. At 3, 5, and 7 hpe, medium was discarded, and cells were treated with 0.5 ml of 5% trichloroacetic acid, washed twice with ethanol, dried under an infrared lamp, and dissolved in 200 μl of 0.1 N NaOH/1% SDS, as previously described.[76] Counts for 100-μl samples were obtained in a liquid scintillation spectrometer.

Measurement of luc activity

Cells were lysed in a buffer containing 0.5% Triton X-100, 25 mM glycylglycine (pH 7.8), and 1 mM dithiothreitol. Luc activity was determined using a Monolith 2010 luminometer (Analytical Luminescence Laboratory), using the Luciferase Assay System (Promega).

Immunofluorescence microscopy

BHK cells were electroporated with the different replicons or infected with SV (100 pfu/cell) and seeded on coverslips. After 7 h, cells were fixed in 4% paraformaldehyde for 15 min, washed twice with PBS, and then permeabilized for 10 min with 0.2% Triton X-100 in PBS. All antibody incubations were carried out for 1 h in PBS containing 0.1% fetal calf serum and 0.1% Triton X-100. Coverslips were washed three times with PBS between primary and secondary antibody incubations, mounted in ProLong Gold anti-fade reagent (Invitrogen), and finally examined with a Radiance 2000 (Bio-Rad/Zeiss) confocal laser scanning microscope. Primary antibodies used were rabbit polyclonal anti-eIF4GI[77] and goat anti-TIA-1 (Acris Antibodies GmbH). Specific antibodies conjugated to Alexa-555 or Alexa-488 were used as secondary antibodies.

Acknowledgements

This study was supported by a DGICYT Grant (BFU2009-07352). E.W. and N.R. are holders of FPU and FPI Fellowships, respectively. The Institutional Grant awarded to the Centro de Biología Molecular "Severo Ochoa" by the Fundación Ramón Areces is acknowledged.

Supplementary Data

Supplementary data associated with this article can be found, in the online version, at doi:10.1016/j.jmb.2010.07.014

References

1. Pestova, T. V., Kolupaeva, V. G., Lomakin, I. B., Pilipenko, E. V., Shatsky, I. N., Agol, V. I. & Hellen, C. U. (2001). Molecular mechanisms of translation initiation in eukaryotes. *Proc. Natl Acad. Sci. USA*, **98**, 7029–7036.
2. Merrick, W. C. (2004). Cap-dependent and cap-independent translation in eukaryotic systems. *Gene*, **332**, 1–11.
3. Pisarev, A. V., Shirokikh, N. E. & Hellen, C. U. (2005). Translation initiation by factor-independent binding of eukaryotic ribosomes to internal ribosomal entry sites. *C. R. Biol.* **328**, 589–605.
4. Sonenberg, N. & Hinnebusch, A. G. (2009). Regulation of translation initiation in eukaryotes: mechanisms and biological targets. *Cell*, **136**, 731–745.
5. Pestova, T. V., Lorsch, J. R. & Hellen, C. U. (2007). The mechanism of translation initiation in eukaryotes. In *Translational control in biology and medicine* (Mathews, N. S. & Hershey, J. W. B., eds), pp. 87–128, Cold Spring Harbor Laboratory Press, Cold Spring Harbor, NY.
6. Kieft, J. S. (2008). Viral IRES RNA structures and ribosome interactions. *Trends Biochem. Sci.* **33**, 274–283.
7. Balvay, L., Soto Rifo, R., Ricci, E. P., Decimo, D. & Ohlmann, T. (2009). Structural and functional diversity of viral IRESes. *Biochim. Biophys. Acta*, **1789**, 542–557.
8. Fitzgerald, K. D. & Semler, B. L. (2009). Bridging IRES

elements in mRNAs to the eukaryotic translation apparatus. *Biochim. Biophys. Acta*, **1789**, 518–528.
9. Jang, S. K. (2006). Internal initiation: IRES elements of picornaviruses and hepatitis c virus. *Virus Res.* **119**, 2–15.
10. Nakashima, N. & Uchiumi, T. (2009). Functional analysis of structural motifs in dicistroviruses. *Virus Res.* **139**, 137–147.
11. Belsham, G. J. (2009). Divergent picornavirus IRES elements. *Virus Res.* **139**, 183–192.
12. Filbin, M. E. & Kieft, J. S. (2009). Toward a structural understanding of IRES RNA function. *Curr. Opin. Struct. Biol.* **19**, 267–276.
13. Lukavsky, P. J. (2009). Structure and function of HCV IRES domains. *Virus Res.* **139**, 166–171.
14. Jan, E., Kinzy, T. G. & Sarnow, P. (2003). Divergent tRNA-like element supports initiation, elongation, and termination of protein biosynthesis. *Proc. Natl Acad. Sci. USA*, **100**, 15410–15415.
15. Jang, C. J., Lo, M. C. & Jan, E. (2009). Conserved element of the dicistrovirus IGR IRES that mimics an E-site tRNA/ribosome interaction mediates multiple functions. *J. Mol. Biol.* **387**, 42–58.
16. Pestova, T. V., Hellen, C. U. & Shatsky, I. N. (1996). Canonical eukaryotic initiation factors determine initiation of translation by internal ribosomal entry. *Mol. Cell. Biol.* **16**, 6859–6869.
17. Niepmann, M. (2009). Internal translation initiation of picornaviruses and hepatitis C virus. *Biochim. Biophys. Acta*, **1789**, 529–541.
18. Borman, A. M. & Kean, K. M. (1997). Intact eukaryotic initiation factor 4G is required for hepatitis A virus internal initiation of translation. *Virology*, **237**, 129–136.
19. Terenin, I. M., Dmitriev, S. E., Andreev, D. E. & Shatsky, I. N. (2008). Eukaryotic translation initiation machinery can operate in a bacterial-like mode without eIF2. *Nat. Struct. Mol. Biol.* **15**, 836–841.
20. Wilson, J. E., Powell, M. J., Hoover, S. E. & Sarnow, P. (2000). Naturally occurring dicistronic cricket paralysis virus RNA is regulated by two internal ribosome entry sites. *Mol. Cell. Biol.* **20**, 4990–4999.
21. Jan, E. & Sarnow, P. (2002). Factorless ribosome assembly on the internal ribosome entry site of cricket paralysis virus. *J. Mol. Biol.* **324**, 889–902.
22. Deniz, N., Lenarcic, E. M., Landry, D. M. & Thompson, S. R. (2009). Translation initiation factors are not required for Dicistroviridae IRES function in vivo. *RNA*, **15**, 932–946.
23. Atkins, G. J., Fleeton, M. N. & Sheahan, B. J. (2008). Therapeutic and prophylactic applications of alphavirus vectors. *Expert Rev. Mol. Med.* **10**, e33.
24. Schlesinger, S. (2001). Alphavirus vectors: development and potential therapeutic applications. *Expert Opin. Biol. Ther.* **1**, 177–191.
25. Lundstrom, K. (2010). Expression of mammalian membrane proteins in mammalian cells using Semliki Forest virus vectors. *Methods Mol. Biol.* **601**, 149–163.
26. Ehrengruber, M. U. & Lundstrom, K. (2007). Alphaviruses: Semliki Forest virus and Sindbis virus vectors for gene transfer into neurons. *Curr. Protoc. Neurosci.*; Chapter 4, Unit 4.22.
27. Schlesinger, S. & Schlesinger, M. J. (2001). Togaviridae. In *Fundamental Virology* (Knipe, D. M. & Howley, P. M., eds), pp. 567–588, Lippincott Williams & Wilkins Press, Philadelphia, PA.
28. Strauss, J. H. & Strauss, E. G. (1994). The alphaviruses: gene expression, replication, and evolution. *Microbiol. Rev.* **58**, 491–562.
29. Tseng, J. C., Granot, T., DiGiacomo, V., Levin, B. & Meruelo, D. (2010). Enhanced specific delivery and targeting of oncolytic Sindbis viral vectors by modulating vascular leakiness in tumor. *Cancer Gene Ther.* **17**, 244–255.
30. Tseng, J. C., Levin, B., Hurtado, A., Yee, H., Perez de Castro, I., Jimenez, M. *et al.* (2004). Systemic tumor targeting and killing by Sindbis viral vectors. *Nat. Biotechnol.* **22**, 70–77.
31. Volkova, E., Frolova, E., Darwin, J. R., Forrester, N. L., Weaver, S. C. & Frolov, I. (2008). IRES-dependent replication of Venezuelan equine encephalitis virus makes it highly attenuated and incapable of replicating in mosquito cells. *Virology*, **377**, 160–169.
32. Li, M. L. & Stollar, V. (2007). Distinct sites on the Sindbis virus RNA-dependent RNA polymerase for binding to the promoters for the synthesis of genomic and subgenomic RNA. *J. Virol.* **81**, 4371–4373.
33. Frolov, I. & Schlesinger, S. (1994). Comparison of the effects of Sindbis virus and Sindbis virus replicons on host cell protein synthesis and cytopathogenicity in BHK cells. *J. Virol.* **68**, 1721–1727.
34. Frolov, I. & Schlesinger, S. (1996). Translation of Sindbis virus mRNA: analysis of sequences downstream of the initiating AUG codon that enhance translation. *J. Virol.* **70**, 1182–1190.
35. Polo, J. M., Belli, B. A., Driver, D. A., Frolov, I., Sherrill, S., Hariharan, M. J. *et al.* (1999). Stable alphavirus packaging cell lines for Sindbis virus and Semliki Forest virus-derived vectors. *Proc. Natl Acad. Sci. USA*, **96**, 4598–4603.
36. Kiiver, K., Merits, A. & Sarand, I. (2008). Novel vectors expressing anti-apoptotic protein Bcl-2 to study cell death in Semliki Forest virus-infected cells. *Virus Res.* **131**, 54–64.
37. Kamrud, K. I., Custer, M., Dudek, J. M., Owens, G., Alterson, K. D., Lee, J. S. *et al.* (2007). Alphavirus replicon approach to promoterless analysis of IRES elements. *Virology*, **360**, 376–387.
38. Rausalu, K., Iofik, A., Ulper, L., Karo-Astover, L., Lulla, V. & Merits, A. (2009). Properties and use of novel replication-competent vectors based on Semliki Forest virus. *Virol. J.* **6**, 33.
39. Ventoso, I., Sanz, M. A., Molina, S., Berlanga, J. J., Carrasco, L. & Esteban, M. (2006). Translational resistance of late alphavirus mRNA to eIF2alpha phosphorylation: a strategy to overcome the antiviral effect of protein kinase PKR. *Genes Dev.* **20**, 87–100.
40. Ou, J. H., Rice, C. M., Dalgarno, L., Strauss, E. G. & Strauss, J. H. (1982). Sequence studies of several alphavirus genomic RNAs in the region containing the start of the subgenomic RNA. *Proc. Natl Acad. Sci. USA*, **79**, 5235–5239.
41. Alonso, M. A. & Carrasco, L. (1982). Translation of capped virus mRNA in encephalomyocarditis virus-infected cells. *J. Gen. Virol.* **60**, 315–325.
42. Perez, L., Irurzun, A. & Carrasco, L. (1994). Action of brefeldin A on translation in Semliki Forest virus-infected HeLa cells and cells doubly infected with poliovirus. *J. Gen. Virol.* **75**, 2197–2203.

43. Sanz, M. A., Castello, A. & Carrasco, L. (2007). Viral translation is coupled to transcription in Sindbis virus-infected cells. *J. Virol.* **81**, 7061–7068.
44. Burgui, I., Yanguez, E., Sonenberg, N. & Nieto, A. (2007). Influenza virus mRNA translation revisited: is the eIF4E cap-binding factor required for viral mRNA translation? *J. Virol.* **81**, 12427–12438.
45. Groft, C. M. & Burley, S. K. (2002). Recognition of eIF4G by rotavirus NSP3 reveals a basis for mRNA circularization. *Mol. Cell*, **9**, 1273–1283.
46. Mir, M. A. & Panganiban, A. T. (2008). A protein that replaces the entire cellular eIF4F complex. *EMBO J.* **27**, 3129–3139.
47. Krausslich, H. G., Nicklin, M. J., Toyoda, H., Etchison, D. & Wimmer, E. (1987). Poliovirus proteinase 2A induces cleavage of eucaryotic initiation factor 4F polypeptide p220. *J. Virol.* **61**, 2711–2718.
48. Ventoso, I., Barco, A. & Carrasco, L. (1998). Mutational analysis of poliovirus 2Apro. Distinct inhibitory functions of 2apro on translation and transcription. *J. Biol. Chem.* **273**, 27960–27967.
49. Borman, A. M., Kirchweger, R., Ziegler, E., Rhoads, R. E., Skern, T. & Kean, K. M. (1997). elF4G and its proteolytic cleavage products: effect on initiation of protein synthesis from capped, uncapped, and IRES-containing mRNAs. *RNA*, **3**, 186–196.
50. Castello, A., Sanz, M. A., Molina, S. & Carrasco, L. (2006). Translation of Sindbis virus 26S mRNA does not require intact eukariotic initiation factor 4G. *J. Mol. Biol.* **355**, 942–956.
51. Lamphear, B. J., Kirchweger, R., Skern, T. & Rhoads, R. E. (1995). Mapping of functional domains in eukaryotic protein synthesis initiation factor 4G (eIF4G) with picornaviral proteases. Implications for cap-dependent and cap-independent translational initiation. *J. Biol. Chem.* **270**, 21975–21983.
52. Soto Rifo, R., Ricci, E. P., Decimo, D., Moncorge, O. & Ohlmann, T. (2007). Back to basics: the untreated rabbit reticulocyte lysate as a competitive system to recapitulate cap/poly(A) synergy and the selective advantage of IRES-driven translation. *Nucleic Acids Res.* **35**, e121.
53. Sanz, M. A., Castello, A., Ventoso, I., Berlanga, J. J. & Carrasco, L. (2009). Dual mechanism for the translation of subgenomic mRNA from Sindbis virus in infected and uninfected cells. *PLoS ONE*, **4**, e4772.
54. White, J. P., Cardenas, A. M., Marissen, W. E. & Lloyd, R. E. (2007). Inhibition of cytoplasmic mRNA stress granule formation by a viral proteinase. *Cell Host Microbe*, **2**, 295–305.
55. Bolte, S. & Cordelieres, F. P. (2006). A guided tour into subcellular colocalization analysis in light microscopy. *J. Microsc.* **224**, 213–232.
56. Bushell, M. & Sarnow, P. (2002). Hijacking the translation apparatus by RNA viruses. *J. Cell Biol.* **158**, 395–399.
57. Schneider, R. J. & Mohr, I. (2003). Translation initiation and viral tricks. *Trends Biochem. Sci.* **28**, 130–136.
58. Castello, A., Alvarez, E. & Carrasco, L. (2006). Differential cleavage of eIF4GI and eIF4GII in mammalian cells. Effects on translation. *J. Biol. Chem.* **281**, 33206–33216.
59. Sarnow, P., Jopling, C. L., Norman, K. L., Schutz, S. & Wehner, K. A. (2006). MicroRNAs: expression, avoidance and subversion by vertebrate viruses. *Nat. Rev., Microbiol.* **4**, 651–659.
60. Henke, J. I., Goergen, D., Zheng, J., Song, Y., Schuttler, C. G., Fehr, C. *et al.* (2008). MicroRNA-122 stimulates translation of hepatitis C virus RNA. *EMBO J.* **27**, 3300–3310.
61. Niepmann, M. (2009). Activation of hepatitis C virus translation by a liver-specific microRNA. *Cell Cycle*, **8**, 1473–1477.
62. Pfingsten, J. S. & Kieft, J. S. (2008). RNA structure-based ribosome recruitment: lessons from the Dicistroviridae intergenic region IRESes. *RNA*, **14**, 1255–1263.
63. Garrey, J. L., Lee, Y. Y., Au, H. H., Bushell, M. & Jan, E. (2010). Host and viral translational mechanisms during cricket paralysis virus infection. *J. Virol.* **84**, 1124–1138.
64. Hunt, S. L., Skern, T., Liebig, H. D., Kuechler, E. & Jackson, R. J. (1999). Rhinovirus 2A proteinase mediated stimulation of rhinovirus RNA translation is additive to the stimulation effected by cellular RNA binding proteins. *Virus Res.* **62**, 119–128.
65. Roberts, L. O., Seamons, R. A. & Belsham, G. J. (1998). Recognition of picornavirus internal ribosome entry sites within cells; influence of cellular and viral proteins. *RNA*, **4**, 520–529.
66. Ziegler, E., Borman, A. M., Kirchweger, R., Skern, T. & Kean, K. M. (1995). Foot-and-mouth disease virus Lb proteinase can stimulate rhinovirus and enterovirus IRES-driven translation and cleave several proteins of cellular and viral origin. *J. Virol.* **69**, 3465–3474.
67. Ohlmann, T., Rau, M., Pain, V. M. & Morley, S. J. (1996). The C-terminal domain of eukaryotic protein synthesis initiation factor (eIF) 4G is sufficient to support cap-independent translation in the absence of eIF4E. *EMBO J.* **15**, 1371–1382.
68. Sanz, M. A. & Carrasco, L. (2001). Sindbis virus variant with a deletion in the 6K gene shows defects in glycoprotein processing and trafficking: lack of complementation by a wild-type 6K gene in trans. *J. Virol.* **75**, 7778–7784.
69. Hahn, C. S., Hahn, Y. S., Braciale, T. J. & Rice, C. M. (1992). Infectious Sindbis virus transient expression vectors for studying antigen processing and presentation. *Proc. Natl Acad. Sci. USA*, **89**, 2679–2683.
70. van der Werf, S., Bradley, J., Wimmer, E., Studier, F. W. & Dunn, J. J. (1986). Synthesis of infectious poliovirus RNA by purified T7 RNA polymerase. *Proc. Natl Acad. Sci. USA*, **83**, 2330–2334.
71. Garcia-Arriaza, J., Manrubia, S. C., Toja, M., Domingo, E. & Escarmis, C. (2004). Evolutionary transition toward defective RNAs that are infectious by complementation. *J. Virol.* **78**, 11678–11685.
72. Ventoso, I. & Carrasco, L. (1995). A poliovirus 2A(pro) mutant unable to cleave 3CD shows inefficient viral protein synthesis and transactivation defects. *J. Virol.* **69**, 6280–6288.
73. Moss, B., Elroy-Stein, O., Mizukami, T., Alexander, W. A. & Fuerst, T. R. (1990). Product review. New mammalian expression vectors. *Nature*, **348**, 91–92.
74. Liljestrom, P., Lusa, S., Huylebroeck, D. & Garoff, H. (1991). In vitro mutagenesis of a full-length cDNA clone of Semliki Forest virus: the small 6,000-

molecular-weight membrane protein modulates virus release. *J. Virol.* **65**, 4107–4113.
75. Sambrook, J. F., Fritsch, E. F. & Maniatis, T. (1989). Molecular Cloning. A Laboratory Manual, 2nd edit., vol. 3. Cold Spring Harbor Laboratory Press, Cold Spring Harbor, NY.
76. Perez, L. & Carrasco, L. (1991). Cerulenin, an inhibitor of lipid synthesis, blocks vesicular stomatitis virus RNA replication. *FEBS Lett.* **280**, 129–133.
77. Feduchi, E., Aldabe, R., Novoa, I. & Carrasco, L. (1995). Effects of poliovirus 2A(pro) on vaccinia virus gene expression. *Eur. J. Biochem.* **234**, 849–854.

OPEN ACCESS Freely available online

PLoS one

Translation of Viral mRNA without Active eIF2: The Case of Picornaviruses

Ewelina Welnowska[◔], **Miguel Angel Sanz***[◔], **Natalia Redondo, Luis Carrasco**

Centro de Biología Molecular "Severo Ochoa" (CSIC-UAM), Universidad Autónoma de Madrid, Madrid, Spain

Abstract

Previous work by several laboratories has established that translation of picornavirus RNA requires active eIF2α for translation in cell free systems or after transfection in culture cells. Strikingly, we have found that encephalomyocarditis virus protein synthesis at late infection times is resistant to inhibitors that induce the phosphorylation of eIF2α whereas translation of encephalomyocarditis virus early during infection is blocked upon inactivation of eIF2α by phosphorylation induced by arsenite. The presence of this compound during the first hour of infection leads to a delay in the appearance of late protein synthesis in encephalomyocarditis virus-infected cells. Depletion of eIF2α also provokes a delay in the kinetics of encephalomyocarditis virus protein synthesis, whereas at late times the levels of viral translation are similar in control or eIF2α-depleted HeLa cells. Immunofluorescence analysis reveals that eIF2α, contrary to eIF4GI, does not colocalize with ribosomes or with encephalomyocarditis virus 3D polymerase. Taken together, these findings support the novel idea that eIF2 is not involved in the translation of encephalomyocarditis virus RNA during late infection. Moreover, other picornaviruses such as foot-and-mouth disease virus, mengovirus and poliovirus do not require active eIF2α when maximal viral translation is taking place. Therefore, translation of picornavirus RNA may exhibit a dual mechanism as regards the participation of eIF2. This factor would be necessary to translate the input genomic RNA, but after viral RNA replication, the mechanism of viral RNA translation switches to one independent of eIF2.

Citation: Welnowska E, Sanz MA, Redondo N, Carrasco L (2011) Translation of Viral mRNA without Active eIF2: The Case of Picornaviruses. PLoS ONE 6(7): e22230. doi:10.1371/journal.pone.0022230

Editor: Eliane F. Meurs, Institut Pasteur, France

Received March 18, 2011; **Accepted** June 17, 2011; **Published** July 14, 2011

Funding: This study was supported by a Grant from Direccion General de Investigacion Cientifica y Tecnica (DGICYT) (BFU2009-07352) and the Institutional Grant awarded to the Centro de Biología Molecular "Severo Ochoa" by the Fundación Ramón Areces. The funders had no role in study design, data collection and analysis, decision to publish, or preparation of the manuscript.

Competing Interests: The authors have declared that no competing interests exist.

* E-mail: masanz@cbm.uam.es

◔ These authors contributed equally to this work.

Introduction

The genome of picornaviruses comprises a molecule of single-stranded RNA of positive polarity that also acts as the only viral mRNA that is translated in infected cells [1]. Upon binding of the virion to its receptor, the naked viral particles deliver the ssRNA molecule to the cytoplasm, where it is recognized and translated by the cellular protein synthesizing machinery [2]. This early viral translation is followed by RNA replication giving rise to large amounts of RNA molecules of positive polarity, some of which may serve as new mRNAs to direct the massive synthesis of viral proteins during the late phase of infection [3,4,5]. This late viral translation is accompanied by a profound inhibition of cellular protein synthesis. The mechanism by which picornavirus mRNA is translated has been analyzed from the early days of research on eukaryotic protein synthesis. In fact, encephalomyocarditis virus (EMCV) RNA was the first viral mRNA to be translated in a mammalian cell free system [6]. Shortly afterwards, the requirements for different eIFs were investigated, revealing that eIF2 was necessary for EMCV mRNA translation [7]. Since then, all experiments with picornavirus mRNAs have provided overwhelming evidence for requirement of eIF2 for the initiation of picornavirus protein synthesis in cell free systems and in culture cells transfected with these mRNAs [8,9,10]. The elegant experiments by Pestova *et al.* [11] using reconstituted translation systems with all the purified components indicate that not all eIFs are necessary for EMCV translation *in vitro*. These investigators have observed that only a central domain of eIF4G was necessary for EMCV RNA translation, while eIF4E and eIF4B were dispensable [12]. The exclusion of eIF2 from these systems abolished protein synthesis directed by picornavirus mRNAs. The presence of IRES elements in mRNAs was also initially found in picornavirus mRNAs [6,13]. The structure and the eIF requirements for the translation of the different IRES-containing picornavirus RNAs may vary among the different species investigated. Based on these differences, at present four classes of picornavirus IRESs can be considered [14], but all of them require eIF2 for efficient translation in cell free systems.

The function of eIF2 is to bind Met-tRNA$_i$ and GTP to form the ternary complex Met-tRNA$_i$-eIF2-GTP, which interacts with the P site on the 40S ribosomal subunit, establishing the interaction between the initiator AUG codon with the anticodon present in Met-tRNA$_i$ [15,16,17]. Binding of the 60S ribosomal subunit to the pre-initiation complex promotes cleavage of GTP, displacing eIF2-GDP from the ribosome. The eIF2-GDP complex is recycled to eIF2-GTP by the activity of the recycling factor eIF2B. Factor eIF2 is composed of three subunits, known as α, β and γ [15,16]. Subunit eIF2α is a 36 kDa protein that contains a serine residue at position 51 (Ser-51), which can be phosphorylated by four different cellular protein kinases. Nutrient deprivation or cellular stresses, such as

heat-shock or viral infection, can activate some of these protein kinases [18,19,20]. GCN2 is activated by amino acid starvation, PKR phosphorylates eIF2 in response to double-stranded RNA, PERK is activated by protein misfolding at the endoplasmic reticulum and HRI phosphorylates eIF2 in the absence of HEME. Phosphorylation of eIF2α impairs the GDP-GTP recycling catalyzed by eIF2B. Therefore, the ternary complex Met-tRNA$_i$ - eIF2-GTP is not generated and thus binding of this complex to the 40S ribosome is hampered. Even partial phosphorylation of eIF2 can lead to total abrogation of translation [21].

Study of eIF2 phosphorylation in picornavirus infected cells has yielded varying results. Some reports suggested that this factor remained unphosphorylated after poliovirus (PV) infection [22,23], while other investigators found substantial eIF2 phosphorylation after PV infection, particularly at late times [24,25]. Of interest, PKR becomes highly activated, yet it is hydrolyzed in PV-infected cells although this hydrolysis is not directly executed by any of the PV proteases (2A or 3C) [24,26]. Mengovirus infection of mouse L-cells provokes a substantial activation of PKR, leading to eIF2 phosphorylation between 3–7 h after virus absorption [27]. The inactivation of eIF2 was coincident with the global inhibition of cellular and viral translation. Interferon treatment of culture cells stimulates, among others, PKR and the 2′-5′ A system blocking EMCV translation [28]. Direct evidence that activation of PKR alone suffices to block EMCV growth was provided by a cell line that stably synthesizes PKR [29]. All these findings pointed to the idea that active eIF2 was necessary to sustain picornavirus translation. The partial phosphorylation of eIF2 arising in picornavirus-infected cells as infection progresses might be partially responsible for the shut-down of cellular translation and the arrest of viral protein synthesis. Recent findings from our laboratory have provided evidence that Sindbis virus subgenomic mRNA exhibits a dual mechanism of translation. This mRNA follows a canonical mechanism when it is directly electroporated in cells or is translated in cell free systems, while it does not require eIF4G nor eIF2 for efficient translation in the infected cells [30]. A similar mechanism may be used by other viruses, including the Cricket paralysis virus [31]. In view of these findings, we reappraised the analysis for the participation of eIF2 during picornavirus RNA translation. Our present results indicate that EMCV protein synthesis does not require active eIF2 at late infection times, while this factor is necessary at early times, suggesting that EMCV mRNA translation can also follow a dual mechanism for the synthesis of viral proteins.

Results

Induction of eIF2α phosphorylation profoundly arrests cellular translation, while EMCV protein synthesis is resistant

Initially, we wished to test the effect of induction of eIF2α phosphorylation on EMCV translation in infected cells. Previous work has established that treatment of culture cells with compounds such as dithiothreitol (DTT), thapsigargin (Tg) or arsenite (Ars) causes phosphorylation of eIF2α leading to a profound arrest of cellular translation [32,33]. Mouse embryo fibroblasts (MEFs) were infected or not with EMCV and at 4 hpi the test compounds were added to the medium and incubated for 1 h. Protein synthesis was estimated by addition of [^{35}S]Met/Cys 15 min after the addition of the different compounds and incubated for 45 min. Protein synthesis was then analyzed by SDS PAGE followed by fluorography and phosphorylation of eIF2α was tested by Western blot (Figures 1A and B). Treatment with 400 μM DTT, 200 μM Ars and 1 μM Tg has no effect on the total amount of eIF2α, while the phosphorylated form of this factor clearly increases in the presence of any of these three compounds in control cells (Figure 1B). As a consequence, cellular protein synthesis strongly diminishes in the presence of these inhibitors (Figure 1A). By contrast, synthesis of EMCV proteins is almost unaffected by treatment with these agents, despite the fact that strong eIF2α phosphorylation is found in the infected cells. For instance, treatment of mock-infected cells with DTT induces 92% inhibition of cellular translation, as calculated by densitometric analysis, while EMCV protein synthesis only decreases by 24% (Figure 1A). Cellular translation was calculated by densitometry of the most prominent band that corresponds to actin, whereas viral translation was calculated by densitometry of all viral proteins. Notably, phosphorylation of eIF2α is clearly apparent in EMCV-infected cells at 5 hpi even in the absence of test compounds. This suggests that EMCV infection induces the phosphorylation of eIF2α.

It should be noted that Ars partially affects the proteolytic cleavage of the EMCV polyprotein, leading to the accumulation of viral precursors and the diminution of viral proteins of low MW. Therefore, we wished to test in more detail the action of DTT on cellular and viral translation. To this end, mock- or EMCV-infected cells were treated at 5 hpi with different DTT concentrations (125, 250 and 500 μM) and protein synthesis was measured from 5.15–6 hpi (Figure 1C). Increasing concentrations of DTT induce an almost total inhibition of cellular translation while EMCV protein synthesis is much less affected under these conditions (Figures 1C and 1D). These findings reveal that substantial EMCV protein synthesis occurs at late times of EMCV infection after induction of eIF2α phosphorylation by different compounds. To estimate the percentage of eIF2α phosphorylated by treatment of culture cells with DTT or Ars, isoelectric focusing was carried out. In untreated cells, most of eIF2α (95%) remains unphosphorylated, whereas in the presence of DTT or Ars almost all eIF2α (90–100%) becomes phosphorylated (Figure S1). These results agree well with our previous observations on the percentage of eIF2α phosphorylated in BHK cells infected with Sindbis virus and treated with Ars [30]. Therefore, this potent phosphorylation of eIF2α leads to the inhibition of cellular translation. The finding that Ars has little effect on late EMCV protein synhtesis suggests that this compound exhibits little toxicity on cellular processes that may influence mRNA translation, such as ATP or GTP synthesis. To further estimate the potential Ars toxicity on cellular protein synthesis, we employed the mouse cell line that expresses a form of eIF2α that cannot be phosphorylated. This cell line expresses an eIF2α bearing a point mutation at serine 51 (S51A). Addition of different Ars concentrations strongly inhibits cellular translation in control MEFs, whereas under these conditions Ars has almost no effect on protein synthesis in MEFs(S51A), demonstrating that the major effect of Ars on translation is mediated by the induction of eIF2α phosphorylation (Figure S2A). To further analyze the differential action of Ars in MEFs and MEFs(S51A), EMC-luc mRNA was transfected in these cells in presence or absence of Ars. Notably, luc synthesis was blocked in MEFs by about 85% in presence of Ars, whereas this compound had almost no effect in MEFs(S51A) (Figure S2B). However, we have found that, for unknown reasons, this variant cell line cannot be infected by several animal viruses tested, including EMCV and Sindbis virus.

EMC-luc translation upon eIF2α phosphorylation in culture cells and in cell free systems

In Sindbis virus-infected cells, we have demonstrated that translation is coupled to transcription. Thus, late viral subgenomic

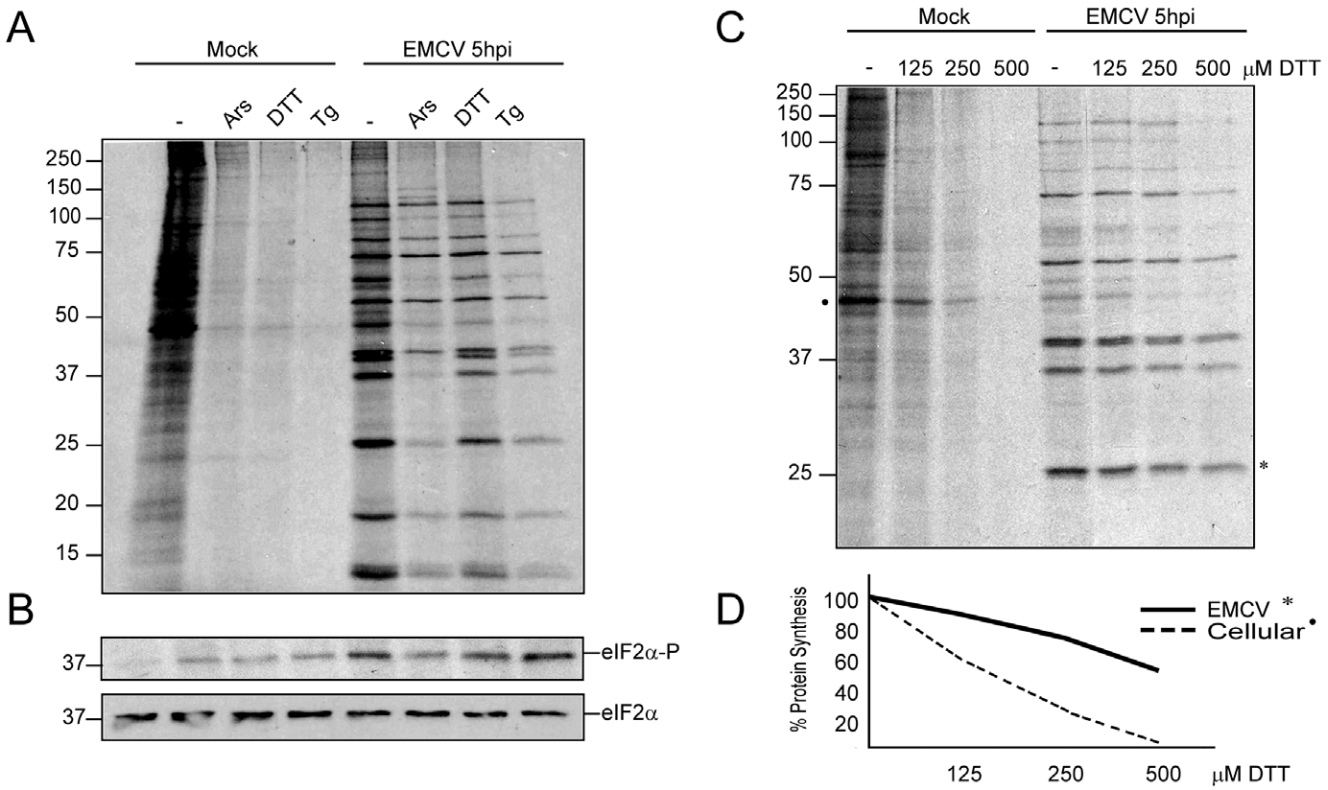

Figure 1. Effect of different inducers of eIF2α phosphorylation on cellular and EMCV translation. A) MEFs were mock- or EMCV-infected at 10 pfu/cell. Cells were subsequently pre-treated with 200 μM arsenite (Ars), 400 μM DTT, or 1 μM thapsigargin (Tg) for 15 min and then labelled for 45 min with [^{35}S]Met-Cys in presence of the same compounds. Samples were submitted to SDS-PAGE, fluorography and autoradiography. B) Western blot analysis of eIF2α and phosphorylated eIF2α using the same samples as in panel A and antibodies anti-phospho-eIF2α (1:1000 dilution) and anti-eIF2α (1:1000 dilution). C) MEFs mock- or EMCV-infected at 10 pfu/cell were pre-treated for 15 min with 0, 125, 250 or 500 μM DTT and then labelled for 45 min with [^{35}S]Met-Cys in presence of the same amounts of DTT. Samples were then collected and submitted to SDS-PAGE, fluorography and autoradiography. D) Cellular and viral protein synthesis examined by densitometric analysis of the autoradiograph shown in panel C. The protein bands analyzed are indicated by an asterisk.
doi:10.1371/journal.pone.0022230.g001

mRNA exhibits a different requirement for eIFs when they are transcribed by the Sindbis virus replication machinery, as compared to their requirements when electroporated into culture cells [30,34]. Overwhelming evidence obtained over the years in many laboratories has established that translation directed by EMCV RNA requires the participation of eIF2 [11,35]. Therefore, our results described above indicating that eIF2 may not participate in the initiation of EMCV RNA translation were quite unexpected. In order to examine the requirement of eIF2 on translation driven by EMCV IRES, we used an EMC-luc mRNA synthesized by *in vitro* transcription, which contains the luc gene immediately behind the IRES sequence of EMCV. BHK cells were electroporated with EMC-luc and the action of Ars was tested. For comparative purposes cells were also electroporated with Cap-luc or CrPV IGR-luc mRNAs and then treated with different concentrations of Ars (0, 50, 100 and 200 μM) for 75 min. After that time luc activity was measured and the amount of phosphorylated eIF2α was analyzed (Figure 2A). At the highest dose of Ars, Cap-luc mRNA was inhibited by about 80%, while CrPV IGR-luc which is resistant to eIF2α phosphorylation was inhibited by only 20% (Figure 2A). Notably, luc synthesis directed by EMC-luc exhibited a high sensitivity to Ars, with 90% inhibition at 50 μM Ars. Analysis of eIF2α indicated that this factor was phosphorylated in Ars-treated cells (Figure 2A).

Next, *in vitro* translation of these different mRNAs was tested and the effect of poly(I:C) analyzed. For this purpose, rabbit reticulocyte lysates were programmed with EMC-luc, Cap-luc and CrPV IGR-luc mRNAs, in the absence or presence of the inhibitor. After incubation, luc activity was estimated. Poly(I:C) rendered an inhibition of EMC-luc translation of about 90%, similar to that found with Cap-luc, while CrPV IGR-luc was almost unaffected by this compound (Figure 2B). These results indicate that unphosphorylated eIF2α must be present in the cell or *in vitro* for efficient initiation of translation of EMC-luc. In addition, these findings contrast with those reported above (Figure 1), illustrating that late viral protein synthesis takes place when eIF2α is phosphorylated in EMCV-infected cells.

In EMCV-infected cells, preferential translation of viral mRNAs synthesized by viral transcription is observed [34]. Thus, EMC-luc mRNAs transfected in these cells at late times of infection are excluded from translation. Taking into account these considerations, we wanted to assay the effect of Tg on the translation of EMC-luc mRNA in EMCV-infected cells. To this end, EMCV-infected MEFs were transfected with EMC-luc mRNA at different hpi and the action of 1 μM Tg was tested (Figure 2C). Translation of exogenous EMC-luc mRNA decreases when it is transfected at late times of EMCV infection, in good agreement with our previous results [34]. Strikingly, Tg blocks EMC-luc mRNA translation at all hpi tested, pointing to a different behavior of EMCV RNA made from transcription or that transfected into cells, as regards to the requirement for active eIF2. Similar findings were obtained in BHK cells infected with EMCV and transfected

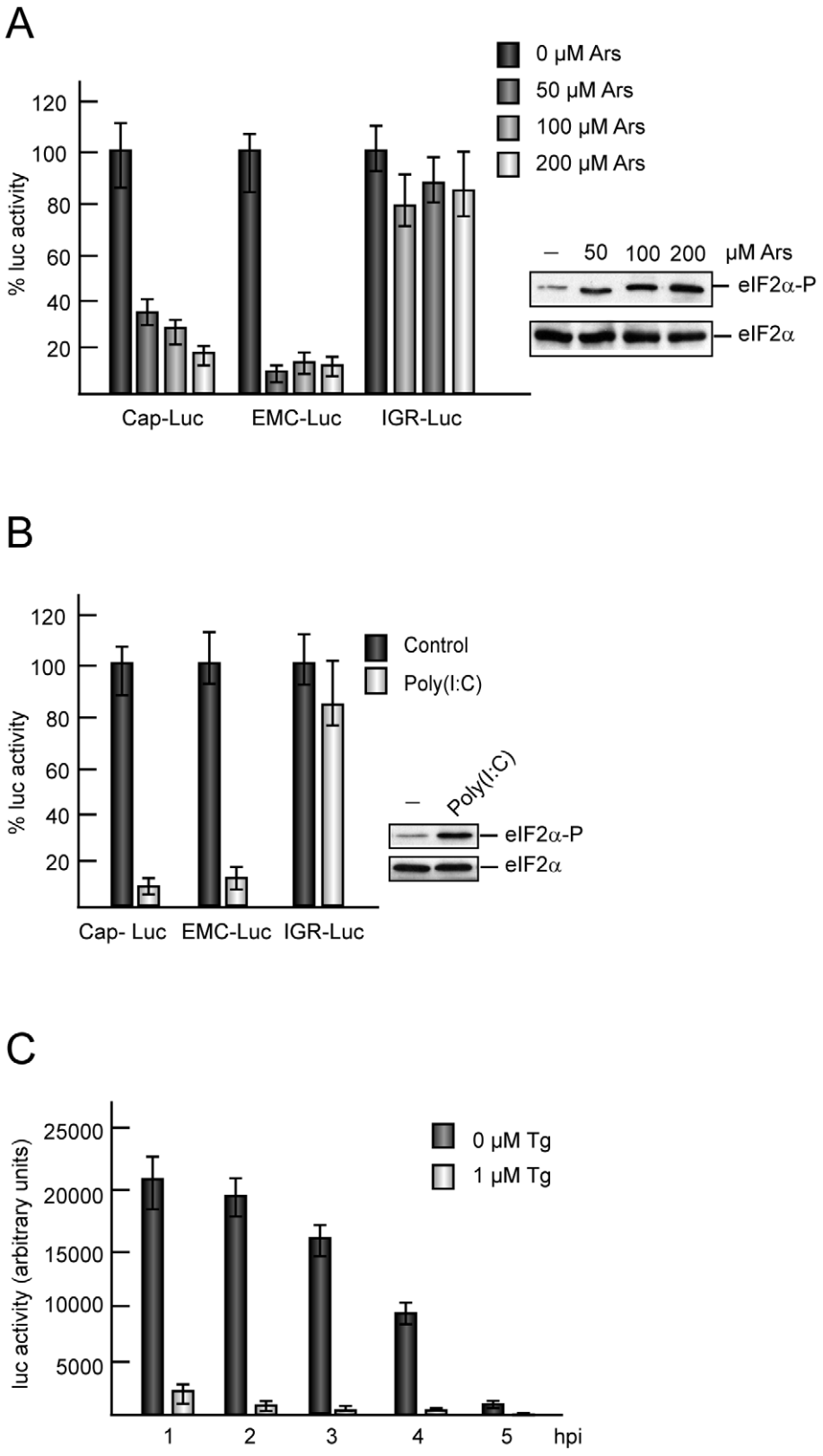

Figure 2. Translation of *in vitro* made mRNAs: Action of eIF2α phosphorylation. A) Cap-luc, EMC-luc, or CrPV IGR-luc mRNAs synthesized *in vitro* by T7 RNA polymerase were electroporated in BHK cells and seeded in DMEM (10% FCS). Different amounts of Ars (0, 50, 100 and 200 μM) were added and cells were incubated for 75 min before harvesting to analyze luc activity. The values shown are percentages of the value of their respective Ars untreated samples and are means ± SD of three independent experiments (left panel). The phosphorylated form of eIF2α and total eIF2α were determined in parallel by Western blot employing specific antibodies (right panel). B) Rabbit reticulocyte lysates were pre-treated or not with 0.5 μg/ml poly(I:C) for 30 minutes. Subsequently, 100 ng Cap-luc, EMCV-luc, or CrPV IGR-luc mRNAs were added and incubated for 1 h at 30°C.

Luc synthesis was estimated by measuring luc activity. The values shown are percentages of the value of their respective poly(I:C) and are means ± SD of three independent experiments untreated samples (left panel). The phosphorylated form of eIF2α and total eIF2α were determined in parallel by Western blot (right panel). C) MEFs cells were infected with EMCV (10 pfu/cell) and next transfected with *in vitro* made EMC-luc mRNA at different times after infection. Cells were incubated for 75 min with the transcription mixture containing 5 μg EMC-luc mRNA for each L-24 well in presence or absence of 1 μM Tg and then collected to measure luc activity. Luc activity values are means ± SD of three independent experiments.
doi:10.1371/journal.pone.0022230.g002

with EMC-luc mRNA (Figure S3). It should be noted that EMCV translation becomes resistant to Tg inhibition as infection progresses. Thus, there is more inhibition of viral translation by Tg at 2–3 and 3–4 hpi than at 4–5 and 5–6 hpi. Once again EMC-luc transfected in these cells is excluded from translation, but Tg was able to strongly inhibit this residual luc synthesis. These observations suggest that in EMCV infected cells there is not a transacting viral factor that could confer eIF2-independence. Therefore, in the same infected cells, EMCV RNAs that are synthesized by the viral transcription machinery are more resistant to the phosphorylation of eIF2α than transfected EMC-luc mRNAs.

Induction of eIF2α phosphorylation at the early stages of EMCV infection

During the early stages of EMCV infection, genomic RNA is released to the cytoplasm for translation, whereas at late times of infection the viral mRNAs that participate in protein synthesis are produced by viral transcription. Our present results indicate that phosphorylation of eIF2α has little effect on viral protein synthesis in the late phase of EMCV infection. Therefore, we wanted to analyze the requirement for active eIF2 during the early stages of EMCV infection. To this end, MEFs were infected with EMCV and next treated or not with 200 μM Ars for 1 h. The cells were then washed and incubated with fresh medium and cell samples were collected at 1, 2, 3, 4, 5 and 6 hpi. EMCV proteins are evidenced by radioactive labelling at 4 hpi (Figure 3A, lane 4). In addition, the appearance of EMCV 3D polymerase can be evidenced by Western blot at 3 hpi (Figure 3B, lane 3). Strikingly, as the infection progresses, an increase in the phosphorylated form of eIF2α was observed (Figure 3B). When Ars is added at the beginning of infection, inhibition of cellular protein synthesis occurs (Figure 3C, lane 1) and this inhibition correlates with phosphorylation of eIF2α (Figure 3D, lane 1). After removal of Ars, the amount of phosphorylated eIF2α decreased to control levels, while cellular translation recovered. Significantly, viral protein synthesis is delayed, such that viral proteins start to be detected at 6 hpi (Figure 3C, lane 6). When eIF2α is phosphorylated at the beginning of infection, viral protein synthesis is delayed by about 2 h as compared to control cells. This finding suggests that for EMCV to begin translation, eIF2α needs to be dephosphorylated. To further analyze the effect of eIF2 phosphorylation on early translation of EMCV, cells were infected with EMCV, and at 2 hpi Ars was added at various concentrations (0, 50, 100, 200 and 400 μM). Then after 1 h of incubation, cells were harvested and samples were analyzed by Western blot using monoclonal anti-3D antibodies. Synthesis of EMCV 3D was strongly inhibited by the presence of Ars at these early times of infection, correlating with the phosphorylation of eIF2α (Figure 3E). In summary, translation of EMCV RNA is blocked at early times of infection if eIF2α is phosphorylated, while during the late phase of EMCV infection, viral protein synthesis can take place in the presence of phosphorylated eIF2α.

Synthesis of EMCV proteins in cells with eIF2α depletion

The use of siRNAs constitutes a useful tool to deplete eIFs in culture cells in order to examine their functioning during viral infection. A difficulty with this approach is that total depletion of the protein to be investigated is rarely achieved, but this approach may nevertheless indicate to what extent a given factor is involved in viral protein synthesis. Another potential problem is that some viral mRNAs may exhibit a dual mode of translation, requiring the factor early in the infection, but not at late times. In this case, a delay in viral protein synthesis may occur in those cells with partial depletion of the factor, while in strongly depleted cells, abrogation of viral translation and replication will occur. To assess the involvement of eIF2α in the translation of EMCV RNA, HeLa cells were depleted with siRNAs. To achieve this, cells were transfected with a mixture of four siRNAs designed to deplete eIF2α mRNA. At 36 h after siRNA transfection, HeLa cells were infected with EMCV. Samples were recovered at 3, 4, 5, 6 and 7 hpi and labeled proteins were analyzed (Figure 4A). Western blot analysis against eIF2α indicates that this factor is silenced by 90% (Figure 4B) and this depletion blocks cellular protein synthesis by 72% as estimated by densitometric analyses (Figure 4A). Notably, EMCV protein synthesis is delayed by about 1–2 h and strongly decreases as compared to undepleted cells infected with EMCV, although it can be clearly detected at late times of infection (6 and 7 hpi). The delay and decrease in EMCV translation in eIF2α-depleted cells are consistent with the idea that this factor participates in viral translation early during infection. To estimate the degree in which EMCV RNA synthesis is affected in eIF2α-depleted HeLa cells, [^{3}H]uridine incorporation was estimated in presence of 5 μg/ml actinomycin D (Figure S4). A very strong inhibition was found in viral RNA replication consistent with the idea that early synthesis of viral proteins is necessary for genome replication. Despite this inhibition, once some viral RNA replication has taken place, translation of EMCV RNA at late times of infection shows little dependence on the presence of eIF2α (5–8 hpi).

Subcellular localization of eIFs and ribosomes in EMCV-infected cells

Another way to analyze the participation of eIFs in viral protein synthesis is to investigate their subcellular localization. Cytoplasmic animal viruses synthesize their proteins in a focal manner, particularly at late times of infection [30,36,37]. Ribosomes are present at those foci together with the eIFs that participate in translation, while those factors that are not involved in protein synthesis or viral replication are excluded from these foci. To investigate the subcellular localization of eIF2α after EMCV infection, MEFs were seeded on glass slides and infected or not with EMCV. At 5 hpi cells were fixed and incubated with the corresponding antibodies as indicated in Figures 5 and 6 prior to immunofluorescence analysis. In mock infected cells, eIF2α colocalizes with ribosomal protein P in the cytoplasm (Figure 5A). By contrast, those two proteins do not colocalize in EMCV infected cells (Figure 5A). EMCV 3D polymerase is clearly observed in the cytoplasm, indicating the viral replicative sites (Figure 5B). Both the cytoplasmic sites for viral translation and RNA replication are located in a perinuclear region and overlap, consistent with the idea that transcription and translation are coupled processes [34]. Notably, EMCV 3D does not colocalize with eIF2α. Using the ImageJ program with the Just Another Co-localization Plugin (JaCoP), the colocalization rate was calculated [38]. For eIF2α and ribosomal protein P the Pearson's Coefficient was 0.96 on the 0 to 1

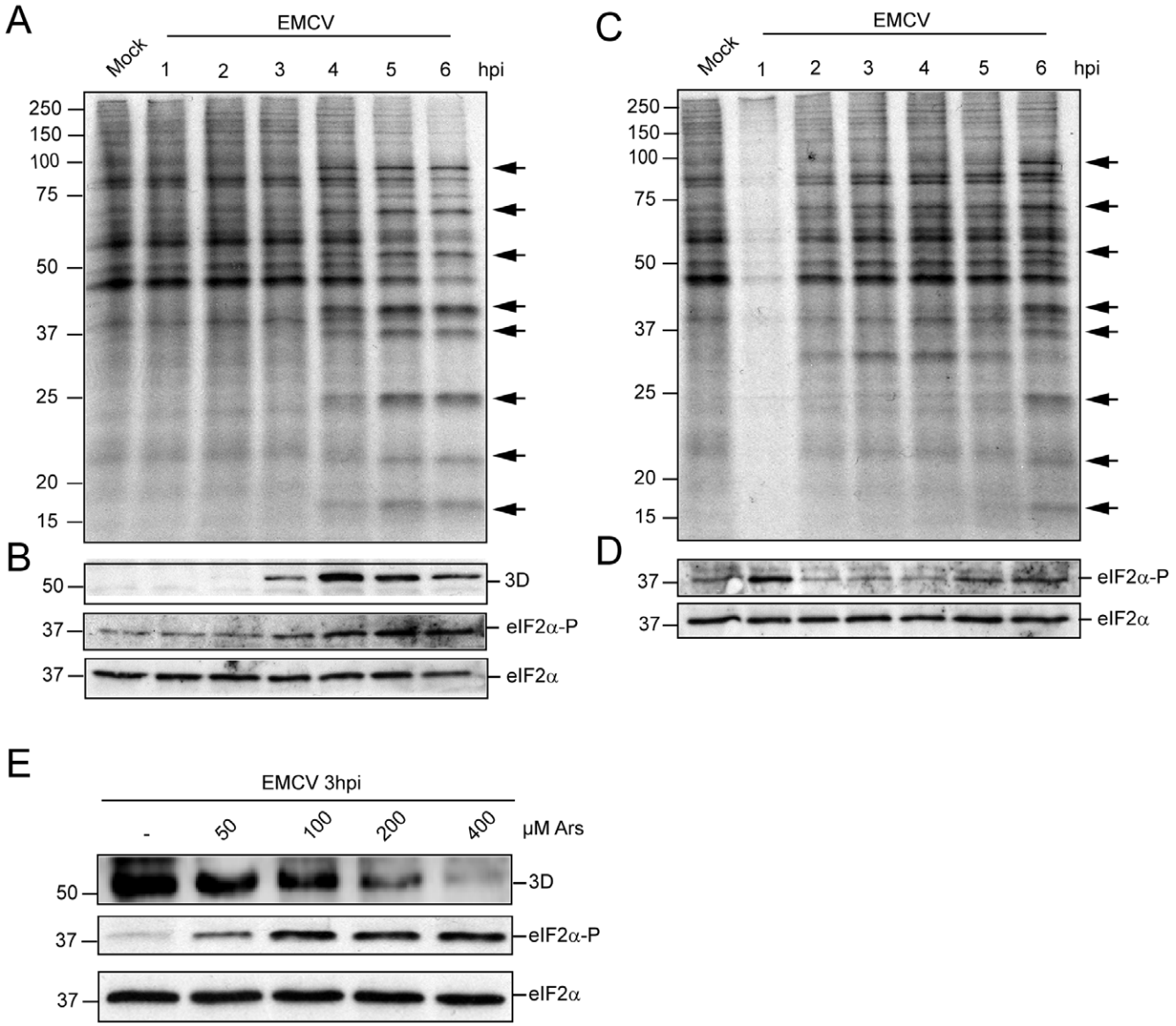

Figure 3. Treatment with Ars at early times of EMCV infection. A) MEFs were infected with EMCV (10 pfu/cell) and then protein synthesis was determined by labelling with [^{35}S]Met-Cys every h from 1 to 6 hpi. B) Western blot analysis of the samples obtained in panel A using anti-3D, anti-phospho-eIF2α or anti-eIF2α antibodies. C) MEFs were infected with EMCV as in panel A and then treated with 200 μM Ars during 1 h (0–1 hpi). Next, Ars was washed and fresh medium was added. Protein synthesis was analyzed at the time of treatment with Ars and every h thereafter until 6 hpi. D) Western blot performed with anti-phospho-eIF2α or anti-eIF2α antibodies using the same samples as in panel C. E) MEFs cells were infected with EMCV (10 pfu/cell) and at 2 hpi treated with different amounts of Ars; one h later samples were harvested and the amount of polymerase 3D produced was determined by Western blot. The amount of eIF2α phosphorylated and total eIF2α was also determined. The arrows indicate viral proteins.

doi:10.1371/journal.pone.0022230.g003

scale (0–0.5 indicates no colocalization and 0.5–1, colocalization), indicating almost total colocalization between eIF2α and ribosomes in mock-infected cells, while in EMCV infected cells this coefficient was 0.28, suggesting that there was no colocalization for eIF2α and ribosomes. In the case of eIF2α and EMCV 3D protein, the Pearson Coefficient was 0.32, which further suggests that there is no colocalization between those two proteins. Therefore, eIF2 is excluded from viral replicative foci.

To compare the above results with other factors that are involved in EMCV translation, eIF4G localization was investigated. This initiation factor is present in the cytoplasm around the nucleus colocalizing completely with ribosomal protein P in both mock and EMCV infected cells (Figure 6A); the Pearson Coefficient for eIF4G and ribosomal protein P was 0.89, and 0.92, respectively. In addition, eIF4GI also colocalizes with EMCV 3D protein (Figure 6B) (Pearson's coefficient 0.9) suggesting that eIF4G participates in EMCV translation. Therefore, the results obtained on the subcellular localization of eIF2α further support the notion that eIF2, contrary to eIF4GI, is not involved in the initiation of EMCV protein synthesis.

Requirement of active eIF2 for RNA translation with other picornaviruses

After demonstrating that EMCV RNA exhibits a dual mode for translation—i.e. this RNA requires the presence of active eIF2 in

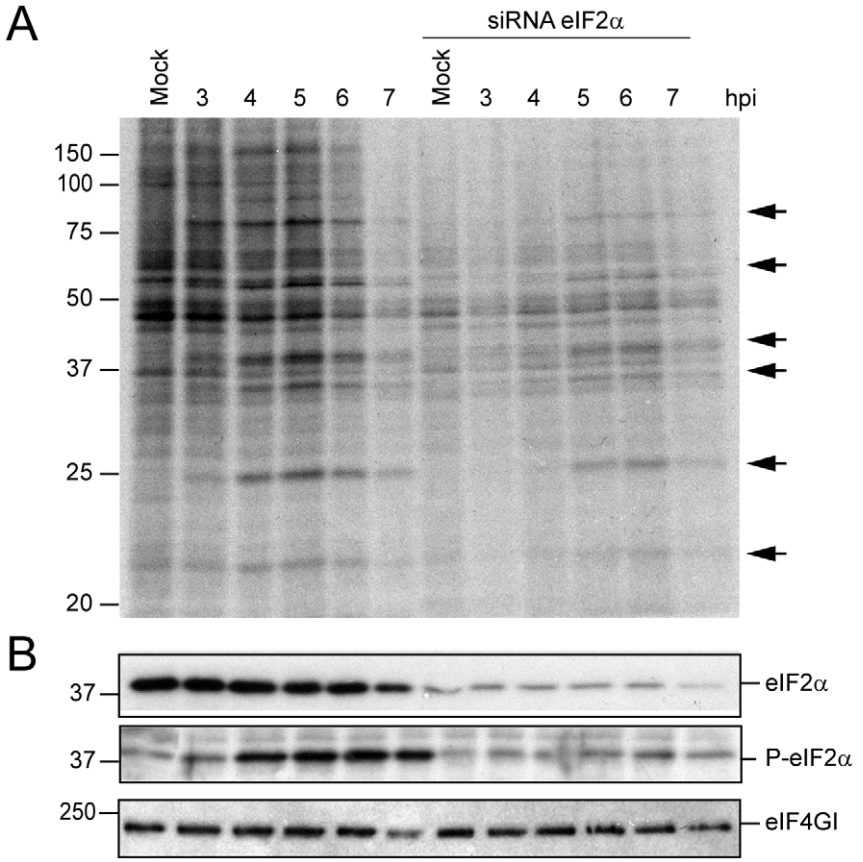

Figure 4. EMCV infection of Hela cells depleted or not of eIF2α. A) Hela cells transfected with a mixture of siRNAs targeting eIF2α mRNA or mock Hela cells were infected with EMCV (10 pfu/cell) at 36 h post-transfection. Next, protein synthesis was determined by [^{35}S]Met-Cys labelling at the hpi indicated. Samples were analyzed by SDS-PAGE, fluorography and autoradiography. B) Western blot analysis of samples from panel A using anti-eIF2α or anti-phospho-eIF2α antibodies. As a control, the amount of eIF4GI in each sample was determined using specific antibodies against this factor. The arrows indicate viral proteins.
doi:10.1371/journal.pone.0022230.g004

infected cells early during infection, but not at late times—we wished to examine the involvement of eIF2 in RNA translation of other picornaviruses. For this purpose, BHK cells were infected with FMDV, a member of the Aphtovirus genus, and at 3 hpi Ars (50, 100 and 200 μM) was added to the medium and incubated for 1 h. Protein synthesis was estimated by incubation with [^{35}S]Met/Cys during 45 min, from 3.15–4 hpi in the presence or absence of Ars. Cells were then collected and the synthesized proteins analyzed (Figure 7A). Phosphorylation of eIF2α and cleavage of eIF4GI were also analyzed (Figure 7B). As expected, addition of Ars strongly induced eIF2α phosphorylation. No inhibition of FMDV protein synthesis was observed by Ars under all the concentrations tested. By contrast, cellular translation was almost totally blocked at 100 μM Ars. These findings clearly indicate that FMDV RNA translation takes place in the presence of phosphorylated eIF2α during the late phase of infection.

To further analyze the effect of inducers of eIF2α phosphorylation on early and late protein synthesis in picornavirus-infected cells, two replicons, one from mengovirus and another from PV, were analyzed. Both replicons contain the luc gene replacing the coding region for viral structural proteins. Mengovirus is closely related to EMCV and both belong to the Cardiovirus genus, while PV is the prototype member of the Enterovirus genus. These replicons have the advantage that early translation can be assayed by estimating luc synthesis, whereas the synthesis of late proteins can be examined by radioactive labelling when the shut-off of host translation has occurred. After electroporation of these replicons into BHK cells, 200 μM Ars were added to the culture medium and luc activity was measured at 75 min. As controls Cap-luc and CrPV IGR-luc were used. Remarkably, luc synthesis from each replicon, as well as from Cap-luc mRNA, was drastically inhibited by Ars, whereas luc synthesis directed by CrPV-luc was unaffected in the presence of Ars (Figure 8A). The effect of this compound on late viral translation was assayed using different Ars concentrations (50, 100 and 200 μM). At late times of replication (5 h post-electroporation), Ars has little effect on Mengovirus protein synthesis (Figure 8C). Thus, only 30% inhibition was found in the presence of 200 μM Ars, whereas cellular translation usually diminished by over 90% under these conditions. The PV replicon exhibited a similar behavior to the Mengovirus one as regards the inhibitory action of Ars (Figure 8D). Altogether, these results provide strong evidence that synthesis of picornavirus proteins does not require eIF2α during the late phase of infection.

Discussion

Participation of eIF2 in the formation of the ternary complex Met-tRNA$_i$–eIF2-GTP is a crucial event in the initiation of translation of most mRNAs whether of cellular or viral origin [16,17]. However, mRNA translation of some viruses, such as HCV or CrPV, does not require this factor [39,40,41,42]. Our present observations indicate that picornavirus RNA translation

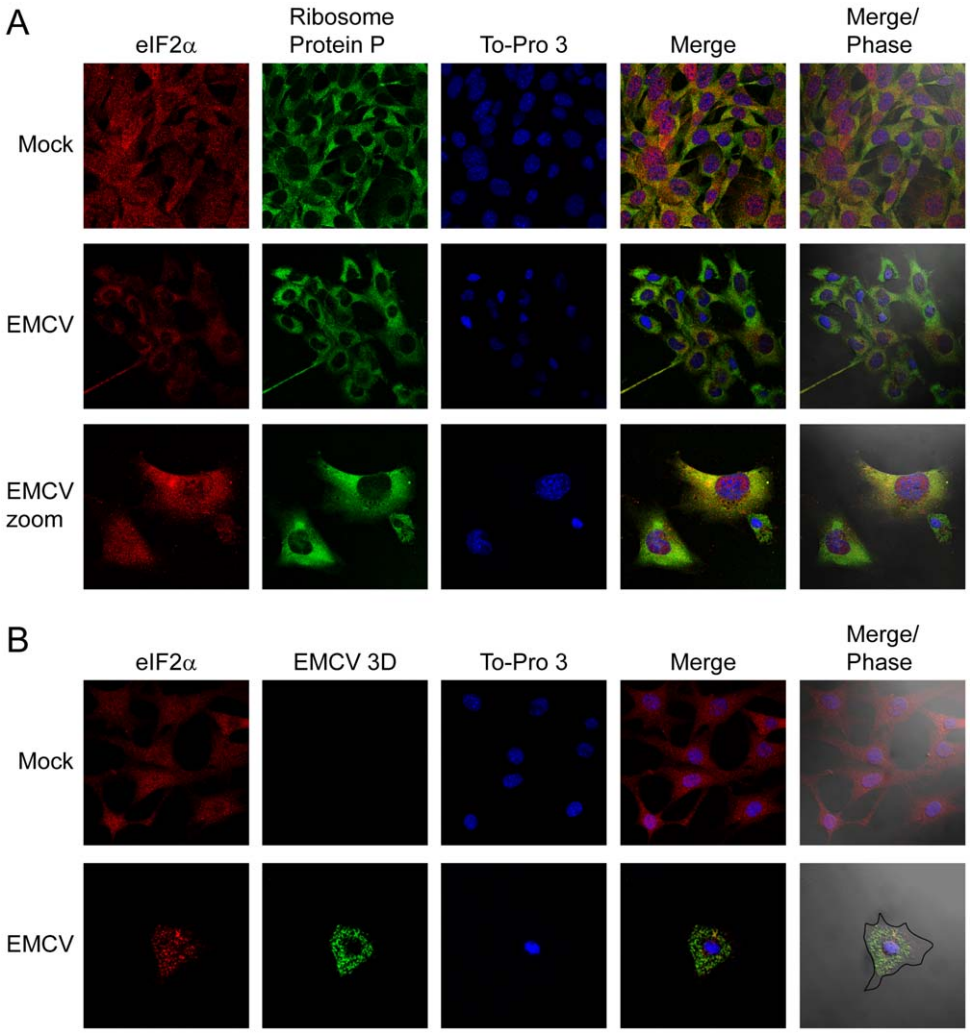

Figure 5. Subcellular localization of eIF2α, ribosomal protein P and EMCV 3D protein in Mock and EMCV infected cells. Hela cells were seeded on glass coverslips and mock infected or infected with EMCV (10 pfu/cell). At 5 hpi, cells were fixed and permeabilized. A) Ribosomal protein P and eIF2αwere detected by indirect immunofluorescence in mock- and EMCV-infected cells. ToPro 3 indicates the localization of the nucleus. B) Localization of eIF2α and EMCV 3D proteins. The cell outline was defined by differential interference contrast microscopy (Nomarski).
doi:10.1371/journal.pone.0022230.g005

takes place when eIF2α is phosphorylated, revealing that this factor is not necessary to translate this RNA at late times of infection. If so, the functioning of IRES elements from HCV, CrPV IGR, and picornaviruses reflects more similarities than previously suspected. Moreover, some cellular mRNAs bearing IRES elements can also be translated when eIF2α becomes phosphorylated [43,44].

Dual mechanism for EMCV translation

The concept that mRNA structure determines the mechanism by which translation takes place has not been supported by our recent findings demonstrating that a viral mRNA such as Sindbis virus subgenomic (SV sg-mRNA) exhibits a dual mode for initiation of translation [30]. This mRNA requires active eIF2 and intact eIF4F complex when it is translated in cell free systems or when electroporated in culture cells. However, SV sg-mRNA efficiently directs translation in the presence of phosphorylated eIF2α or upon eIF4G cleavage in virus-infected cells [30,45]. Consistent with these findings, our present results support the notion that picornavirus RNA also exhibits a dual mode for its translation. Thus, EMCV RNA is efficiently translated at late times of infection when eIF2α has been phosphorylated. By contrast, as shown in this and other studies, *in vitro* protein synthesis driven by EMCV IRES is profoundly blocked upon phosphorylation of eIF2α [41,46]. A similar situation is found when this IRES containing RNA is transfected in cells or at early times of EMCV infection. Our conclusion is that EMCV RNA can be translated following a canonical mechanism as regards to the use of eIF2, early during infection. As infection progresses, the cellular environment is modified such that this RNA can now direct translation in the absence of active eIF2. Therefore, EMCV RNA has a dual mode for translation, despite the fact that this RNA possesses the same structure at early and late times of infection. If true, the mechanism by which picornavirus RNA is translated would depend on two parameters: 1) the structure of this mRNA and 2) the environment in which translation is examined. In addition, our present findings provide an explanation for the partial resistance of EMCV in cells that express PKR [29].

The dual mode of translation for viral mRNAs occurs not only with SV sg- mRNA and picornavirus RNAs, but also with CrPV

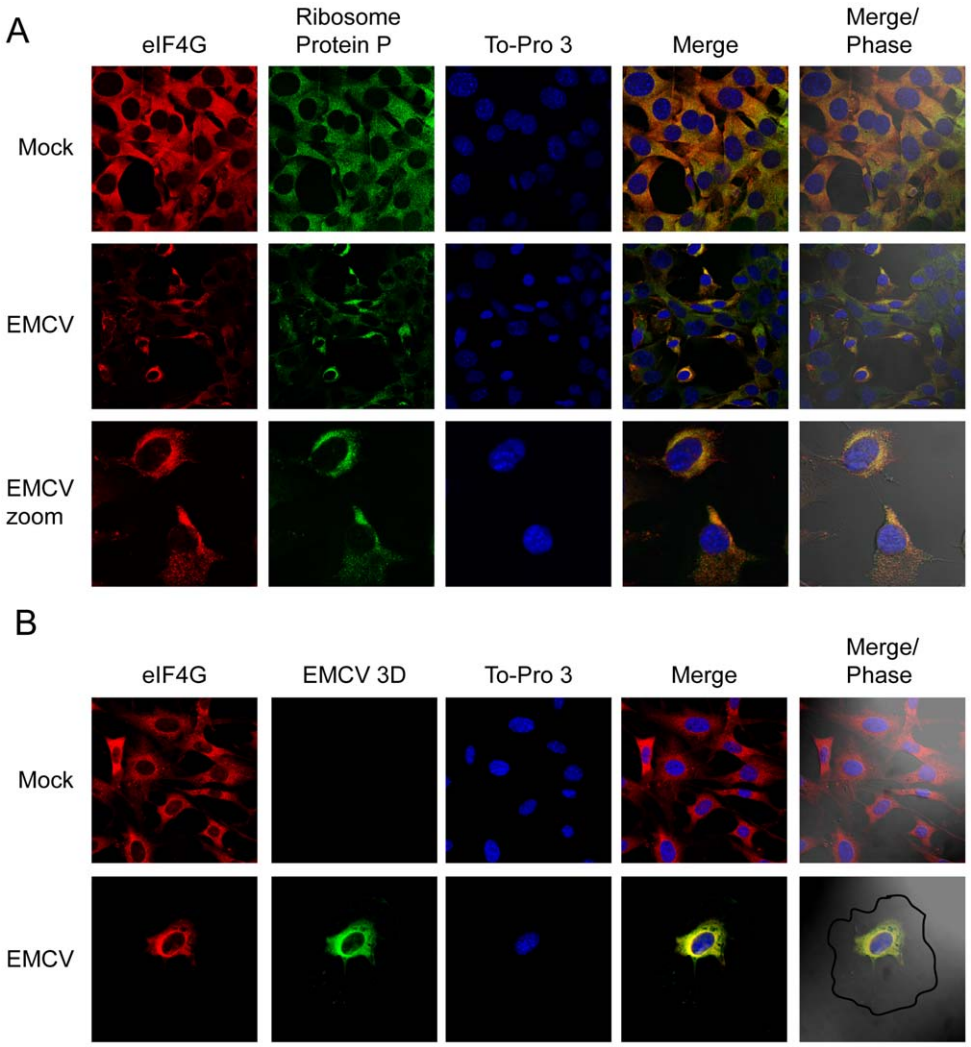

Figure 6. Subcellular localization of eIF4G, ribosomal protein P and EMCV 3D protein in infected cells. Hela cells were seeded on glass coverslips and mock infected or infected with EMCV (10 pfu/cell). At 5 hpi cells were fixed and permeabilized. A) Ribosomal protein P and eIF4G were detected by indirect immunofluorescence in mock- and EMCV-infected cells. ToPro 3 indicates the localization of the nucleus. B) Localization of eIF4G and EMCV 3D proteins. The cell outline was defined by differential interference contrast microscopy (Nomarski).
doi:10.1371/journal.pone.0022230.g006

mRNA [31]. We have speculated that the presence of viral proteins is responsible for the switch between these two modes to initiate translation [30]. In this regard, Hantavirus N protein is able to replace the eIF4F complex, thus the mechanism of viral translation in this instance is due to N protein [47]. Also, PV $2A^{pro}$ can rescue the translatability of SV sg-mRNAs bearing a picornavirus IRES [48].

Picornavirus translation in the presence of phosphorylated eIF2

It is puzzling to envisage how EMCV RNA initiation might occur in the absence of eIF2. Several possibilities exist: one is that a cellular protein or factor can act as a substitute for eIF2. This may be the case for HCV RNA translation, where eIF5B acts as a substitute for eIF2 [39]. It has also been proposed that eIF2A could act as a substitute for eIF2 in infections with Sindbis virus [49]. These data have been questioned recently as it has been suggested that other cellular proteins such as ligatin or MCT-1 and DENR can replace eIF2 during the initiation of HCV protein synthesis or during the translation of SV sg-mRNA [50]. However, the authors of that study did not find that ligatin can replace eIF2 for the initiation on EMCV RNA. In fact, ligatin has been identified as eIF2D [51]. This factor can replace eIF2 for the translation of some cellular mRNAs. Binding of aminoacyl-tRNA to the ribosomal P-site is promoted by eIF2D in a GTP-independent fashion [51]. In principle, it should be possible that the function of eIF2 was replaced by eIF2A or eIF2D in picornavirus infected cells. Another possibility is that the IRES itself directly binds to the 40S, or even to the 80S ribosome, at the P site late during infection, directly triggering the elongation phase. If so, the activity of picornavirus IRESs may be more similar to CrPV IGR IRES than previously thought [40,52]. Therefore, to know exactly which mechanism is acting during initiation with the different IRES-containing mRNAs thus far identified in virus species, the mechanism of translation has to be examined in virus-infected cells. The results obtained in cell free systems or even in culture cells transfected with these mRNAs may be misleading and cannot be extrapolated to the physiological situation. As illustrated in the present work, the mechanism for initiation of translation on EMCV RNA requires active eIF2 *in*

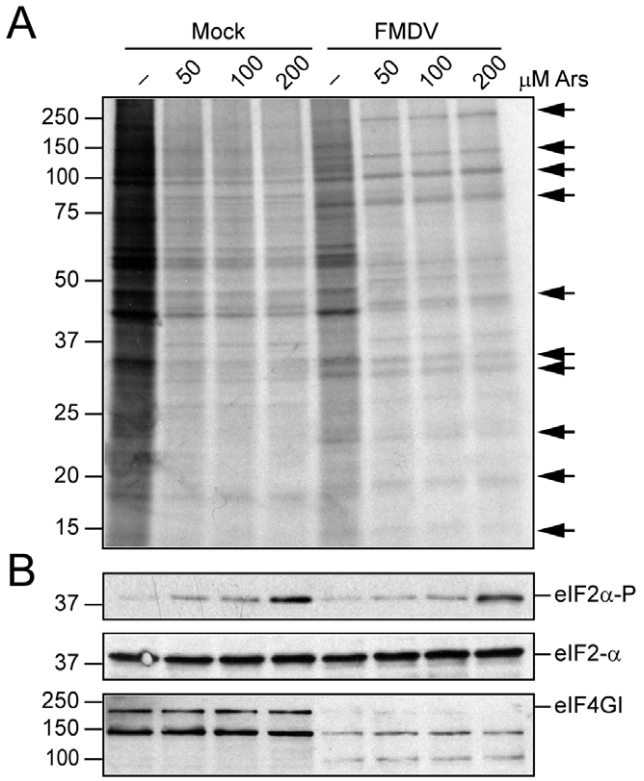

Figure 7. Action of Ars on FMDV infection. A) BHK cells were mock infected or infected with FMDV (10 pfu/cell). At 3 hpicultures were treated with different amounts of Ars (0, 50, 100 and 200 μM) for 15 min and next labeled by [^{35}S]Met-Cys labelling in presence of the same concentrations of Ars from 3.15–4 hpi. Samples were collected and analyzed by SDS-PAGE, fluorography and autoradiography. B) The phosphorylated form of eIF2α and total eIF2α were determined in parallel by Western blot with specific antibodies. The cleavage of eIF4GI was also analyzed by Western blot using specific antibodies against this factor. The arrows indicate viral proteins.
doi:10.1371/journal.pone.0022230.g007

vitro, this being the mode of translation closer to the canonical mechanism than that observed in the infected cells during the bulk of viral translation.

A variety of mechanisms to initiate translation on viral mRNAs

Two major mechanisms for the initiation of translation are known in eukaryotic cells: m7G cap-dependent or m7G cap-independent [16,17]. This division is mainly based on whether or not a m7G cap structure is present at the 5′ end of mRNAs and/or the requirement for eIF4E during mRNA translation. However, this simplistic classification may lead to some confusion because there are capped mRNAs that do not require eIF4E. In some instances, such as Adenoviruses, Influenza virus or Hantavirus, a viral protein recognizes the m7G cap structure of viral mRNA and replaces eIF4E or even eIF4F [47,53,54]. Thus, translation depends on the presence of a m7G cap structure, but eIF4E is dispensable. This is also the case of SV sg-mRNA, which does not require intact eIF4G but still needs the m7G cap structure at the 5′-end of this mRNA [45,48]. When defining the mechanism of initiation it seems more adequate to refer to the eIFs that are involved in translation [55]. According to whether eIF2 is required for translation, one of two different mechanisms of initiation is defined. One is the canonical mechanism that uses the ternary complex Met-tRNA$_i$-eIF2-GTP while the other does not require this factor. In this last case a variety of mechanisms can be operative depending on the type of mRNA examined and the conditions analyzed. The situation is that depending on the cellular or viral mRNA considered and the type of assay employed (*in vitro*, intact cells, stress situations, viral infections, etc.) the requirements for eIFs can vary. This picture may be slightly more complicated if we bear in mind that a given mRNA can exhibit different mechanisms of initiation, reflecting the plasticity of some RNAs in accommodating stress situations.

Materials and Methods

Cell Cultures and Viruses

The cell lines used in this work were: HeLa, BHK-21 and mouse embryo fibroblasts (MEFs). The mouse cell line MEFs(S51A) that contains an unphosphorylatable form of eIF2α was kindly provided by D. Ron and R.J. Kaufman (Department of Biological Chemistry, MI, USA). Cells were grown at 37°C in Dulbecco's Modified Eagle's Medium (DMEM) supplemented with 5% fetal calf serum (FCS) (HeLa and BHK) or 10% FCS (MEFs) and nonessential amino acids. Infection with EMCV or with foot-and-mouth disease virus (FMDV) was carried out at a multiplicity of 10 pfu/cell.

Plasmids

The constructs pKs luc and pTM1-luc have been already described [48]. These plasmids were used as DNA template to obtain Cap-luc and EMC-luc mRNA by *in vitro* transcription using the T7 RNA polymerase. Plasmid T7 Rluc ΔEMCV IGR-Fluc [56] was employed to obtain CrPV IGR-luc mRNA. The constructs encoding the PV replicon pRluc31 [57] and the mengovirus replicon RZ-pMluz [58] have been already described.

Protein metabolic labeling and Western blot analysis

Protein synthesis was analyzed by replacing DMEM growth media with 0.2 ml methionine–cysteine free DMEM supplemented with 2 μl EasyTag^{TM} EXPRESS ^{35}S Protein Labeling mix, [^{35}S]Met-Cys (11 mCi/ml, 37.0 Tbq/mmol; Perkin Elmer) per well of an L-24 plate. Cultures were pre-treated with the amounts indicated in each case of dithiothreitol (DTT), thapsigargin (Tg) or arsenite (Ars) for 15 min, before labeling for 45 min in the presence of the tested compounds. The cells were then collected in the appropriate gel loading buffer (62.5 mM Tris–HCl, pH 6.8, 2% SDS, 0.1 M DTT, 17% glycerol, and 0.024% bromophenol blue) and analyzed by electrophoresis in SDS-polyacrylamide gels (SDS-PAGE), followed by fluorography and autoradiography. Specific rabbit polyclonal antibodies raised against phospho-eIF2α (Ser 51) (Cell Signaling Technology) or total eIF2α (Santa Cruz Biotechnology) were used in Western blot analysis at 1:1000 dilution antisera. Mouse monoclonal antibodies raised against EMCV 3D protein (a generous gift from A. Palmenberg, University of Wisconsin, Madison, USA) were used at 1:1000 dilution. Rabbit polyclonal antibodies raised against peptides derived from the N- and C-terminal regions of human eIF4GI were also used at a 1:1000 dilution [59]. Anti-rabbit and anti-mouse immunoglobulin G antibodies coupled to peroxidase (Promega) were used at a 1:5000 dilution.

In vitro transcription and transfection

Plasmids were used as templates for *in vitro* RNA transcription with T7 RNA polymerase (Promega). To obtain Cap-luc mRNA, an m^{7}G(5′)ppp(5′)G cap analog was added to the transcription mixture. For transfection, subconfluent BHK cells were harvested, washed with ice-cold phosphate-buffered saline (PBS), and

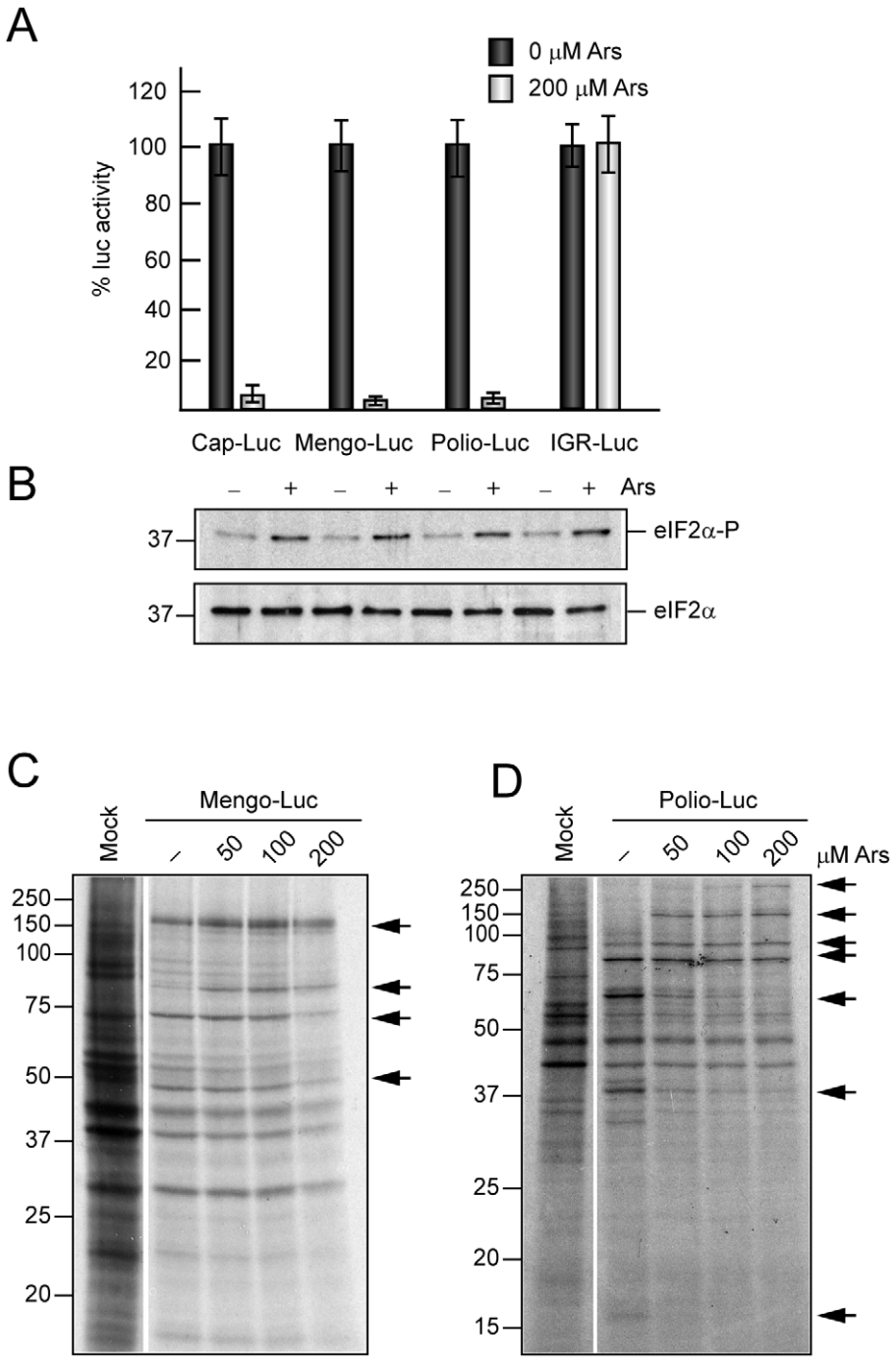

Figure 8. Translation of Mengovirus and PV replicons. Effect of Ars on early and late viral protein synthesis. A) BHK cells were electroporated with Mengo-luc, Polio-luc replicons, Cap-luc or CrPV IGR-luc mRNAs; all these RNAs were synthesized by *in vitro* transcription. Electroporated cells were seeded in DMEM (10% FCS) in presence or absence of 200 μM Ars. 75 min later cells were collected and lysed to measure luc activity. The values shown are percentages of the value of their respective Ars untreated samples and are means ± SD of three independent experiments. B) The phosphorylated form of eIF2α and total eIF2α were determined in parallel by Western blot with specific antibodies. C and D) BHK cells were electroporated with Mengo-luc replicon (C) or polio-luc replicon (D) and at 5 h post-electroporation protein synthesis was determined by [^{35}S]Met-Cys labelling in presence of different concentrations of Ars (0, 50, 100 and 200 μM). The arrows indicate viral proteins.
doi:10.1371/journal.pone.0022230.g008

resuspended at a density of approximately 2.5×10^6 cells/ml in the same buffer. Subsequently, 20 μg of *in vitro* transcribed RNA were added to 0.4 ml cell suspension and the mixture was transferred to a 2-mm cuvette. Electroporation was carried out at room temperature by generating two consecutive 1.5-kV, 25-mF pulses with a Gene Pulser apparatus (Bio-Rad), as previously described [48].

In vitro translation

In vitro translation was carried out in rabbit reticulocyte lysates. To induce phosphorylation of eIF2α, extracts were treated with 0.5 μg/ml poly(I:C) (Pharmacia Biotech) for 30 min. Subsequently, 100 ng of different mRNAs were added and incubated for 1 h at 30°C. Protein synthesis was estimated by measuring luc activity.

Transfection of HeLa cells

To transfect interference RNAs (siRNAs), HeLa cells were grown in 24-well plates with antibiotic- and antimycotic free DMEM supplemented with 5% FCS to 60–70% confluence. To make up the transfection mixture, 2 µl of Lipofectamine 2000 (Invitrogen) were added to 50 µl of Opti-MEM I Reduced Serum Medium (Opti-MEM I) (Invitrogen) and then incubated for 5 min at room temperature. Simultaneously, the siRNA mixture was prepared with 100 pmol of a mixture of four siRNAs targeting eIF2α mRNA (Dharmacon; Thermo Scientific) in 50 µl of the Opti-MEM I for each L-24 well and then incubated at room temperature for 5 min. The final mixture was subsequently prepared with 50 µl of Lipofectamine suspension and 50 µl of the siRNA mixture by incubation for 30 minutes at room temperature. To transfect HeLa cells with siRNAs, cell medium was removed and 100 µl of Opti-MEM I followed by 100 µl of the transfection/siRNAs mixture obtained were added to each well. Cells were then incubated at 37°C for 4 h. After incubation, the transfection medium was removed and the cultures continued in fresh medium. At 36 h post-transfection HeLa cells were infected with EMCV (10 pfu/cell) to determine viral protein synthesis.

Luciferase activity measurement

HeLa cells were harvested with buffer containing 25 mM glycylglycine (pH 7.8), 0.5% of Triton X-100 and 1 mM dithiothreitol. Luciferase (luc) activity was measured using Moonlight 2000 apparatus (Analytical Luminescence Laboratory) using the Luciferase Assay System (Promega).

Immunofluorescence analysis

HeLa cells were seeded on glass cover slips prior to infection with EMCV (10 pfu/cell). At 5 hpi, cells were fixed in 4% PFA for 15 min, washed twice with PBS, and then permeabilized for 10 min with 0.2% Triton X-100 in PBS. Subsequent antibody incubations were carried out for 2 h with specified primary antisera and corresponding fluorescence-conjugated secondary antibody at room temperature. Cover slips were then mounted in ProLong Gold antifade reagent (Invitrogen) and examined with a Zeiss LSM510 Inverted confocal laser-scanning microscope (Bio-Rad/Zeiss) with Plan-Apochromat 63X/1.4 oil objective. Mouse monoclonal antibodies raised against eukaryotic ribosomal P protein [60], or EMCV 3D protein (a gift from A. Palmenberg, University of Wisconsin, Madison, USA) were used for immunofluorescence at 1:10 and 1:200 dilutions, respectively. Rabbit polyclonal antibodies raised against eIF4GI or eIF2α were used at 1:100 dilution. To-pro3 (Invitrogen) was employed at 1:500 dilution.

Supporting Information

Figure S1 Analysis of phosphorylated and unphosphorylated eIF2α in culture cells. Effect of inhibitors. HeLa cells were untreated or treated for 60 min with 200 µM Ars or 400 µM DTT. Afterwards cell monolayers were collected and proteins were separated by isoelectric focusing and transferred to a nitrocellulose membrane as described before [30]. The phosphorylated and unphosphorylated forms of eIF2α were detected by anti-eIF2α rabbit polyclonal antibodies and quantified by densitometric scanning of the corresponding bands.
(TIF)

Figure S2 Effects of Ars on translation in MEFs. A) Protein synthesis was analyzed in MEFs or MEFs(S51A) treated with different concentrations of Ars as indicated in the Figure. Culture cells were pretreated for 15 min with Ars in DMEM without methionine and cysteine. Then, 15 µCi of [^{35}S]Met-Cys for each L-24 well were added and incubation was continued for 1 h. Cells were collected in sample buffer and proteins synthesized during this time were analyzed by SDS-PAGE, fluorography and autoradiography as described in Materials and Methods. B) Luc synthesis in MEFs or MEFs(S51A) transfected with EMC-luc mRNA in the presence of different concentrations of Ars. Culture cells were transfected with 5 µg of EMC-luc mRNA per well of an L-24 plate in the presence of 0, 200 or 400 µM Ars. 75 min later cell monlayers were collected and lysed to measure luc activity. The percentage to the values of the respective samples untreated with Ars is represented. Luc activity values are means ± SD of three independent experiments.
(TIF)

Figure S3 Translation of EMC-luc mRNA transfected in EMCV-infected cells. A) BHK cells were infected with EMCV (10 pfu/cell) and next transfected with EMC-luc mRNA at different times after infection. The cells were incubated for 75 min with the transcription mixture containing 5 µg EMC-luc mRNA per well of an L-24 plate in presence or absence of 1 µM Tg and then collected to measure luc activity. Luc activity values are means ± SD of three measures of the same experiment. B) Protein synthesis was analyzed in parallel. In this case the cultures were treated or not with 1 µM Tg for 15 min before adding 15 µCi of [35S]-Met, Cys per well of an L-24 plate, and continue the incubation for 1 h. The arrows indicate viral proteins.
(TIF)

Figure S4 EMCV RNA synthesis in eIF2-depleted HeLa cells. Hela cells transfected with a mixture of siRNAs targeting eIF2αmRNA or mock Hela cells were infected with EMCV (10 pfu/cell) at 36 h post-transfection. Viral RNA was subsequently labeled with [^{3}H]uridine (20 µCi/ml, final concentration) in the presence of 5 µg/ml actinomycin D. At the indicated hpi [^{3}H]uridine incorporated was quantified in a liquid scintillation spectrometer as described before [48]. Cpm values are means ± SD of three measures of the same experiment.
(TIF)

Acknowledgments

We wish to thank J.P.G.-Ballesta (Centro de Biologia Molecular "Severo Ochoa", Madrid) for kindly providing the anti-ribosome antibodies, A. Palmenberg, (University of Wisconsin, Madison, USA) for the mouse monoclonal antibodies against EMCV 3D protein and the mengovirus replicon RZ-pMluz, E. Martínez-Salas (Centro de Biologia Molecular "Severo Ochoa", Madrid) for providing a sample of FMDV, P. Sarnow (Stanford University, California, USA) and Y. Kusov (University of Lübeck, Germany) for providing plasmids T7 Rluc ΔEMCV IGR-Fluc and the PV replicon pRluc31 respectively.

Author Contributions

Conceived and designed the experiments: EW MAS NR LC. Performed the experiments: EW MAS NR. Analyzed the data: EW MAS NR LC. Wrote the paper: LC MAS.

References

1. Agol V (2002) Picornavirus genome: an overview. In: BLSaE W, ed. Molecular biology of picornavirus. Washington, D.C.: ASM Press. pp 127–148.
2. Rieder EaW E (2002) Cellular receptors of picornaviruses: an overview. In: BLSaE W, ed. Molecular biology of picornaviruses. WhasingtonD.C.: ASM Press. pp 61–70.

3. Hogle JM (2002) Poliovirus cell entry: common structural themes in viral cell entry pathways. Annu Rev Microbiol 56: 677–702.
4. Paul A (2002) Possible Unyfying Mechanism of picornavirus Genome Replication. In: Semler BWE, ed. Molecular biology of picornaviruses. Washington, D.C.: ASM Press. pp 227–246.
5. Belov GA, Ehrenfeld E (2007) Involvement of cellular membrane traffic proteins in poliovirus replication. Cell Cycle 6: 36–38.
6. Kerr IM, Martin EM (1971) Virus protein synthesis in animal cell-free systems: nature of the products synthesized in resonse to ribonucleic acid of encephalomyocarditis virus. J Virol 7: 438–447.
7. Schreier MH, Staehelin T (1973) Initiation of eukaryotic protein synthesis: (Met-tRNA f -40S ribosome) initiation complex catalysed by purified initiation factors in the absence of mRNA. Nat New Biol 242: 35–38.
8. Scheper GC, Thomas AA, Voorma HO (1991) The 5′ untranslated region of encephalomyocarditis virus contains a sequence for very efficient binding of eukaryotic initiation factor eIF-2/2B. Biochim Biophys Acta 1089: 220–226.
9. Svitkin YV, Meerovitch K, Lee HS, Dholakia JN, Kenan DJ, et al. (1994) Internal translation initiation on poliovirus RNA: further characterization of La function in poliovirus translation in vitro. J Virol 68: 1544–1550.
10. Thomas AA, Rijnbrand R, Voorma HO (1996) Recognition of the initiation codon for protein synthesis in foot-and-mouth disease virus RNA. J Gen Virol 77(Pt 2): 265–272.
11. Pestova TV, Kolupaeva VG, Lomakin IB, Pilipenko EV, Shatsky IN, et al. (2001) Molecular mechanisms of translation initiation in eukaryotes. Proc Natl Acad Sci U S A 98: 7029–7036.
12. Kolupaeva VG, Lomakin IB, Pestova TV, Hellen CU (2003) Eukaryotic initiation factors 4G and 4A mediate conformational changes downstream of the initiation codon of the encephalomyocarditis virus internal ribosomal entry site. Mol Cell Biol 23: 687–698.
13. Pelletier J, Sonenberg N (1988) Internal initiation of translation of eukaryotic mRNA directed by a sequence derived from poliovirus RNA. Nature 334: 320–325.
14. Belsham GJ (2009) Divergent picornavirus IRES elements. Virus Res 139: 183–192.
15. Merrick WC (2004) Cap-dependent and cap-independent translation in eukaryotic systems. Gene 332: 1–11.
16. Pestova TIJR, Hellen CU (2007) The mechanism of translation initiation in eukaryotes. In: MB Matheus NS JH, ed. Translational Control in Biology and Medicine. New York, USA: Cold Spring Harbor Laboratory Press. pp 87–128.
17. Sonenberg N, Hinnebusch AG (2009) Regulation of translation initiation in eukaryotes: mechanisms and biological targets. Cell 136: 731–745.
18. Chen JJ, London IM (1995) Regulation of protein synthesis by heme-regulated eIF-2 alpha kinase. Trends Biochem Sci 20: 105–108.
19. Fernandez J, Yaman I, Sarnow P, Snider MD, Hatzoglou M (2002) Regulation of internal ribosomal entry site-mediated translation by phosphorylation of the translation initiation factor eIF2alpha. J Biol Chem 277: 19198–19205.
20. Wek RC, Jiang HY, Anthony TG (2006) Coping with stress: eIF2 kinases and translational control. Biochem Soc Trans 34: 7–11.
21. Hershey JW (1989) Protein phosphorylation controls translation rates. J Biol Chem 264: 20823–20826.
22. Ransone LJ, Dasgupta A (1987) Activation of double-stranded RNA-activated protein kinase in HeLa cells after poliovirus infection does not result in increased phosphorylation of eucaryotic initiation factor-2. J Virol 61: 1781–1787.
23. Ransone LJ, Dasgupta A (1988) A heat-sensitive inhibitor in poliovirus-infected cells which selectively blocks phosphorylation of the alpha subunit of eucaryotic initiation factor 2 by the double-stranded RNA-activated protein kinase. J Virol 62: 3551–3557.
24. Black TL, Safer B, Hovanessian A, Katze MG (1989) The cellular 68,000-Mr protein kinase is highly autophosphorylated and activated yet significantly degraded during poliovirus infection: implications for translational regulation. J Virol 63: 2244–2251.
25. O'Neill RE, Racaniello VR (1989) Inhibition of translation in cells infected with a poliovirus 2Apro mutant correlates with phosphorylation of the alpha subunit of eucaryotic initiation factor 2. J Virol 63: 5069–5075.
26. Black TL, Barber GN, Katze MG (1993) Degradation of the interferon-induced 68,000-M(r) protein kinase by poliovirus requires RNA. J Virol 67: 791–800.
27. DeStefano J, Olmsted E, Panniers R, Lucas-Lenard J (1990) The alpha subunit of eucaryotic initiation factor 2 is phosphorylated in mengovirus-infected mouse L cells. J Virol 64: 4445–4453.
28. Rice AP, Duncan R, Hershey JW, Kerr IM (1985) Double-stranded RNA-dependent protein kinase and 2-5A system are both activated in interferon-treated, encephalomyocarditis virus-infected HeLa cells. J Virol 54: 894–898.
29. Meurs EF, Watanabe Y, Kadereit S, Barber GN, Katze MG, et al. (1992) Constitutive expression of human double-stranded RNA-activated p68 kinase in murine cells mediates phosphorylation of eukaryotic initiation factor 2 and partial resistance to encephalomyocarditis virus growth. J Virol 66: 5805–5814.
30. Sanz MA, Castello A, Ventoso I, Berlanga JJ, Carrasco L (2009) Dual mechanism for the translation of subgenomic mRNA from Sindbis virus in infected and uninfected cells. PLoS One 4: e4772.
31. Garrey JL, Lee YY, Au HH, Bushell M, Jan E (2010) Host and viral translational mechanisms during cricket paralysis virus infection. J Virol 84: 1124–1138.
32. Harding HP, Zhang Y, Ron D (1999) Protein translation and folding are coupled by an endoplasmic-reticulum-resident kinase. Nature 397: 271–274.
33. Brostrom CO, Brostrom MA (1998) Regulation of translational initiation during cellular responses to stress. Prog Nucleic Acid Res Mol Biol 58: 79–125.
34. Sanz MA, Castello A, Carrasco L (2007) Viral translation is coupled to transcription in Sindbis virus-infected cells. J Virol 81: 7061–7068.
35. Pestova TV, Hellen CU, Shatsky IN (1996) Canonical eukaryotic initiation factors determine initiation of translation by internal ribosomal entry. Mol Cell Biol 16: 6859–6869.
36. Katsafanas GC, Moss B (2007) Colocalization of transcription and translation within cytoplasmic poxvirus factories coordinates viral expression and subjugates host functions. Cell Host Microbe 2: 221–228.
37. Castello A, Quintas A, Sanchez EG, Sabina P, Nogal M, et al. (2009) Regulation of host translational machinery by African swine fever virus. PLoS Pathog 5: e1000562.
38. Bolte S, Cordelieres FP (2006) A guided tour into subcellular colocalization analysis in light microscopy. J Microsc 224: 213–232.
39. Terenin IM, Dmitriev SE, Andreev DE, Shatsky IN (2008) Eukaryotic translation initiation machinery can operate in a bacterial-like mode without eIF2. Nat Struct Mol Biol 15: 836–841.
40. Deniz N, Lenarcic EM, Landry DM, Thompson SR (2009) Translation initiation factors are not required for Dicistroviridae IRES function in vivo. RNA 15: 932–946.
41. Wilson JE, Pestova TV, Hellen CU, Sarnow P (2000) Initiation of protein synthesis from the A site of the ribosome. Cell 102: 511–520.
42. Lancaster AM, Jan E, Sarnow P (2006) Initiation factor-independent translation mediated by the hepatitis C virus internal ribosome entry site. RNA 12: 894–902.
43. Gerlitz G, Jagus R, Elroy-Stein O (2002) Phosphorylation of initiation factor-2 alpha is required for activation of internal translation initiation during cell differentiation. Eur J Biochem 269: 2810–2819.
44. Fernandez J, Yaman I, Merrick WC, Koromilas A, Wek RC, et al. (2002) Regulation of internal ribosome entry site-mediated translation by eukaryotic initiation factor-2alpha phosphorylation and translation of a small upstream open reading frame. J Biol Chem 277: 2050–2058.
45. Castello A, Sanz MA, Molina S, Carrasco L (2006) Translation of Sindbis virus 26S mRNA does not require intact eukariotic initiation factor 4G. J Mol Biol 355: 942–956.
46. Shimoike T, McKenna SA, Lindhout DA, Puglisi JD (2009) Translational insensitivity to potent activation of PKR by HCV IRES RNA. Antiviral Res 83: 228–237.
47. Mir MA, Panganiban AT (2008) A protein that replaces the entire cellular eIF4F complex. EMBO J 27: 3129–3139.
48. Sanz MA, Welnowska E, Redondo N, Carrasco L (2010) Translation driven by picornavirus IRES is hampered from Sindbis virus replicons: rescue by poliovirus 2A protease. J Mol Biol 402: 101–117.
49. Ventoso I, Sanz MA, Molina S, Berlanga JJ, Carrasco L, et al. (2006) Translational resistance of late alphavirus mRNA to eIF2alpha phosphorylation: a strategy to overcome the antiviral effect of protein kinase PKR. Genes Dev 20: 87–100.
50. Skabkin MA, Skabkina OV, Dhote V, Komar AA, Hellen CU, et al. (2010) Activities of Ligatin and MCT-1/DENR in eukaryotic translation initiation and ribosomal recycling. Genes Dev 24: 1787–1801.
51. Dmitriev SE, Terenin IM, Andreev DE, Ivanov PA, Dunaevsky JE, et al. (2010) GTP-independent tRNA delivery to the ribosomal P-site by a novel eukaryotic translation factor. J Biol Chem 285: 26779–26787.
52. Pestova TV, Lomakin IB, Hellen CU (2004) Position of the CrPV IRES on the 40S subunit and factor dependence of IRES/80S ribosome assembly. EMBO Rep 5: 906–913.
53. Xi Q, Cuesta R, Schneider RJ (2004) Tethering of eIF4G to adenoviral mRNAs by viral 100k protein drives ribosome shunting. Genes Dev 18: 1997–2009.
54. Burgui I, Yanguez E, Sonenberg N, Nieto A (2007) Influenza virus mRNA translation revisited: is the eIF4E cap-binding factor required for viral mRNA translation? J Virol 81: 12427–12438.
55. Shatsky IN, Dmitriev SE, Terenin IM, Andreev DE (2010) Cap- and IRES-independent scanning mechanism of translation initiation as an alternative to the concept of cellular IRESs. Mol Cells 30: 285–293.
56. Wilson JE, Powell MJ, Hoover SE, Sarnow P (2000) Naturally occurring dicistronic cricket paralysis virus RNA is regulated by two internal ribosome entry sites. Mol Cell Biol 20: 4990–4999.
57. Andino R, Rieckhof GE, Achacoso PL, Baltimore D (1993) Poliovirus RNA synthesis utilizes an RNP complex formed around the 5′-end of viral RNA. EMBO J 12: 3587–3598.
58. Fata-Hartley CL, Palmenberg AC (2005) Dipyridamole reversibly inhibits mengovirus RNA replication. J Virol 79: 11062–11070.
59. Aldabe R, Feduchi E, Novoa I, Carrasco L (1995) Efficient cleavage of p220 by poliovirus 2Apro expression in mammalian cells: effects on vaccinia virus. Biochem Biophys Res Commun 215: 928–936.
60. Vilella MD, Remacha M, Ortiz BL, Mendez E, Ballesta JP (1991) Characterization of the yeast acidic ribosomal phosphoproteins using monoclonal antibodies. Proteins L44/L45 and L44′ have different functional roles. Eur J Biochem 196: 407–414.

Journal of Virology

Membrane Integration of Poliovirus 2B Viroporin

Luis Martínez-Gil, Manuel Bañó-Polo, Natalia Redondo, Silvia Sánchez-Martínez, José Luis Nieva, Luis Carrasco and Ismael Mingarro

J. Virol. **2011, 85(21):11315. DOI: 10.1128/JVI.05421-11. Published Ahead of Print 10 August 2011.**

JOURNAL OF VIROLOGY, Nov. 2011, p. 11315–11324 Vol. 85, No. 21
0022-538X/11/$12.00 doi:10.1128/JVI.05421-11

Membrane Integration of Poliovirus 2B Viroporin▽

Luis Martínez-Gil,[1]† Manuel Bañó-Polo,[1]† Natalia Redondo,[2] Silvia Sánchez-Martínez,[3] José Luis Nieva,[3] Luis Carrasco,[2] and Ismael Mingarro[1]*

Departament de Bioquímica i Biologia Molecular, Universitat de València, E-46100 Burjassot, Spain[1]; Centro de Biología Molecular (CSIC-UAM), Universidad Autónoma de Madrid, E-28049 Madrid, Spain[2]; and Unidad de Biofísica (CSIC-UPV/EHU) and Departamento de Bioquímica, Universidad del País Vasco, E-48080 Bilbao, Spain[3]

Received 16 June 2011/Accepted 29 July 2011

Virus infections can result in a variety of cellular injuries, and these often involve the permeabilization of host membranes by viral proteins of the viroporin family. Prototypical viroporin 2B is responsible for the alterations in host cell membrane permeability that take place in enterovirus-infected cells. 2B protein can be localized at the endoplasmic reticulum (ER) and the Golgi complex, inducing membrane remodeling and the blockade of glycoprotein trafficking. These findings suggest that 2B has the potential to integrate into the ER membrane, but specific information regarding its biogenesis and mechanism of membrane insertion is lacking. Here, we report experimental results of *in vitro* translation-glycosylation compatible with the translocon-mediated insertion of the 2B product into the ER membrane as a double-spanning integral membrane protein with an N-/C-terminal cytoplasmic orientation. A similar topology was found when 2B was synthesized in cultured cells. In addition, the *in vitro* translation of several truncated versions of the 2B protein suggests that the two hydrophobic regions cooperate to insert into the ER-derived microsomal membranes.

Virus infections can lead to a variety of cellular injuries, and usually these involve the restructuring of host membrane systems. Viroporins are a group of small virally encoded proteins that interact with cellular membranes to modify permeability and promote the release of viral particles. A typical feature exhibited by viroporins is the presence of at least one membrane-spanning helix anchoring the protein into membranes. After membrane insertion, their oligomerization creates hydrophilic channels or pores (22).

Poliovirus is the enterovirus prototype member of the *Picornaviridae* family. This small, nonenveloped, icosahedral virus possesses a single-stranded 7.5-kb positive-sense RNA genome that encodes a single polyprotein. Polyprotein processing by virus-encoded proteases yields the structural P1 region proteins that encapsidate viral RNA and the nonstructural P2 and P3 region proteins involved in the replication of the viral RNA and membrane permeabilization (2). Nonstructural 2B protein is one of the products generated on processing the P2 region (62). Viroporin 2B has been identified as one of the viral proteins responsible for the alterations in host cell membrane permeability that take place in enterovirus-infected cells. Different 2B proteins expressed in cells have been localized at the endoplasmic reticulum (ER), Golgi complex, and, to a lesser extent, to the plasma and mitochondrial membranes (18, 31, 49, 58). Biochemical and structural data indicate that viroporins form homo-oligomers that create pores in the ER and Golgi complex membranes (1, 16, 17, 30, 59). However, experimental data dealing with the mechanism of the membrane integration of the 2B product are lacking to date.

The poliovirus 2B viroporin protein is hydrophobic overall and rather small (97 amino acids). Hydrophobicity within the viroporin 2B sequence seems to cluster in two main regions (Fig. 1), one predicted to form a cationic amphipathic α-helix located between residues 35 and 55 (HR1) and a second, more hydrophobic, α-helix located between residues 61 and 81 (HR2), as previously suggested (1). Mutations in the amphipathic α-helix or the second hydrophobic region were shown to interfere with the ability of 2B to increase membrane permeability to promote virus release (3, 8, 58) and with viral RNA replication (57), indicating that the soundness of these regions is essential for viral infection. The amphipathic α-helices of several 2B proteins contain three lysine residues at similar positions, and the presence of an aspartic acid residue also is common in the hydrophobic HR2 region (15), suggesting an α-helical hairpin structure.

Two views of the insertion process of α-helical hairpins into the membrane bilayer can be envisioned. One view postulates α-helical hairpin insertion to be a spontaneous process that does not require specific machinery (9, 19). The other supposes a role for the translocon, which is responsible for facilitating the translocation of secreted proteins across the membrane and insertion of membrane proteins into the lipid bilayer (27, 46), allowing *en bloc* α-helical hairpin insertion from a proteinaceous environment into the lipid bilayer (51).

In the present study, we find that viroporin 2B is an integral membrane protein that can be inserted into the ER membrane through the translocon. The *in vitro* translation of model integral membrane protein constructs in the presence of microsomal membranes initially suggested that when expressed separately, only the amphipathic helix (HR1) can span the membrane. However, the *in vitro* translation of truncated versions of the 2B protein carrying appropriate C-terminal re-

* Corresponding author. Mailing address: Departament de Bioquímica i Biologia Molecular, Universitat de València, E-46100 Burjassot, Spain. Phone: 34-96-354 3796. Fax: 34-96-354 4635. E-mail: Ismael.Mingarro@uv.es.
† These authors contributed equally to this work.
▽ Published ahead of print on 10 August 2011.

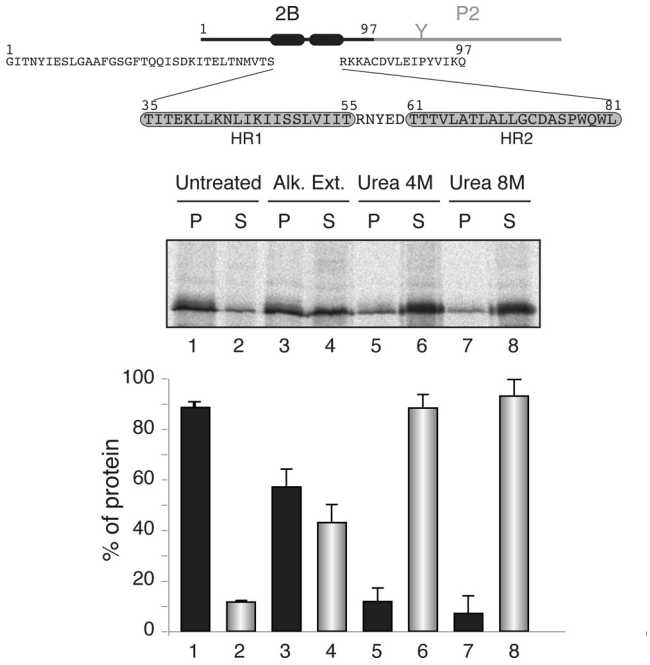

FIG. 1. Membrane association of the chimeric viroporin 2B/P2 protein. At the top is a schematic representation of the poliovirus 2B/P2 chimeric protein (the fused P2 domain is shown in gray). Amino acid residues are shown (HR1 and HR2 are highlighted in gray boxes). The gel in the middle shows the segregation of [^{35}S]Met/Cys-labeled viroporin 2B/P2 fusion protein into membranous and soluble fractions (untreated) and after alkaline wash (Alk. Ext.; sodium carbonate buffer) or urea treatments. P and S denote pellet and supernatant, respectively. In the graph at the bottom, to calculate the percentages of protein the signals present in each pellet and supernatant pair were summed and set to 100%. Data correspond to averages from at least three independent experiments; error bars show standard deviations.

porter glycosylation tags further demonstrated that (i) the N-terminal hydrophobic domain may be stably inserted into the ER-derived microsomal membranes through the translocon, provided that an N_{cyt}/C_{lum} topology is preserved (N_{cy+}, N-terminal end of the transmembrane [TM] segment is oriented toward the cytosol; C_{lum}, C-terminal end of the TM segment is oriented toward the lumen); and (ii) within the complete 2B protein the two hydrophobic regions cooperate to insert into the ER membrane as a helical hairpin with an N-/C-terminal cytoplasmic orientation. In addition, a similar topology was adopted by viroporin 2B expressed in cultured cells under conditions leading to plasma membrane permeabilization.

MATERIALS AND METHODS

Enzymes and chemicals. All enzymes (unless indicated otherwise) as well as plasmid pGEM1, the RiboMAX SP6 RNA polymerase system, and rabbit reticulocyte lysate (a cell-free translation system) were purchased from Promega (Madison, WI). The ER rough microsomes from dog pancreas were purchased from tRNA Probes (College Station, TX). To ensure consistent performance with minimal translational inhibition and background noise, microsomes have been isolated free from contaminating membrane fractions and stripped of endogenous membrane-bound ribosomes and mRNA. The [^{35}S]Met/Cys and ^{14}C-methylated markers were purchased from GE Healthcare. The restriction enzymes and endoglycosidase H (EndoH) were purchased from Roche Molecular Biochemicals. The DNA plasmid, RNA clean-up, and PCR purification kits were from Qiagen (Hilden, Germany). The PCR QuikChange mutagenesis kit was from Stratagene (La Jolla, CA). All oligonucleotides were purchased from Thermo (Ulm, Germany).

Computer-assisted analysis of viroporin 2B sequence. The prediction of TM helices was done using up to 10 of the most common methods available on the Internet: DAS (14) (http://www.sbc.su.se/~miklos/DAS), PHDhtm (47) (http://www.predictprotein.org/), MEMSAT3 (28) (http://bioinf.cs.ucl.ac.uk/psipred/), MEMSAT-SVM (43) (http://bioinf.cs.ucl.ac.uk/psipred/), SOSUI (26) (http://bp.nuap.nagoya-u.ac.jp/sosui/), TMHMM (29) (http://www.cbs.dtu.dk/services/TMHMM), TMPred (http://www.ch.embnet.org/software/TMPRED_form.html), ΔG Prediction Server (24, 25) (http://www.cbr.su.se/DGpred/), SPOCTOPUS (60) (http://octopus.cbr.su.se/), and TopPRED (12) (http://www.sbc.su.se/~erikw/toppred2/).

DNA manipulations. Plasmids encoding full-length 2B sequence (without a stop codon) were constructed by subcloning poliovirus serotype 1 (PV1) Mahoney strain 2B-encoding DNA (kindly provided by E. Wimmer, Stony Brook University) (56) into pGEM1 vector between the NcoI and NdeI restriction sites. This construct contained the P2 domain of the *Escherichia coli* leader peptidase (Lep) fused in frame at the C terminus, as described previously (41). Alternatively, we prepared templates for the *in vitro* transcription of the truncated *2B* mRNA with a 3′ glycosylation tag. The truncated viroporin 2B sequence was prepared by the PCR amplification of a fragment of the pGEM1 plasmid. The 5′ primer was the same for all PCRs and had the sequence 5′-TTCGTCCAACC AAACCGACTC-3′. This primer was situated 210 bases upstream of the *2B* translational start codon; thus, all amplified fragments contained the SP6 transcriptional promoter from pGEM1. The 3′ primers were designed to have approximately the same annealing temperature as the 5′ primer. They contained an optimized glycosylation tag followed by tandem translational stop codons, TAG and TAA, and annealed at specific positions to obtain the desired polypeptide length. PCR amplification comprised a total of 30 cycles with an annealing temperature of 52°C. The amplified DNA products were purified with the Qiagen PCR purification kit according to the manufacturer's protocol and verified on a 1% agarose gel.

In addition, the hydrophobic regions from 2B were introduced into the modified Lep sequence from the pGEM1 plasmid (24, 34) between the SpeI and KpnI sites using two double-stranded oligonucleotides with overlapping overhangs at the ends. The complementary oligonucleotide pairs first were annealed at 85°C for 10 min and then slowly cooled to 30°C, after which the two annealed double-stranded oligonucleotides were mixed, incubated at 65°C for 5 min, cooled slowly to room temperature, and ligated into the vector. The replacements of Lys 46 by Gly, Glu, Gln, and Arg in the LepHR1 construct were done using the QuikChange mutagenesis kit from Stratagene (La Jolla, CA) according to the manufacturer's protocol. All DNA manipulations were confirmed by the sequencing of plasmid DNAs.

Expression *in vitro*. Full-length 2B DNA was amplified from 2B/P2 plasmid using a reverse primer with a stop codon at the end of the 2B sequence (2B-derived expressions), or the DNA derived from the pGEM1 plasmid was transcribed directly (2B/P2 construct). Alternatively, viroporin 2B was amplified fused to the first 50 amino acids from P2 using a reverse primer with tandem stop codons at the 3′ end (2B/50P2). The transcription of the DNA derived from the pGEM1 plasmid was done as described previously (61). Briefly, the transcription mixture was incubated at 37°C for 2 h. The mRNA products were purified with a Qiagen RNeasy clean-up kit and verified on a 1% agarose gel.

In vitro translation of *in vitro*-transcribed mRNA was performed in the presence of reticulocyte lysate, [^{35}S]Met/Cys, and dog pancreas microsomes as described previously (21, 61). Lep constructs with HR-tested segments were transcribed and translated as previously reported (33, 34). For the posttranslational membrane insertion experiments, 2B-derived mRNAs were translated (37°C for 1 h) in the absence of rough microsomal membranes (RMs). Translation then was inhibited with cycloheximide (10 min at 26°C; 2 mg/ml final concentration), after which RMs were added and incubated for an additional hour at 37°C. In all cases, after translation membranes were collected by ultracentrifugation and analyzed by sodium-dodecyl sulfate-polyacrylamide gel electrophoresis (SDS-PAGE). Finally, the gels were visualized on a Fuji FLA3000 phosphorimager with ImageGauge software.

For EndoH treatment, the translation mixture was diluted in 4 volumes of 70 mM sodium citrate (pH 5.6) and centrifuged (100,000 × *g* for 20 min at 4°C). The pellet was resuspended in 50 μl of sodium citrate buffer with 0.5% SDS and 1% β-mercaptoethanol, boiled for 5 min, and incubated for 1 h at 37°C with 0.1 mU of EndoH. The samples were analyzed by SDS-PAGE.

For the proteinase K protection assay, the translation mixture was supplemented with 1 μl of 50 mM $CaCl_2$ and 1 μl of proteinase K (4 mg/ml) and then digested for 40 min on ice. The reaction was stopped by adding 1 mM phenylmethylsulfonyl fluoride (PMSF) before SDS-PAGE analysis.

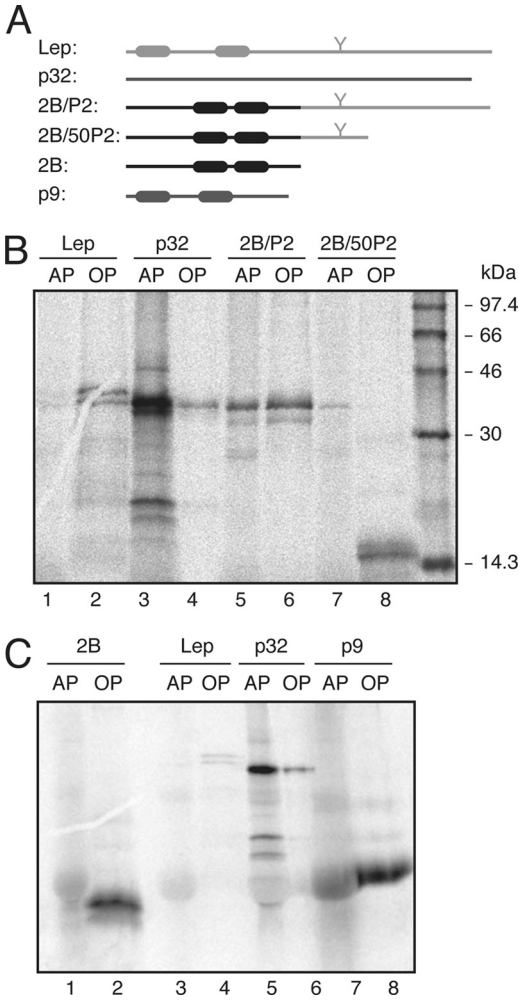

FIG. 2. Triton X-114 partition of viroporin 2B and 2B-derived proteins. (A) Structural organization of the proteins used in the Triton X-114 partition experiments. (B) SDS-PAGE (12% polyacrylamide) analysis after Triton X-114 treatment of 2B/P2 (~38 kDa) and 2B/50P2 (~16 kDa) proteins. Integral membrane protein Lep (~37 kDa; the nonglycosylated form) and peripheral PNRSV movement protein (~32 kDa) were processed in parallel as control samples. (C) Phase separation of viroporin 2B. As a control for small integral membrane protein, Turnip crinkle virus p9 movement protein (~9 kDa) was included. The gels used contained 20% polyacrylamide. AP and OP refer to aqueous and organic phases, respectively.

Membrane sedimentation, alkaline wash, and urea treatments. The translation mixture was diluted in 8 volumes of buffer A (35 mM Tris-HCl at pH 7.4 and 140 mM NaCl) for the membrane sedimentation, 4 volumes of buffer A supplemented with 100 mM Na_2CO_3 (pH 11.5) for the alkaline wash, and 4 or 8 M urea for urea treatments. The samples were incubated on ice for 30 min and clarified by centrifugation (10,000 × *g* for 20 min). Membranes were collected by the ultracentrifugation (100,000 × *g* for 20 min at 4°C) of the supernatant onto 50-μl sucrose cushions. Pellets (P) and supernatants (S) of the ultracentrifugation were analyzed by SDS-PAGE.

Phase separation in Triton X-114 solution. The phase separation of integral membrane proteins using the detergent Triton X-114 was performed as described previously (10, 41). Triton X-114 (1%, vol/vol) was added to a translation mixture that previously had been diluted with 180 μl of phosphate-buffered saline (PBS). After mixing, the samples were incubated at 0°C for 1 h and overlaid onto 300 μl of PBS supplemented with 6% (wt/vol) sucrose and 1% (vol/vol) Triton X-114. After 10 min at 30°C, an organic droplet was obtained by centrifugation for 3 min at 1,500 × *g*. The resulting aqueous upper phase (AP; 200 μl) was collected, and the organic droplet at the bottom of the tube was diluted with PBS (organic phase [OP]). Both OP and AP were supplemented with sample buffer and boiled for 10 min prior to 12% (Fig. 2B) or 20% (Fig. 2C) SDS-PAGE analysis.

Transfection assay. Baby hamster kidney (BHK) cells that stably express the T7 RNA polymerase (clone BSR-T7/5), designated BHKT7 (11), were used. Cells were grown at 37°C in Dulbecco's modified Eagle's medium (DMEM) supplemented with 5 or 10% fetal calf serum (FCS) and nonessential amino acids. BHKT7 cells additionally were treated with Geneticin G418 (Sigma) on every third passage at a final concentration of 2 mg/ml. Cells were transfected with 1 μg of plasmid pTM1-2B (3, 4) or the different constructs plus 2 μl of Lipofectamine per well in Opti-mem medium (Invitrogen) for 2 h at 37°C. After 2 h, Lipofectamine was removed and the cells were supplemented with fresh medium containing 5% FCS.

RESULTS

Viroporin 2B is an integral membrane protein. Viroporin 2B amino acid sequence (Fig. 1) has been parsed to test the performance of several commonly used algorithms for predicting the topology of integral membrane proteins. As shown in Table 1, the predicted outcome showed great variability according to the methods used, likely due to the limited hydrophobicity of the membrane-associating regions of 2B. The membrane association properties of the full-length viroporin 2B were studied using an *in vitro* system that closely mimics the *in vivo* situation, in which cytosolic and membrane fractions of *in vitro*-translated [^{35}S]Met/Cys-labeled 2B/P2 fusions in the presence of ER-derived microsomes were collected and analyzed by SDS-PAGE and autoradiography. In this system, the microsomes provide all of the membrane insertion and glycosylation components (i.e., the translocon machinery and the oligosaccharyltransferase enzyme). The reporter P2 domain is the extramembrane C-terminal domain from the bacterial leader peptidase (Lep) that carries an N-glycosylation site extensively used to report membrane translocation (Fig. 1, top). The viroporin 2B/P2 chimera was recovered mainly from the 100,000 × *g* pellet fraction (Fig. 1, untreated lanes) after the centrifugation of the microsome-containing translation reaction mixture, indicating that it could be either a membrane-associated protein or a lumenally translocated protein. The absence of glycosylation suggested that the chimeric protein was not translocated into the lumen of the microsomes. Nevertheless, to differentiate between these possibilities the translation reaction mixtures were washed with sodium carbonate (pH 11.5), which renders microsomes into membranous sheets, releasing the soluble luminal proteins (35, 41). As shown in Fig. 1, the 2B/P2 fusion appeared to be preferentially associ-

TABLE 1. Computer analysis of viroporin 2B amino acid sequence

Algorithm	Membrane protein	No. of TM segments (starting aa/ending aa)
DAS	Yes	2 (45/53–64/71)
PHDhtm	Yes	2 (41/57–64/72)
MEMSAT3	Yes	1 (44/63)
MEMSAT-SVM	Yes	1 (40/55)
SOSUI	No	0
TMHMM	No	0
TMPred	Yes	1 (58/78)
ΔG Prediction Server	Yes	1 (61/82)
SPOCTOPUS	Yes	1 (48/73)
TopPRED	Yes	1 (38/58)

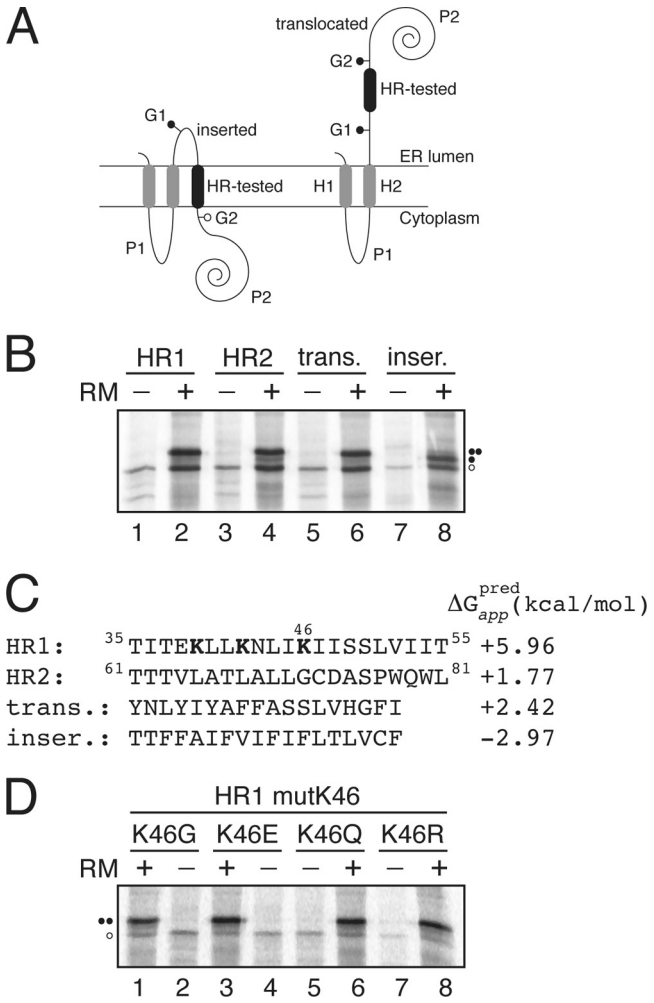

FIG. 3. Insertion of viroporin 2B hydrophobic regions 1 (HR1) and 2 (HR2) into microsomal membranes using Lep as a model protein. (A) Schematic representation of the leader peptidase (Lep) construct used to report insertion into the ER membrane of 2B HR1 and HR2. The HR under study is inserted into the P2 domain of Lep flanked by two artificial glycosylation acceptor sites (G1 and G2). The recognition of the HR by the translocon machinery as a TM domain locates only G1 in the luminal side of the ER membrane, preventing G2 glycosylation. The Lep chimera will be doubly glycosylated when the HR being tested is translocated into the lumen of the microsomes. (B) *In vitro* translation in the presence of membranes of the different Lep constructs. Constructs containing HR1 (residues 35 to 55; lanes 1 and 2) and HR2 (residues 61 to 81; lanes 3 and 4) were transcribed and translated in the presence of membranes. Control HRs were used to verify sequence translocation (trans.; lanes 5 and 6) and membrane integration (inser.; lanes 7 and 8). Bands of nonglycosylated protein are indicated by a white dot; singly and doubly glycosylated proteins are indicated by one and two black dots, respectively. (C) The HR sequence in each construct is shown together with the predicted ΔG apparent value, which was estimated using the ΔG prediction algorithm available on the Internet (http://dgpred.cbr.su.se/). Lysine residues in HR1 are shown in boldface. (D) *In vitro* translation of HR1-derived mutants at lysine 46.

ated (approximately 58%; lanes 3 and 4) with the membranous pellet fraction, suggesting a tight association with membranes. Further treatment with 4 M urea demonstrated that approximately 88% of the protein was in the supernatant fraction (Fig. 1, lanes 5 and 6). More than 93% of the protein was extracted from the supernatant fraction by 8 M urea (Fig. 1, lanes 7 and 8), suggesting that 2B/P2 is released from the membrane environment when the secondary and tertiary structures of the protein are lost.

The translation reaction mixtures also were treated with Triton X-114, a nonionic detergent that forms a separate organic phase into which membrane lipids and hydrophobic proteins are segregated from the aqueous phase, which contains nonintegral membrane proteins (10, 35). The 2B/P2 fusion protein (Fig. 2A) was detected in both the aqueous and organic phases (Fig. 2B, lanes 5 and 6), while a reduction of the P2 domain to its 50 N-terminal residues (Fig. 2A) led to the organic-phase detection of the chimera (Fig. 2B, lanes 7 and 8). Control analyses of Lep and Prune necrotic ring-spot virus (PNRSV) p32 movement protein showed, as previously demonstrated (35), organic- and aqueous-phase detections, respectively. Finally, viroporin 2B translated in the absence of fused domains was detected only in the organic phase (Fig. 2C, lanes 1 and 2), indicating that viroporin 2B is an integral membrane protein.

Insertion of the viroporin 2B hydrophobic regions into biological membranes. We assayed the membrane insertion capacities of the viroporin 2B hydrophobic regions using an *in vitro* experimental system (24), which accurately reports the integration of transmembrane (TM) helices into microsomal membranes. This system uses ER-derived microsomal membranes and provides a sensitive way to detect the insertion or translocation of hydrophobic regions through the Sec translocon (25). An obvious advantage of this system is that the insertion assays are performed in the context of a biological membrane. The system is based on the cotranslational glycosylation performed by the oligosaccharyltransferase (OST) enzyme. OST adds sugar residues to an NX(S/T) consensus sequence (53), with X being any amino acid except proline (52), after the protein emerges from the translocon channel. The glycosylation of a protein region translated *in vitro* in the presence of microsomal membranes therefore indicates the exposure of this region to the OST active site on the luminal side of the ER membrane. In our first experimental assay (Fig. 3), a segment to be assayed (HR tested) is engineered into the luminal P2 domain of the integral membrane protein Lep from *E. coli*, where it is flanked by two acceptor sites (G1 and G2) for *N*-linked glycosylation (Fig. 3A). Both engineered glycosylation sites are to be used as membrane insertion reporters. The rationale behind using two glycosylation sites is that G1 will always be glycosylated due to its native luminal localization, while G2 will be glycosylated only on the translocation of the tested TM region through the microsomal membrane. Thus, single glycosylation indicates a correct TM integration (Fig. 3A, left), whereas double glycosylation reports the nonintegration capability of the tested HR segment (Fig. 3A, right). The single glycosylation of the molecule results in an increase in molecular mass of about 2.5 kDa relative to the observed molecular mass of Lep expressed in the absence of microsomes, and the mass is around 5 kDa in the case of double glycosylation.

The translation of the chimeric constructs harboring the predicted viroporin 2B hydrophobic regions as HR-tested segments resulted mainly in double-glycosylated forms (Fig. 3B,

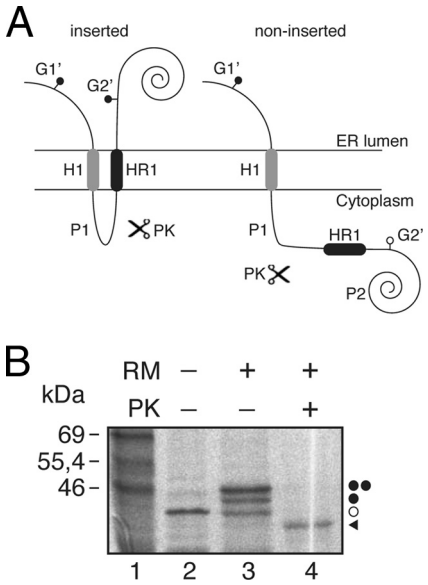

FIG. 4. Insertion of HR1 into microsomal membranes using the Lep′ construct. (A) Schematic representation of the Lep-derived construct (Lep′). In this Lep′ construct (~40 kDa; the nonglycosylated form), HR1 replaces the H2 domain from Lep. The glycosylation acceptor site (G2′) located in the beginning of the P2 domain will be modified only if HR1 inserts into the membrane, while the G1′ site, embedded in an extended N-terminal sequence of 24 amino acids, is always glycosylated. (B) *In vitro* translation in the presence of membranes. Bands of nonglycosylated protein are indicated by a white dot; singly and doubly glycosylated proteins are indicated by one and two black dots, respectively. The protected glycosylated HR1/P2 fragment (~36.5 kDa) is indicated by a black triangle.

lanes 2 and 4), which is consistent with the translocation of these regions into the lumen of the ER. Control constructs with previously tested (37) translocation and integration sequences are shown in lanes 6 and 8, and they disclose the expected double and single glycosylation patterns, respectively (Fig. 3B). The permeabilization induced by an overlapping peptide library that spanned the complete viroporin 2B sequence mapped the cell plasma membrane-porating activity to the partially amphipathic HR1 domain (32). This region contains three lysine residues that would preclude TM disposition (Fig. 3C), especially in the case of lysine 46, since it would be located roughly in the center of the hydrophobic core of the lipid bilayer. Nevertheless, the replacement of this residue by glycine, glutamic acid, glutamine, or arginine renders glycosylation patterns consistent with the translocation of the hydrophobic region into the ER lumen (Fig. 3D). Taken together, these results suggest that an isolated HR1 segment does not span ER-derived membranes in an N_{lum}/C_{cyt} orientation.

Since native 2B does not have a cleavable signal sequence, it seems likely that HR1 acts as a signal-anchor sequence having an N_{cyt}/C_{lum} orientation in the membrane (36). To test HR1 insertion in a reverse orientation, another Lep construct (Lep′) was used. In this Lep′ construct, HR1 replaces the second TM segment (H2) from Lep (Fig. 4A). The glycosylation acceptor site (G2′) located in the beginning of the P2 domain will be modified only if the HR1 segment inserts into the membrane, while the G1′ site, embedded in an extended N-terminal sequence of 24 amino acid residues, is always glycosylated. We found that HR1 significantly inserts into the membrane (up to 60% of the molecules) with the appropriate topology (Fig. 4B). The nature of the cytosolic/luminal domains was further examined by proteinase K (PK) digestions. Treatment with PK degrades domains of membrane proteins that protrude into the cytosol, but membrane-embedded or luminally exposed domains are protected. The addition of PK to a Lep′HR1 translation mixture (Fig. 4B, lane 4) rendered a protected, glycosylated HR1-P2 fragment, suggesting the proper insertion of HR1 sequence with an N_{cyt}/C_{lum} orientation.

Viroporin 2B integrates into the ER membrane through the translocon with an N-terminal/C-terminal cytoplasmic orientation. The microsomal *in vitro* system closely mimics the conditions of *in vivo* membrane protein assembly into the ER membrane. HR1 is properly recognized by the translocon as a TM segment out of its native context (Fig. 4). However, the presence of fused domains can influence its membrane insertion capacity. Hence, we next sought to investigate whether HR1 also could direct the integration into the ER membrane of the native 2B sequence (i.e., in the absence of nonviral fused domains) through the translocon.

Because N-glycosylation acceptor sites are absent from the viroporin 2B sequence, several modifications were prepared to determine the TM disposition of different 2B-derived proteins. First, to gain topological information, an N-glycosylation acceptor site was engineered at the hydrophilic N-terminal region of the 2B sequence by mutating glutamine 20 to an acceptor asparagine (…^{20}NIS…; construct 2BNtGlyc). Second, we added a C-terminal N-glycosylation tag (CtGlyc; **NST**-MMM [the glycosylation sequon is in boldface]) that has been proven to be efficiently glycosylated (6). The first 60 residues of the viroporin 2B carrying an N-terminal glycosylation site were translated using C-terminal tags (Fig. 5A) either with an N-glycosylation acceptor site as a C-terminal tag (2BNt/Ct; Fig. 5B, lanes 1, 3, and 5) or with a nonacceptor site (2BNt/CtØ; Fig. 5B, lanes 2, 4, and 6). The lack of glycosylation at the N-terminal engineered acceptor site together with the efficient glycosylation observed only when using the C-terminal acceptor site (Fig. 5B, lane 3), as proven after EndoH treatment (Fig. 5B, lane 5), strongly indicates that HR1 in the viroporin context is acting as a noncleavable signal sequence and is properly recognized by the translocon machinery to be inserted into the membrane with its N terminus facing the cytoplasm (N_{cyt}/C_{lum} topology). In addition, by blocking protein synthesis after 2BNt/Ct has been translated in the absence of membranes, we confirmed that the truncated version of 2B (2BNt/Ct) needs to be cotranslationally inserted into the ER membrane. As shown in Fig. 5C, 2BNt/Ct was glycosylated when microsomal membranes were added to the translation mixture cotranslationally. In contrast, when microsomal membranes were included posttranslationally (i.e., after translation had been inhibited by cycloheximide), the C-terminal acceptor site was not glycosylated (Fig. 5C, lane 3), thereby emphasizing that truncated 2B is integrated cotranslationally through the ER translocon.

Because of the low hydrophobicity and the relatively poor insertion propensity found in the Lep system for HR2 (Fig. 3), it is predicted that the 2B C-terminal region will be translocated into the ER lumen. However, 2B hydrophobic regions also are responsible for the membrane anchoring of the 2BC

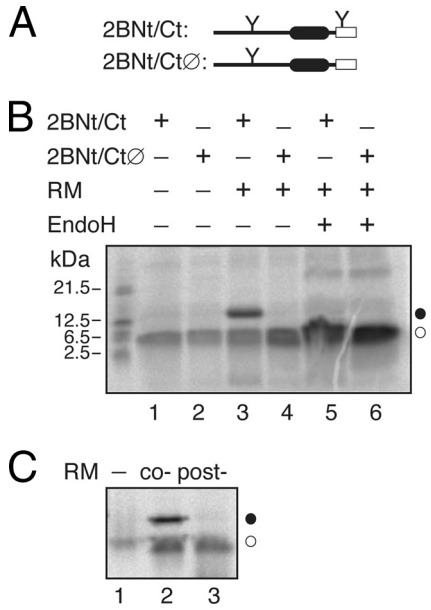

FIG. 5. Membrane insertion of 60-mer viroporin 2B. (A) Structural organization of the 2B 60-mer truncated construct. (B) *In vitro* translations were performed in the presence (+) or in the absence of C-terminal glycosylation tag, RMs, and EndoH as indicated. (C) The 2BNt/Ct construct was translated in either the absence (lanes 1 and 3) or the presence (lane 2) of RMs. Lane 2, cotranslationally added microsomes. Lane 3, RMs were added posttranslationally (after 1 h of translation and 10 min of cycloheximide treatment; Post-), and incubation was continued for another 1 h.

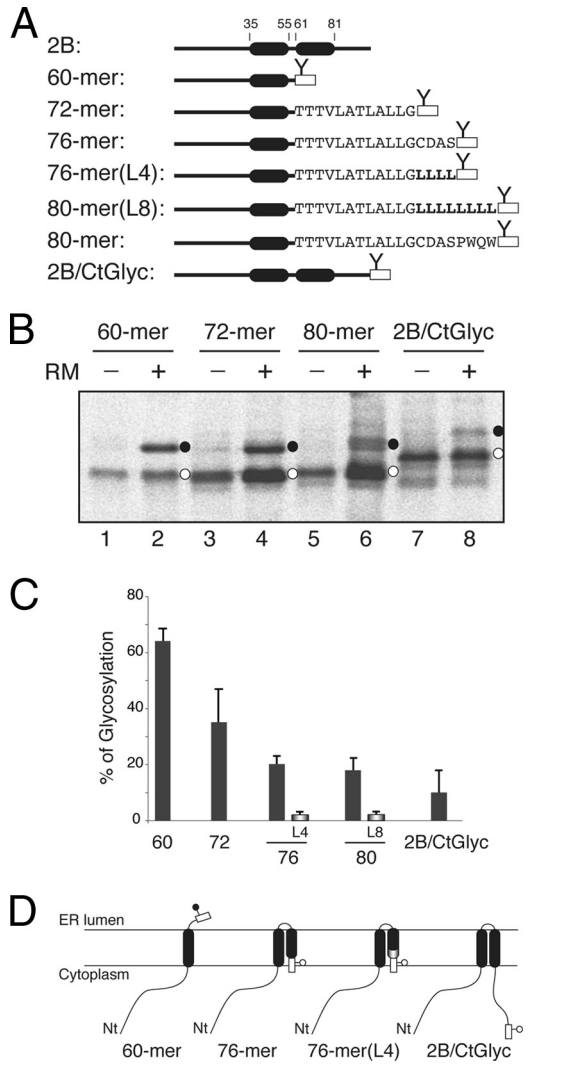

FIG. 6. Effect of HR2 on 2B 60-mer insertion and topology. (A) Structural organization of full-length and truncated viroporin 2B constructs. (B) *In vitro* translation of truncated viroporin 2B 60-mer, 72-mer, 80-mer, and full-length (2B/CtGlyc) constructs in which a fused C-terminal N-glycosylation tag (rectangle) provides a simple readout for topology determination. The presence of RMs and nonglycosylated and glycosylated proteins (empty and black dots, respectively) is indicated. (C) *In vitro* glycosylation of truncated viroporin 2B-derived proteins. The level of glycosylation is quantified from SDS-PAGE gels by measuring the fraction of glycosylated (f_g) versus glycosylated-plus-nonglycosylated (f_{ng}) molecules, using the equation $p = f_g/f_g + f_{ng}$. Data correspond to averages from at least four independent experiments, and error bars show standard deviations. (D) Topological models for 2B constructs. Nt, N terminus.

precursor, which performs its enzymatic and RNA binding activities in the cytosolic compartment. Thus, we speculated that some type of helix-helix interaction stabilizes the insertion of HR2 to keep an N_{cyt}/C_{cyt} 2B topology. It has been shown recently that in some cases the insertion of poorly hydrophobic regions depends on the presence of neighboring loops and/or TM segments (20), especially in the case of the preceding TM segment (23, 55). In our attempts to unravel the disposition of 2B in biological membranes, we focused on the insertion of truncated C-terminal reporter tag fusions. In Fig. 6 we show a series of experiments where HR1 and various lengths of downstream sequence were translated as truncated proteins with an N-glycosylation C-terminal tag (Fig. 6A). A mutant polypeptide truncated at the end of the hydrophilic loop between HR1 and HR2 (60-mer) is highly glycosylated (~65%; Fig. 6B, lane 2), indicating that, similarly to what is shown in Fig. 5B, the C-terminal glycosylation tag has been translocated into the lumen of the ER, and thus HR1 is integrated into the ER membrane in a N_{cyt}/C_{lum} orientation in this construct (Fig. 6D, left). The percentage of glycosylated truncated proteins is reported in Fig. 6C. Extending the 2B sequence to include roughly half of HR2 has a significant effect on this pattern (72-mer; Fig. 6B and 6C), suggesting some tendency of these truncated molecules to insert the C-terminal tag into the membrane. Moreover, extending the 2B sequence four residues (roughly one helical turn; 76-mer) (Fig. 6C) substantially diminished glycosylation (~21%). The glycosylation level for the truncated protein shown in Fig. 6C cannot be explained by an increased hydrophobicity of the added amino acids, since the total free energy predicted (ΔG^{pred}) for the ^{73}CDAS^{76} sequence is 4.31 kcal/mol, where a positive value is indicative of extramembrane disposition (the calculation of ΔG^{pred} was carried out using the scale of Hessa and collaborators [24]). Interestingly, the addition of four leucine residues (ΔG^{pred} = −2.2 kcal/mol) instead of the ^{73}CDAS^{76} sequence [76-mer(L4)] strongly precludes glycosylation (<3%) (Fig. 6C), demonstrating the clear hydrophobic effect of the leucine residues in this construct. This was further corroborated by extending the protein to include up to eight leucine residues

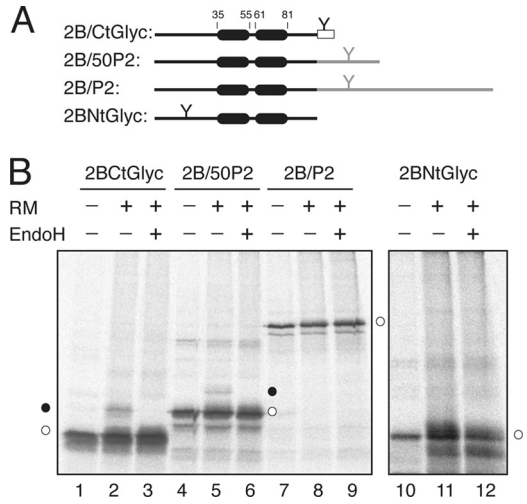

FIG. 7. Insertion and topology of full-length viroporin 2B protein. (A) The structural organization of the 2B-derived constructs is shown at the top. The N-glycosylation site is highlighted by a Y-shaped symbol both when inserted in the protein sequence and when added as a C-terminal reporter tag (rectangles). (B) *In vitro* translation was performed in the presence (+) and in the absence (−) of RMs and EndoH as indicated. Nonglycosylated and singly glycosylated proteins are indicated by empty and black dots, respectively.

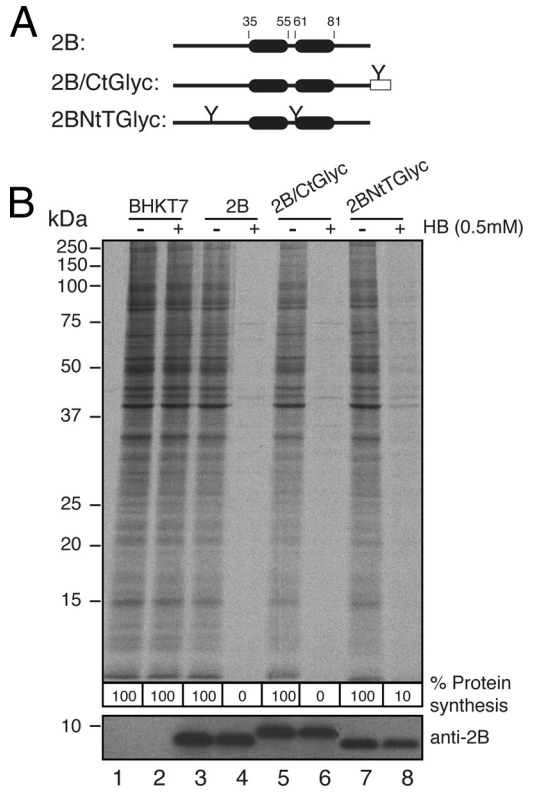

FIG. 8. Permeabilization activity of 2B-derived constructs in BHKT7 cells. (A) Structural organization of the transfected 2B variants. (B) BHKT7 cells were transfected with pTM1-2Bwt or with pTM1-2B variants. At 3 h posttransfection, cells were pretreated with hygromycin B (HB) at 0.5 mM for 15 min and then labeled with [^{35}S]Met/Cys for 45 min in the presence of the inhibitor. After labeling, the proteins were analyzed by SDS-PAGE (17.5%) followed by fluorography and autoradiography (top). The synthesis of 2B protein was detected by Western blotting using specific rabbit polyclonal antibodies (bottom). The numbers below each lane represent the percentage of protein synthesis in the presence of hygromycin B as calculated by densitometric scanning.

[80-mer(L8)] (Fig. 6C). Finally, both the mutant truncated at the end of HR2 (80-mer) and the 2B full-length construct (2B/CtGlyc) had little effect on this pattern (~17 and ~10% glycosylation, respectively), indicating that the C terminus of the majority of these tagged proteins is cytosolic, and thus the HR2 sequence included in these constructs is integrated into the membrane in an N_{lum}/C_{cyt} orientation (Fig. 6D, right).

To confirm that the same topology is adopted by the full-length 2B protein, several 2B-derived constructs were prepared and their membrane disposition experimentally determined. The translation of the C-terminal-tagged 2B protein (2B/CtGlyc) (Fig. 7A) in the presence of RMs resulted in glycosylation in <8% of the molecules, as demonstrated by EndoH (a glycan-removing enzyme) treatment (Fig. 7B, lanes 1 to 3). The addition of the first 50 residues of the Lep P2 domain (2B/50P2) (Fig. 7A), which contains an N-glycosylation acceptor site as a topological reporter, yielded glycosylation in <5% of the viroporin 2B-derived molecules (Fig. 7B, lanes 4 to 6). Furthermore, when full-length Lep P2 domain was used as a reporter domain, the chimera was not glycosylated at all (2B/P2) (Fig. 7B, lanes 7 to 9). Finally, the *in vitro* translation of a construct harboring an N-terminal glycosylation acceptor site (2BNtGlyc, Fig. 7A) in the presence of RM only resulted in unmodified molecules (Fig. 7B, lanes 10 to 12). Taken together, these results suggest a preferential N-/C-terminal cytoplasmic orientation for viroporin 2B when expressed in the presence of ER-derived microsomal membranes.

Viroporin 2B topology in mammalian cells. To further assess the topology adopted by functional viroporin 2B in membranes, 2B variants containing designed N-glycosylation sites at different positions were expressed in cultured cells, and their plasma membrane-permeabilizing capacities were assessed (Fig. 8). For this purpose, the 2B variants were cloned in pTM1 vector and transfected in BHK cells that stably express the T7 RNA polymerase. These cells posses the machinery required for synthesizing the virion components and even to assemble infectious particles. As expected, 2B expression permeabilized BHK cells to the antibiotic hygromycin B (31) (Fig. 8B, lane 4). Although the synthesis of unmodified 2B is not detectable by radioactive labeling in the permeabilized cells (Fig. 8B, top), it can be detected by Western blotting using a specific 2B antibody (Fig. 8B, bottom). No glycosylation of 2B was observed when this protein bears the N-glycosylation site at the amino terminus, in the turn, or at the carboxy terminus of this viroporin (Fig. 8B, lanes 5 to 8). In addition, these two viroporin 2B variants retain their capacity to permeabilize cells to hygromycin B, suggesting that they are located at the membrane and exhibit the ability to alter membrane permeability. It should be noted that in the case of the N-glycosylation site located at the turn, although the location is luminal the absence of glycosylation is due to its proximity to the TM domains as previously reported (42, 44). In conclusion, the *in vitro* and *in vivo* assays consistently indicate that both the N and

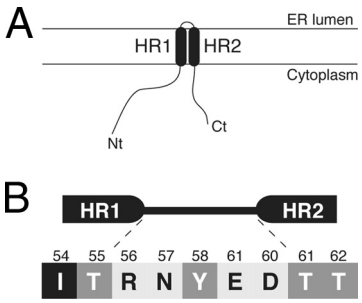

FIG. 9. (A) Topological model for 2B association with membranes. (B) Turn-inducing propensity at the interhelical region of the viroporin 2B helical hairpin according to the scale of Monné and coworkers (39). The five amino acid residues interconnecting HR1 and HR2 are shown flanked by the putative last two residues from the HR1 helix and the putative first two residues from HR2. All residues connecting HR1 and HR2 are turn inducers (normalized turn potential, >1). The residues are highlighted according to their turn potential: black for a potential lower than 1 (Ile54), dark gray for a potential between 1 and 2 (Thr55, Tyr58, and Thr61), and light gray for a potential above 2 (Arg56, Asn57, Glu59, and Asp60).

C termini of viroporin 2B face the cytoplasm, as displayed in Fig. 9A.

DISCUSSION

Viroporins are a group of proteins responsible for alterations in the permeability of cellular membranes during virus infection, favoring the release of viral particles from infected cells (reviewed in reference 22). The molecular mechanisms by which viroporins insert into cell membranes remain largely unknown. In this study, we demonstrate that poliovirus viroporin 2B is a double-spanning integral membrane protein that can be inserted into the ER membrane through the translocon machinery.

Computer-assisted membrane protein topology prediction is a useful starting point for experimental studies of membrane proteins. We have used 10 popular prediction methods and found large discrepancies between their predictions. Two of the algorithms failed to predict 2B as an integral membrane protein, and two of them assigned two TM segments for the protein. It should be noted that the reliability of a topology prediction can be estimated by the number of prediction methods that agree. Since six of the algorithms predicted 2B as a membrane protein with only one TM segment, these results clearly highlight that the presence of helical hairpin structures, which was not detected even by the methods predicting reentrant loops (MEMSAT-SVM and SPOCTOPUS), may be missed by current predictive methods, as previously suggested for a different TM helical hairpin (40).

The membrane association of 2B/P2 fusion protein was resistant to alkaline extraction. Since this treatment disrupts microsomal membranes and releases any soluble luminal protein, this result indicates that the fusion protein is not translocated to the lumen of the microsomes. Urea treatments solubilized our fusion protein (Fig. 1), indicating that secondary and tertiary structures in 2B play an important role in 2B insertion. The latter results contrast with previous work that showed that coxsackievirus 2B/enhanced green fluorescent protein fusions were resistant to urea extraction (18). This discrepancy could be derived either from the differences found in the amino acid sequence of both 2B proteins or from the use of different fusion proteins in both cases. In fact, a significant influence of the P2 domain can be observed in our Triton X-114 partition experiments. Fusions containing the full P2 domain partition significantly into the aqueous phase, whereas the addition of the 50 N-terminal residues from this domain promoted the partitioning of the shorter chimera into the organic phase. These results clearly demonstrated integral membrane protein behavior (compare lanes 5 and 6 with lanes 7 and 8 in Fig. 2B), as corroborated by partition experiments using full-length 2B (Fig. 2C, lanes 1 and 2).

By challenging the hydrophobic regions of 2B in a model protein construct (Lep), we demonstrate first that these regions do not integrate as TM segments in the presence of ER-derived membranes when expressed separately (Fig. 3). It should be mentioned that, in these Lep-derived constructs, the HR1 segment is forced to insert into the membrane with an N_{lum}/C_{cyt} topology, and this topological effect can prevent the proper TM disposition of this region. In fact, using a Lep-derived variant (Lep′), we demonstrated the TM disposition of HR1 when expressed with an N_{cyt}/C_{lum} orientation (Fig. 4). The glycosylation data obtained in the context of the parental 2B sequence using engineered and truncated proteins provided compelling evidence that HR1-HR2 also may integrate cotranslationally into the membrane in the absence of fused domains. Hence, a truncated 2B protein containing HR1 inserted efficiently into ER microsomal membranes adopting an N_{cyt}/C_{lum} topology (Fig. 5), and the addition of HR2 residues to this construct resulted in the cytoplasmic reorientation of the C terminus (Fig. 6). Furthermore, the lack of glycosylation at N-glycosylation acceptor sites engineered at different positions, both in an *in vitro* microsomal system (Fig. 7) and in cultured cells (Fig. 8), suggests that both the N and C termini of viroporin 2B protein reside on the cytosolic side of the membrane. In the context of the P2 polyprotein, the membrane topology found in the present work leaves the protease cleavage sites of P2 facing the cytosol, which is suitable for polypeptide processing by viral proteases.

Taken together, these data support the capacity of the HR domains to act as interacting TM segments in their natural contexts. In this sense, we have described previously the integration into the ER membrane of two closely spaced membrane-spanning segments of viral origin, where both TM segments of the nascent protein bind to one or more translocon proteins and are held until the termination of translation, whereupon they are released laterally as a helical hairpin into the lipid phase (50, 51). More recently, this mechanism of partition into the membrane as a pair of helices has been observed by others using a nonviral membrane protein (13). Thus, the retention of a first cationic amphipathic segment (HR1) at the ER translocon to generate a helical hairpin might facilitate partitioning into the lipid phase by shielding the polar amino acids that could compromise effective membrane integration (36).

These findings provide important new insights into the molecular architecture and the molecular mechanism of 2B integration into the membrane. The synergic effect found for pore formation between HR1 and HR2 in a previous peptide-based

analysis, which indicated that both HRs cooperate in membrane permeabilization (48), suggests that HR1 and HR2 interact with each other to form a helix-turn-helix (helical hairpin) motif that traverses the lipid bilayer. An additional source of stability of this motif can be the turn between the two helices. It has been shown that charged and polar residues (plus prolines and glycines) display turn induction in a TM polyleucine stretch (38); in our case, we do not know exactly which amino acid residues form the turn in the membrane-bound viroporin, although in all likelihood the turn occurs between the highly hydrophilic residues 55 and 61. Figure 9B shows this region of viroporin 2B, where the residues are highlighted according to their turn-inducing propensities (38). All residues present in this region are strongly turn inducing (normalized turn potential, >1). Among them, four (Arg56, Asn57, Glu59, and Asp60) have a high turn potential (>2). In essence, a great concentration of turn-promoting residues is found in the region connecting HR1 and HR2. Thus, in the membrane-bound form, we can expect the turn of viroporin 2B to be centered on ^{56}RNYED^{60}. Interestingly, previous mutagenesis studies using the CBV 2B protein showed that the negatively charged residues found in this short hydrophilic turn between HR1 and HR2 are indeed important for the membrane-active character of 2B protein (16). Moreover, recent molecular dynamic simulations of the poliovirus 2B channel/pore-forming regions suggested that Glu59 and Asp60 are involved in the helical hairpin formation (45). In any case, it seems clear that the turn may play a significant role in the stability and integration of the membrane-bound 2B protein. In addition, the topology observed in the present work agrees with previous data obtained with different fusion proteins (18). Furthermore, the localization of the C terminus at the cytosolic side of the membrane is consistent with the need for the proteolytic liberation of the 2B protein from the precursor 2BC polyprotein by a cytosolic viral protease cleavage, which is accomplished by 3C^{pro} (54). This could occur after the membrane insertion of 2BC or even the entire P2 precursor (2ABC).

Our findings further suggest a physiological role for translocon-mediated 2B integration into the ER membrane. Our combined analysis predicts a marginal propensity for 2B polypeptide to insert into membranes (Table 1 and Fig. 3D). On the other hand, upon viral entry, initially synthesized 2B or 2BC proteins will remain diluted in the cytosol of the infected cell. Marginal hydrophobicity together with low concentration are predicted to reduce the probability of the spontaneous insertion of 2B and 2BC into their primary target organelle: the Golgi complex (18, 49). Thus, we speculate that cotranslational insertion into the ER membrane is a particularly relevant phenomenon at the initial stages of the infectious cycle, during which both the viral mRNA levels and the concentration of the translated viral proteins are predictably low. Under those conditions, the cellular protein biosynthesis and vesicular transport machineries remain functional, and 2B and its 2BC precursor likely are synthesized as additional cell membrane proteins. From the ER, these proteins may reach the Golgi compartment membrane to fulfill regulatory and/or signaling functions that result in the disruption of Ca^{2+} homeostasis (5, 15) and vesicular transport inhibition (7, 15). At later stages, the canonical ER-Golgi protein-trafficking pathway no longer is functional and/or required for viral replication. The massive proliferation of cell endomembranes (viroplasm) and the high levels of viral protein synthesis result in higher effective concentrations of these components inside the infected cell system. Under those conditions, it is predicted that the spontaneous insertion into the membrane of a significant amount of synthesized 2B and 2BC will ensue.

In summary, viroporin 2B may use common structural arrangements to integrate into the ER membrane through the translocon, at least during the initial stages of the viral replicative cycle. The development of *in vitro* assays designed to dissect the membrane integration process will lead to a better understanding of the membrane permeabilization mechanisms that act during enterovirus infection.

ACKNOWLEDGMENTS

We thank Arne Elofsson (Stockholm University) for helpful comments on the manuscript.

This work was supported by grants BFU2009-08401 (to I.M.), BFU2009-07352 (to L.C.), and BIO2008-00772 (to J.L.N.) from the Spanish Ministry of Science and Innovation (MICINN, ERDF; supported by the European Union), as well as by ACOMP/2011/025 from the Generalitat Valenciana to I.M. M.B.-P. was the recipient of an FPU fellowship from the Spanish Ministry of Education.

REFERENCES

1. **Agirre, A., A. Barco, L. Carrasco, and J. L. Nieva.** 2002. Viroporin-mediated membrane permeabilization. Pore formation by nonstructural poliovirus 2B protein. J. Biol. Chem. **277:**40434–40441.
2. **Agol, V.** 2002. Picornavirus genome: an overview, p. 127–148. *In* B. L. Semler and E. Wimmer (ed.), Molecular biology of picornaviruses. ASM Press, Washington, DC.
3. **Aldabe, R., A. Barco, and L. Carrasco.** 1996. Membrane permeabilization by poliovirus proteins 2B and 2BC. J. Biol. Chem. **271:**23134–23137.
4. **Aldabe, R., and L. Carrasco.** 1995. Induction of membrane proliferation by poliovirus proteins 2C and 2BC. Biochem. Biophys. Res. Commun. **206:**64–76.
5. **Aldabe, R., A. Irurzun, and L. Carrasco.** 1997. Poliovirus protein 2BC increases cytosolic free calcium concentrations. J. Virol. **71:**6214–6217.
6. **Bañó-Polo, M., F. Baldin, S. Tamborero, M. A. Marti-Renom, and I. Mingarro.** 2011. N-glycosylation efficiency is determined by the distance to the C-terminus and the amino acid preceding an Asn-Ser-Thr sequon. Protein Sci. **20:**179–186.
7. **Barco, A., and L. Carrasco.** 1995. A human virus protein, poliovirus protein 2BC, induces membrane proliferation and blocks the exocytic pathway in the yeast Saccharomyces cerevisiae. EMBO J. **14:**3349–3364.
8. **Barco, A., and L. Carrasco.** 1998. Identification of regions of poliovirus 2BC protein that are involved in cytotoxicity. J. Virol. **72:**3560–3570.
9. **Baumgärtner, A.** 1996. Insertion and hairpin formation of membrane proteins: a Monte Carlo study. Biophys. J. **71:**1248–1255.
10. **Bordier, C.** 1981. Phase separation of integral membrane proteins in Triton X-114 solution. J. Biol. Chem. **256:**1604–1607.
11. **Buchholz, U. J., S. Finke, and K. K. Conzelmann.** 1999. Generation of bovine respiratory syncytial virus (BRSV) from cDNA: BRSV NS2 is not essential for virus replication in tissue culture, and the human RSV leader region acts as a functional BRSV genome promoter. J. Virol. **73:**251–259.
12. **Claros, M. G., and G. von Heijne.** 1994. TopPred II: an improved software for membrane protein structure prediction. Comput. Appl. Biosci. (Cambridge) **10:**685–686.
13. **Cross, B. C., and S. High.** 2009. Dissecting the physiological role of selective transmembrane-segment retention at the ER translocon. J. Cell Sci. **122:**1768–1777.
14. **Cserzö, M., E. Wallin, I. Simon, G. von Heijne, and A. Elofsson.** 1997. Prediction of transmembrane a-helices in prokaryotic membrane proteins: the dense alignment surface method. Protein Eng. **10:**673–676.
15. **de Jong, A. S., et al.** 2008. Functional analysis of picornavirus 2B proteins: effects on calcium homeostasis and intracellular protein trafficking. J. Virol. **82:**3782–3790.
16. **de Jong, A. S., W. J. Melchers, D. H. Glaudemans, P. H. Willems, and F. J. van Kuppeveld.** 2004. Mutational analysis of different regions in the coxsackievirus 2B protein: requirements for homo-multimerization, membrane permeabilization, subcellular localization, and virus replication. J. Biol. Chem. **279:**19924–19935.
17. **de Jong, A. S., et al.** 2002. Multimerization reactions of coxsackievirus pro-

teins 2B, 2C and 2BC: a mammalian two-hybrid analysis. J. Gen. Virol. **83:**783–793.
18. **de Jong, A. S., et al.** 2003. Determinants for membrane association and permeabilization of the coxsackievirus 2B protein and the identification of the Golgi complex as the target organelle. J. Biol. Chem. **278:**1012–1021.
19. **Engelman, D. M., and T. A. Steitz.** 1981. The spontaneous insertion of proteins into and across membranes: the helical hairpin hypothesis. Cell **23:**411–422.
20. **Enquist, K., et al.** 2009. Membrane-integration characteristics of two ABC transporters, CFTR and P-glycoprotein. J. Mol. Biol. **387:**1153–1164.
21. **García-Sáez, A. J., I. Mingarro, E. Perez-Paya, and J. Salgado.** 2004. Membrane-insertion fragments of Bcl-xL, Bax, and Bid. Biochemistry **43:**10930–10943.
22. **Gonzalez, M. E., and L. Carrasco.** 2003. Viroporins. FEBS Lett. **552:**28–34.
23. **Hedin, L. E., et al.** 2010. Membrane insertion of marginally hydrophobic transmembrane helices depends on sequence context. J. Mol. Biol. **396:**221–229.
24. **Hessa, T., et al.** 2005. Recognition of transmembrane helices by the endoplasmic reticulum translocon. Nature **433:**377–381.
25. **Hessa, T., et al.** 2007. Molecular code for transmembrane-helix recognition by the Sec61 translocon. Nature **450:**1026–1030.
26. **Hirokawa, T., S. Boon-Chieng, and S. Mitaku.** 1998. SOSUI: classification and secondary structure prediction system for membrane proteins. Bioinformatics **14:**378–379.
27. **Johnson, A. E., and M. A. van Waes.** 1999. The translocon: a dynamic gateway at the ER membrane. Annu. Rev. Cell Dev. Biol. **15:**799–842.
28. **Jones, D. T.** 2007. Improving the accuracy of transmembrane protein topology prediction using evolutionary information. Bioinformatics **23:**538–544.
29. **Krogh, A., B. Larsson, G. von Heijne, and E. L. Sonnhammer.** 2001. Predicting transmembrane protein topology with a hidden Markov model: application to complete genomes. J. Mol. Biol. **305:**567–580.
30. **Luik, P., et al.** 2009. The 3-dimensional structure of a hepatitis C virus p7 ion channel by electron microscopy. Proc. Natl. Acad. Sci. U. S. A. **106:**12712–12716.
31. **Madan, V., A. Castello, and L. Carrasco.** 2008. Viroporins from RNA viruses induce caspase-dependent apoptosis. Cell Microbiol. **10:**437–451.
32. **Madan, V., et al.** 2007. Plasma membrane-porating domain in poliovirus 2B protein. A short peptide mimics viroporin activity. J. Mol. Biol. **374:**951–964.
33. **Martínez-Gil, L., A. E. Johnson, and I. Mingarro.** 2010. Membrane insertion and biogenesis of the Turnip crinkle virus p9 movement protein. J. Virol. **84:**5520–5527.
34. **Martínez-Gil, L., J. Perez-Gil, and I. Mingarro.** 2008. The surfactant peptide KL4 sequence is inserted with a transmembrane orientation into the endoplasmic reticulum membrane. Biophys. J. **95:**L36–L38.
35. **Martínez-Gil, L., et al.** 2009. Plant virus cell-to-cell movement is not dependent on the transmembrane disposition of its movement protein. J. Virol. **83:**5535–5543.
36. **Martínez-Gil, L., A. Sauri, M. A. Marti-Renom, and I. Mingarro.** 2011. Membrane protein integration into the ER. FEBS J. [Epub ahead of print.] doi:10.1111/j.1742-4658.2011.08185.x.
37. **Martínez-Gil, L., A. Sauri, M. Vilar, V. Pallas, and I. Mingarro.** 2007. Membrane insertion and topology of the p7B movement protein of melon necrotic spot virus (MNSV). Virology **367:**348–357.
38. **Monné, M., M. Hermansson, and G. von Heijne.** 1999. A turn propensity scale for transmembrane helices. J. Mol. Biol. **288:**141–145.
39. **Monné, M., I. Nilsson, A. Elofsson, and G. von Heijne.** 1999. Turns in transmembrane helices: determination of the minimal length of a "helical hairpin" and derivation of a fine-grained turn propensity scale. J. Mol. Biol. **293:**807–814.
40. **Nagy, A., and R. J. Turner.** 2007. The membrane integration of a naturally occurring alpha-helical hairpin. Biochem. Biophys. Res. Commun. **356:**392–397.
41. **Navarro, J. A., et al.** 2006. RNA-binding properties and membrane insertion of Melon necrotic spot virus (MNSV) double gene block movement proteins. Virology **356:**57–67.
42. **Nilsson, I., and G. von Heijne.** 1993. Determination of the distance between the oligosaccharyltransferase active site and the endoplasmic reticulum membrane. J. Biol. Chem. **268:**5798–5801.
43. **Nugent, T., and D. T. Jones.** 2009. Transmembrane protein topology prediction using support vector machines. BMC Bioinformatics **10:**159.
44. **Orzáez, M., J. Salgado, A. Gimenez-Giner, E. Perez-Paya, and I. Mingarro.** 2004. Influence of proline residues in transmembrane helix packing. J. Mol. Biol. **335:**631–640.
45. **Patargias, G., T. Barke, A. Watts, and W. B. Fischer.** 2009. Model generation of viral channel forming 2B protein bundles from polio and coxsackie viruses. Mol. Membr. Biol. **26:**309–320.
46. **Rapoport, T. A., V. Goder, S. U. Heinrich, and K. E. Matlack.** 2004. Membrane-protein integration and the role of the translocation channel. Trends Cell Biol. **14:**568–575.
47. **Rost, B., P. Fariselli, and R. Casadio.** 1996. Topology prediction for helical transmembrane proteins at 86% accuracy. Protein Sci. **5:**1704–1718.
48. **Sánchez-Martínez, S., et al.** 2008. Functional and structural characterization of 2B viroporin membranolytic domains. Biochemistry **47:**10731–10739.
49. **Sandoval, I. V., and L. Carrasco.** 1997. Poliovirus infection and expression of the poliovirus protein 2B provoke the disassembly of the Golgi complex, the organelle target for the antipoliovirus drug Ro-090179. J. Virol. **71:**4679–4693.
50. **Saurí, A., P. J. McCormick, A. E. Johnson, and I. Mingarro.** 2007. Sec61alpha and TRAM are sequentially adjacent to a nascent viral membrane protein during its ER integration. J. Mol. Biol. **366:**366–374.
51. **Saurí, A., S. Saksena, J. Salgado, A. E. Johnson, and I. Mingarro.** 2005. Double-spanning plant viral movement protein integration into the endoplasmic reticulum membrane is signal recognition particle-dependent, translocon-mediated, and concerted. J. Biol. Chem. **280:**25907–25912.
52. **Shakin-Eshleman, S. H., S. L. Spitalnik, and L. Kasturi.** 1996. The amino acid at the X position of an Asn-X-ser sequon is an important determinant of N-linked core-glycosylation efficiency. J. Biol. Chem. **271:**6363–6366.
53. **Silberstein, S., and R. Gilmore.** 1996. Biochemistry, molecular biology, and genetics of the oligosaccharyltransferase. FASEB J. **10:**849–858.
54. **Skern, T., et al.** 2002. Structure and function of picornavirus proteinases, p. 199–212. *In* B. L. Semler and E. Wimmer (ed.), Molecular biology of picornaviruses. ASM Press, Washington, DC.
55. **Tamborero, S., M. Vilar, L. Martinez-Gil, A. E. Johnson, and I. Mingarro.** 2011. Membrane insertion and topology of the translocating chain-associating membrane protein (TRAM). J. Mol. Biol. **406:**571–582.
56. **van der Werf, S., J. Bradley, E. Wimmer, F. W. Studier, and J. J. Dunn.** 1986. Synthesis of infectious poliovirus RNA by purified T7 RNA polymerase. Proc. Natl. Acad. Sci. U. S. A. **83:**2330–2334.
57. **van Kuppeveld, F. J., J. M. Galama, J. Zoll, P. J. van den Hurk, and W. J. Melchers.** 1996. Coxsackie B3 virus protein 2B contains cationic amphipathic helix that is required for viral RNA replication. J. Virol. **70:**3876–3886.
58. **van Kuppeveld, F. J., et al.** 1997. Coxsackievirus protein 2B modifies endoplasmic reticulum membrane and plasma membrane permeability and facilitates virus release. EMBO J. **16:**3519–3532.
59. **van Kuppeveld, F. J., W. J. Melchers, P. H. Willems, and T. W. Gadella, Jr.** 2002. Homomultimerization of the coxsackievirus 2B protein in living cells visualized by fluorescence resonance energy transfer microscopy. J. Virol. **76:**9446–9456.
60. **Viklund, H., A. Bernsel, M. Skwark, and A. Elofsson.** 2008. SPOCTOPUS: a combined predictor of signal peptides and membrane protein topology. Bioinformatics **24:**2928–2929.
61. **Vilar, M., et al.** 2002. Insertion and topology of a plant viral movement protein in the endoplasmic reticulum membrane. J. Biol. Chem. **277:**23447–23452.
62. **Wimmer, E., C. U. Hellen, and X. Cao.** 1993. Genetics of poliovirus. Annu. Rev. Genet. **27:**353–436.

OPEN ACCESS Freely available online

PLoS one

Translation without eIF2 Promoted by Poliovirus 2A Protease

Natalia Redondo*, Miguel Angel Sanz, Ewelina Welnowska, Luis Carrasco

Centro de Biología Molecular "Severo Ochoa" (CSIC-UAM), Universidad Autónoma de Madrid, Madrid, Spain

Abstract

Poliovirus RNA utilizes eIF2 for the initiation of translation in cell free systems. Remarkably, we now describe that poliovirus translation takes place at late times of infection when eIF2 is inactivated by phosphorylation. By contrast, translation directed by poliovirus RNA is blocked when eIF2 is inactivated at earlier times. Thus, poliovirus RNA translation exhibits a dual mechanism for the initiation of protein synthesis as regards to the requirement for eIF2. Analysis of individual poliovirus non-structural proteins indicates that the presence of $2A^{pro}$ alone is sufficient to provide eIF2 independence for IRES-driven translation. This effect is not observed with a $2A^{pro}$ variant unable to cleave eIF4G. The level of $2A^{pro}$ synthesized in culture cells is crucial for obtaining eIF2 independence. Expression of the N-or C-terminus fragments of eIF4G did not stimulate IRES-driven translation, nor provide eIF2 independence, consistent with the idea that the presence of $2A^{pro}$ at high concentrations is necessary. The finding that $2A^{pro}$ provides eIF2-independent translation opens a new and unsuspected area of research in the field of picornavirus protein synthesis.

Citation: Redondo N, Sanz MA, Welnowska E, Carrasco L (2011) Translation without eIF2 Promoted by Poliovirus 2A Protease. PLoS ONE 6(10): e25699. doi:10.1371/journal.pone.0025699

Editor: Robert J. Geraghty, University of Minnesota, United States of America

Received July 5, 2011; **Accepted** September 8, 2011; **Published** October 7, 2011

Funding: This study was supported by a DGICYT (Direccion General de Investigacion Cientifica y Tecnica. Ministerio de Educacion y Ciencia. SPAIN) grant (BFU2009-07352). NR and EW are holders of FPI (Formación de Personal Investigador) and FPU (Formación de Profesorado Universitario) fellowships, respectively. The Institutional Grant awarded to the Centro de Biología Molecular "Severo Ochoa" by the Fundación Ramón Areces is acknowledged. The funders had no role in study design, data collection and analysis, decision to publish, or preparation of the manuscript.

Competing Interests: The authors have declared that no competing interests exist.

* E-mail: nsevillano@cbm.uam.es

Introduction

Viral proteases play an important part both in the generation of mature viral proteins and in the modulation of cellular functions [1,2]. Three proteases have been described in different picornavirus species: $2A^{pro}$, L^{pro} and $3C^{pro}$ [3].This last protease, $3C^{pro}$, and its precursor $3CD^{pro}$, are present in all picornavirus species and are responsible for most proteolytic cleavages of the viral polyprotein . The three proteases are capable of cis-autoproteolysis, by which they are excised from the viral polyprotein. It seems reasonable to think that the main purpose of PV $2A^{pro}$ and FMDV L^{pro} is to modify cellular functions. Indeed, both proteases bisect eIF4G at a position close to each other. The cleavage site of PV $2A^{pro}$ on eIF4GI is located between amino acids 681–682 [4]. Bisection of eIF4G takes place soon after PV infection, leading to inhibition of cellular translation, while the bulk of PV proteins is synthesized at late times when virtually all eIF4G has been proteolyzed. Thus, hydrolysis of eIF4G by PV $2A^{pro}$ inhibits the canonical mechanism of translation, which is cap-dependent and promotes a non-canonical mechanism in which eIF4E and cap recognition are not necessary [4]. Apart from this cleavage, PV $2A^{pro}$ can hydrolyze other cellular proteins, although the exact degradome for this protease has still not been defined. Some of these hydrolytic events associated with PV $2A^{pro}$ involve the proteolysis of nucleoporins, thereby altering RNA and protein trafficking between nucleus and cytoplasm [4]. Therefore, PV $2A^{pro}$ blocks cap-dependent translation upon eIF4G cleavage and interferes with mRNA export to the cytoplasm; both events abolish cellular gene expression and abrogate cellular responses to viral infection.

The translation initiation factor eIF4G is a large polypeptide which can interact with several cellular and viral proteins. Two forms of eIF4G encoded by two different genes are known, eIF4GI and eIF4GII [5]. The exact functioning of each of these two forms in the process of translation remains unclear, although it has been suggested that these forms are functionally interchangeable. Three regions have been distinguished in eIF4G, each of which harbours the interaction sites with several cellular proteins. Binding of eIF4E and eIF4A to eIF4G gives rise to the formation of the eIF4F complex [6,7]. Interaction of eIF4F with mRNA may take place directly or indirectly. Thus, eIF4E directly binds to the cap structure present at the 5′ end of mRNAs, while eIF4A unwinds the secondary structure of the mRNA leader sequence. In addition, eIF4G itself interacts with picornavirus IRESs by means of its central domain [8,9,10]. Apart from these direct interactions of the eIF4F complex with mRNAs, eIF4G also interacts with eIF3 and PABP, both of which also can directly bind to mRNA. Joining of the eIF4F complex to the 40S ribosomal subunit is mediated by the interaction between eIF4G and eIF3. Therefore, during the initiation of translation, eIF4G plays a pivotal role as a scaffolding molecule organizing the architecture of different initiation factors, mRNA and the preinitiation complex [6,7]. The central role of eIF4G in mRNA translation makes it a key target for a variety of animal viruses. Indeed, modulation of eIF4G activity by viral proteins may be essential for cytopathic viruses to control translation. Calicivirus as well as some picornavirus and retrovirus species encode proteases that hydrolyze eIF4G during infection [4,11,12,13]. Alternatively, a number of viral proteins are able to interact with eIF4G, modulating its activity. This is the case of

rotavirus NSP3 [14], influenza virus NS1 and PB2 [15,16] and adenovirus 100 K protein [17]. Cleavage of eIF4G by picornavirus proteases $2A^{pro}$ or L^{pro} leads to the stimulation of IRES-driven translation [4]. Pestova and colaborators demonstrated that the central domain of eIF4G together with eIF4A interacts with EMCV IRES and promotes the formation of the preinitiation complex [18,19]. Consistent with this finding, the C-terminal fragment or even the core domain of eIF4G suffices to promote IRES-driven translation both in vivo and in cell free systems [20,21].

eIF4F activity is regulated in eukaryotic cells by extra- and intracellular signals through phosphorylation [4]. eIF4E activity is also controlled by phosphorylation by the protein kinase Mnk1 or by interaction with eIF4G, which is modulated by eIF4E binding proteins (4E-BPs) [7]. Phosphorylation also represents the most important mechanism to regulate eIF2 activity. Factor eIF2 is composed of three subunits, known as α, β and γ [6,22]. Several kinases target eIF2α leading to phosphorylation of Ser-51 residue. The function of eIF2 is to bind Met-$tRNA_i$ and GTP to form the ternary complex Met-$tRNA_i$-eIF2-GTP, which interacts with the 40S ribosomal subunit, establishing the interaction between the initiator AUG codon with the anticodon present in Met-$tRNA_i$ [6,7]. The hydrolysis of eIF2-bound GTP is promoted by eIF5, while the eIF5B–GTP complex facilitates recruitment of the 60S subunit to the 48S initiation complex. This joining promotes that the translation initiation factors except for eIF5B–GTP and eIF1A are displaced. The eIF2-GDP complex is recycled to eIF2-GTP by the activity of the recycling factor eIF2B. Phosphorylation of eIF2α impairs the GDP-GTP recycling catalyzed by eIF2B. Therefore, the ternary complex Met-$tRNA_i$ -eIF2-GTP is not generated and thus, binding of this complex to the 40S ribosome is hampered. Even partial phosphorylation of eIF2 can lead to substantial abrogation of translation. Some reports suggested that this factor remained unphosphorylated after poliovirus (PV) infection [23,24], while other workers found substantial eIF2 phosphorylation under the same conditions after PV infection, particularly at late times [25,26]. Of interest, Protein Kinase R (PKR) becomes highly activated, yet it is hydrolyzed in PV-infected cells although this hydrolysis is not directly executed by any of the PV proteases (2A or 3C) [25,26,27]. All these findings pointed to the idea that active eIF2 was necessary to sustain picornavirus translation. In contrast to this idea, we described recently that several picornaviruses do not require active eIF2 at late times of infection [28], similar findings have been reported for PV-infected cells [29]. In the present work we provide evidence that cleavage of eIF4G by PV $2A^{pro}$ in mammalian cells modifies the requirement for eIF2 in translation directed by picornavirus IRESs. Thus, cleavage of eIF4G by PV $2A^{pro}$ establishes a mechanism for IRES-driven translation that is cap- and eIF2 independent. These unexpected findings indicate that PV $2A^{pro}$ induces eIF2 independence IRES-driven translation by a mechanism that is still unknown.

Results

Dual mode for translation of PV RNA

Some viral mRNAs, when they are translated in virus-infected cells, have different requirements for eIFs as compared to cell-free systems or transfected cells [30,31]. This is the case of Sindbis virus 26S mRNA, which does not require intact eIF4G [32] or active eIF2 [33] for translation in the infected cells, whereas these eIFs are necessary to initiate protein synthesis on this viral mRNA in cell-free systems [31]. Although it is generally accepted that picornavirus RNA needs eIF2 to initiate translation, there is some evidence that this factor can be phosphorylated at late times of infection [26,34]. Indeed, recently we found that several picornaviruses exhibit this dual mode for translation of the viral mRNA [28]. So we hypothesized that this factor might be dispensable at late times in the PV life cycle, when the bulk of viral proteins are being synthesized. To test this possibility, eIF2 was inactivated by treating culture cells with Ars to induce phosphorylation of eIF2α. This compound induces oxidative stressand has been widely used to inactivate eIF2 [35,36,37]. A PV replicon (pRLuc31) containing the luciferase (luc) gene replacing the viral structural proteins was used [38]. As controls, cells were also electroporated with Cap-luc or CrPV IGR-luc mRNAs [28,29] and at 1 hpe cells were treated with different concentrations of Ars (0, 50, 100 and 200 μM) for 1 h. Electroporation of these RNAs into BHK-21 cells gives rise to luc synthesis from the beginning of transfection. This early luc synthesis was produced by translation of the input RNA and was drastically blocked by Ars treatment in the case of PV replicon to an extent similar to that found with a capped mRNA whereas CrPV IGR-luc was inhibited by only 20% (Figure 1A). At 7 hours post transfection (hpt), PV proteins can be detected by radioactive labelling because cellular protein synthesis is abrogated. Notably, Ars treatment has little inhibitory effect on the translation of PV RNA, whereas translation of cellular mRNAs was blocked by about 90% under the same conditions (Figure 1B). It should be noted that Ars interferes with the cleavage of the PV polyprotein as already observed [28,29]. Certainly, Ars treatment led to eIF2α phosphorylation, both in control and in PV RNA transfected cells. Of interest was that phosphorylation of eIF2α was also found in PV-replicating cells in the absence of Ars (Figure 1C, middle panel). In addition, cleavage of eIF4G was progressively observed along the PV replication cycle (Figure S1B, upper panel). Analysis of eIF2α phosphorylation throughout the time course of PV replication provides evidence that this factor became phosphorylated at times when PV protein synthesis was maximal and eIF4G had been cleaved (Figure S1A). These findings demonstrate that PV RNA exhibits a dual mechanism for the initiation of translation as regards the participation of eIF2. At early times, before viral RNA replication has occurred, active eIF2 is required to translate PV RNA, whereas this factor is dispensable at late times when massive production of viral proteins is taking place.

Analysis of PV non-structural proteins that confer eIF2 independence for viral RNA translation

Since the PV replicon tested above only encodes PV non-structural proteins in addition to luc, we reasoned that perhaps extensive individual expression of each PV non-structural protein might establish conditions similar to those observed during PV replication. Under these conditions of high PV protein synthesis, active eIF2 might not be necessary to translate PV RNA. Moreover, it may be that synthesis of a single PV protein was able to confer eIF2-independence for IRES-driven translation. To test this possibility, the system used was the BHKT7 cell line, which stably expresses T7 RNA polymerase. Although this polymerase is devoid of capping activity, transfection of plasmids encoding different PV non-structural proteins under the control of a T7 promoter gives rise to extensive translation of mRNAs bearing a picornavirus IRES sequence. The different pTM1 constructs encoding for each PV non-structural protein were transfected into BHKT7 cells and the synthesis of PV proteins was analyzed by radioactive labelling in presence or absence of Ars (Figure 2A), as well as by western blot (Figure 2B). As shown in Figure 2A, all PV proteins can be clearly detected by radioactive

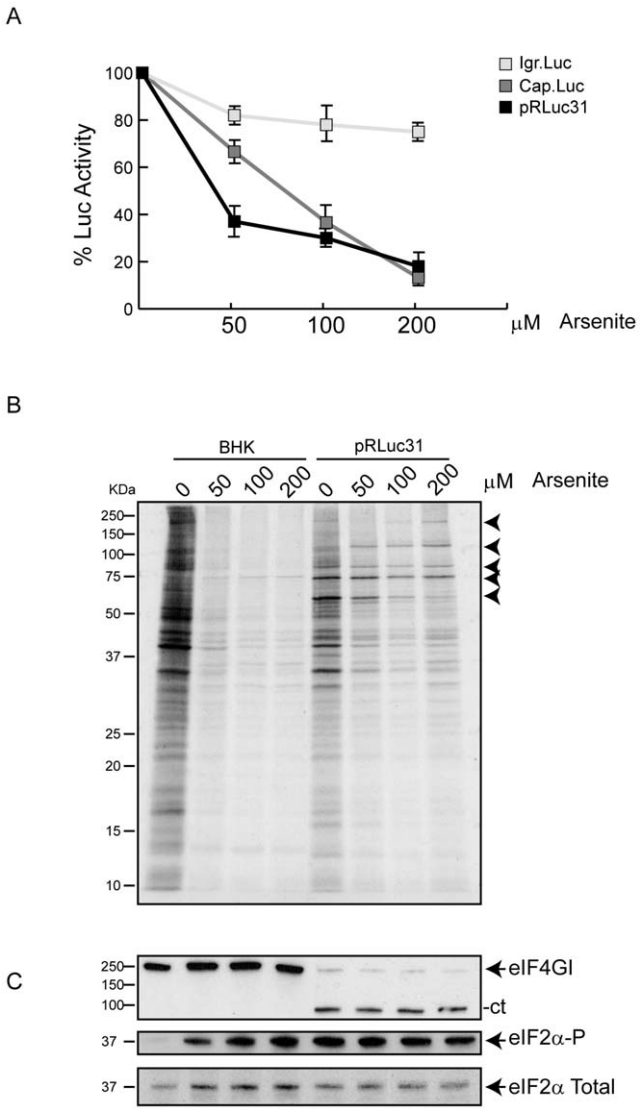

Figure 1. Effect of eIF2 phosphorylation induced by Ars on PV protein synthesis. A) Cap-luc, PV replicon-luc or CrPV IGR-luc mRNAs synthesized *in vitro* by T7 RNA polymerase were electroporated in BHK-21 cells and seeded in DMEM (10% FCS). Different amounts of Ars (0, 50, 100 and 200 μM) were added and cells were incubated for 60 min before harvesting to analyze luc. Error bars indicate standard deviations (SD) obtained from three measurements of each sample. B) BHK-21 cells were electroporated with RNA of PV replicon. At 7 hpe cells were treated with different concentrations of Ars and labelled with [^{35}S]Met/Cys for 45 minutes. Samples were analyzed by SDS-PAGE (17.5%) followed by fluorography and autoradiography. Arrows indicate viral proteins. C) eIF4GI, eIF2α and phosphorylated eIF2α were detected by western blot.
doi:10.1371/journal.pone.0025699.g001

labelling in absence of Ars. Strikingly, PV 2A^{pro} is extensively synthesized even in the presence of Ars, when eIF2α has become phosphorylated. Thus, Ars inhibited cellular translation more than 90%, whereas the synthesis of PV 2A^{pro} was blocked by only 35% (Figure 2C). The inhibition of the other PV non-structural proteins by Ars treatment was around 80% (Figure 2C) and in some cases such as 2B, 3A and 3C their synthesis was almost undetectable (Figure 2A). Therefore, the expression of one individual PV protein, 2A^{pro}, can confer independence from active eIF2 for picornavirus–IRES-driven translation.

Translation of mRNAs containing different picornavirus IRESs in the presence of 2A^{pro}: Requirement for active eIF2α

Our next goal was to assess whether PV 2A^{pro} was able to confer eIF2 independence *in trans* for the translation of other mRNAs bearing a picornavirus IRES. To this end, the synthesis of luc directed by EMCV-, PV- and HAV-IRES was tested in the presence or absence of Ars, when culture cells did or did not co-express PV 2A^{pro}. The synthesis of this protease in culture cells rescues the inhibition of Ars by about 70% when EMCV or PV IRESs are tested (Figure 3A). Notably, translation driven by HAV IRES is abolished when co-expressed with PV 2A^{pro} in presence or absence of Ars. These results agree well with previous studies indicating that HAV IRES requires the intact form of eIF4F for functionality [39,40,41]. Similar results were obtained in the human hepatoma Huh7-T7 cell line (Figure S2). Therefore, translation of luc mRNA bearing different picornavirus IRESs is hampered when eIF2α phosphorylation is induced by Ars. Of interest, PV 2A^{pro} is able to confer translatability to EMCV and PV IRESs, but not to HAV IRES under these conditions.

In addition to Ars, there are other treatments for inducing phosphorylation of eIF2α, such as incubation of culture cells with hypertonic medium or Thapsigargin (Tg) [30,42]. To assay the effect of these treatments on IRES-directed translation, BHKT7 cells were transfected with pTM1-luc, pTM1-2A or co-transfected with pTM1-luc and pTM1-2A. Extensive inhibition of cellular translation was observed when cells were treated either with Ars, hypertonic medium or both (Figure 4A). Inhibition of luc synthesis also occurs when pTM1-luc is transfected alone. However, when PV 2A^{pro} is synthesized under these conditions, significant levels of IRES-2A translation are detected (Figure 4A). Hypertonic medium promotes eIF2α phosphorylation, particularly when combined with Ars (Figure 4B). A similar conclusion can be drawn when cells are transfected with pTM1-2A and treated with Tg (Figure 4C) or with dithiothreitol (results not shown). These findings support the idea that translation of IRES-2A mRNA is resistant to different compounds and treatments that induce phosphorylation of eIF2α when high levels of PV 2A^{pro} are synthesized.

PV infection induces partial PKR degradation, as well as its phosphorylation which correlates with increased eIF2α phosphorylation as infection progresses. To test whether PV 2A^{pro} expression diminished the amount of PKR in our culture cells, a western blot analysis was carried out using specific antibodies against PKR. The levels of this enzyme were similar in cells that either did or did not express PV 2A^{pro} (Figure S3).

Proteolytic activity of PV 2A^{pro} is necessary to confer eIF2 independence

Next, we wished to examine the effect of eIF2 phosphorylation on IRES-driven translation when eIF4G remained uncleaved. To this end, a PV 2A^{pro} variant bearing a point mutation (G60R) devoid of eIF4G cleavage activity [43,44] was employed. In this case, plasmid pTM1-2C was co-transfected with pTM1-2A or pTM1-2A (G60R). As a control, the same constructs were expressed alone. PV 2A^{pro} and 2C synthesis were analyzed both in the presence or absence of Ars. Cellular translation was abolished by Ars, as well as the synthesis of PV 2C and PV 2A (G60R) (Figure 5A). By contrast, PV proteins 2C and 2A^{pro} are still synthesized in presence of Ars, when PV 2A^{pro} is expressed alone or when PV 2C is co-expressed with PV 2A^{pro}. The labelled proteins separated by SDS-PAGE were quantified by densitometric analyses (Figure 5C). Synthesis of PV 2C was inhibited by only 30–35% in presence of Ars and PV 2A^{pro}, while this inhibition was

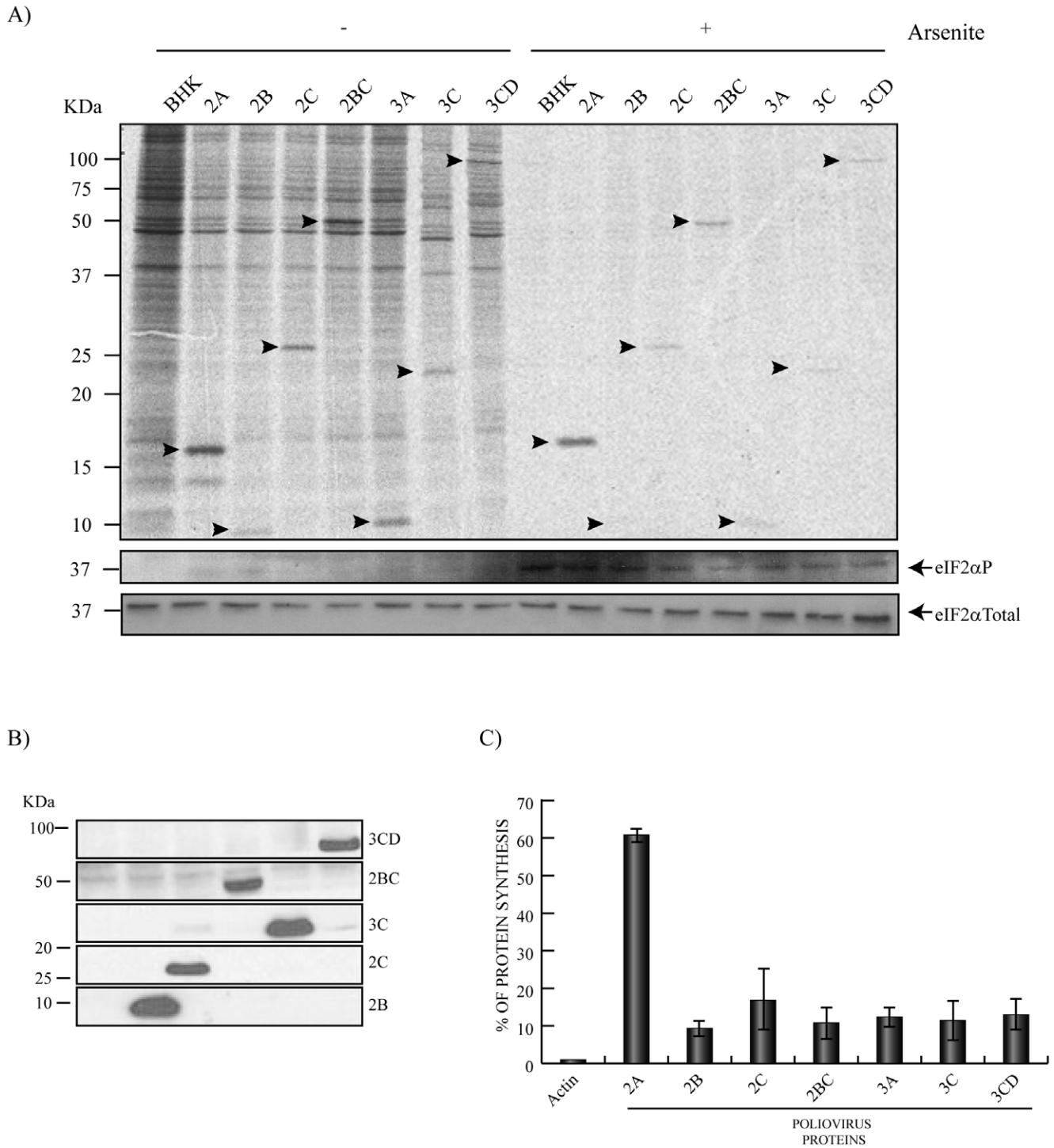

Figure 2. Individual expression of PV non structural proteins. Action of eIF2 phosphorylation. BHKT7 cells were transfected with pTM1 plasmids encoding different PV non-structural proteins and were(+) or were not(−) treated with Ars. A) After 2 hpt cells were pre-treated with 200 μM Ars for 15 minutes and then labelled with [^{35}S]Met/Cys for 45 minutes in presence of the inhibitor. Then, samples were processed by SDS-PAGE (17.5%), fluorography and autoradiography. Western blot of total eIF2α and phosphorylated eIF2α using the same samples is shown at the bottom of this panel. B) PV non-structural proteins were detected by western-blot. C) The percentage of actin (*) and each PV protein synthesis was estimated by densitometric scanning of the corresponding band (arrows) from three independent experiments. Error bars indicate SD.
doi:10.1371/journal.pone.0025699.g002

of 85–90% when 2A^{pro} (G60R) was present (Figure 5C, lower graphs). This result indicates that the presence of high levels of 2A^{pro} in the absence of eIF4G cleavage does not induce eIF2 independence for IRES-directed translation.

Another approach to abolishing eIF4G cleavage is to use PV 2A^{pro} inhibitors. Addition of methoxysuccinyl-Ala-Ala-Pro-Val-chloromethylketone (MPCMK) strongly blocks cleavage of eIF4G [45] even when high levels of PV 2A^{pro} are synthesized in BHKT7

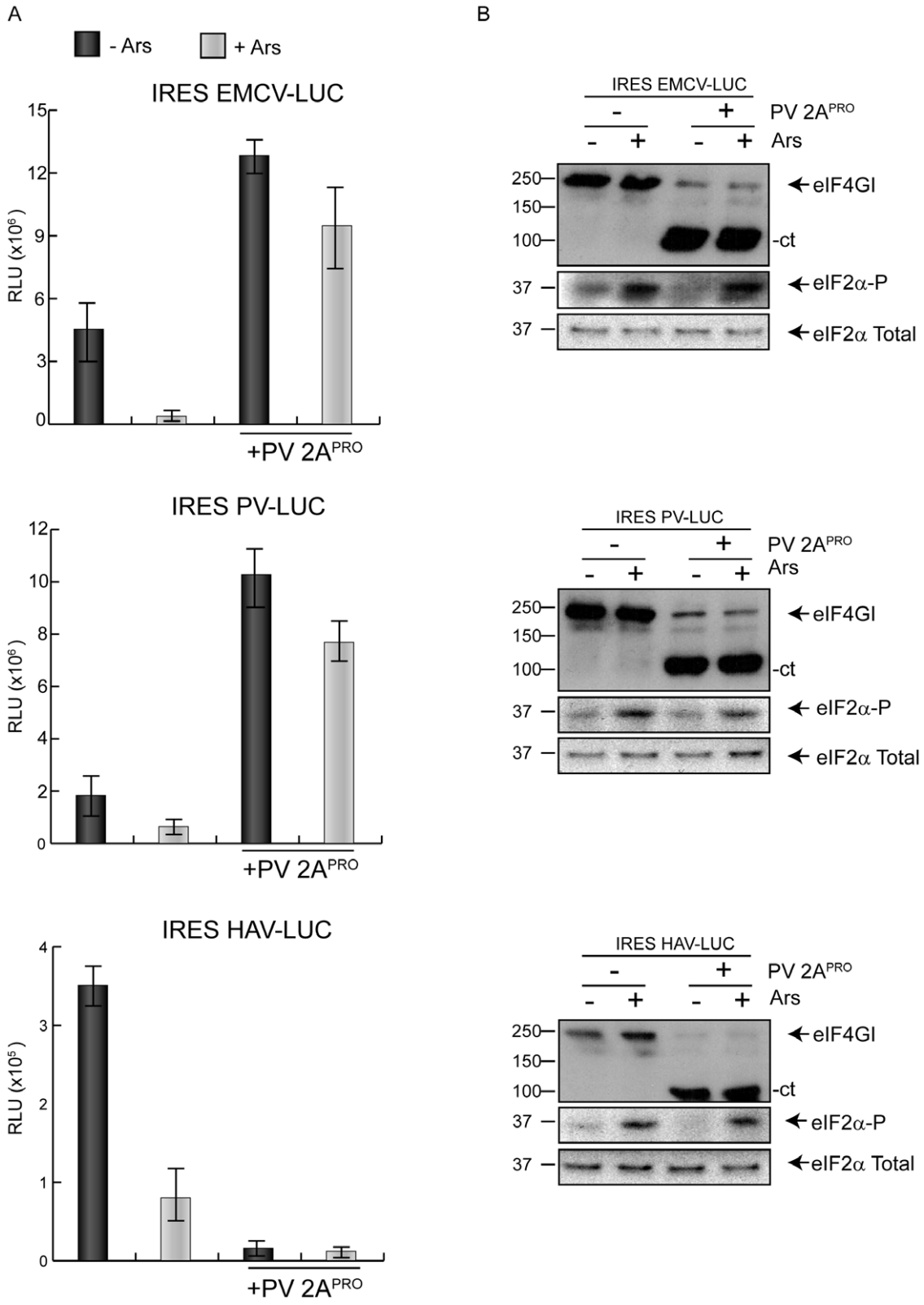

Figure 3. Inhibition of translation directed by PV or EMCV IRES by Ars. Rescue by PV $2A^{pro}$. A) BHKT7 cells were transfected with plasmids containing EMCV IRES-luc, PV IRES-luc or HAV IRES-luc alone or co-transfected with pTM1-2A. At 2 hpt cells were treated or not with Ars for 1 hour. Then, cells were harvested and lysated in luciferase buffer and luc activity was measured (as described in Materials and Methods) and represented from at least three independent experiments. Error bars indicate standard deviation (SD). B) eIF4GI, eIF2α and phosphorylated eIF2α were detected by western blot.

doi:10.1371/journal.pone.0025699.g003

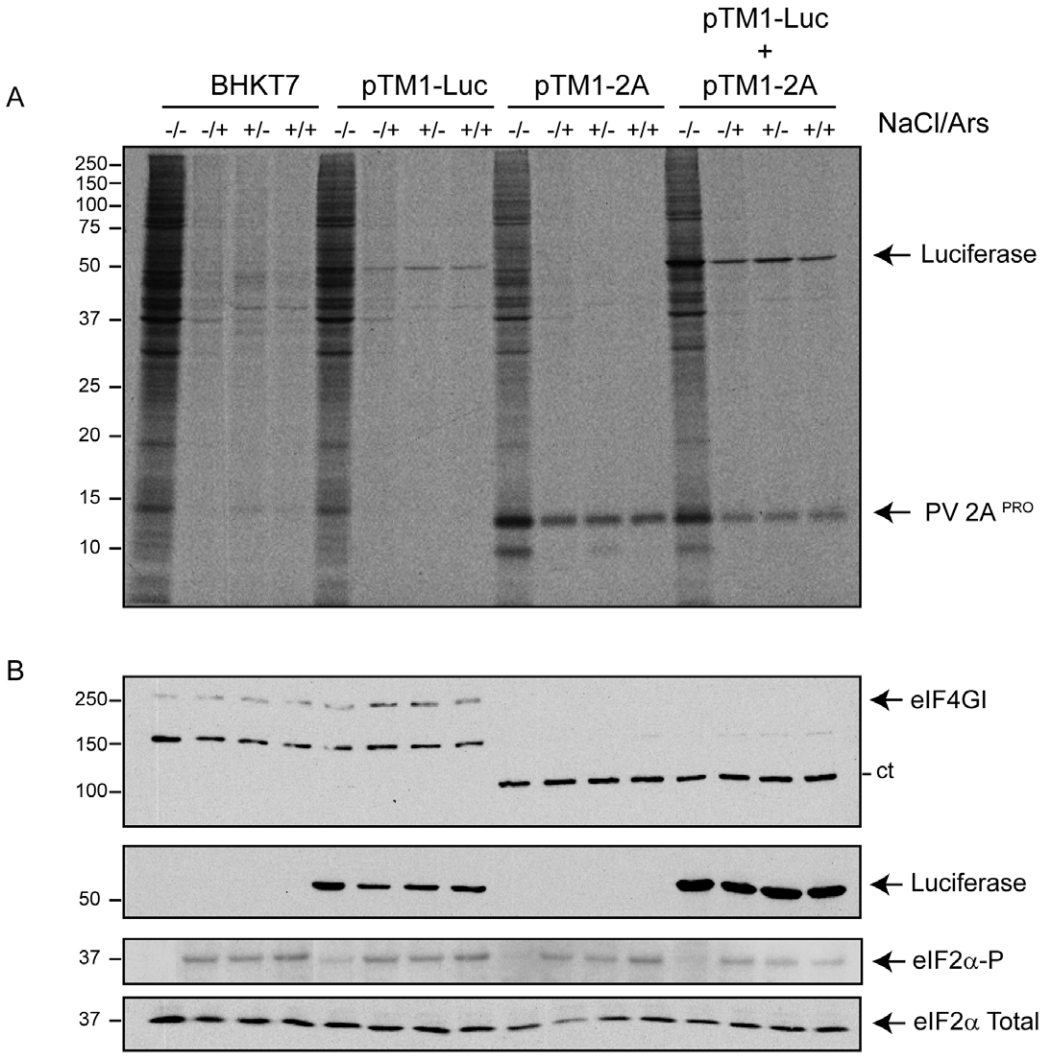
A
BHKT7
pTM1-Luc
pTM1-2A
pTM1-Luc + pTM1-2A
-/- -/+ +/- +/+
NaCl/Ars
250
150
100
75
50
37
25
20
15
10
Luciferase
PV 2A PRO
B
eIF4GI
ct
Luciferase
eIF2α-P
eIF2α Total
C
BHKT7
pTM1-2A
Thapsigargin 2 μM
NaCl 120 μM
PV 2A PRO
100 64 55 47 % PV 2A PRO SYNTHESIS
100 30 0 0
100 21 0 0 % CELLULAR SYNTHESIS
eIF2α-P
eIF2α Total

Figure 4. Effect of different inducers of eIF2α phosphorylation on IRES-driven translation. A) BHKT7 cells were transfected with pTM1-luc, pTM1-2A or both. At 2 hpt cells were pretreated with Ars(−/+), NaCl(+/−) or both(+/+) for 15 minutes and then labelled with [^{35}S]Met/Cys for 45 minutes in presence of the inhibitors. After labelling, the proteins were analyzed by SDS-PAGE(17.5%), fluorography and autoradiography. B) Western blot analysis of samples from panel A using anti-eIF4GI, anti-Luc, anti-phosphorylated eIF2α and anti-total eIF2 antibodies. C) Cells were mock transfected or transfected with pTM1-2A. At 2 hpt cells were pretreated with 1 μM Tg or additional 120 mM NaCl or both for 15 minutes and then were labelled with [^{35}S]Met/Cys for 45 minutes in presence of the inhibitors. After labelling, proteins were analyzed by SDS-PAGE, fluorography and autoradiography. Numbers below each lane indicate the percentage of cell protein (*) and PV 2A^{pro} synthesis in cells treated with inhibitor compared with untreated cells quantified by densitometry of the corresponding bands. A western blot using antibodies against eIF2α and phosphorylated eIF2α was performed.
doi:10.1371/journal.pone.0025699.g004

cells. The presence of this 2A^{pro} inhibitor abolishes eIF2 independence for translation of picornavirus IRES (see below). In conclusion, cleavage of eIF4G (together with other putative cellular protein (s)) accomplished by active 2A^{pro} is necessary for this phenomenon.

Cleavage of eIF4G is not sufficient to provide eIF2-independent translation

The only known direct effect of PV 2A^{pro} on translation is that this protease cleaves eIF4G, leading to stimulation of picornavirus RNA translation [8]. Thus, it is possible that eIF2-independent translation is the consequence of the generation of the two eIF4G fragments after bisection by PV 2A^{pro}. Alternatively, it is possible that in addition to eIF4G, other host proteins could be hydrolyzed by this protease providing eIF2-independent translation. Moreover, the presence of PV 2A^{pro} itself could be necessary, and in this scenario 2A might play an IRES trans-acting role. To distinguish between these possibilities different experiments were conducted. Initially, we tested the effect of Ars on EMCV IRES-driven translation in the presence of low or high levels of PV 2A^{pro}. Low amounts of this protease are produced in cells when in vitro synthesized IRES-2A mRNA is transfected [46], whereas high levels of 2A^{pro} are found in culture cells using the system described in this work. Under both conditions, eIF4G becomes extensively cleaved. Addition of Ars to cell cultures transfected with IRES 2A mRNA and later with plasmid encoding IRES-luc (pTM1-luc) profoundly blocked translation, irrespective of whether or not PV 2A^{pro} was present (Figure 5D). Under those conditions, eIF4G was almost totally cleaved and both eIF4G fragments were present (Figure 5E), but the levels of 2A^{pro} are low and do not confer eIF2-independence. By contrast, when high amounts of PV 2A^{pro} are synthesized in BHKT7 cells, Ars has little inhibitory effect on EMCV IRES-driven translation. These findings support the notion that the presence of eIF4G fragments (or the cleavage of other cellular proteins) is necessary but not sufficient to confer eIF2 independence for picornavirus IRES-driven translation.

To provide further support for this conclusion, the two eIF4G fragments generated by PV 2A^{pro} cleavage were synthesized in BHKT7 cells by transfection of the corresponding pTM1 plasmids. These two fragments correspond to the cleavage products of eIF4G accomplished by PV 2A^{pro}. The synthesis of each fragment was detected by immunoblotting (Figure 6B). Synthesis of luc from EMCV -luc was sensitive to Ars even when cells expressed either of the eIF4G fragments (Figure 6A). A densitometric analysis of the corresponding products synthesized is represented in Figure 6C. The inhibition of luc synthesis by Ars is around 40% when PV 2A^{pro} is present but is greater than 80% when luc is expressed either alone or with the N-terminal or C-terminal fragments of eIF4GI. In conclusion, the idea that the C-terminus fragment of eIF4GI interacts with EMCV IRES thereby allowing mRNA to be translated without eIF2 is not supported by these results. In fact, we demonstrate that high levels of PV 2A^{pro} must be present to translate picornavirus RNA when eIF2α is phosphorylated.

In addition, we tested whether the presence of high levels of both the inactive mutant 2A G60R and the carboxy fragment of eIF4G can switch translation to an eIF2-independent mode. When PV 2A^{pro} is or is not synthesized together with the C-fragment of eIF4GI, Ars has little effect on translation driven by EMCV IRES (Figure 6D). In fact, the synthesis of the C-terminal fragment of eIF4G is stimulated when co-expressed with PV 2A^{pro}. The percentage of luc synthesis is about 70% in presence of Ars when is co-expressed with PV 2A^{pro} with or without the eIF4GI C terminal fragment (Figure 6F). However, luc synthesis is notably diminished by Ars to around 20% when luc is synthesized either with PV 2A (G60R) alone or with PV 2A (G60R) together with the C-terminal fragment of eIF4GI. These observations indicate that to achieve resistance to eIF2 phosphorylation, both the cleavage of eIF4G (or other cellular protein (s)) and the synthesis of high levels of active PV 2A^{pro} are necessary.

Two possibilities can be envisaged to account for the above findings. One is that PV 2A^{pro} cleaves a putative cellular protein other than eIF4G when present at high levels. This putative cleavage would be necessary to confer eIF2 independence. Another possibility is that active 2A^{pro} must be present to observe this phenomenon. To distinguish between these two possibilities, cells were transfected with pTM1-2A and after 1 h of incubation, when eIF4G and other putative cellular proteins had been cleaved, pTM1-luc was transfected in the presence or absence of MPCMK, which is an inhibitor of the proteolytic activity of 2A^{pro} (Figure 7A) . Addition of this inhibitor, even after PV 2A^{pro} has exerted its proteolytic activity renders IRES-driven translation dependent on active eIF2 (Figure 7B). These findings therefore demonstrate that cleavage of other putative cellular protein is not involved in this phenomenon. In conclusion, both cleavage of eIF4G and active PV 2A^{pro} are required to render IRES driven translation independent of eIF2.

Discussion

Progressive inactivation of eIF2 by phosphorylation takes place upon infection of culture cells with some PV variants and other picornaviruses [24,26,34]. This eIF2 inactivation was previously thought to play a role in the abrogation of cellular and viral protein synthesis at late times of infection, since the prevailing idea was that picornavirus RNA translation needs active eIF2. Our present data demonstrate that significant phosphorylation of eIF2α is found in PV-replicating cells from about 3 hpi. Moreover, induction of substantial eIF2 phosphorylation by Ars has little effect on PV protein synthesis, while cellular translation is drastically abolished under these conditions. Our present results are in good agreement with recent findings indicating that several picornaviruses, including PV, can translate their mRNA when eIF2α is phosphorylated at late times of infection [28,29]. The claim that cleavage of eIF5B by PV 3C^{pro} as responsible for eIF2-independent translation [29] is not supported by our results illustrating that upon the individual expression of each PV protein only 2A^{pro} is endowed with this activity. If this is so, the

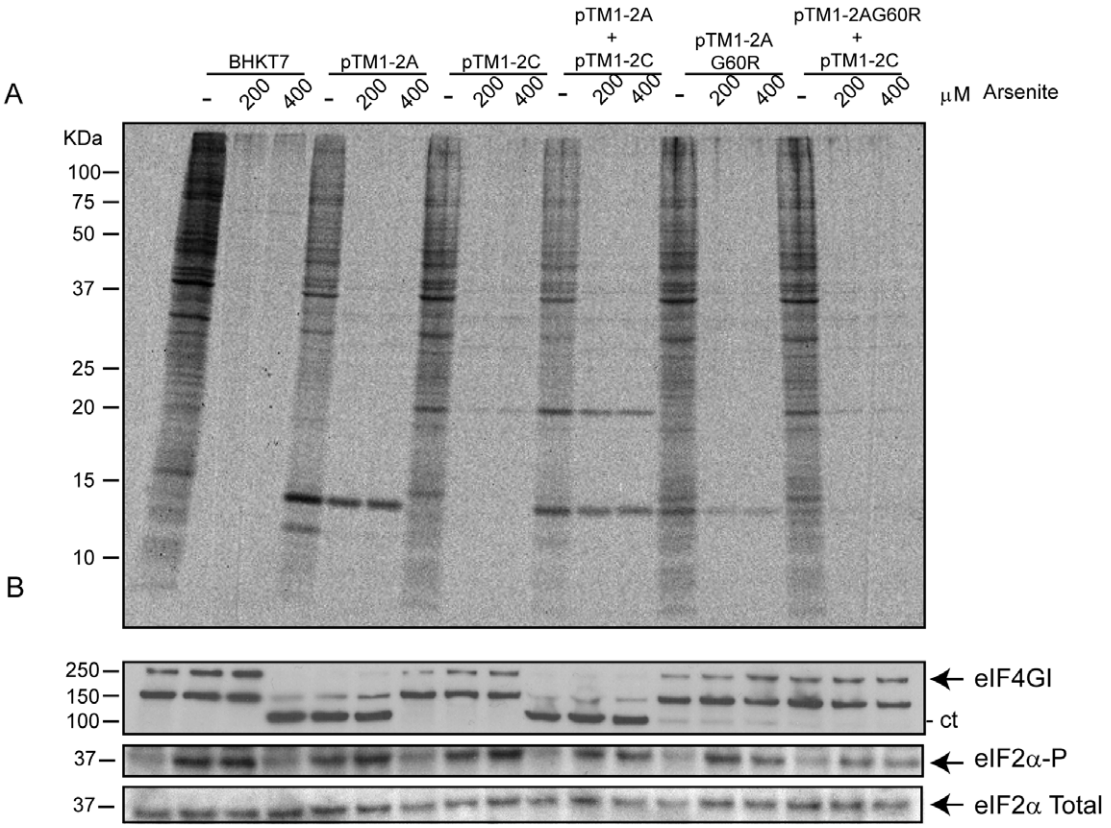
A
BHKT7
pTM1-2A
pTM1-2C
pTM1-2A + pTM1-2C
pTM1-2A G60R
pTM1-2AG60R + pTM1-2C
- 200 400
μM Arsenite
KDa
100
75
50
37
25
20
15
10
B
250
150
100
eIF4GI
ct
37
eIF2α-P
37
eIF2α Total

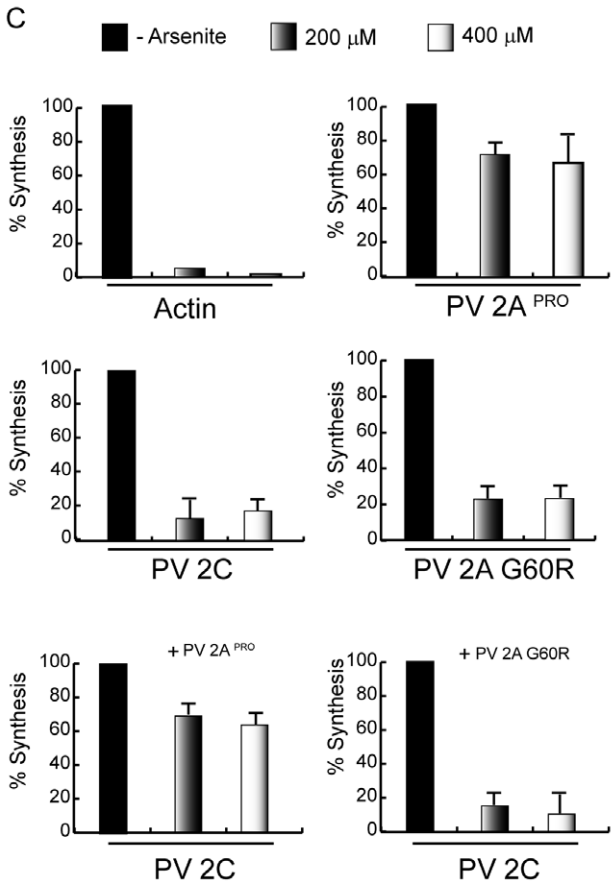
C
- Arsenite
200 μM
400 μM
% Synthesis
Actin
PV 2A PRO
PV 2C
PV 2A G60R
+ PV 2A PRO
+ PV 2A G60R

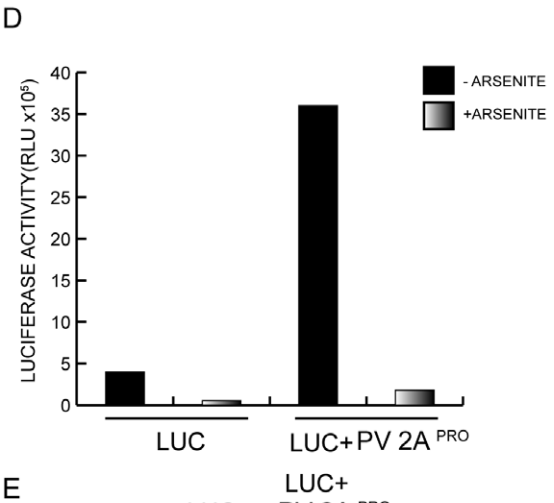
D
- ARSENITE
+ARSENITE
LUCIFERASE ACTIVITY(RLU x10⁵)
LUC
LUC+ PV 2A PRO

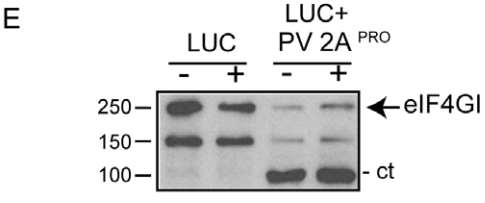
E
LUC
LUC+ PV 2A PRO
- + - +
250
150
100
eIF4GI
ct

Figure 5. Proteolytic activity is necessary for eIF2α independent translation. BHKT7 cells were transfected or co-transfected with either pTM1-2A or pTM1-2A G60R, which encodes for an inactive $2A^{pro}$, and pTM1-2C. A) At 2 hpt cells were treated with different Ars concentrations and incubated with [^{35}S]Met/Cys for 45 minutes. Samples were analyzed by SDS-PAGE (17.5%), fluorography and autoradiography. B) eIF4GI, phosphorylated eIF2α and total eIF2α of the same samples were detected by western blot. C) The percentage of cellular and viral protein synthesis, measured by densitometric scanning of the corresponding band from at least three independent experiments, is shown. Upper panels show the synthesis of actin (representing cellular protein synthesis), 2A wt, 2C and 2A G60R when they are expressed by separate. Lower panels show the synthesis of PV 2C protein alone, either in presence of 2A wt or in presence of 2A G60R. All data are shown as the mean ±SD of at least three independent experiments. D) BHKT7 cells were first transfected with IRES-2A mRNA. After 2 hpt, cell monolayers were washed and incubated in fresh medium (DMEM plus 5% FCS) for 1 h to accomplish the cleavage of eIF4G. Then, pTM1-luc was transfected during 2 h, afterwards transfection medium was removed and cells were incubated in fresh medium and after 15 minutes were treated or not with 200 μM Ars during 1 h . Finally, cell monolayers were harvested in luciferase buffer and luc activity was measured and represented. E) Cleavage of eIF4GI of the samples used in panel D was detected by western blot.
doi:10.1371/journal.pone.0025699.g005

mechanism of picornavirus RNA translation may be more similar to the situation reported for flaviviruses, since translation of their viral RNAs may not use eIF2, when this factor is absent [36,47,48]. We also have demonstrated that the individual expression of PV $2A^{pro}$, but not other PV non-structural proteins, is sufficient to render picornavirus IRES-driven translation independent for active eIF2. This effect is observed both in *cis* and in *trans* on mRNAs bearing picornavirus IRES elements. These mRNAs are little affected upon phosphorylation of eIF2 induced by different inhibitors when high levels of PV $2A^{pro}$ are synthesized.

PV $2A^{pro}$ is a multifunctional protease that targets a number of cellular processes, including translation [4,49]. Indeed, this viral protease bisects eIF4G thereby disrupting cap-dependent translation of the vast majority of cellular mRNAs. By contrast, this modification of eIF4G enhances PV protein synthesis [8]. Most evidence indicated that simple cleavage of eIF4G is not sufficient for this stimulation [21,50]. Indirect evidence points to a direct activity of $2A^{pro}$ in PV RNA translation [49,51], thus the actual presence of $2A^{pro}$ together with cellular protein cleavage would be necessary to stimulate IRES-driven translation. The C-terminal fragment of eIF4G is able to replace the entire factor in cell free systems [18]. However, overexpression of this fragment in intact cells does not stimulate picornavirus IRES-driven translation [21,50,52]. Consistent with these findings, our present observations indicate that the expression of either the N-or C-terminus fragments of eIF4G in our system does not stimulate translation directed by EMCV IRES. Our findings support the concept that for eIF2 independence during initiation of IRES-containing mRNAs, both cellular protein cleavage and the presence of high levels of PV $2A^{pro}$ are necessary.

It is most striking that after several decades of studies on the mechanism of picornavirus translation, the possibility that eIF2 may not participate in this process has not been uncovered. It is generally thought that translation on picornavirus RNA requires active eIF2 [22]. This mechanism has been supported by many studies using cell free systems. However, to our knowledge the idea that eIF2 might not participate in the initiation of translation of PV RNA in the infected cells has not been investigated. Notably, PV translation is blocked by Ars during the early period of infection, supporting the notion that PV RNA exhibits a dual mode for its translation, as occurs for instance with Sindbis virus 26S mRNA [31]. Therefore, PV RNA may follow two different mechanisms for the initiation of translation: one canonical mechanism using entire eIF4G and eIF2 early during infection and another mechanism at the late phase of the virus life cycle. This last mechanism does not require intact eIF4G or active eIF2. Remarkably, the presence of PV $2A^{pro}$ alone suffices to provide independence from active eIF2.

The new and unsuspected findings that the translation of mRNAs bearing picornavirus IRESs takes place when eIF2 has been inactivated by phosphorylation open a future area for research in the field of picornavirus translation. In addition, the fact that PV $2A^{pro}$ can switch picornavirus RNA translation from an eIF2 dependent mechanism to a different mode of initiation establishes the first molecular basis for this phenomenon. Future work will target the elucidation of potential cellular proteins or factors that can replace eIF2 during picornavirus RNA translation. It is even possible that in the infected cells or in the presence of PV $2A^{pro}$ the IRES structure is sufficient to signal the initiation codon in a way akin to that described for Cricket paralysis virus IGR IRES [53,54]. Several reports have appeared about the potential replacement of eIF2 by other cellular proteins for the translation of hepatitis C virus (HCV) RNA [48,55], but these experiments have always been carried out in *in vitro* systems in the absence of any viral protein. Some authors believe that eIF5B can replace eIF2 for the translation of HCV RNA in reconstituted cell free systems [36]. A recent report suggests that ligatin (also known as eIF2D) could replace eIF2 for HCV, but not EMCV RNA translation [48]. Although cell free systems have been very useful for unravelling the mechanisms of protein synthesis, they may provide some artefacts. Therefore, the observations found in *in vitro* systems must be contrasted with the situation present in intact cells and in virus-infected cells.

Materials and Methods

Cell Cultures

Baby Hamster Kidney (BHK-21 and clon BSR-T7/5, designated as BHKT7) cells [56] and Huh7-T7 (Human Hepatoma,) were used in this work. Cells were grown at 37°C in Dulbecco's Modified Eagle's Medium (DMEM) supplemented with 5% or 10% fetal calf serum (FCS) and non-essential amino acids. Cells BHKT7 were additionally provided with Geneticin G418 (Sigma) on every third passage at a final concentration of 2 mg ml^{-1} cell culture medium. For Huh7-T7 cells the medium was supplemented with Zeocin (5 μM).

Plasmids and transfections

The pTM1-derived plasmids containing the poliovirus proteins were described in detail earlier [44,57,58,59] . The constructs pKs.Luc and pTM1-luc have been already described [60]. The pTM1-eIF4GInt and pTM1-eIF4GIct were constructed using the pcDNA3 HAeIF4G-I [5] as DNA template. In the case of N-terminal fragment, were used the primers 5′NcoI4GInt: GCGCGCCCCATGGCCACGCCTTCTCAG and 3′BclI4GInt: GCGCTGATCATTAGCCAAGGTTGGCCAAG and, in the case of C-terminal the primers used were 5′EcoRI4GIct: GCGCGCAAATTCGGACAACCCTTAGC and 3′BclI4GIct: CCGCTGATCAGTTGTGGTCAGACTCCTCC. The PCR products were digested with NcoI/BclI or EcoRI/BclI respectively and inserted into the pTM1, previousy digested with the same

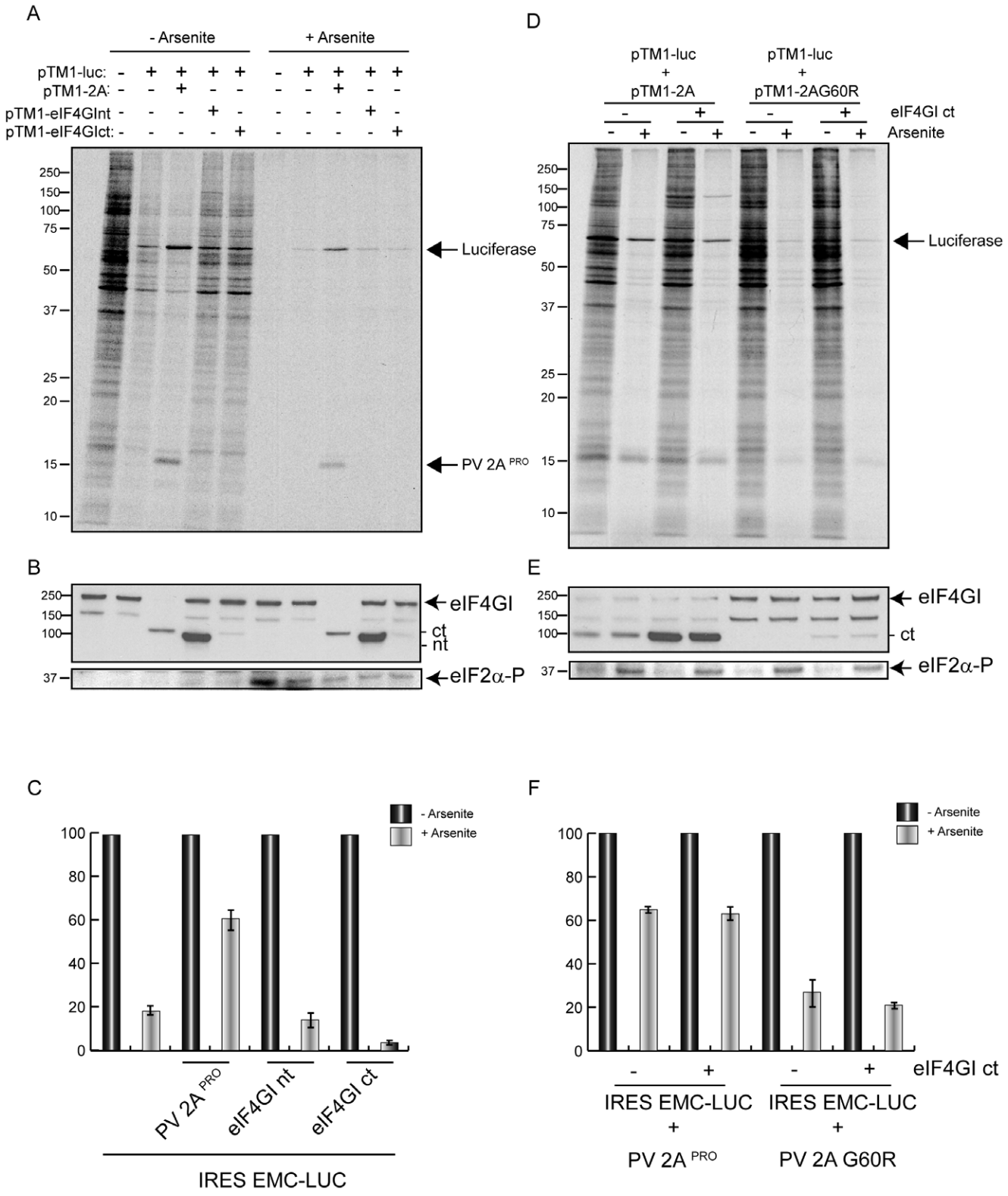

Figure 6. Influence on IRES-directed translation of expression of eIF4G fragments. pTM1-luc was co-transfected with a combination of the next plasmids: pTM1-2A , pTM1-eIF4Gnt and pTM1-eIF4Gct. A) At 2 hpe cells were pre-treated with 200 μM Ars for 15 minutes and then labelled with [^{35}S]Met/Cys for 45 minutes in presence of the inhibitor. Samples were processed by SDS-PAGE (17.5%) followed by fluorography and autoradiography. B) The amount of eIF4GI, eIF2α and phosphorylated eIF2α of the samples were detected by western blot. C) The percentage of luc synthesis, measured by densitometric scanning of the corresponding band, was represented. Error bars indicate SD from at least two independent experiments. D) BHKT7 cells were co-transfected with pTM1-luc and either pTM1-2A wt or pTM1-2A G60R. To each mixture, plasmid expressing c-terminal fragment of eIF4GI was or was not added. At 3 hpt samples were first pretreated with Ars for 15 minutes and then radiolabeled with [^{35}S]Met/Cys for 45 minutes and were or were not treated with Ars. Samples were then processed by SDS-PAGE (17.5%) followed by fluorography and

autoradiography. E) eIF4GI, eIF2α and phosphorylated eIF2α were detected by western blot. F) The percentage of luc synthesis, measured by densitometric scanning of the corresponding band, was represented. Error bars indicate SD from at least three independent experiments.
doi:10.1371/journal.pone.0025699.g006

enzymes. BHKT7 cells were transfected using Lipofectamine 2000 (Invitrogen). Cells were transfected or co-transfected with 1 μg of plasmid DNA or a mixture comprising 1 μg of each plasmid; in the case of RNA transfection, 2 μg of 2A mRNA were added plus 2 μl of Lipofectamine per well in Opti-mem medium (Invitrogen) for 2 hours at 37°C. After 2 hours, Lipofectamine was removed, and the cells were supplemented with fresh medium containing 5% FCS. BHK-21 cells were electroporated with *in vitro* synthesized mRNAs using as DNA templates the PV replicon, pKS.Luc or T7 Rluc ΔEMCV IGR-Fluc (this plasmid was employed to obtain CrPV IGR-luc mRNA). To obtain Cap-luc mRNA from pKS.luc, an $m^7G(5')ppp(5')G$ cap analog was added to the transcription mixture. Transcription reactions were carried out with T7 RNA polymerase (Promega) according to the manufacturer's instructions. For transfection, subconfluent BHK cells were harvested, washed with ice-cold phosphate-buffered saline (PBS), and resuspended at a density of approximately 2.5×10^6 cells/ml in the same buffer. Subsequently, 40 μg of *in vitro* transcribed RNA were added to 0.8 ml cell suspension and the mixture was transferred to a 4-mm cuvette (Bio-Rad). Electroporation was performed at room temperature by generating one pulse at 350 V and 975 μF using a Gene Pulser II apparatus (Bio-Rad). Finally, cells were diluted in DMEM supplemented with 10% FCS and seeded onto culture plates.

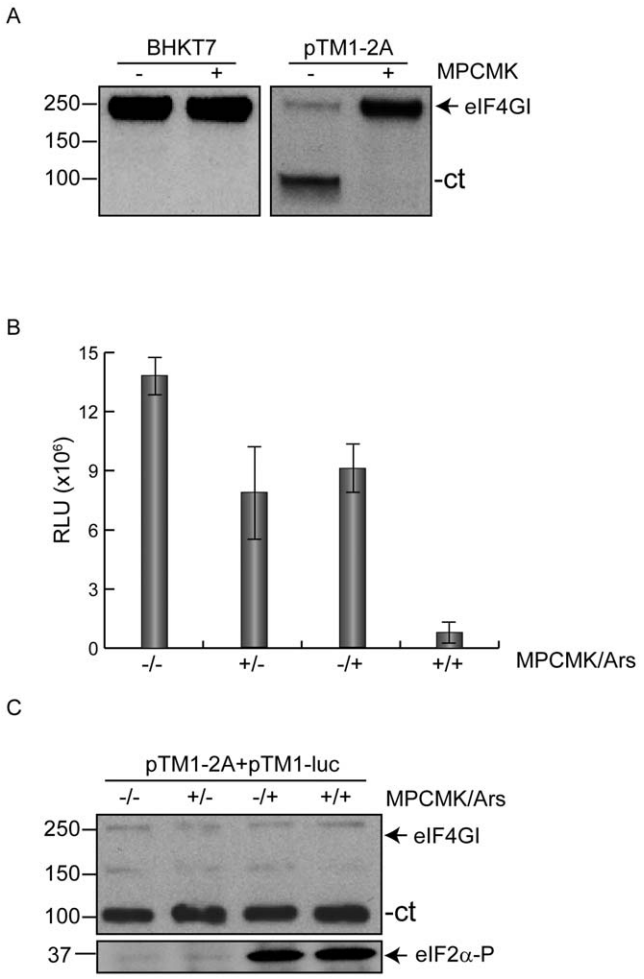

Figure 7. Active PV 2A^{pro} is necessary for eIF2 independence. A) BHKT7 cells were transfected or not with pTM1-2A and at the same time, in the mixture of transfection, cells were incubated without or with (−/+) 750 μM MPCMK. The transfection mixture was removed and cell monolayers were incubated for 1 h with or without (−/+) the inhibitor. To analyze the inhibitory effect on the proteolytic activity of PV 2A^{pro}, eIF4GI was detected by western blot. B) BHKT7 cells were transfected with pTM1-2A. After, cell cultures were incubated for 1 h at 37°C, then cells were transfected with pTM1-luc for 30 minutes. Afterwards, transfection mixture was removed and cells were incubated with or without 750 μM MPCMK (+/−), with 200 μM Ars (−/+) or both of them (+/+) for 1 h. Finally, cells were harvested and lysated in luciferase buffer and luc activity was measured and represented from at least three independent experiments. Error bars indicate SD. C) The samples obtained in panel B were used to examine eIF4GI by western blot. Phosphorylated eIF2α also was detected by western blot.
doi:10.1371/journal.pone.0025699.g007

Inhibitor treatments and analysis of protein synthesis by radioactive labelling

BHKT7 cells were transfected or co-transfected with the corresponding plasmids. At different time points, after two hours of incubation with transfection mixture, cells were pre-treated with 200 μM sodium arsenite (Ars) (Riedel-de Haën) or 2 μM Thapsigargin (Tg) (Sigma) for 15 min at 37°C, or left untreated. Next, proteins were radiolabelled for 45 min with [^{35}S]Met/Cys (Promix; Amersham Pharmacia) in methionine/cysteine-free DMEM in the presence or absence of the corresponding concentration of Ars or Tg. Finally, cells were collected in sample buffer, boiled for 4 min and analysed by SDS-PAGE (17,5%) and fluorography. Protein synthesis was quantified by densitometry using a GS-710 calibrated Imaging Densitometer (Bio-Rad). In the case of NaCl treatment, a methionine/cysteine-free DMEM with a final concentration of 265 (120+145) mM NaCl was used. Proteins were then radiolabelled for 45 minutes. Finally, cell monolayers were resuspended in sample buffer and processed as described above.

Western blotting

Transfected cells were collected in sample buffer, boiled and processed by SDS-PAGE. After electrophoresis, proteins were transferred to a nitrocellulose membrane as described previously [61]. To detect PV non-structural proteins, specific rabbit polyclonal antibodies [43,61,62] were used at dilution 1:1000. To detect eIF4GI a rabbit antibodies mix against the N-terminal and C-terminal portion of this protein [63] were used at dilutions of 1:1000. Polyclonal rabbit antibodies against eIF2α (Santa Cruz biotechnologies) and phosphorylated eIF2α (Cell Signaling) were used at a 1:1000 dilution. Rabbit antisera were raised against firefly luciferase (Promega). Incubation with primary antibodies was performed for 2 h at room temperature, and then the membrane was washed three times with PBS containing 0.2% Tween-20 and incubated for 1 h with horseradish peroxidase-conjugated anti-mouse (Promega) or anti-rabbit IgG antibodies (Amersham) at a 1:5000 dilution. After washing three times, protein bands were visualized with the ECL detection system (Amersham).

Measurement of Luciferase Activity

Cells were recovered in a buffer containing 25 mM glycylglycine (pH 7.8), 0.5% Triton X-100 and 1 mM dithiothreitol. Luc

activity was determined using *luciferase assay system* (Promega) and Mononlight 2010 apparatus (Analytical Luminescence Laboratory) as described previously [11,12].

Supporting Information

Figure S1 Kinetics of PV Replicon. BHKT7 cells were transfected withPV replicon. A) Protein synthesis was determined by labelling with [^{35}S]Met-Cys for 45 minutes every two hours from 1 to 7 hpt. B) Western blot analysis of the samples obtained in panel A using anti-eIF4G, anti-Luciferase and anti-phospho-eIF2α.
(TIF)

Figure S2 Rescue of picornavirus IRES translation by PV 2A^{pro} in Huh7-T7 cells. A) Hepatoma cells were transfected with plasmids encoding EMCV IRES-luc, PV IRES-luc or HAV IRES-luc alone or co-transfected with pTM1-2A. At 2 hpt cells were treated or not with 200 μM Ars for 1 hour. Then, cells were harvested and lysated in luciferase buffer and luc activity was measured and represented as percentage from at least three independent experiments. Error bars indicate SD. B) eIF4GI were detected by western blot.
(TIF)

Figure S3 Effect of 2A^{pro} on PKR. BHKT7 cells were mock- or transfected with pTM1-2A in presence or absence of Ars. Protein kinase RNA-activated (PKR) was detected by western blot.
(TIF)

Acknowledgments

We wish to express our gratitude to Dr. Y. Kusov for kindly providing us with plasmid pRLuc31 encoding the poliovirus replicon and plasmids encoding HAV and PV IRES-luc, Dr. P. Sarnow for plasmid T7 Rluc ΔEMCV IGR-Fluc, Dr. J. Berlanga for antibodies against PKR and Dr R. Bartenschlager for Huh7-T7. Dr. A. Castelló is acknowledged for critical reading of this manuscript.

Author Contributions

Conceived and designed the experiments: NR LC. Performed the experiments: NR MAS EW. Analyzed the data: NR MAS LC. Wrote the paper: NR MAS LC.

References

1. Dougherty WG, Semler BL (1993) Expression of virus-encoded proteinases: functional and structural similarities with cellular enzymes. Microbiol Rev 57: 781–822.
2. Tong L (2002) Viral proteases. Chem Rev 102: 4609–4626.
3. Foeger N, Glaser W, Skern T (2002) Recognition of eukaryotic initiation factor 4G isoforms by picornaviral proteinases. J Biol Chem 277: 44300–44309.
4. Castello A, Alvarez E, Carrasco L (2011) The Multifaceted Poliovirus 2A Protease: Regulation of Gene Expression by Picornavirus Proteases. J Biomed Biotechnol 2011: 369648.
5. Gradi A, Imataka H, Svitkin YV, Rom E, Raught B, et al. (1998) A novel functional human eukaryotic translation initiation factor 4G. Mol Cell Biol 18: 334–342.
6. Merrick WC (2004) Cap-dependent and cap-independent translation in eukaryotic systems. Gene 332: 1–11.
7. Sonenberg N, Hinnebusch AG (2009) Regulation of translation initiation in eukaryotes: mechanisms and biological targets. Cell 136: 731–745.
8. Belsham GJ (2009) Divergent picornavirus IRES elements. Virus Res 139: 183–192.
9. de Breyne S, Yu Y, Unbehaun A, Pestova TV, Hellen CU (2009) Direct functional interaction of initiation factor eIF4G with type 1 internal ribosomal entry sites. Proc Natl Acad Sci U S A 106: 9197–9202.
10. Yanagiya A, Svitkin YV, Shibata S, Mikami S, Imataka H, et al. (2009) Requirement of RNA binding of mammalian eukaryotic translation initiation factor 4GI (eIF4GI) for efficient interaction of eIF4E with the mRNA cap. Mol Cell Biol 29: 1661–1669.
11. Alvarez E, Menendez-Arias L, Carrasco L (2003) The eukaryotic translation initiation factor 4GI is cleaved by different retroviral proteases. J Virol 77: 12392–12400.
12. Ventoso I, Blanco R, Perales C, Carrasco L (2001) HIV-1 protease cleaves eukaryotic initiation factor 4G and inhibits cap-dependent translation. Proc Natl Acad Sci U S A 98: 12966–12971.
13. Willcocks MM, Carter MJ, Roberts LO (2004) Cleavage of eukaryotic initiation factor eIF4G and inhibition of host-cell protein synthesis during feline calicivirus infection. J Gen Virol 85: 1125–1130.
14. Piron M, Vende P, Cohen J, Poncet D (1998) Rotavirus RNA-binding protein NSP3 interacts with eIF4GI and evicts the poly(A) binding protein from eIF4F. Embo J 17: 5811–5821.
15. Aragon T, de la Luna S, Novoa I, Carrasco L, Ortin J, et al. (2000) Eukaryotic translation initiation factor 4GI is a cellular target for NS1 protein, a translational activator of influenza virus. Mol Cell Biol 20: 6259–6268.
16. Burgui I, Yanguez E, Sonenberg N, Nieto A (2007) Influenza virus mRNA translation revisited: is the eIF4E cap-binding factor required for viral mRNA translation? J Virol 81: 12427–12438.
17. Xi Q, Cuesta R, Schneider RJ (2004) Tethering of eIF4G to adenoviral mRNAs by viral 100 k protein drives ribosome shunting. Genes Dev 18: 1997–2009.
18. Lomakin IB, Hellen CU, Pestova TV (2000) Physical association of eukaryotic initiation factor 4G (eIF4G) with eIF4A strongly enhances binding of eIF4G to the internal ribosomal entry site of encephalomyocarditis virus and is required for internal initiation of translation. Mol Cell Biol 20: 6019–6029.
19. Pestova TV, Shatsky IN, Hellen CU (1996) Functional dissection of eukaryotic initiation factor 4F: the 4A subunit and the central domain of the 4G subunit are sufficient to mediate internal entry of 43S preinitiation complexes. Mol Cell Biol 16: 6870–6878.
20. Hundsdoerfer P, Thoma C, Hentze MW (2005) Eukaryotic translation initiation factor 4GI and p97 promote cellular internal ribosome entry sequence-driven translation. Proc Natl Acad Sci U S A 102: 13421–13426.
21. Kaiser C, Dobrikova EY, Bradrick SS, Shveygert M, Herbert JT, et al. (2008) Activation of cap-independent translation by variant eukaryotic initiation factor 4G in vivo. Rna 14: 2170–2182.
22. Pestova TV, Kolupaeva VG, Lomakin IB, Pilipenko EV, Shatsky IN, et al. (2001) Molecular mechanisms of translation initiation in eukaryotes. Proc Natl Acad Sci U S A 98: 7029–7036.
23. Ransone LJ, Dasgupta A (1987) Activation of double-stranded RNA-activated protein kinase in HeLa cells after poliovirus infection does not result in increased phosphorylation of eucaryotic initiation factor-2. J Virol 61: 1781–1787.
24. Ransone LJ, Dasgupta A (1988) A heat-sensitive inhibitor in poliovirus-infected cells which selectively blocks phosphorylation of the alpha subunit of eucaryotic initiation factor 2 by the double-stranded RNA-activated protein kinase. J Virol 62: 3551–3557.
25. Black TL, Safer B, Hovanessian A, Katze MG (1989) The cellular 68,000-Mr protein kinase is highly autophosphorylated and activated yet significantly degraded during poliovirus infection: implications for translational regulation. J Virol 63: 2244–2251.
26. O'Neill RE, Racaniello VR (1989) Inhibition of translation in cells infected with a poliovirus 2Apro mutant correlates with phosphorylation of the alpha subunit of eucaryotic initiation factor 2. J Virol 63: 5069–5075.
27. Black TL, Barber GN, Katze MG (1993) Degradation of the interferon-induced 68,000-M(r) protein kinase by poliovirus requires RNA. J Virol 67: 791–800.
28. Welnowska E, Sanz MA, Redondo N, Carrasco L (2011) Translation of Viral mRNA without Active eIF2: The Case of Picornaviruses. PLoS One 6: e22230.
29. White JP, Reineke LC, Lloyd RE (2011) Poliovirus Switches to an eIF2-Independent Mode of Translation during Infection. J Virol 85: 8884–8893.
30. Garrey JL, Lee YY, Au HH, Bushell M, Jan E (2010) Host and viral translational mechanisms during cricket paralysis virus infection. J Virol 84: 1124–1138.
31. Sanz MA, Castello A, Ventoso I, Berlanga JJ, Carrasco L (2009) Dual mechanism for the translation of subgenomic mRNA from Sindbis virus in infected and uninfected cells. PLoS One 4: e4772.
32. Castello A, Sanz MA, Molina S, Carrasco L (2006) Translation of Sindbis virus 26S mRNA does not require intact eukariotic initiation factor 4G. J Mol Biol 355: 942–956.
33. Ventoso I, Sanz MA, Molina S, Berlanga JJ, Carrasco L, et al. (2006) Translational resistance of late alphavirus mRNA to eIF2alpha phosphorylation: a strategy to overcome the antiviral effect of protein kinase PKR. Genes Dev 20: 87–100.
34. Neznanov N, Dragunsky EM, Chumakov KM, Neznanova L, Wek RC, et al. (2008) Different effect of proteasome inhibition on vesicular stomatitis virus and poliovirus replication. PLoS One 3: e1887.
35. Fernandez J, Yaman I, Sarnow P, Snider MD, Hatzoglou M (2002) Regulation of internal ribosomal entry site-mediated translation by phosphorylation of the translation initiation factor eIF2alpha. J Biol Chem 277: 19198–19205.
36. Terenin IM, Dmitriev SE, Andreev DE, Shatsky IN (2008) Eukaryotic translation initiation machinery can operate in a bacterial-like mode without eIF2. Nat Struct Mol Biol 15: 836–841.
37. Wehner KA, Schutz S, Sarnow P (2010) OGFOD1, a novel modulator of eukaryotic translation initiation factor 2alpha phosphorylation and the cellular response to stress. Mol Cell Biol 30: 2006–2016.

38. Andino R, Rieckhof GE, Achacoso PL, Baltimore D (1993) Poliovirus RNA synthesis utilizes an RNP complex formed around the 5′-end of viral RNA. Embo J 12: 3587–3598.
39. Ali IK, McKendrick L, Morley SJ, Jackson RJ (2001) Activity of the hepatitis A virus IRES requires association between the cap-binding translation initiation factor (eIF4E) and eIF4G. J Virol 75: 7854–7863.
40. Borman AM, Kean KM (1997) Intact eukaryotic initiation factor 4G is required for hepatitis A virus internal initiation of translation. Virology 237: 129–136.
41. Whetter LE, Day SP, Elroy-Stein O, Brown EA, Lemon SM (1994) Low efficiency of the 5′ nontranslated region of hepatitis A virus RNA in directing cap-independent translation in permissive monkey kidney cells. J Virol 68: 5253–5263.
42. Novoa I, Zeng H, Harding HP, Ron D (2001) Feedback inhibition of the unfolded protein response by GADD34-mediated dephosphorylation of eIF2alpha. J Cell Biol 153: 1011–1022.
43. Barco A, Ventoso I, Carrasco L (1997) The yeast Saccharomyces cerevisiae as a genetic system for obtaining variants of poliovirus protease 2A. J Biol Chem 272: 12683–12691.
44. Ventoso I, Barco A, Carrasco L (1998) Mutational analysis of poliovirus 2Apro. Distinct inhibitory functions of 2apro on translation and transcription. J Biol Chem 273: 27960–27967.
45. Molla A, Hellen CU, Wimmer E (1993) Inhibition of proteolytic activity of poliovirus and rhinovirus 2A proteinases by elastase-specific inhibitors. J Virol 67: 4688–4695.
46. Castello A, Alvarez E, Carrasco L (2006) Differential cleavage of eIF4GI and eIF4GII in mammalian cells. Effects on translation. J Biol Chem 281: 33206–33216.
47. Lukavsky PJ (2009) Structure and function of HCV IRES domains. Virus Res 139: 166–171.
48. Skabkin MA, Skabkina OV, Dhote V, Komar AA, Hellen CU, et al. (2010) Activities of Ligatin and MCT-1/DENR in eukaryotic translation initiation and ribosomal recycling. Genes Dev 24: 1787–1801.
49. Hambidge SJ, Sarnow P (1992) Translational enhancement of the poliovirus 5′ noncoding region mediated by virus-encoded polypeptide 2A. Proc Natl Acad Sci U S A 89: 10272–10276.
50. Roberts LO, Seamons RA, Belsham GJ (1998) Recognition of picornavirus internal ribosome entry sites within cells; influence of cellular and viral proteins. Rna 4: 520–529.
51. Macadam AJ, Ferguson G, Fleming T, Stone DM, Almond JW, et al. (1994) Role for poliovirus protease 2A in cap independent translation. Embo J 13: 924–927.
52. De Gregorio E, Preiss T, Hentze MW (1999) Translation driven by an eIF4G core domain in vivo. Embo J 18: 4865–4874.
53. Deniz N, Lenarcic EM, Landry DM, Thompson SR (2009) Translation initiation factors are not required for Dicistroviridae IRES function in vivo. Rna 15: 932–946.
54. Wilson JE, Powell MJ, Hoover SE, Sarnow P (2000) Naturally occurring dicistronic cricket paralysis virus RNA is regulated by two internal ribosome entry sites. Mol Cell Biol 20: 4990–4999.
55. Dmitriev SE, Terenin IM, Andreev DE, Ivanov PA, Dunaevsky JE, et al. (2010) GTP-independent tRNA delivery to the ribosomal P-site by a novel eukaryotic translation factor. J Biol Chem 285: 26779–26787.
56. Buchholz UJ, Finke S, Conzelmann KK (1999) Generation of bovine respiratory syncytial virus (BRSV) from cDNA: BRSV NS2 is not essential for virus replication in tissue culture, and the human RSV leader region acts as a functional BRSV genome promoter. J Virol 73: 251–259.
57. Aldabe R, Barco A, Carrasco L (1996) Membrane permeabilization by poliovirus proteins 2B and 2BC. J Biol Chem 271: 23134–23137.
58. Aldabe R, Carrasco L (1995) Induction of membrane proliferation by poliovirus proteins 2C and 2BC. Biochem Biophys Res Commun 206: 64–76.
59. Aldabe R, Feduchi E, Novoa I, Carrasco L (1995) Expression of poliovirus 2Apro in mammalian cells: effects on translation. FEBS Lett 377: 1–5.
60. Sanz MA, Welnowska E, Redondo N, Carrasco L (2010) Translation driven by picornavirus IRES is hampered from Sindbis virus replicons: rescue by poliovirus 2A protease. J Mol Biol 402: 101–117.
61. Barco A, Carrasco L (1995) A human virus protein, poliovirus protein 2BC, induces membrane proliferation and blocks the exocytic pathway in the yeast Saccharomyces cerevisiae. Embo J 14: 3349–3364.
62. Rodriguez PL, Carrasco L (1993) Poliovirus protein 2C has ATPase and GTPase activities. J Biol Chem 268: 8105–8110.
63. Aldabe R, Feduchi E, Novoa I, Carrasco L (1995) Efficient cleavage of p220 by poliovirus 2Apro expression in mammalian cells: effects on vaccinia virus. Biochem Biophys Res Commun 215: 928–936.

ARTÍCULO ENVIADO PARA PUBLICACIÓN

PHOSPHORYLATION OF eIF2α IS RESPONSIBLE FOR THE FAILURE OF PICORNAVIRUS IRES TO DIRECT TRANSLATION FROM SINDBIS VIRUS REPLICONS

Miguel Angel Sanz, Natalia Redondo, Manuel García-Moreno and Luis Carrasco

Centro de Biología Molecular Severo Ochoa

CSIC-UAM

c/Nicolás Cabrera, 1

Cantoblanco, 28049 Madrid, Spain

Running title: Phosphorylation of eIF2 blocks picornavirus IRES

Keywords: Poliovirus IRES; alphavirus; initiation factor; protein kinase R; regulation of translation

Abbreviations: SV, Sindbis virus; PV, poliovirus; $2A^{pro}$, 2A protease; sgmRNA, subgenomic mRNA; luc, luciferase; hpe, hour post-electropotation; hpt, hour post-transfection; Ars, arsenite; Tg, thapsigargin; MEFs, mouse embryo fibroblasts; BHK, Baby Hamster Kidney-21 cells; PKR, protein kinase R.

ARTÍCULO ENVIADO PARA PUBLICACIÓN

TRANSLATION DIRECTED BY HEPATITIS A VIRUS IRES IN THE ABSENCE OF ACTIVE eIF4F COMPLEX AND eIF2

Natalia Redondo[1], Miguel Angel Sanz[1], Jutta Steinberger[2], Tim Skern[2], Yuri Kousov[3] and Luis Carrasco[1]

[1]Centro de Biologia Molecular Severo Ochoa (CSIC-UAM)

c/Nicolás Cabrera 1. Universidad Autónoma de Madrid

Cantoblanco, 28049 Madrid. Spain

[2]Max F. Perutz Laboratories, Medical University of Vienna, Dr. Bohr-Gasse 9/3, A-1030 Vienna, Austria

[3]Institute of Biochemistry, Center for Structural and Cell Biology in Medicine, University of Lubeck, D-23538 Lubeck, Germany

Key words: Hepatitis A virus; picornavirus IRES; initiation factor of translation; eIF4G; eIF2

Running title: IRES-driven translation without eIFs